Development of a Premixed Burner Integrated Thermoelectric Power Generator for Insect Control

A Thesis Submitted to Cardiff University for the Degree of

Doctor of Philosophy

by

Tanuj Deep Singh

BE (Mech.) MBA (Operations)

March 2014

Cardiff Institute of Energy

Cardiff University, Wales, United Kingdom

Abstract

Electrical power generation using hydrocarbons presents a huge potential owing to their higher power densities and environmental factors associated with lithium ion batteries. Small scale combustors have been widely developed and tested for power generation purpose employing Thermoelectrics and Thermophotovoltaic conversion of combustion heat into electricity. This thesis is concerned with development and investigation of a novel non-catalytic meso scale self-aspirating premixed burner integrated thermoelectric generator for a CO_2 Generator device having its application in the insect control industry.

Flame stabilisation has been one of the main issues in small scale combustion systems due to higher surface to volume ratio associated with small size of the combustor. Previous research has shown that catalytic combustion is one way of improving flame stabilisation, however employing a catalyst into the system increases the manufacturing cost which can be a significant downside. This research work studies flame stabilisation mechanisms in meso-scale burner which mainly focuses on Backward Facing Step or Sudden Expansion Step and secondary air addition into the combustion chamber. A 250 W premixed burner was developed which was classified as a meso scale burner whose operating parameters were in a range of micro-combustors whereas the size was comparatively bigger due to its integration with standard size thermoelectric modules.

The first phase of the research was concerned with development of the burner which included optimisation of the design to achieve a stable enclosed premixed flame as per the design and operational requirements. It was found that flame blowoff can be prevented by addition of secondary air into the combustion chamber downstream of the step. The second phase of the research focused on the integration of the burner with thermoelectric power generators. This involved investigation of various configurations to optimise the electrical power output. The burner integrated thermoelectric unit was then tested in the actual field to validate the concept of integrating combustion and thermoelectrics for small scale power generation applications. The final phase of the research involved a study on the effect of secondary air addition on flame stabilisation in burners employing backward facing step. The minimum secondary air requirement for burner with different step heights was determined. The addition of secondary air cross-stream into the combustion chamber creates stable recirculation zone which reduces the local stream velocity and hence prevents flame blowoff.

Acknowledgments

I would like to thank Dr Richard Marsh whose excellent technical and managerial abilities have helped me to carry out the present work. Dr Marsh has been a great source of motivation and has provided me with all the necessary resources whenever they were needed which I really appreciate.

I am grateful to Dr Gao Min whose immense knowledge in the field of Thermoelectrics has helped me to better understand the subject and for always guiding me to the right path.

I would also like to thank Malcolm Seaborn and Steve Meads for their technical assistance in carrying out the experiments. I also thank the members of GTRC group for their help with experiments at various phases of the research.

I thank Dr Owen Jones and others associated with the KTP project for giving me opportunity to undertake this study.

Finally, I would like to thank my parents for their support and accepting my decision to pursue this study. I can't thank them enough for giving me everything I have ever asked for. Also, thanks to my brother for the encouragement he has given me throughout the past three years.

Tanuj Deep Singh

Declaration

This work has not previously been accepted in substance for any degree and is not being concurrently submitted in candidature for any degree.

Signed……. (Tanuj Deep Singh)
Date…….

Statement 1

This thesis is being submitted in partial fulfilment of the requirements for the degree of PhD.

Signed……. (Tanuj Deep Singh)
Date…….

Statement 2

This thesis is the result of my own independent work/investigation, except where otherwise stated. Other sources are acknowledged by footnotes giving explicit references.

Signed……. (Tanuj Deep Singh)
Date…….

Statement 3

I hereby give consent for my thesis, if accepted, to be available for photocopying and for inter-library loan, and for the title and summary to be made available to outside organisations.

Signed……. (Tanuj Deep Singh)
Date…….

Contents

List of Figures

List of Tables

Nomenclature

Symbol	Definition	Unit
Q	Burner Thermal Output	Watt
P	Electrical Power Output	Watt
P_1	Power output of Primary Power Generator	Watt
P_2	Power output of Secondary Power Generator	Watt
S	Backward Facing Step, Step Height	millimetre
T	Temperature	degree
R	Resistance	Ohms
Ri	Internal resistance of TEG	
V	Voltage output	Volts
V_1	Voltage output of Primary Power Generator	Volts
V_2	Voltage output of Secondary Power Generator	Volts
ΔT, dT	Temperature Difference across the two sides of TEG	degree
ΔT_1	Temperature Difference of Primary Power Generator	degree
ΔT_2	Temperature Difference of Secondary Power Generator	degree
α_{ab}, α_{np}	Seebeck coefficient	V.K-1
β	Thomson coefficient	W.I-1.K-1
I	Current	Ampere
ZT	Thermoelectric Figure of Merit	-
T_H, T_h	Temperature of Hot Side of the TEG	degree
T_{H1}	Temperature of Hot Side of the TEG of Primary Power Generator	degree
T_{H2}	Temperature of Hot Side of the TEG of Secondary Power Generator	degree
T_C, T_c	Temperature of Cold Side of the TEG	degree
T_{C1}	Temperature of Cold Side of the TEG of Primary Power Generator	degree
T_{C2}	Temperature of Cold Side of the TEG of Secondary Power Generator	degree
η	Efficiency	-
P_{max}	Maximum Power	Watts
d	Diameter	millimetre

r	Radius	millimetre
V_f	Volumetric flow rate of fuel	mL/min
Vpa	Volumetric flow rate of primary combustion air	L/min
V_{sa}	Volumetric flow rate of Secondary combustion air	L/min
V_{ta}	Volumentri flow rate of total combustion air	L/min
ϕ	Equivalence Ratio	
C1	Configuration 1	-
C2	Configuration 2	-
C3	Configuration 3	-
C4	Configuration 4	-
C5	Configuration 5	-
BC, NC	Nominal Configuration	-
v_f	Velocity of fuel	m/s
v_{pa}	Velocity of primary combustion air	m/s
v_{sa}	Velocity of secondary combustion air	m/s

Abbreviations

KTP	Knowledge Transfer Partnership
TSB	Technology Strategy Board
TEG	Thermoelectric Generator
EDM	Electro Discharge Machining
LBM	Laser Beam Machining
FIBM	Focused Ion Beam Machining
BFS	Backward Facing Step
PIV	Particle Image Velocimetry
TPV	Thermo-photo-voltaic
FTIR	Fourier Transform Infrared Spectroscopy
HE	Heat Exchanger
IHS	Internal Heat Sink
HS	Heat Sink
UHC	Unburnt Hydrocarbons
THC	Total Hydrocarbons

Chapter 1

Introduction

1.1 Project Motivation

The present study was performed under a Knowledge Transfer Partnership (KTP) project between Cardiff University and Suterra. The duration of the project was three years and it was funded by Technology Strategy Board (TSB). Suterra develops and markets products based on pheromone attractants for monitoring and control of insect pests in agriculture and public health sectors. The company was established in 1984 in Pontypridd, South Wales, and exports its products to over 50 countries.

The aim of the project was development, testing and commercialisation of a Carbon Dioxide (CO_2) Generator. Experimental studies have proved that CO_2 is a powerful attractant for biting insects such as mosquitoes and midges [1]. Thus a device producing CO_2 would therefore deliver a unique product with huge potential as various mosquito/midge catching apparatus are available in the market which does not have a source of CO_2 and the CO_2 Generator can be used in conjunction with them to improve their efficiency in terms of number of insects trapped. A non-catalytic CO_2 Generator which was proposed to be manufactured at a cost of less than $ 100, with capability of generating its own electrical power does not currently exist in the marketplace [2]. Also, developing such a product had strategic significance to the company as it would allow it to grow into a global market leader for monitoring and control of mosquitoes and other biting insects which is the aim is part of the company's future business plan.

The company proposed that the CO_2 Generator would produce CO_2 in small quantities through combustion of a hydrocarbon fuel. The device would generate electrical power to drive a fan and LED by converting heat of combustion into electricity via thermoelectric power generation (TEG) modules. This provided opportunity to carry out the present work which deals with the development and experimental investigation of a novel meso-scale non-catalytic premixed burner integrated with thermoelectric device for electrical power generation.

The KTP project was successfully completed in February 2013 with the development of a CO_2 Generator which satisfies all the operational and design requirements. The product has been tested in the laboratory as well as in the actual field with live insects for its operational capabilities and has passed all the important criteria.

1.2 CO_2 Generator Device Concept

The concept behind the device is entomological evidence suggesting that flying biting insects are attracted to CO_2, which is the reason mosquitoes and midges are attracted to animals and human beings as they emit CO_2 while respiration. Many flying biting insect traps are available in the market which uses this concept to attract mosquito and a have particular mechanism to catch/kill them [3-11] [100]. Some of the methods used for producing CO_2 include bottled CO_2, dry ice, photocatalytic reaction of Ultraviolet light rays on the surface of Titanium Dioxide [103] and catalytic combustion of hydrocarbon fuel. Mechanisms used for trapping/killing insects include sticky surfaces on the trap and a small fan to suck insects into the trap. The device which has been proposed in this study involves usage of a fan to capture mosquitoes/midges into a 'catch bag'. Many mosquito traps are present in the market which do not have a CO_2 source but are compatible to be used along a device which produces CO_2. One such mosquito trap [12] can be seen in Figure 1.1 which shows a schematic drawing of operation of an insect catching apparatus and CO_2 Generator. This particular apparatus has an opening at the top from where the insects are sucked inside the traps and collected in an 'insect catch bag' by a fan located inside the trap body. In operation a CO_2 Generator device would burn a hydrocarbon fuel supplied from a gas bottle to produce CO_2 at a fixed rate which would form a cloud in the surrounding area. Mosquitoes or midges in the near vicinity will be attracted to the CO_2 and when they are sufficiently near enough for the suction fan to come into effect, gets sucked into the catch bag. The consumer can change the catch bag when it is full.

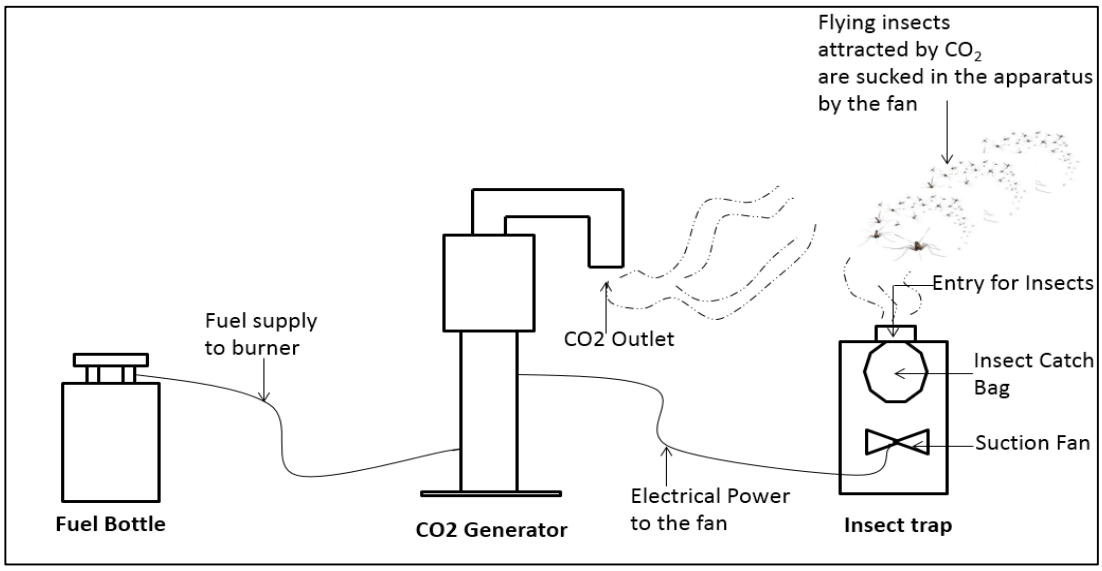

Figure 1.1: Schematic showing operation of an insect catching apparatus and CO_2 Generator

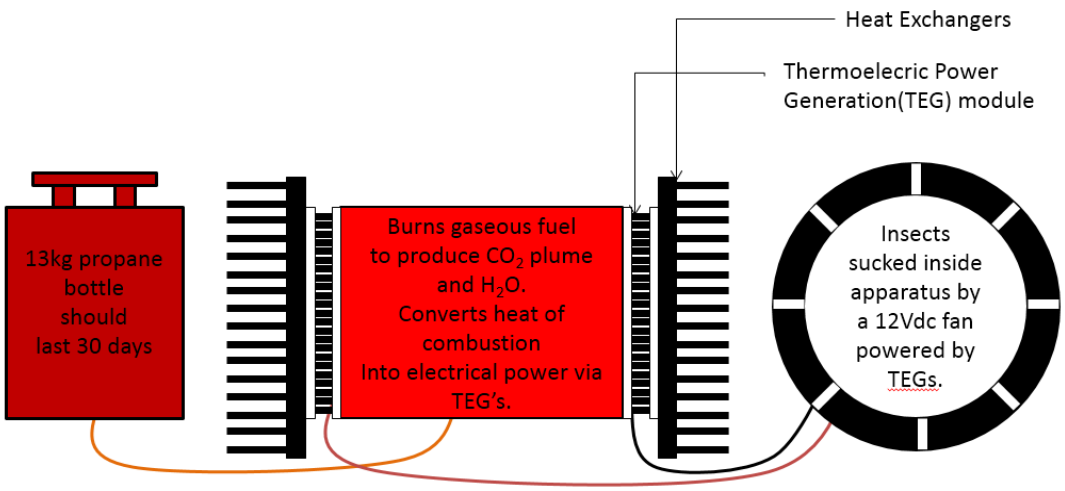

Figure 1.2: A schematic diagram showing the working concept of the device involving combustion of a hydrocarbon fuel to produce CO_2 and conversion of heat into electricity via thermoelectric to run a 12 V fan and other electrical components such as LEDs.

The figure above presents the working concept of the device which includes a burner providing source of heat through combustion of a hydrocarbon fuel supplied from a gas bottle such as a 13 kg propane bottle shown in the diagram; and TEG modules integrated on the sides of the burner which generates electrical power to drive electrical components included in the insect catching apparatus. For example, suction fan which is a 12 vdc, device requires around 3.2 W power. So, a means by which the device can generate electricity would bring added benefit to the product by allowing its application in remote areas. Two TEG modules have been integrated on the burner walls which converts the heat of combustion into electrical power via the Seebeck effect [13]. This eliminates the use of batteries and increases the longevity of operation as well, as thermoelectric modules are using the heat to produce electricity which would have been wasted.

1.3 Target Markets

Following are the target markets for the proposed CO_2 Generator:

- Governments: Mosquito Abatement Groups in EU and US. The Bill and Melinda Gates Foundation (B&MGF) estimate that about $ 750 million is spent by municipalities and other government organisations on mosquito abatement programmes.
- Military: There has been rising number of cases in armed forces suffering from vector borne diseases such as malaria, dengue, or leishmaniasis. Monitoring and control of

vector presence costs the countries concerned hundreds of millions of pounds per annum. Consumer: The B&MGF has estimated that consumers worldwide spend over $8 billion protecting themselves from mosquito borne diseases.

- Pest Control Operators (PCO) – Pest control operators provide professional insect control solutions to households, schools and hotels etc. This market is estimated by B&MGF to be about $ 100 million worldwide.

  Most of these markets are in remote locations where electrical power is not easily available.

1.4 Design Objectives

The CO_2 Generator was designed based on the following objectives:

1. The quality of the combustion products was of high importance as any toxic/harmful compound in the exhaust other than CO_2 and water can affect the attraction of insects towards it. So, the requirement was to design a burner in a way that it permits complete combustion and produces no harmful compounds. A non-catalytic premixed gas burner with a backward facing step and mixing zones has been designed and extensively tested to enhance mixing of the reactants. The benefits of having a sudden expansion or backward facing step have been mentioned in detail in the literature review.
2. The burner should not have a catalyst to achieve conversion of harmful compounds like carbon monoxide, nitrogen oxides and sulphur oxide into CO_2 and water. The reason being low cost design.
3. The flame needed to be enclosed so that the heat of combustion can be supplied to the burners walls which would heat up thermoelectric modules placed on them. So the location of the flame was very much important for electrical power generation aspect as well as environmental factors as the burner will be operating outdoors. A strong wind or rain should not have an impact on burner operation and flame should sustain for long duration of operation.
4. Flame stability was a major aspect which has been extensively explored in this work. The flame was supposed to sustain throughout an insect catching season which can be as long as 3 months. Environmental factors were needed to be considered during design as the burner will have to operate under rain, strong winds and temperature fluctuations. For this purpose, secondary air supply has been studied to understand its

effect on the flame stability or flame anchoring as well as completeness of combustion.

5. The unit is a low cost design so the emphasis was given to eliminate expensive moving parts such as pumps etc. So the objective was to design the burner which would operate without any forced means of air supply. In other words, the burner has to be a 'Self Aspirating Type', where the air is entrained into the burner by the flow of fuel downstream.
6. As one of the aims of the project was to develop a low cost design, the TEG modules cannot be customised according to the requirements as it would increase the cost. So, the modules which were chosen to be integrated with this device were those ones which are commercially available. A comprehensive market research was performed for the module keeping focus on the price and performance along with experimental investigations were done to select the best performing modules. Results from the experimental investigation will be presented in the later sections. The modules which are selected are square in shape and have the dimension - 40mmx40mmx3mm [93]. The principle of thermoelectric power generation states that the higher the temperature difference between hot and cold side of the module, higher the power generation will be. Keeping this in focus, the requirement was to increase the heat flowing through the module. One way of achieving this is by capturing maximum heat from the combustion exhaust. So the burners should be designed in a way that it accommodates flat surfaced TEG modules which are square in shape and allowing maximum heat absorption at the burner walls.
7. Temperature difference will be optimised when there is an efficient way of dissipating heat at the cold side of the TEG module. So the next objective was to use efficient and at the same time inexpensive heat exchangers which would result in higher temperature difference and hence higher electrical power output. An investigation has been done to identify the most appropriate heat sinks.

1.5 Operating Requirements

1. Propane was selected as fuel because of its easy availability in the countries where the final product will be sold. These devices are generally used with a 13 kg propane bottle. Similar devices sold by competitors consume 13 kg propane in 30 days [3-11] [100], so the first operating requirement was the longevity of the operation. The concept was that a customer should only have to change the gas bottle once a month

when he/she is supposed to empty insect bags from the traps (as explained in the Device Concept).

2. The device was required to produce 300-450 mL/min of CO_2 as this is the ideal rate for mosquito/midge attraction according to entomological experts. The stoichiometric combustion equation for propane would show that around 150 mL/min of propane combustion would result in 450 mL/min of CO_2 and a 13 kg gas bottle would last 30 days. A burner combusting 150 mL/min of propane would have a heat output rating of 250 W.
3. The electrical power generation requirement was ~3.5 W based on the power requirements of the fans studied for this concept. This was an important design aspect as consistent power generation is required throughout the operation as the whole concept of catching insects by attracting them through CO_2 is only logical if the suction fan is operating at a consistent speed and developing enough suction power to capture the insects and eliminate them from the infected area.
4. The external structure of the unit should not go above 60 ^oC as high temperatures can be sensed as a danger by insects according to entomological research. Also, this aspect was important in terms of human safety.
5. The outlet temperature of the CO_2 should not exceed 30 ^oC which is for the same entomological and safety reasons.

1.6 About the present research

The CO_2 generator described earlier involves electrical power generation using hydrocarbons which presents a huge potential alternative to traditional batteries. It is a well-known fact that hydrocarbons have notably higher energy density as compared to batteries. For example, propane has an energy density of 40 MJ/kg where as a lithium-ion battery has 0.5 MJ/kg. Hydrocarbon fuels provide around 10 times more energy storage density than batteries. There are several other benefits of using hydrocarbons over batteries such as ease of availability, longer shelf lives, low cost and no need of pre-processing [15][16].

Some small scale combustion systems employed for power generation are shown in Figure 1.3.

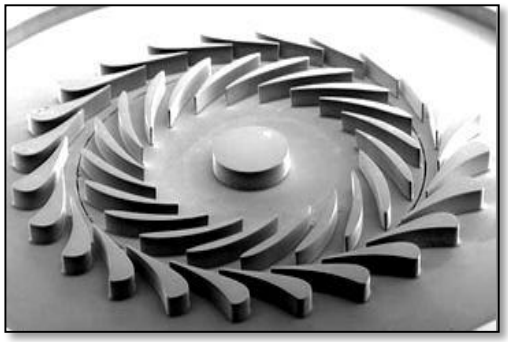

(a)

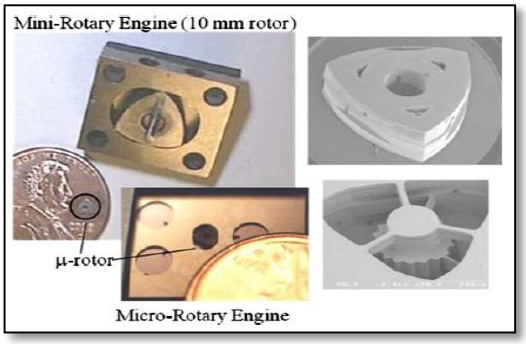

(b)

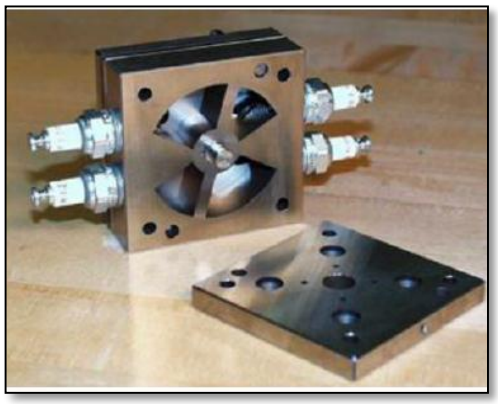

(c)

(d)

Figure 1.3: Small scale combustion based power generation devices

A photograph of a micro gas turbine is shown in Figure 1.3 (a), the main components are a radial compressor/turbine unit, a combustion chamber and an electrical generator incorporated in the compressor. The microcombustor has been successfully tested for continuous operation using Hydrogen/air mixtures and hydrocarbon-air mixtures [17]. Figure 1.3 (b) shows a mini rotary engine developed by researchers at the University of California, Berkeley [17] [18] using EDM. The engine uses H_2 as fuel and with 10-mm rotor produced 4 W at 9300 rpm. A meso-scale internal combustion swing engine (MICSE) with four combustion chambers developed by the University of Michigan is

shown in Figure 1.3(c). The engine operates in a four-stroke Otto cycle and energy is converted is by an inductive alternator connected to the shaft of the swinging piston [17]. Figure 1.3(d) shows a two-dimensional Swiss-roll (i) and three-dimensional toroidal (ii and iii) burners developed at the University of Southern California [17]. The toroidal three-dimensional Swiss-roll burner was designed based on the Weinberg's heat recirculating Swiss-roll burners. Power generation is achieved by thermoelectric elements embedded in the walls of these burners [19-23].

Thermoelectric power generation using small scale combustion is a promising field for power generation. This research work involves a detailed study of integration of thermoelectric power generating devices with small combustors. The basic principle of thermoelectric power generation is based on the Seebeck effect, which has been studied in detail in the literature review, states that a voltage is generated when there is a temperature difference at the two sides of a semiconductor or metal [13]. Combustion of hydrocarbon such as propane provides the heat required to raise the temperature of the hot side of a thermoelectric power generator (TEG) module with cooling is provided at the cold side via heat exchangers.

The main focus in this research has been given to flame stabilisation in a meso-scale self-aspirating burners. The main feature of this burner is secondary air supply over a backward facing step for the purpose of widening the burners flammability limits. This experimental study has shown that flame blowoff can be prevented by supplying secondary air to the backward facing step thus producing hydro-dynamically stable recirculation zone. The main area of focus is:

- Effect of varying step height on flame stabilisation in a self-aspirating meso-scale premix burner
- Effect of secondary combustion air addition on the flame stabilisation in the burner

The novelty of this work lies in the scale of operation and the justification for the feasibility of the concept of integrating combustion and thermoelectrics to generate electrical power for small scale applications. Previous experimental research in this field is focussed on either micro-scale where the size of the burner and thermoelectric generator is in order of few millimetres and electrical output is in milli-watts [15-22] or comparatively larger ones having sub-cm size range [23][97]. This research is focussed on the design and testing of thermoelectric generator integrated meso-scale combustor having heat output of around 250W and an electrical output of 3-5 W. The literature review carried out in this work has shown that the burner of the current research work has

the dimensions of a meso-scale burner while operating requirement of a micro-scale, which is a novel area of research involving investigation flame stabilisation issues in these type of small scale burners. This research work will provide reference for future work in this field and present an analysis of how thermoelectric power is dependent on the ambient conditions. The results also prove the durability of these devices when it comes to continuous operation for long durations.

The next chapter will cover a literature review on micro and meso-scale combustion principles. The major topics covered in the literature review includes flame stabilisation and combustion dynamics in burners employing a backward facing step, premix burner design principles, thermoelectric principles, micro-scale thermoelectric power generators and burner configurations. The Research Methodology chapter comprises of the test rig set up, burner's description and plan of experiments. This also includes description of the major equipment and tools used to carry out experiments and record the data. This is followed by a chapter giving an account of major design and operational challenges emerged during the product development cycle which provided with opportunities to study novel combustion and thermoelectric phenomena. This is followed by an application of fundamental data in order to develop the CO_2 Generator device. It is important to understand the design, geometry and working principle of the device developed during the project which will be presented in this chapter. Results from the integration of thermoelectric power generation modules on the burner will be presented with their effect on each other. Product gas analysis was also conducted via Fourier Transform Infrared Spectroscopy (FTIR) in support of the findings. The next chapter includes experimental results and discussion on the effect of varying step height and secondary air supply on flame stabilisation.

The thesis also presents results from endurance tests of the device, tests conducted in environmental chamber and field trial results. The aim of these tests was to validate the concept of integration of meso-scale combustion system with thermoelectric.

1.7 Structure of Thesis

The structure of the thesis is as follows:

Chapter 2: Literature Review - This chapter deals with the literature associated with premix combustion and thermoelectrics. It includes a study of previous work done in the field of integrating combustion and thermoelectric phenomena in one system.

Chapter 3: Research Methodology - This chapter is concerned with the research approach employed to develop the premix burner and integrated thermoelectric power generator, discusses the test performed and data collected, describes test rig, system components and combustion product analysers.

Chapter 4: Challenges/Issues - This chapter is concerned with the major design challenges and problems faced in achieving stable flame in a self-aspirating non-catalytic burner and electrical power output during the development stages of the mentioned device.

Chapter 5: Development and Investigation of a meso-scale premix burner - Development of a novel self-aspirating premix meso-scale burner has been explained along with various experimental results from different prototypes and configurations are presented.

Chapter 6: Integration with thermoelectrics - This chapter consists of results from integration of combustor developed in the previous chapter with thermoelectric power generation modules.

Chapter 8: Effect of Secondary air on flame stabilisation in self-aspirating premix burners- This chapter is concerned with an experimental study of understanding flame stabilisation using secondary air supply.

Chapter 9: Conclusion and Future work – The chapter will summarise the thesis and mentions any future work recommended.

Chapter 2

Literature Review

2.1 Introduction

A comprehensive literature review was carried out to form a firm foundation for the research to be carried out in the present research involving development and investigation of a burner integrated thermoelectric unit. This chapter will include a study of premixed combustion followed by an introduction of small scale combustion. Previous study on micro-scale combustion and compact energy module solutions and the application of small premix, possibly flameless burners has been carried out. Small scale electrical power generators involving integration of thermoelectric and other power generation methods employing combustion as a source of energy input have been studied.

2.2 Premixed Combustion

Premixed combustion involves complete mixing of fuel and oxidiser before combustion is allowed to take place. The fuel and oxidiser are intimately mixed prior to their arrival in the ignition zone [24]. The practical examples of combustion systems employing premixed combustion are spark ignition engines, lean burn gas turbines and household burners; where the fuel and air are mixed prior to their entry into the combustion chamber. The reactant mixture is then ignited with a source of heat and the flame propagates through the mixture. The mixture will only burn when the equivalence ratio lies within the flammability range which is approximately from 0.5 to 1.5 [25].The simplest example of a premixed flame is a Bunsen flame in which a mixture of gaseous fuel and air travels downstream a tube at a velocity higher than the burning velocity of the fuel. The invention of the Bunsen burner led to a major change in the industry as the previously used diffusion combustion system produced flames which were luminous, smoky and had a tendency to form carbon deposits on burner components and causing damage to them and their temperatures were low as well. On the other hand premixed flames involve much more intense combustion, have a higher flame temperature and are relatively soot free [26]. Mishra [27] performed experimental studies of flame stability limits of CNG-air premixed flames in simple Bunsen burner having two different port diameters operating between flashback and blowoff limits. He plotted a stability map which could be used

while designing CNG-air premix burners. The main conclusion was that the flame stability decreased when the diameter of the port was increased from 12 to 15mm.

Lean premixed burners investigated by several researchers will be discussed in this section of the literature review. The effect of premixing of fuel and air on NOx formation has been investigated by Hase and Kori [28]. They have suggested that lean premixed combustion is a promising method for reducing NOx emissions but however if the mixing of fuel and air is not sufficient, the NOx may not be as low as expected despite being premixed combustion system. Reduction in NOx with premixed combustion has been reported by Ghoniem et al. [29] as well where they discussed about flame stabilisation by injecting air and H_2 jet perpendicular to the main fuel stream near a backward facing step. Extinction and flame propagation has been extensively investigated in premix combustion systems, a numerical study was performed by Alliche et al. [30] on extinction condition of premixed flame in a channel and concluded that the quenching depends upon the heat losses imposed at the walls of the combustion chamber. Xu and Ju [31] undertook a theoretical and experimental investigation into meso-scale premixed flame propagation and extinction and obtained a general flame dynamics for small scale premixed burners due to flame wall interactions. Their results showed existence of multiple flame regimes and the nonlinear dependence of flame speed on the equivalence ratio affected by flow speed, Nusselt number and wall heat conductivity. Some of the other works on premixed combustion includes an investigation of flammability limits of stationary flames in tubes at low pressure by Kim et al. [32] which involved flame-wall interactions, measurement of flame thickness and quenching of stationary premixed flames, combustion characteristics of propane-hydrogen-air premixed flames and their burning velocities were studied by Tang et al. [33] where they explored the flame stability behaviour with hydrogen addition in the propane-air mixture, Li et al. [34] studied premixed combustion in cylindrical micro combustors with focus on transient flame behaviour and wall heat flux where they employed a backward facing step in a premixed micro burner for flame stabilisation, lean premixed swirl combustion has been studied by Huang and Yang [35] focussing on premixed combustion systems in gas turbines and included discussion on swirl injector configurations and swirl flow characteristics and another study on flashback in premixed flames has been experimentally and numerically done by Kurdyumov et al. [36] indicating heat transfer to walls contributing to flashback.

Premixed combustion has been used in porous burners which present various advantages such as enhanced efficiencies, higher power densities, higher dynamic power ranges, high

compactness and controlled pollutant emissions making them superior of conventional free flame burners. Preheating of incoming reactants is achieved in porous burners through heating up of the porous solid by the post flame zone by radiation and conduction heat transfer mechanisms. A numerical study was performed by Akbari and Rihai [37] on a porous burner and the results showed that the inlet mixture characteristics and the structural properties of the solid matrix determine the flame stability and thermal performance of a porous burner. They also suggested that burner length does not play any role in thermal characteristics of the burner. Furthermore, the efficiency of the preheating zone can be increased and increase in the solid matrix porosity and burner firing rate. The recirculation of heat from the hot combustion products to the incoming reactants in porous burners is studied by Wood and Harris [38], who suggests that increased flame speeds, extended flammability range, flame stability across wide range of flow rates and low emission are characteristics of premix combustion in porous burners.

2.3 Small Scale Combustion - Micro and Meso-Scales

Combustion at small scale has gained attention over the past few years for its wide potential applications in power generation as well as heat and mechanical power sources [39]. There has been an upward trend in the miniaturisation of mechanical and electromechanical engineering devices motivated by the progress made in micro-fabrication techniques like electro discharge machining (EDM), laser beam machining (LBM) and focused ion beam machining (FIBM) [40]. As already mentioned in the introduction chapter, the energy density of hydrocarbon fuels is substantially higher than the conventional batteries currently available in the market. The high energy density along with other advantages such as elimination of moving parts, small size, low weight and longevity of operation is growing interest of researcher in developing small scale combustion devices. Several micro and meso combustors have been developed and tested with satisfactory combustion efficiency. Some of the combustors have been integrated with electrical power generators such as thermoelectric power generators and thermo-photovoltaic cells, though the conversion efficiency has been found to be low. Combustion at small scale presents various technical challenges which will be studied in this section. The definition of micro and meso combustion scales will also be explored through a comparison of design and operating characteristics of small scale burners developed and tested by researchers [40][87].

2.3.1 Challenges in Micro and Meso-Scale Combustion

Combustion in small scale systems presents issues related to the time available for the combustion reaction to take place and to the quenching of the combustion reaction by the wall. The fundamental requirement for combustion to take place in micro combustors is that the residence should be larger than the time required for the reaction to occur. The residence time in gas turbines is determined by the size of the combustion chamber and flow rate of the fuel and air stream through the chamber. In the case of combustion in internal combustion engines the residence time is determined by both the engine speed as well as the size of combustion chamber. Catalytic combustion involves diffusion of species to the wall and species absorption/desorption at the wall which determines the residence time. Micro combustors have small residence time which makes it important to have small chemical times to make sure complete combustion of the reactants take place. Various ways are used to achieve this small chemical time which includes ensuring high combustion temperatures which requires the heat losses to be reduced from the combustors walls, preheating of reactants, stoichiometric operating conditions and using fuels with high energy densities [82][87][40].

One of the main technical challenges with micro and meso-scale combustion is the quenching issues due to the large surface to volume ratio [82]. These small scale combustors differ from conventional scale ones in terms of heat transfer and surface reactions that take place at the burner's wall because of high surface to volume ratio in micro-scale burners. As the scale of the combustor is reduced, the surface to volume ratio increases due to small characteristic length. This high ratio results in heat losses causing flame stability issues which are also governed by the ratio of heat loss to heat generation in non-adiabatic flames. Quenching of the flame takes place as a result of high chemical time. Walther and Ahn [40] suggests that thermochemical management techniques can be used to overcome quenching which includes the use of excess enthalpy combustors, generating adiabatic walls by stacking planar devices in a symmetrical fashion (insulated temperature boundary condition), establishing high-temperature ceramic walls, and using surface coatings.

Weinberg et al. [18][19][20][21] conducted work on recirculating burners named as 'swiss-roll' combustors as shown in the Figure 1. Their study involved optimisation of combustion reaction by using the enthalpy of the products to pre-heat the fuel air mixture. This enthalpy exchange obtained by recirculating the exhaust resulted in steady combustion with mixtures well below the normal flammability limits.

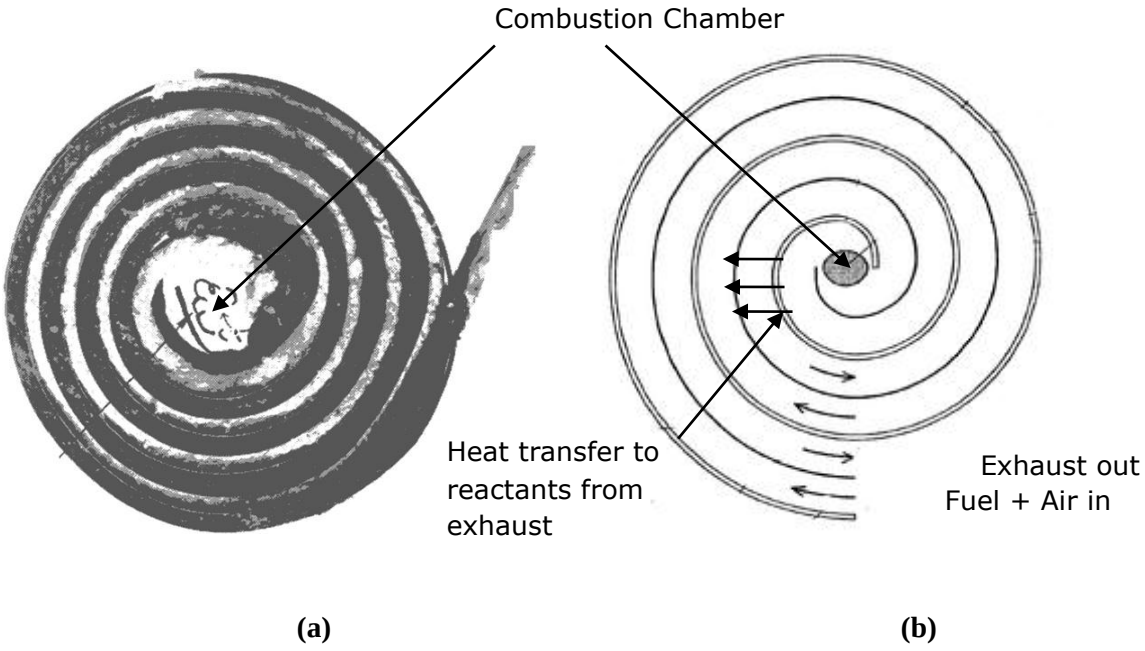

Figure 2.1: (a) A photo of Weinberg's 'swiss roll' heat recirculating burner [40] (b) A figure explaining the concept of heat recirculating burners

Figure 2.1 shows 'swiss roll' type Weinberg's heat recirculating burner in which the combustion chamber is located at the centre of the burner. The incoming reactant and exhaust channels are coiled around each other allowing heat transfer from the hot exhaust to the cold incoming reactants. Stable combustion has also been observed at temperatures below the expected homogeneous combustion temperatures of the fuels tested but above their normal catalytic temperatures [18][21][19]. The preheating of the incoming reactants by recirculating the exhaust has been implemented in to obtain stable combustion in thin tubes with diameters smaller than the quenching distances [41][42].

As mentioned before, quenching is one of the major problems in micro combustors. The author advises that the problem of wall quenching can be prevented by increasing the wall temperature as the quenching distance is approximately inversely proportional to the square root of the temperature, preventing heat losses to the wall (adiabatic wall), or by using catalyst on the combustor wall [40]. Coating the combustor walls with inert materials such as Mullite can also reduce radical recombination and chemical quenching at relatively low temperatures [43].

The high surface to volume ratio in micro combustors although presents issues in gas phase combustion but it favours catalytic combustion. It must be noted that regardless of

the attractive nature of catalytic combustion at large surface-to-volume ratios, the kinetic reaction rate is typically lower than the gas phase for the temperatures expected in micro-devices. Hence, the use of catalysis in gas turbine combustors, which is a chemical time limited system, may not be ideal [43]. While in combustion systems which are not limited by reaction times, the relative increase of surface area and the lower temperatures of the catalytic reaction advocate that micro-scale combustors using catalyst may be easier to realize than those using gas-phase reactions. The above mentioned Swiss role burner based on preheating of the reactants involves the use of a catalyst. The results showed that combustion of hydrogen-air mixtures and other fuels such as butane and propane at less than 200^{o}C in the Swiss burner which confirms the potential of micro catalytic combustors [21][[44][45][46]. Some other work on the employment of catalytically active surfaces in micro and meso channels to stabilize the flame structure, determine extinction limits, optimize combustion efficiencies and reduce emissions has been mentioned in [18][46][21][44][45]. A single pass counter flow heat exchanger developed by Peterson RB [48] is designed with an incorporated catalytic surface. Volumetric heat generation rates of up to 101 W/mm^3 are achieved due to the small scale greatly enhancing both thermal and mass transfer.

Various experimental and numerical investigations have been carried out to analyse the combustion regimes and phenomena which occur in micro-scale combustion systems. Jackson et al. [49] addressed the thermal issues in micro combustors made up of narrow ducts. Their calculations identified the unique oscillatory phenomena made possible by surface interactions in micro-scale combustion that have been observed by Maruta [50], and more recently by Evans and Kyritsis [51]. Other works on micro combustion includes recent work with PIV characterizing the flow fields around catalytically coated micro-wires [52] and micro-flat plates for boundary layer interruption [53].

Kaisare et al. [54] investigated the mechanisms of extinction and blowoff and how these are affected by thermal conductivity and heat losses in small scale channels. The research involved study of effect of reactor dimensions and system parameters on extinction and blowout in premixed flame using a 1D model. They found that extinction occurs when the heat released by reaction is insufficient to sustain combustion due to heat loss or in other words the ratio of heat losses to the total heat generated is high and the maximum temperature is low. On the other hand, blow-out occurs when the flame gets swept out of the channel at higher velocities due to lower residence times. At blowout limits, the heat losses are comparatively lower and the maximum temperatures higher. The research suggested that when the flame stabilisation in small channels is obtained through heat

recirculation through the burner, the solid thermal conductivity has a stronger effect on the blowout limit and a comparatively weaker effect on the extinction limit. A small scale combustor can be enabled to operate at higher inlet velocities when they are made up of higher thermal conductivity.

The research was also concerned with the study of effect of reactor dimensions such as reactor length, gap size, and plate thickness on flame stability. It was found that increasing channel length results in an increase in heat loss and residence time. The research work further mentions the channel gap width has a strong effect on quenching limits which depends upon the fuel. The rate of heat transfer to the wall is inversely proportional (approximately) to the gap width. Thus, the net heat loss as well as the heat recirculation towards the upstream of the reactor increases when the gap width is reduced. The increase in heat losses makes the flames less stable near the extinction limit, whereas the heat recirculation stabilizes the flames at higher velocities which allow the blowout to occur at much higher velocities. They also suggested that material integrity in terms of high wall temperatures should also be carefully considered while designing small scale burners.

Pan et al. [89] investigated the effects of fuel to oxygen mixing ratio, nozzle to combustor diameter ratio, and wall thickness to combustor diameter ratio on combustion in small scale combustors. They found that oxygen rich mixing rates results in high wall surface temperatures (At hydrogen to oxygen mixing rate of 1.8:1, the wall temperature was found to be higher than mixing rate of 1.5:1). It was observed that the flame tends to relocate in the combustion chamber with changes in volumetric flow rate and nozzle to combustor diameter ratio for a given flow rate and hence affects the distribution of wall temperature. It was also shown that photovoltaic energy conversion efficiency is affected by the wall thickness of the combustor, thin wall combustor resulted in an increase of surface temperature about 150 K which eventually increases the conversion efficiency. This effect will be important in the present research as wall temperature is an important aspect of power generation in thermoelectrics. A thin wall combustor will provide more heat at the hot side of the thermoelectric module, thus help in achieving large temperature difference, provided an efficient mechanism of heat removal at the cold side of the thermoelectric module, which would result in higher power generation.

In other research by Yang et al. [56], experiments were performed employing porous media foam in the combustion chamber. It was observed that heat transfer between the hot gas and the combustor wall enhanced which maximised the output power of the system as the foam provided a high and uniform temperature distribution along the

combustor. The results indicated an increase in peak wall temperature by 90-120 K with SiC porous media. This increase in wall temperature significantly enhances radiation energy which is useful for electricity generation. Similar method of heat extraction from the combustion has been employed in the present research to obtain higher power generation through thermoelectrics which would be discussed in other chapters later.

2.3.2 Defining Scale of Combustion

Three premix burners were developed and tested in the present work. The three types of burners differ from each other based on the diameter of the combustion chamber while the length has been kept same. The diameters of combustion chamber are 20mm, 26mm and 36mm while the length is 30 mm. The burner is designed to operate with propane as fuel at 150ml/min of flow rate which corresponds to a burner thermal heat output of 250W. The following discussion will involve an attempt to define the scale of the burner based on the previous work done by various authors in small scale combustion.

Table 2.1: Specifications of some small scale combustion systems

Author(s)	Scale	Mode of combustion	Mode of Power Generation	Combustion chamber dimensions	Q (W)	P (W)
Kania and Dreizler	Micro	Catalytic	Thermoelectric	4 mm dia, 5 mm-25 mm length	50	2.16
Norton et al.	Micro	Catalytic	Thermoelectric	10 mm wide and 60 mm long	150	0.25
US Government - Patent US 6613972B2	Micro	Catalytic	Thermoelectric	1 mm characteristic length	-	-
Li et al.	Micro	Non-catalytic	Thermophotov-oltaics	-	-	0.7-0.70
Wu et al.	Micro /Meso	Non-catalytic	-	2.38, 3.18, 3.97, 4.76 and 5.16 mm dia	25-170	-
Scarpa et al.	Meso	Catalytic	-	10.6 mm x 6.6 mm cross section, 100 mm long		-
Belmont el at.	Meso	Non-catalytic	-	4 mm channel height, 173 mm long	75	-
Kariuki and Balachandran	Micro	Non-catalytic	-	3 mm wide, 27 mm long and 1 mm high 5 channels	25-250	-

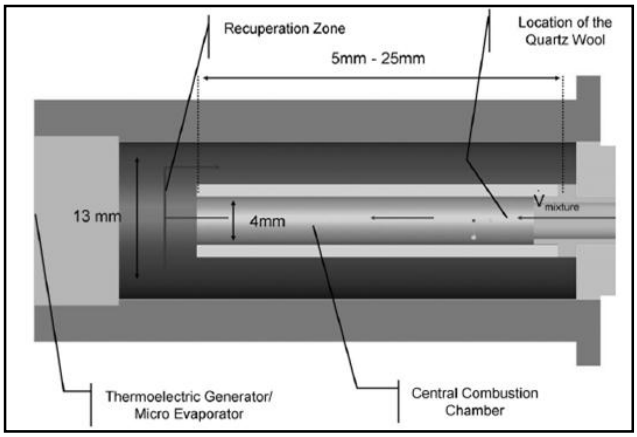

Figure 2.2

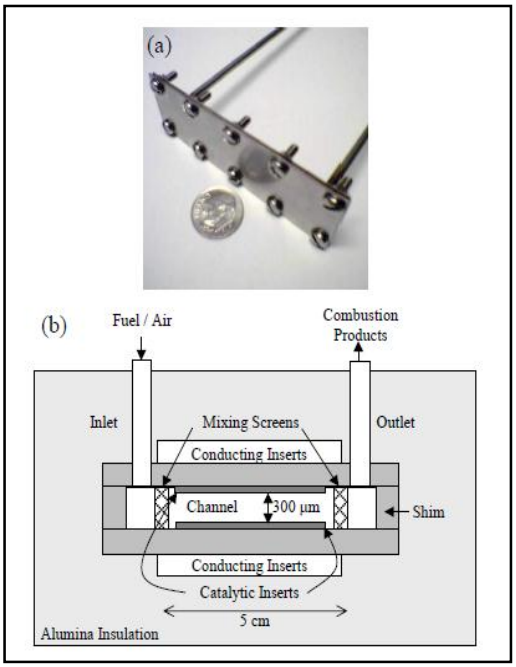

Figure 2.3

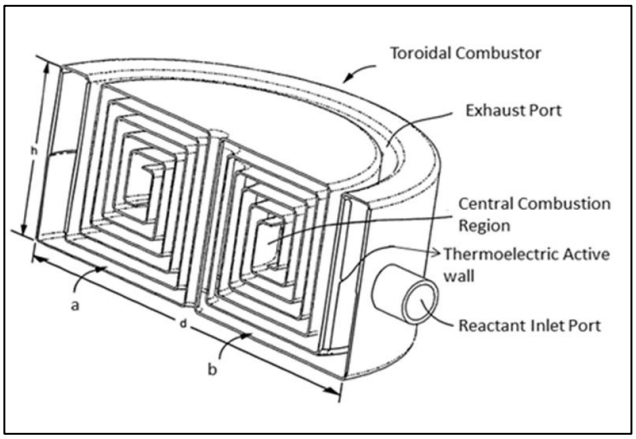

Figure 2.4

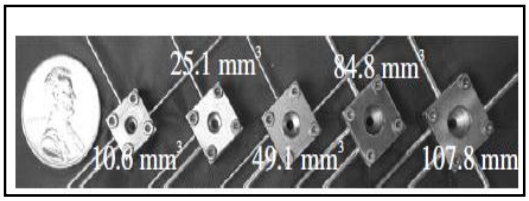

Figure 2.5

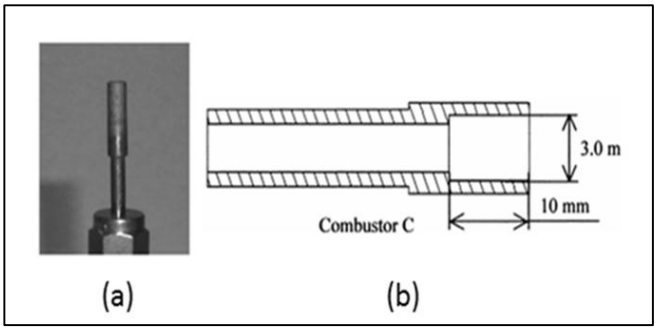

Figure 2.6

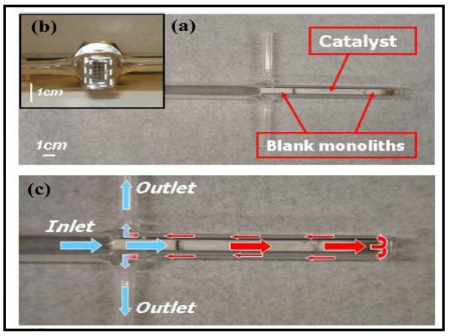

Figure 2.7

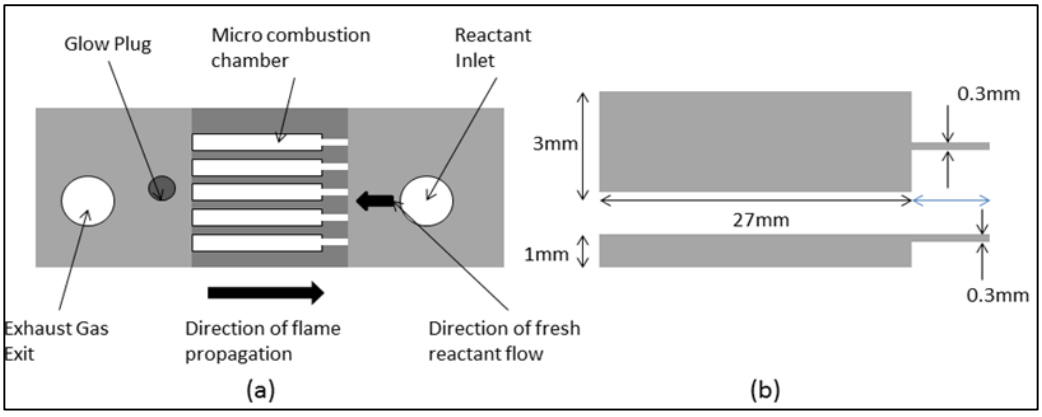

Figure 2.6

Various small scale burners have been developed and tested all around the world in the past decade. Based on the literature review carried out in this research work, a clear classification of the scale of combustion has not been found. Table 2.1 shows a list of various small scale burners developed and their size, scale as the authors claimed, mode of combustion, mode of power generation, heat input and power generation. Based on the information given in table, it is clearly evident that different authors have different opinion on classifying burners as micro and meso burners. Kariuki and Balachandran [57] developed a burner having combustion chamber made up of 5 channels each having dimensions as 3 mm wide, 27 mm long and 1mm high. The burner was operated at a thermal output of 25-250 W and has been classified as micro combustors. Norton et al. [78] developed and tested a catalytic burner having a heat output of 150 W and termed it as 'micro'. Similar examples of combustors classified under micro-scale are the burners developed by Kania and Dreizler [59] (burner rating 50 W), US government [60] and Li et al [34]. In the work of Wu et al. [61], a clear differentiation among micro and meso-scales has not been shown and their heat outputs are between 25-170 W. Hence, based on the operating range or burner heat output, the burners developed and tested in the present work can be classified as micro-scale combustors as their heat output range is 250 W which is similar to the above discussed micro combustors.

However, a comparison based on the size of combustion chamber shows that the combustion chamber in the burners of the present study have comparatively bigger size. The micro burner developed by US government has a characteristic length of just 1 mm, also the combustion chamber in Kania and Dreizler burner is 25mm long and the diameter is just 4 mm and the micro combustors of Kariuki and Balachandran's work has combustion chamber which is just 3 mm wide, 27 mm long and 1 mm high. It is evident that the size of all these micro burners is substantially smaller than the burners of the present work which consists of combustion chamber having diameter 20 mm, 26 mm and

36 mm and length 30 mm. This suggests that classifying the burners of this study as micro may not be justified based on their large combustion chamber size.

It is worth noting here that Belmont et al. [62] developed a burner which was operated at a thermal power output of 75 W and they have classified it as a meso-scale burner.

Hence, it can be seen that the burners developed in this study does not exactly fall in either micro or meso-scales of combustion as according to operating parameters the burners are required to operate under micro-scale, while in terms of size they have to be big enough to be integrated with thermoelectric modules which are commercially available modules of fixed size.

2.4 Backward Facing Step

One of the most important challenges in designing a micro-combustor is to achieve an optimal balance between stable combustion and maximizing heat output. Micro combustors have high surface to volume ratio which increases heat losses causing unstable combustion due to quenching of the flame. Residence time is also small in micro combustors which lead to difficulties in sustaining combustion. Previous studies have suggested that the sudden expansion step was able to facilitate recirculation of the combustion mixture near the wall, thereby enhancing the mixing process of combustion around the rim of the tube (normal-scale) and ensure a complete and stable combustion [55][63][85]. Previous results implies that the micro-combustors with backward facing step are very effective for application to direct energy conversion where the wall heat flux/temperatures are the required as heat source, such as thermoelectric power generators, the present will focus on meso-combustors with backward facing step for the same application.

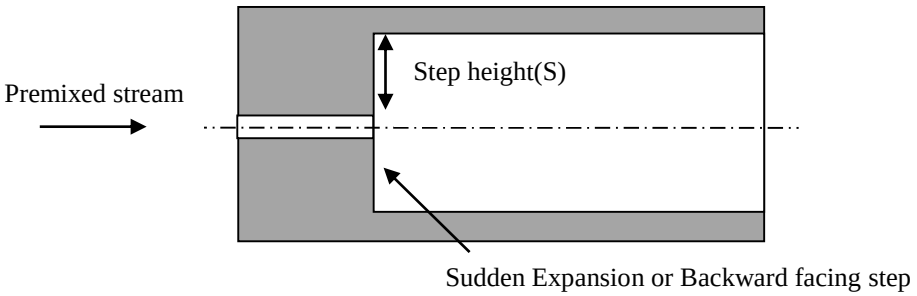

Figure 2.9: A premixed burner with backward facing step

Figure 2.9 shows a premixed burner with a backward facing step, also known as a sudden expansion step. The distance between the internal diameter of the burner and the diameter of the premix zone is termed as Step height (S).

2.4.1 Backward Facing Step and Wall Temperature

The effects of step height on the external wall temperature and the emissive power of a micro combustors having premixed laminar flame have been investigated by Li et al. [63]. Numerical simulation of a premixed hydrogen–air flame has been carried out in micro-combustors having different step heights. A comparison of results from numerical simulation and experiments on the micro combustors with different step heights has been conducted. The microcombustor, similar to the one shown in Figure 2.9, investigated in the study is made up of stainless steel with length 20 mm and wall thickness 1mm. A sudden expansion step is introduced at the inlet of the chamber for flame stabilisation and to facilitate recirculation of the combustion mixture near the wall which enhances the mixing and ensuring a complete and stable combustion. Three step heights are considered in the study – 1 mm, 2 mm and 3 mm.

The results from simulated and measured external wall temperatures were in agreement. Both experiment and simulation show that the external wall temperature increases with decreasing step height. The emissive power decreases with increasing step height. An increase in step height increases the external wall surface area, but it decreases drastically the external wall temperature of the microcombustor. As a result, the emissive power decreases.

Yang et al. [55] studied combustion in micro cylindrical combustors with and without a back backward facing step. The research basically involved comparison of three stainless steel micro combustor designs shown in Figure 2.10:

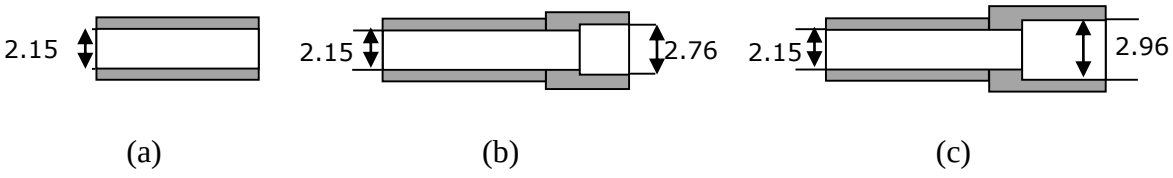

Figure 2.10: (a) Type 1 – Cylindrical tube without backward facing step, (b) Type 2 – Cylindrical tube with backward facing step and (c) Type 3 – Slightly bigger tube length after step and step height.

The major parameters measured in the experiments were wall temperature and the distribution of temperatures at the exit plane. The wall temperature is a major factor

reflecting the heat transported through the solid boundary. Compared to the total heat release during combustion, the heat transported becomes significantly large as the size of the combustor shrinks because of high surface to volume ratio. The exhaust temperature provides an indication of whether combustion is complete.

The experimental studies indicated that stable combustion can be achieved in a small combustor with a diameter of 2–3 mm under certain ranges of inlet flow velocity and equivalence ratios. As suggested by Yang et al., the micro-combustors are mostly constrained by inadequate residence time of the combustion mixture. For the type 1 micro-combustor, the combustion took place either outside the tube when flow speed was greater than 8 m/s or flame extinguished when the flow speed fell below 1.3 m/s. The experimental results of the micro-combustor without backward facing step indicate that stable condition can only be achieved under a narrow flammability range. Major problems associated with this design are the difficult to control the position of the flame and unstable combustion at low fuel/air ratio at high flow rates. To address these problems, a backward facing step prior to the combustion section of the tube was investigated and it was observed that the position of peak temperature on the wall moves slightly from the location near the exit towards the backward facing step in the Type-2 micro-combustor. The temperature along the wall is almost uniform and the variation is less than 5%. The backward facing step through flow separation and reattachment, largely enhance the mixing process and prolong the residence time of the fuel mixture, which results in a higher temperature near the wall of the combustor. The flammability range for stable combustion has been significantly extended especially at high flow rates. The temperatures near the wall are higher than the temperatures in the central region. This implies that the micro-combustor with the proposed design of backward facing step is very effective for application to direct energy conversion where the wall heat flux/temperatures are the required output of the power system [55].

An experimental study of premixed combustion in cylindrical micro combustor was performed by Li et al. [90] at the National University of Singapore. A micro Thermo-photo-voltaic (TPV) system was developed with main components: micro combustor, an emitter, a dielectric filter and a photo voltaic cell array. The objective of study was to systematically investigate the effects of combustor length, combustor diameter, inlet velocity and fuel–air equivalence ratio on the wall temperature and the radiation power through the combustor wall by measuring wall temperature profiles of the micro combustors. The micro combustors used in the experiments were made of stainless steel 316 with a backward-facing step for flame stabilisation. The study basically involves

experiments on burners with diameter 2 mm and 3 mm respectively. Acoustic emissions were observed in the case of smaller combustors (d=2 mm), the main reasons leading to acoustic emission include flow instabilities, flame-flow/flame-structure interactions, heat loss induced high-frequency extinction-re ignition and mass transfer (diffusion of species) limitations. A stable flame was obtained after a while after ignition at the exit in the d = 3 mm micro combustors. Results showed a larger mean wall temperature with a small combustor diameter which keeps on rising with increasing inlet flow velocity. The results further showed that a successful ignition depends on the combustor length, fuel–air equivalence ratio, flow velocity and the combustor diameter. The effects of combustor length are more prominent for the mixtures with fuel equivalence ratio 0.8 and 1.0. Results further showed that the zone of stable flame without noise decreases with increase in combustor length because of large surface to volume ratio for longer combustors which causes more thermal losses. So it was concluded that as the combustor length increases, the range for successful ignition becomes smaller. Results showed a significant increase in wall temperature when the equivalence ratio increased from 0.6 to 0.8 for both d = 2 mm and d = 3 mm burner tube. The radiation heat flux through the combustor wall is very important in thermo- photovoltaic generators as these utilises the thermal radiation from the combustor wall for power generation. Experimental results showed that the smaller combustor represent higher emitter efficiency than the larger ones under the same flow conditions, which is attributed to the fact that smaller combustors experience higher heat loss through the combustor wall. Further, it was observed that a longer burner gives higher emitter efficiency because of a larger surface area. The study also discussed about flame stabilisation with backward facing step which is an important aspect of the present research. A backward facing step was integrated in the design to promote flame stabilisation and determination of peak wall temperature which is an important aspect in small scale power generation devices employing thermal energy for energy conversion [85][89].

2.4.2 *Previous Studies on Flow Interactions at Backward Facing Step*

Altay et al. [64] explored the mechanism of flame vortex interactions in a combustion chamber having backward facing step, which is significant to large scale gas turbine combustors. They carried out a parametric study by varying the equivalence ratio, Reynolds Number, inlet temperature and the fuel composition to study the flame-vortex interaction driven combustion dynamics in an atmospheric backward facing step combustor.

Flame images of four operating modes were examined: unstable, high-frequency unstable, quasi-stable and stable operating. Each of the four operating modes corresponds to specific equivalence ratio, Reynolds number and fuel inlet temperature. Experiments were conducted for the operating modes to determine the flame dynamics at different equivalence ratios, Reynolds number and fuel inlet temperature. Flame images corresponding to one cycle of the unstable mode taken at $\phi = 0.80$, Re = 8500, Tin = 300 K, without hydrogen enrichment were studied (Figure 2.11). The flame dynamics is described as follows: a wake vortex is formed in the recirculation zone downstream of the step which is represented as step 1 in the figure. The velocity is rising at this moment and the acceleration and pressure are at maximum. The vortex convects downstream with increase in the velocity at the step, while moving toward the upper wall of the combustor. As a result, a packet of unburned reactants forms between the growing vortex and the flame of the previous cycle (2, 3). In addition, the heat release rate is decreasing following the end of the intense burning from the previous cycle. Between instants 2 and 3, heat release rate reaches its minimum, and the velocity is near its maximum value.

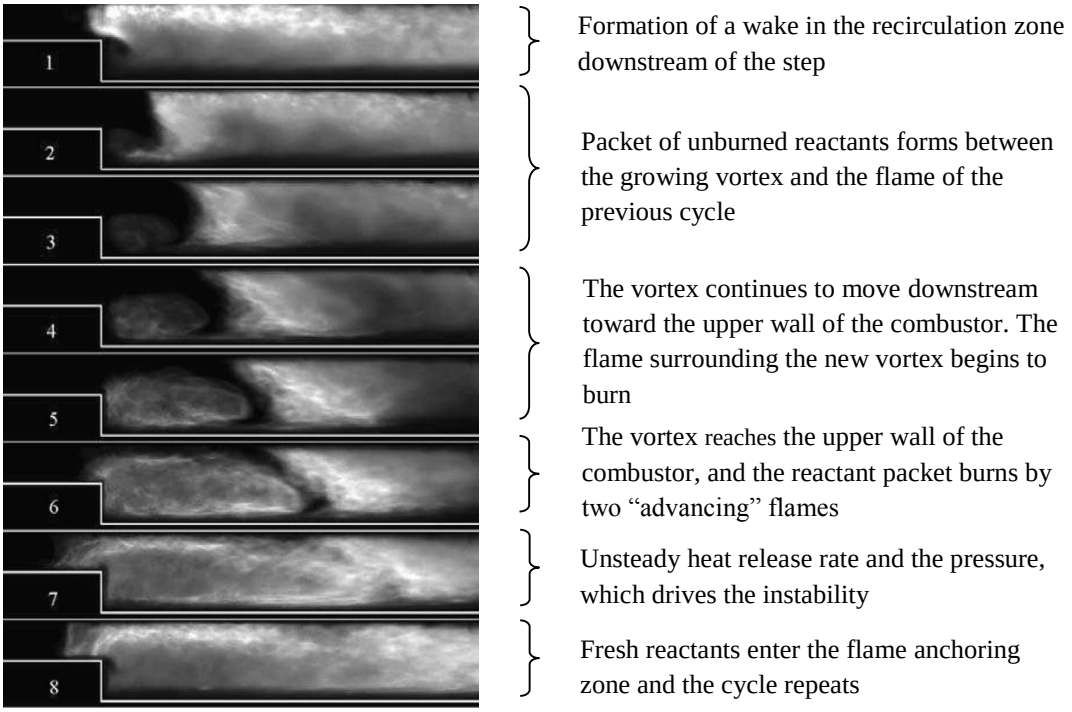

Figure 2.11: Flame Images at $\phi = 0.80$, Re = 8500 *T*in = 300 K, without hydrogen enrichment [64]

As the velocity drops from its maximum value, the vortex continues to move downstream toward the upper wall of the combustor. The heat release rate starts to rise as the reactant packet sandwiched between the flame from the earlier cycle and the flame surrounding the new vortex begins to burn (4–6). As the velocity reaches its minimum value between

images 6 and 7, the vortex reaches the upper wall of the combustor, and the reactant packet burns by two “advancing” flames on both sides causing intense burning. As a result, the heat release rate reaches its maximum near the moment of maximum pressure, resulting in the positive feedback between the unsteady heat release rate and the pressure, which drives the instability (7). The flame moving upstream of the step indicates very small or negative velocity at the step (6, 7). Next, as the velocity starts to rise again, the heat release rate starts to drop, fresh reactants enter the flame anchoring zone and the cycle repeats.

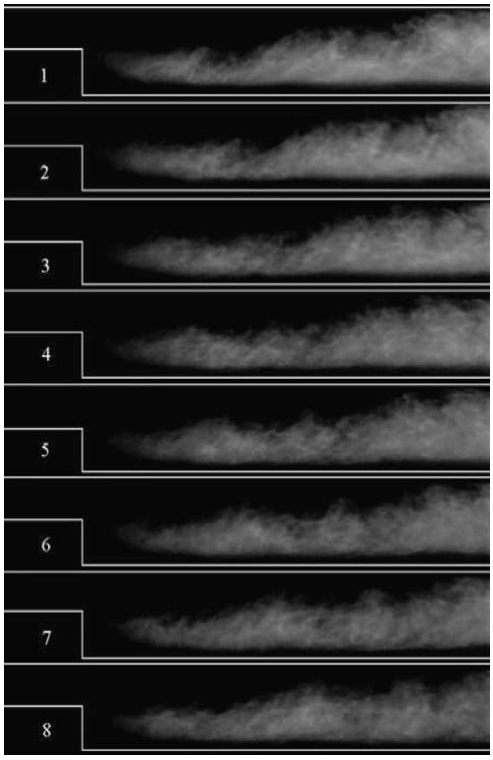

Figure 2.12: Flame Images at ϕ= 0.57, Re = 6500, Tin = 300 K, with 50% by volume hydrogen enrichment [64]

The flame images corresponding to the stable mode observed at ϕ = 0.57, Re = 6500, *T*in = 300 K, with 50% by volume hydrogen enrichment are shown in Figure 2.12. It is observed that in the stable operating mode, there is no coupling between the heat release rate and pressure. The heat release rate is steady, and the pressure oscillates at very small amplitude and high frequency, which corresponds to the vortex shedding frequency [64].

Roy et al. [68] performed a numerical analysis of the turbulent fluid flow through an axi-symmetric sudden expansion passage. The focus of their research is the effect of Reynolds number and expansion ratios on the size and strength of the recirculation bubble. As shown on the Figure 2.13 (a), they observed that the reattachment point moves towards

upstream side of the passage with the increase in the axial inlet velocity. This shifting of the reattachment point with the increase in inlet velocity or the Reynolds number implies the reduction of the size of the recirculation bubble.

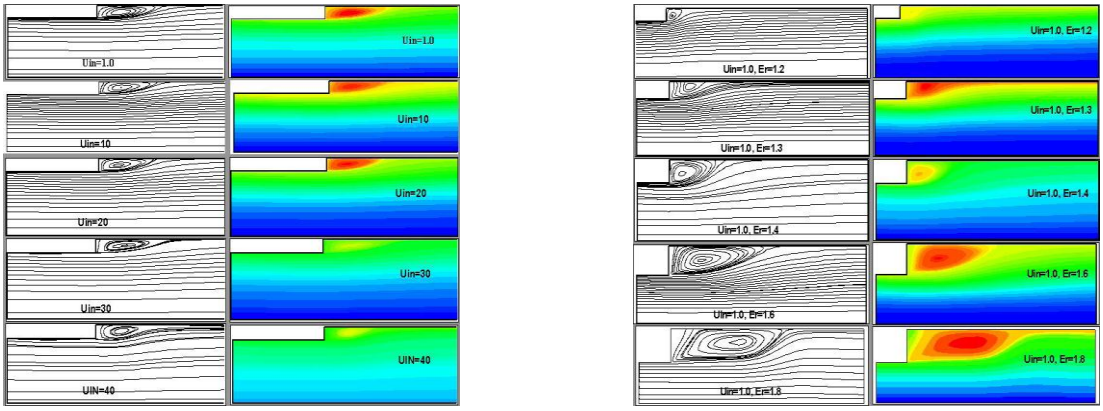

(a) (b)

Figure 2.13: (a) Reattachment point moving towards upstream side of the passage with the increase in the axial inlet velocity; (b) Showing increase in width of recirculation zone with increase in expansion ratio [68]

This is physically realistic as the average inlet flow velocity is increasing and this causes decrease in the generation of adverse pressure gradient which is responsible for generation of recirculation zone. Though the inlet flow is not able to eliminate the recirculation zone completely and the effect of the recirculation zone in the downstream flow is still present. Thus they concluded in their study that for the same expansion ratio the size and strength of the recirculation region decreases with the increase in Reynolds number. Thus the increase in Reynolds number provides the stabilizing effect on the flow field of the downstream. The numerical simulation further suggested that the recirculation region increases with the increase in expansion ratio as shown in the Figure 2.13 (b). It was observed that the maximum width of the recirculation zone generated for different cases by varying the expansion ratio is roughly equal to the lateral expansion of the expanded portion of the passage. It was shown that turbulent energy is generated from the region where the geometry of the passage changes. It is maximum at the sudden expansion or recirculation region which is followed by decrease in the turbulent energy as there exist the laminar sub layer. The sudden expansion passage is a typical geometry where the generation of turbulent energy takes place due to the sudden change of geometrical conditions causing the instability which ultimately culminate in turbulence.

Abu-Mulaweh et al. [69] performed experiments to study the effect of backward facing step heights on turbulent mixed convection flow along a vertical flat plate. The step

geometry consisted of an adiabatic backward-facing step, an upstream wall and a downstream wall. The results showed that the turbulence intensity of the streamwise and transverse velocity fluctuations and the intensity of temperature fluctuations downstream of the step increase as the step height increases. It was also found that both the reattachment length and the heat transfer rate from the downstream heated wall increase with increasing step height.

Ko and Sung [70] discussed the importance of flame stabilisation in a premixed burner with a sudden expansion step as the flame can be easily extinguished during turbulent mixing and combustion reactions.

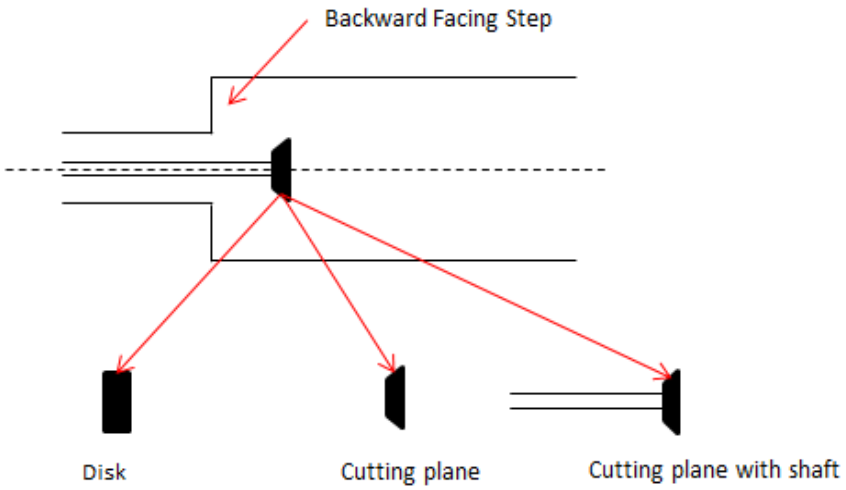

Figure 2.14: Sudden expansion premix burner with three types of flame holders explored by Ko and Sung [70]

The premix burner having a backward facing step or sudden expansion step is shown in the Figure 2.14 with three different types of flame holders located after the step. A large-eddy simulation for turbulent flow inside the combustion device shown in the figure above was carried out with three different types of flame holders: a disc type, a cutting plane type, and a cutting plane with shaft type. The function of the flame holder as discussed in the study is to promote turbulent mixing and to accommodate flame stability in the combustion chamber. Figure 2.14 shows a schematic diagram of the flame holder and the combustion device.

The results for the axial turbulent intensity for three flame holders showed that two peaks of turbulent intensities exist – the inner peak value is larger than the outer peak because

of the strong-recirculation region behind the flame holder. The peak value was found to be largest in the case of the 'disc'. These peaks develop spatially downward and are then attenuated.

The study further reveals that the recirculation region behind the flame holder is affected by the shape of the flame holder. The size of the recirculation region for the 'disc' was found to be bigger than the 'cutting plane' which was attributed to the impinging area of the 'cutting plane' is smaller than that of the 'disc'. In the case of the 'cutting edge with shaft', the boundary layer develops along the shaft surface and a small recirculation region is formed in front of the corner part between the shaft and the flame holder. The recirculation region is seen to be the smallest for this type of flame holder. Axisymmetric vortex rings were generated on the inside and outside of the annular jet around the flame holder which were deformed downstream in a round jet. The vortex rings were observed to be widely spread and quickly deformed in the case of disc whereas the vortex ring had small size and its shape was maintained at the end of the recirculation region.

2.5 Addition of Secondary Air as a Flame Stabilisation Mechanism

Atlay et al. [66] experimentally investigated the effect of air injection near the flame anchoring zone in reducing thermoacoustic instabilities which were driven by flame–vortex interactions.

They performed experiments on a 33 kW propane burner employed with a backward facing step by varying the equivalence ratio and the inlet temperature. Two modes of operations were studied, in the first mode the air was injected cross-stream through a row of micro-diameter holes just upstream of the step while in the second mode the air was injected stream wise through micro-diameter holes. They found that flame flashback occurs at higher equivalence ratio of the reactant mixture. However, flame stability was improved when air was injected in the cross-stream direction with the flame anchoring slightly upstream of the step and thus eliminating the instability. On the other hand, the addition of air steam-wise only resulted in a stable flame at optimum secondary air flow rate [66].

In a study by Ghoniem et al. [65] on lean premixed combustion in a backward facing step combustor, a high speed air jet was injected from a small slot cross-stream into the main stream upstream of the step. The results showed that when the momentum ratio of jet to main flow was below unity, complete blowout occurred as the jet diluted the mixture. However when the ratio was above unity the pressure oscillations were eliminated and the flame became stable. They found through flow visualisation and chemiluminescence

that injection of a strong jet produces a more compact flame which is less dependent to the wake vortex and stabilises closer to the step. They also performed experiments by injecting hydrogen instead of air and found similar results with flame stability improved upon injection of hydrogen. The results also showed that the injection of air near the step reduced NOx in the exhaust whereas the injection of hydrogen showed an increase in NOx concentration due to higher combustion temperature [65].

Flame stability by injecting an air jet has been studied by Uhm and Acharya [67] where they found that high momentum air jet helps in reducing pressure oscillations and improves flame stability. They also suggested that only a small amount of air jet is required to be effective. The control air-jet was found to have an effect on the droplet and the heat release distributions to positively influence the combustion dynamics. Their results showed that 90% reduction in the peak pressure oscillation amplitude can be achieved with air jet injection [67].

2.6 Thermoelectric Power Generation Using Combustion

Thermal energy is generated in many industrial as well as natural processes and a large amount of it is wasted. Some of the examples of such processes include heat waste from automobile exhausts, industrial processes such as involved in steel plants, geothermal from undergrounds and temperature difference between the surface and bottom of the oceans etc. Thermoelectric devices have the potential to convert the heat wasted in the above mentioned processes into electricity [95-99]. As discussed in the introduction chapter, the present research is concerned with development of a CO_2 Generator device for insect catching apparatus which consists of a premixed burner to produce the required carbon dioxide by burning a hydrocarbon fuel. The thermal energy generated during the combustion can be harvested using thermoelectric devices which convert it into electricity required to run the insect apparatus. Thus, making the carbon dioxide generator device capable of producing its own electricity in remote areas where external electricity is not available. In this way the device not only performs its primary function which is to burn a hydrocarbon fuel to generate carbon dioxide, but it also converts the heat of combustion into electricity using thermoelectric devices which would have been wasted otherwise. This section will discuss principles of Thermoelectrics followed by an introduction to thermoelectric power generator and its efficiencies, a discussion about typical configurations of thermoelectric modules and heat exchangers, thermoelectric figure of merit and finally various thermoelectric generators incorporating combustion will be explored [95-99].

2.6.1 Principles of Thermoelectric

There are three types of thermoelectric effects and based on these effects, thermoelectric devices can be developed and employed for power generation, refrigeration and temperature sensing [96].

The Seebeck Effect

The Seebeck effect states that when two dissimilar metals or semiconductors are joined together, a voltage V is produced when a temperature difference is applied across the two junctions [71]. Figure 2.15 shows two dissimilar materials *a* and *b* joined together at the ends, when a heat source is applied to one junction to raise the temperature to T_H and a temperature T_C is maintained at the other junction such that $T_H > T_C$, the Seebeck voltage produced is:

$$V = \propto_{ab} \Delta T \qquad \text{Equation 2.1}$$

where ΔT= (T_H-T_C) is the temperature difference across the two junctions and α_{ab} is referred to as Seebeck coefficient.

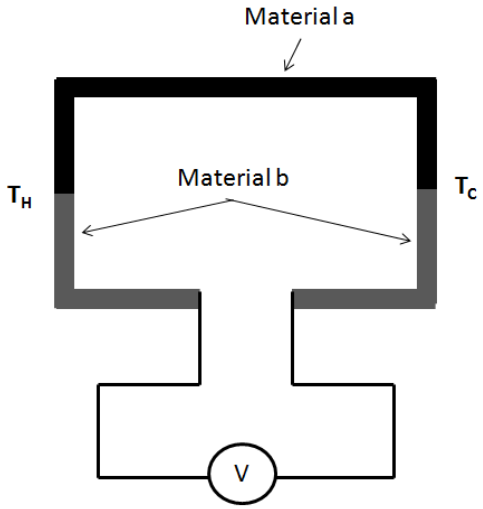

Figure 2.15: Seebeck effect

The Seebeck coefficient α_{ab} remains approximately constant over a certain range of temperature for most of the metals and alloys. It can be determined by:

$$\alpha_{ab} \cong \frac{V}{\Delta T}$$

Seebeck coefficient depends upon the properties of material *a* and *b* and hence it is called as relative Seebeck coefficient. The unit of $\propto_{ab}$ is $V.K^{-1}$. When a thermoelectric device is operated under Seebeck effect, it is a generator which converts heat into electricity [72].

Peltier effect

Peltier effect is observed when a voltage is applied to the circuit instead of a temperature difference across the junction causing heat absorption at one junction and heat dissipation at the other due to thermal transport of electrons as a result of flow of current around the circuit. This will result in one junction getting cold and the other becoming hot. With the change in direction of the electric current the heat absorption and dissipation at the junction will be reversed too.

Figure 2.16 shows two dissimilar materials *a* and *b* joined together at the ends and a voltage V is applied to the circuit causing heat absorption at one end and heat dissipation

at the other. The amount of heat removed per unit time from one junction to the other is given by:

$$Q = \pi_{ab} I \qquad \text{Equation 2.2}$$

Where I is the electric current and π_{ab} is the Peltier coefficient.

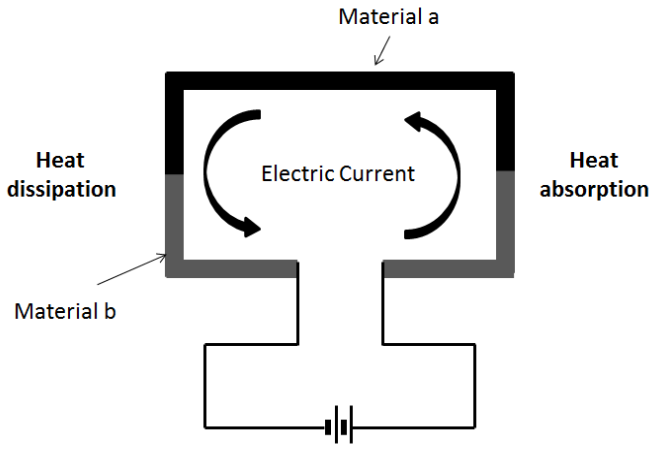

Figure 2.16: Peltier effect

Similar to Seebeck coefficient, Peltier coefficient is a relating quantity too. The unit of Peltier coefficient is $W.I^{-1}$. When a thermoelectric device is operating under Peltier mode, it is a refrigerator which pumps heat from one junction to another [72].

Thomson effect

Thomson effect involves heat dissipation or absorption along a single material when it is subjected to a temperature difference and electric current simultaneously. Figure 2.17 shows a single material being subjected to temperature difference, ΔT and current, I, the total heat absorption (or dissipation) according to Thomson effect is given by:

$$Q_T = \beta I \Delta T \qquad \text{Equation 2.3}$$

Where β is the Thomson effect and its unit is $W.I^{-1}.K^{-1}$.

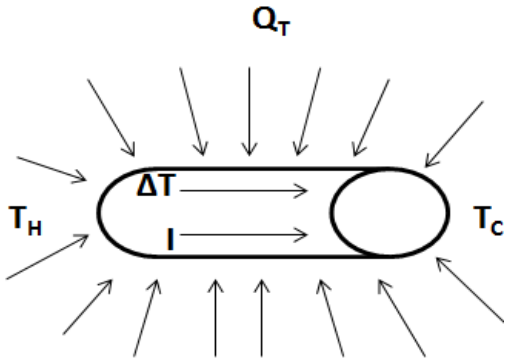

Figure 2.17: Thomson effect

It is known that no thermoelectric device has been developed to work under Thomson effect but it exists in other thermoelectric devices and in fact its effect is quite considerable when temperature difference across the device is large[71][72].

2.6.2 Thermoelectric Generator

A thermoelectric generator is a solid state energy converter which uses electrons as its working fluid. It is extremely reliable, environmental friendly and consists of no moving parts. It has been widely studied Heat recirculation can improve efficiency by 20 %. It basically consists of n-type and p-type semiconductors connected electrically in series by highly conducting metal stripes and sandwiched between thermally conducting but electrically insulating plates. Efficiency of module is measured as the ratio of power generated to heat absorbed at the hot end [73].

2.6.3 Module Efficiencies

Thermoelectric Module efficiencies can be expressed according to heat transfer to the module. When there is a uniform heat transfer along the length of a thermoelectric module, then its efficiency is give as:

$$\eta(T_h, T_c) = \frac{T_h - T_c}{T_h} \quad \frac{\{\sqrt{(1+ZT)}\}-1}{\{\sqrt{(1+ZT)}\}+\frac{T_c}{T_h}} \qquad \text{Equation 2.4}$$

When thermoelectric modules are used in applications where hot liquids or gases are used as heat sources, the temperature distribution along the module is not uniform and varies with position due to heat being extracted via thermoelectric elements, as shown in the Figure 2.18.

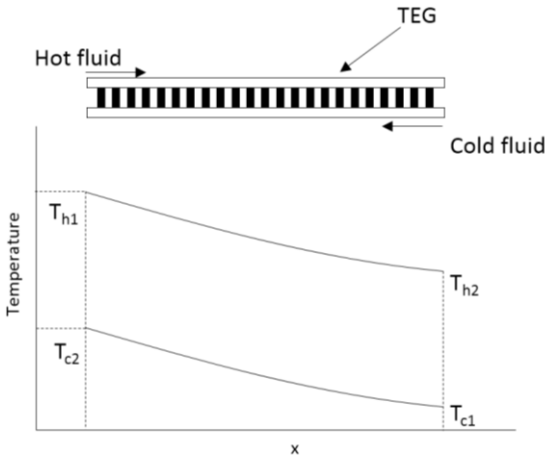

Figure 2.18: Temperature distribution on the hot and cold sides of a TEG along the heat flow direction

The Figure 2.18 shows the temperature distribution on the hot and cold surfaces of a TEG along the direction of heat flow. When heat transfer across a TEG module is non uniform, the efficiency is measured in terms of overall efficiency which is the ratio of total output power to the total heat extracted by the entire module:

$$\eta = \frac{-Mc \int \eta(Th,Tc) dT_h}{Mc(T_{h1} - T_{h2})} \qquad \text{Equation 2.5}$$

When the amount of heat that flows through a TEG is only a portion of the total available heat from a heat source, efficiency is given as:

$$\text{System heat transfer, } Q_s = Mc(T_h - T_c)$$

$$\eta = \frac{-Mc \int \eta(Th,Tc) dT_h}{Mc(T_h - T_c)} \qquad \text{Equation 2.6}$$

2.6.4 Typical Configurations

The configuration of a thermoelectric conversion system largely depends upon the type of heat source used. Rowe and Min [73] explains that the overall efficiency and system efficiency are directly related to the arrangement of heat source, thermoelectric module and heat exchangers which basically determines the temperature distribution and the amount of heat flowing through the TEG. Following are three important configurations explained by Rowe and Min in their work on conversion efficiency of thermoelectric combustion systems.

i) Maximum temperature difference without heat recirculation

This configuration is widely used when the heat source is 'waste heat' from combustion systems. The hot exhaust gases from combustors are made to flow through a heat exchanger which supplies a part of heat from gases to the hot side of thermoelectric module. The cold side of the module is attached to a heat sink which is assumed to be maintaining a constant temperature.

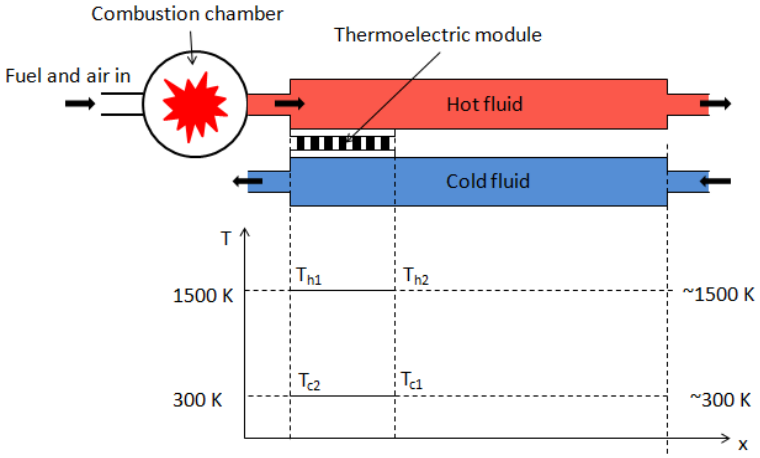

Figure 2.19: Configuration showing 'Maximum temperature difference without heat recirculation'

As shown in the Figure 2.19, there are separate hot and cold fluid streams flowing through the TEG module in this configuration. The overall efficiency of such a system is high but system efficiency will be low because only a small heat is extracted from the hot gases. This type of configuration is only useful where system efficiency is not a primary requirement.

ii) Maximum heat extraction without heat exchanger

In this configuration, more than one thermoelectric module is used in order to increase the heat extraction which results in increase in the system efficiency.

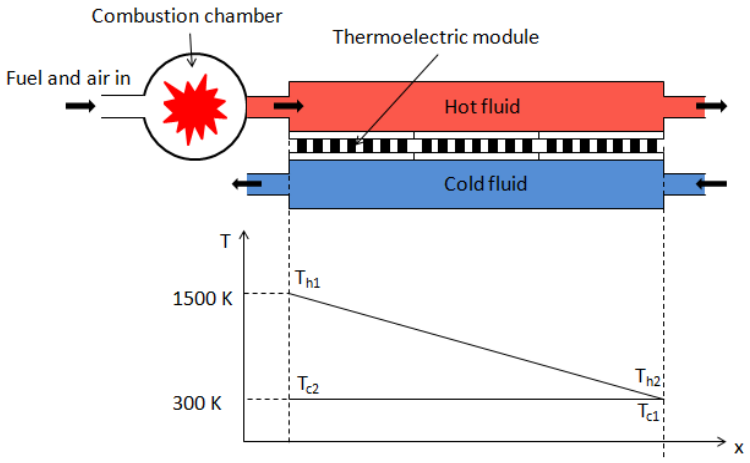

Figure 2.20: Configuration showing 'Maximum heat extraction without heat exchanger

It is seen that the temperature of the hot gases will decrease as heat is being extracted from the exhaust gases. The figure above shows the temperature distribution when the cold side temperature is kept at a constant value.

iii) Heat recirculation via thermoelectric modules

The cold side of a thermoelectric module rejects a large amount of heat as it has a very low efficiency. If this heat can be used back in the system then the system efficiency can be improved.

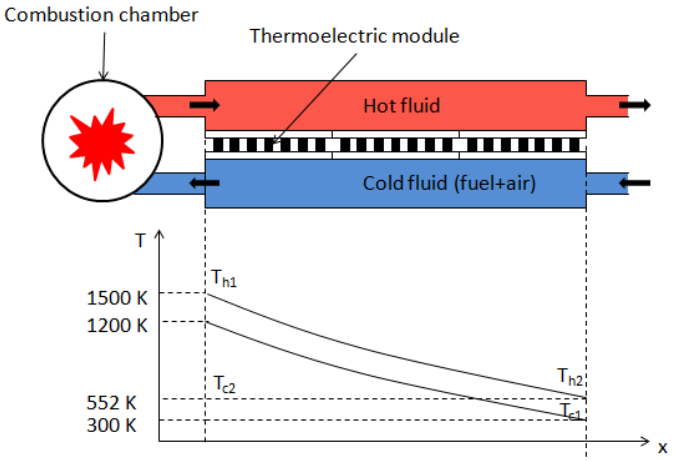

Figure 2.21: Configuration showing 'Heat recirculation via thermoelectric modules'

As shown in the Figure 2.21, heat rejected at the cold end is recycled to preheat the cold inlet gases that are fed to the combustor chamber. System efficiency increases with the increase in preheat temperature as more heat returning to combustion chamber. Overall

efficiency decreases with the increase in preheat temperature which is a result of low temperature difference across thermoelectric module.

2.6.5 Thermoelectric Figure of merit (ZT)

Figure of merit is a dimensionless figure of merit which evaluates the performance of a thermoelectric material both in cooling (the Peltier effect) and in generation (the Seebeck effect). Figure of merit is denoted by ZT. Where $Z = \alpha^2/(\rho\lambda)$, where α is the Seebeck coefficient, ρ the electrical resistivity and λ the thermal conductivity and T is the absolute temperature. A high figure of merit is desired as the conversional efficiency of thermoelectric devices depends upon it.

A paper has been presented by Rowe and Min [74] which presents an accurate, fast and simple method of evaluating figure of merit. The main feature of this method is the simplicity of instruments used to measure ZT.

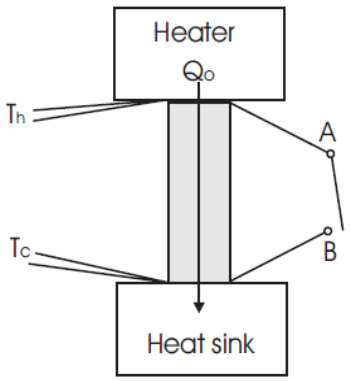

Figure 2.22: Arrangement for measurement of ZT [74]

The paper presents a relationship between temperature difference when the circuit is open and when short circuited. Figure of merit can be obtained using the following formula:

$$ZT = \left(\frac{dT_o}{dT_s}\right) - 1 \qquad \text{Equation 2.7}$$

The difference in temperature between the hot and cold ends of a specimen, dT_o, is obtained when terminals are open and dT_s is obtained when A and B are short-circuited.

Another research has been done by Min et al. [75] in their paper "Thermoelectric figure of merit under large temperature difference". This paper presents an important aspect which states that figure of merit keeps on decreasing with an increase in temperature

difference. This aspect has significance in the present research as the thermoelectric configuration employed in the present study is aimed at achieving large temperature difference to obtain high electrical output but as per the findings of Min et al. in their above mentioned paper, higher temperature difference should lower the conversion efficiency which will be a concern to be addressed due to the application of the system.

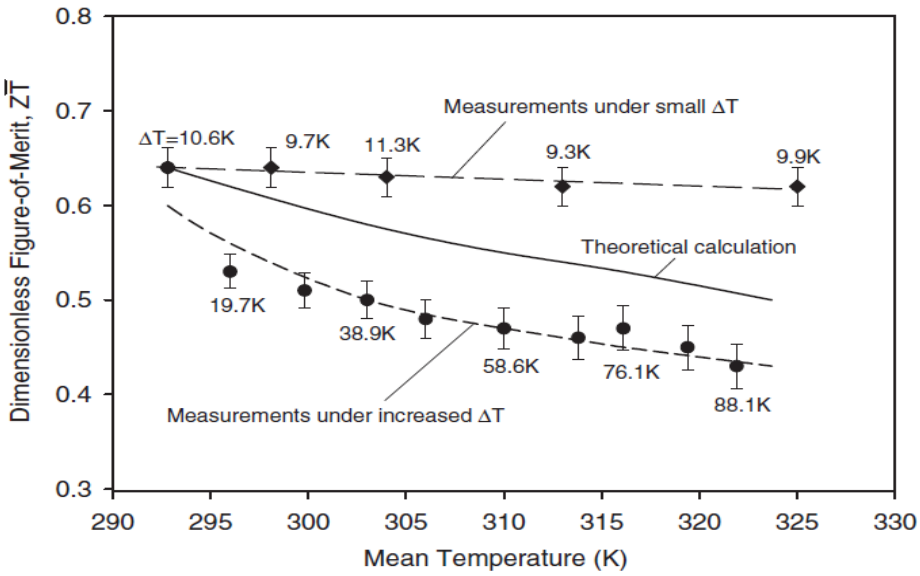

Figure 2.23: Graph showing ZT at different mean temperatures [75]

From the above figure, it is evident that the figure of merit decreases with an increase in temperature difference. For a given mean temperature, the ZT value obtained under a large temperature difference is smaller than that obtained under a small temperature difference.

The results suggest that the Thomson effect is likely to be one of the main phenomena responsible for the observed trend of reduction in figure of merit with temperature difference.

Two configurations have been discussed to overcome this issue:

- Segment Configuration: In this configuration two or three pieces of different thermoelectric materials with different operating temperatures but similar ZT are joined together to form a ‘segmented thermo element.
- Cascade configuration: In this configuration thermo elements for different operating temperatures are arranged on different stages, which are separated by electrically insulating but thermally conducting ceramic plates. The overall temperature difference across a module is the sum of the temperature differences across each stage in the cascade configuration. Currently, the segmented configuration is considered desirable

because of its fewer interfaces, which decrease the thermoelectric performance. However, the paper concluded that that the segmented configuration may exhibit a much large ZT reduction than the cascade configuration due to the thermo elements operating under a very large temperature difference. Although the cascade configuration may exhibit a significant interface problem, the accompanying reduction in ZT is less considerable. As anticipated, the design of an efficient thermoelectric converter will be a compromise between its ZT reduction and interface deterioration

2.6.6 Previous Work on Combustion System with Thermoelectric Generators

A study of previous work on combustion systems integrated with thermoelectric for power generation was carried out in this section. Various research papers and patent documents have been investigated to understand the interaction between the two fields of science - combustion and thermoelectric. A lot of theoretical and experimental work related to the topic has been done previously which concentrates on integration of these phenomena's at micro and meso level which would produce milli-volts/watts and consists of micro combustors and micro thermoelectric generator devices [84]. The present study will examine the interaction at slightly bigger level which will be termed as meso-scale in the thesis. These meso-scale thermoelectric generators will have the capability to generate around 3-5 W of electrical output while maintaining an efficient and stable combustion.

Kania and Dreizler [59] presented a paper concerned with the development of a micro energy converter which employs thermoelectric effect to generate electrical output. In the micro combustor designed by Kania and Dreizler, methanol was used as a fuel, which was evaporated in a micro evaporator, mixed with air and combusted in a micro combustion chamber. The evaporator acts as heat sink which uses the evaporation enthalpy of the liquid fuel and the heat source is combustor. A thermoelectric generator was located at between the cold micro evaporator and combustion zone, which generates electric power. This design was aimed at high temperature difference, which is a primary requirement to generate high power output.

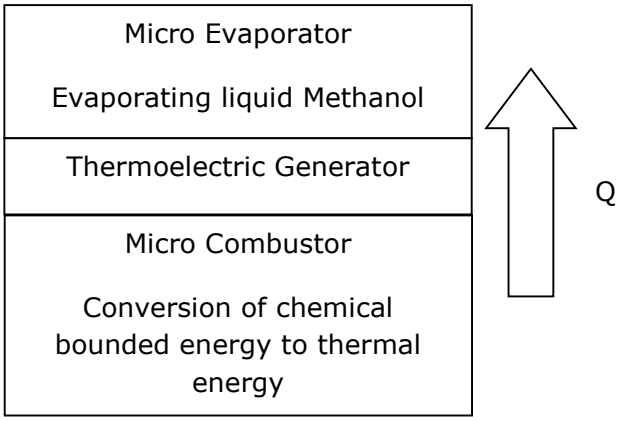

Figure 2.24: Flow of heat through the system in micro combustor integrated thermoelectric generator designed by Kania and Dreizler [59].

This configuration ensures high temperature difference across the thermoelectric generator and thus a high thermodynamic efficiency. The micro evaporator design consists of an evaporation and condensation cycle. A small amount of methanol was supplied to the combustion chamber for combustion. Condensation of evaporated methanol takes place in the micro condenser which was insulated from all other components in the system. In this way a large temperature difference was achieved with this configuration.

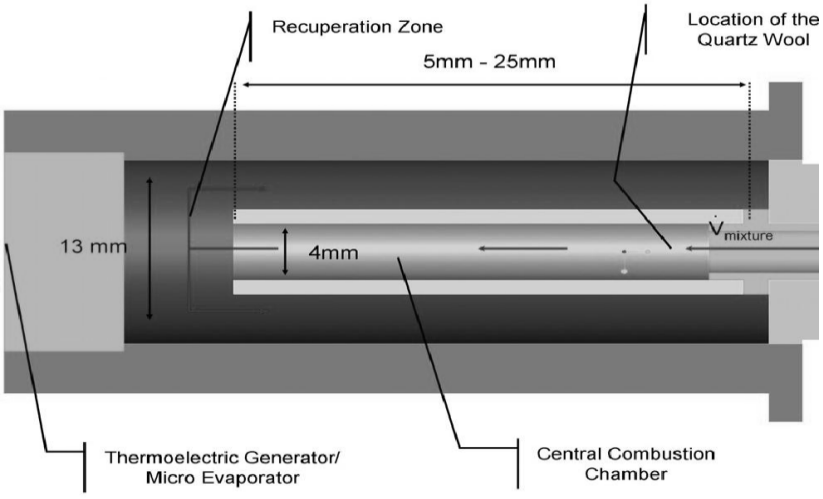

Figure 2.25: A drawing showing the design, components and dimensions of the micro combustor integrated thermoelectric generator [59]

The chamber was made up stainless steel sheet of 0.5 mm thickness and was cylindrical in shape as shown in the Figure 2.25. The central combustion zone was 4 mm-6 mm in diameter and 5 mm-25 mm long. It was surrounded by exhaust recuperation zone which had a diameter of 13 mm. Fuel inlet and exhaust was on the same side. The micro

combustor have high surface to volume ration which causes problems related to flame stabilisation. To overcome these problems, Quartz wool coated with a catalytic material was used to stabilise the combustion process, which was placed at the entrance of the chamber. The influence of combustion chamber dimensions, equivalence ratio and heat losses on the combustion and system efficiency were studied. The output efficiency of this design was claimed to be 4.3%.

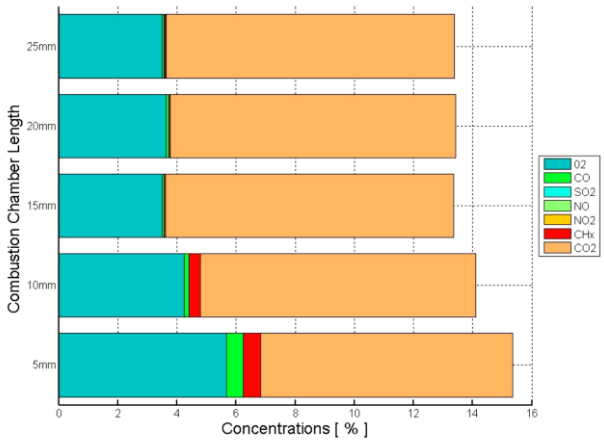

Figure 2.26: Graph showing concentrations of various compounds at different combustion chamber lengths [59]

The Figure 2.26 shows combustion products obtained at different central combustion chamber lengths. High CH_4 concentration shows that the combustion was not complete for 5 mm and 10 mm lengths. The combustion seemed to be stable for 15 mm and longer combustion chambers. The face temperature of the evaporator was important as it was the source of heat for thermoelectric generator and hence system efficiency was largely dependent on it. Higher temperatures were obtained using 15mm or longer combustion chamber lengths. The 15 mm combustion chamber, being small and stable, was investigated at different equivalence ratios as shown in Figure 2.27. The exhaust analysis did not show any CH_4 for any of the equivalence ratios while CO was observed to be high for equivalence ratio 1.0 and 1.1. Equivalence ratio 0.2 was concluded to be optimum for 15mm long combustion chamber.

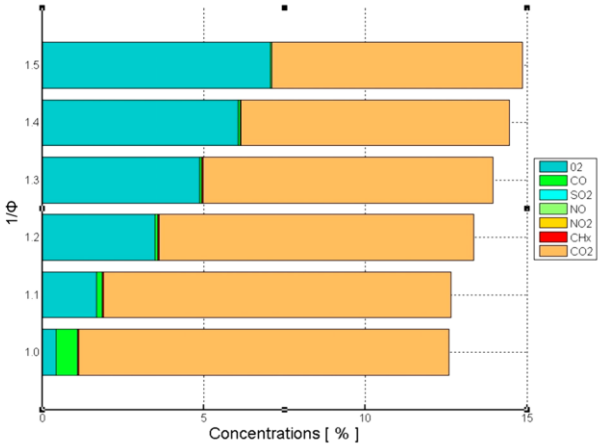

Figure 2.27: Concentration of products of combustion at different equivalence ratios [59]

The thermoelectric generator efficiency of 5.4% and system efficiency of 4.3% was suggested to be realistic with this design operating at 190^{o}C of temperature difference and figure of merit 0.8 [59].

Norton et al. [78] fabricated and characterised a catalytic micro combustor utilizing hydrocarbon fuels with a thermal efficiency of 1%. The combustion chamber consisted of stainless steel gasket sandwiched between two thicker stainless steel plates as shown in the Figure 2.28.

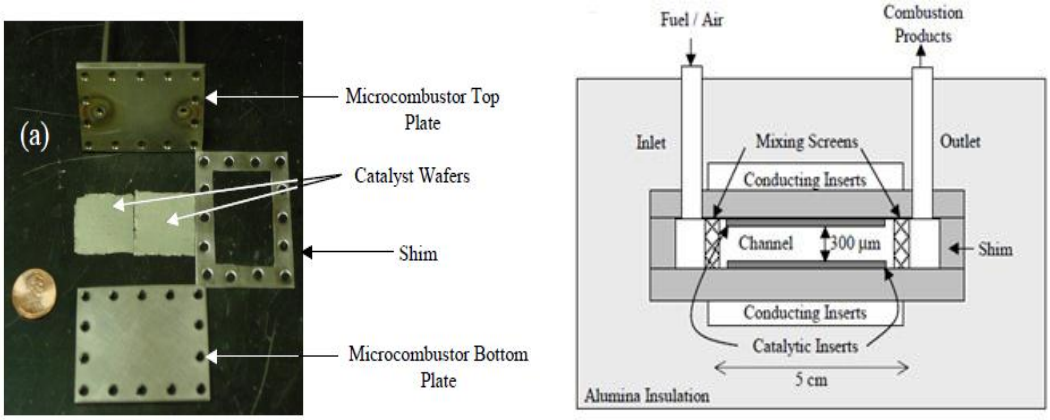

Figure 2.28: (a) A photograph of various components (b) Drawing/Schematic of the microcombustor with dimensions of the combustion chamber [78]

The study was performed on two sets of micro combustors both of same design but one slightly bigger in size than the other. The combustion chamber consists of a thin stainless steel gasket of thickness 500 µm packed in between two thicker stainless steel plates. Inlet and outlet tubes were made up of stainless steel and were welded to the top plate at

opposite ends of the combustion zone. Fine metal screens were placed at the entrance and exit of the combustion zone to act as static mixers, promoting uniform flow over the entire length of the catalyst, and preventing "jetting" of the reactants. Catalyst was deposited on thin alumina inserts, which were separated in the combustion chamber by 1 mm wide alumina shims to create a total channel height of 300 μm. Outer walls of the burner had conducting wall inserts in order to vary the axial thermal conductivity of the combustion zone walls. The entire burner was enclosed in an insulating, 6.4 mm thick fibrous alumina jacket. For the small microcombustor, Copper and stainless steel wall inserts were tested. Experiments were also carried out by removing the inserts and leaving a static air gap between the combustor wall and the insulation material. For the large microcombustor, a 3.2 mm thick copper wall insert was used between the top plate of the microcombustor and the thermoelectric device.

Aluminium heat sink was used on the cold side of the thermoelectric generator. The experimental data showed that copper had the highest temperature uniformity, followed by stainless steel and air. It was evident from this that as the material conductivity increases, the temperature uniformity improves. The wall temperature decreases as the flow continues downstream. This basically showed that combustion occurred at the beginning of the catalytic zone, after that cooling occurred due to heat losses. Next, the maximum temperature against equivalence ratio for hydrogen and propane combustion was analysed. Stable combustion was observed at the leanest equivalent ratios with Hydrogen. Propane flame extinguished at equivalence ratio of 0.6. Also, it was also seen that at small equivalence ratio, Hydrogen showed complete conversion whereas propane showed complete conversion near the extinction limit, after that the combustion fell sharply. Another study was done to investigate the difference in maximum temperature and minimum temperatures measured within the catalytic zone of the burner. It was evident that walls with highly conductive insert, in this case copper, reduce the temperature differential for both the fuels. This temperature differential should be as small as possible to achieve high power output of a TEG module, the large microcombustor was integrated with thermoelectric generator and the maximum power output for propane was measured to be 0.4 W at a temperature difference of 123 ^{o}C. Copper inserts were used as they were found to be more favourable than stainless steel and air based on the findings mentioned above.

A thermoelectric power generator has been fabricated and tested at the Massachusetts Institute of Technology by Samuel et al. [76]. The generator was stable at temperature of

up to 500 ^{o}C, with thermopile voltages up to 7 V and device thermal efficiency up to 0.02%.

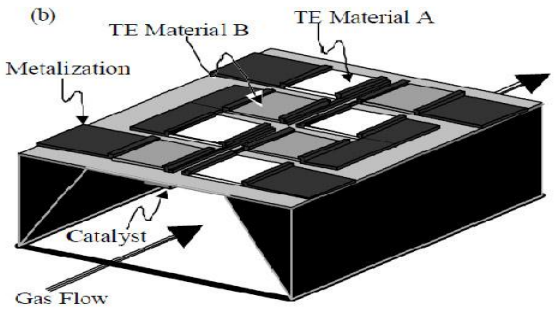

Figure 2.29: Thermoelectric power generator fabricated and tested in the MIT by Samuel et al. [76]

As shown in the Figure 2.29, the power generator basically consists of a channel etched through a silicon wafer capped by a thin membrane and the channel was sealed by an aluminium plate. The research explained the importance of catalyst location in the thermoelectric power generation system. Platinum as catalyst was used which was in line with hot end of the thermopile. A greater temperature difference was achieved by this alignment as it made sure that the reaction took place below the thermopile. The reaction products observed were mainly carbon dioxide and water.

Heat recycling in regenerative burner was examined by Weinberg et al. [86] in order to analyse the effect of preheating the incoming reactants on conversion efficiencies. Higher system efficiencies have been aimed in this theoretical approach by studying different arrangements of thermoelectric modules and heat exchangers.

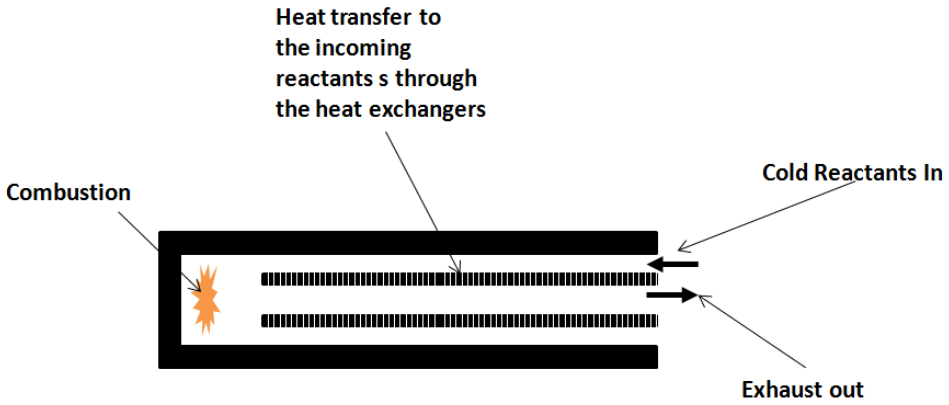

Figure 2.30: Heat recycling regenerative burner

One such configuration consisted of a coaxial assembly of a large number of flat annular 'washers' made up of alternating n and p-type thermoelectric materials connected in series shown in Figure 2.30. The washers were joined alternatively at the inner and outer peripheries; in the manner of compressed concertina bellows. The cold junction faces the incoming reactants; in this way the device works in the thermoelectric power generation mode as well as heats up the incoming reactants on the cold side. A comparison between the device operating with and without preheating of incoming reactants suggested that reaction zone temperature increases with heat recirculation and heat extraction. This is advantageous in terms of improvement in thermal efficiency as higher combustion zone temperature will allow complete combustion of fuel and hence, improve the combustion efficiency [86].

The research further compares three different configurations of thermoelectric converter, heat exchanger and insulation.

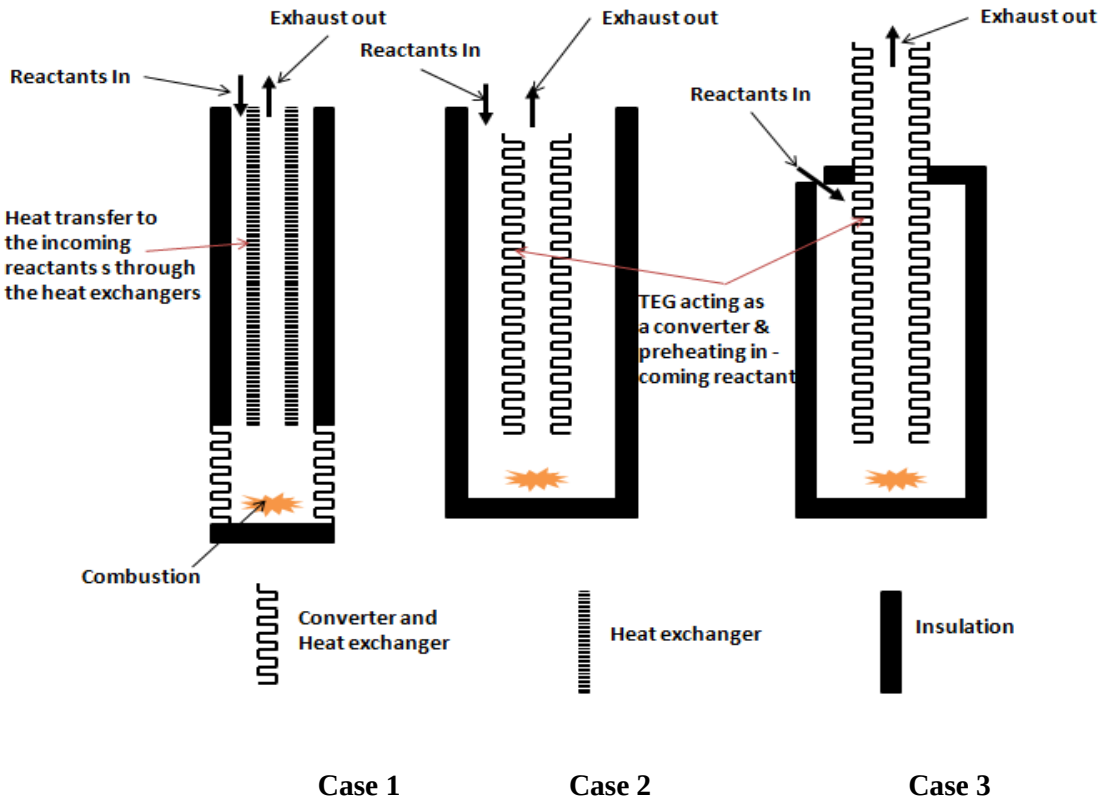

Figure 2.31: A demonstration of three configurations studied by Min et al. involving varying arrangement of heat sinks and TEGs

The three configurations are shown in the figure above which differs from each other based on the arrangement of thermoelectric converter and heat sinks. In Case 1, the cold

side is maintained at the ambient temperature, the hot side is the combustion chamber. The cold reactants enter from top, burns at the bottom and hot gases moves out with preheating the incoming fuel. In Case 2, thermoelectric material acts as converter as well as heat exchanger. The temperature of cold side is the temperature of incoming reactants and temperature of the hot side is the temperature of exhaust gases. The exhaust gases while flowing over the thermoelectric length, preheats the incoming fuel. The configuration in Case 3 is combination of case 1 and case 2. Thermoelectric material acts as both converter as well as heat exchanger, some part of it is extended outside the insulation. It should be noted that the outlet temperature of exhaust gases is equal to ambient temperature. The configuration in case 3 is found to be superior to the other two configurations. A large portion of heat losses are eliminated in case 3, as they occur from the cold side of the heat exchanger while in the second stage, they are essential part of the generating process [77][83].

A 'toroidal' counter-flow heat exchanger combustor integrated with thermoelectric generators was constructed and tested which relates to the theoretical work of Weinberg et al. discussed above. This work has been mentioned in the patent document, US 6,613,972 B2 [79]. The device was constructed by a three dimensional micro fabrication technique in a monolithic process. In this counter flow heat exchanger combustor, the inlet and exhaust channels were coiled around each other. The reactant and exhaust channels were separated by channel wall, one side of the channel wall was in contact with the reactant channel and the other side was in contact with the exhaust channel as shown in the Figure 2.32. This arrangement is also known as 'Swiss roll' combustors.

Table 2.2: The dimensions of 'toroidal' counter-flow heat exchanger combustor [79]

Outer diameter	Height	Chamber Size	Reactant channels
2-15 mm	1-6 mm	Less than 1 mm	100 micro m- 1 mm

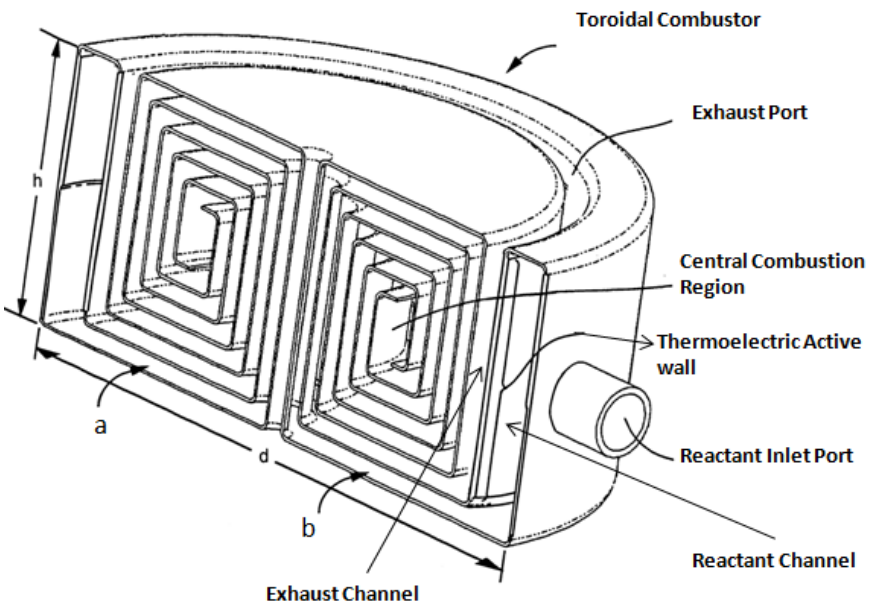

Figure 2.32: Cut away view of 'toroidal' combustor [79]

As shown in the Figure 2.32 fuel enters from the reactant inlet port, flows through reactant channel and burns in the central combustion zone. The burnt gas flow through the exhaust channel and leaves the heat exchanger from outlet port while preheating the incoming reactants.

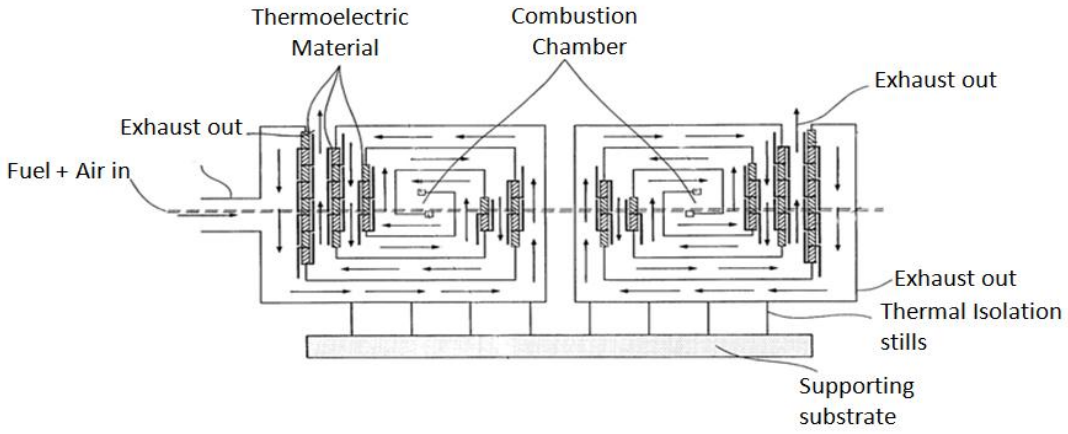

Figure 2.33: Cross sectional view of 'toroidal' combustor [79]

The figure above shows the cross sectional view of the 'toroidal' combustor showing the location of thermoelectric element. Channel wall was made up of thermoelectric module. As it can be seen in the figure that one side of the thermoelectric wall is in contact with the hot exhaust gases while the other is in contact with the cold inlet gases. In this way

the fuel entering the heat exchanger is pre heated by the exhaust gases in a Swiss roll configuration and power generation is achieved simultaneously. Benefits of 'Swiss roll' type 'toroidal' combustors are: reduced heat losses, less fuel consumption, elimination of quenching limits and combustion of fuel in a flameless mode.

Another patent document, US20110083710 A1 [80], titled "Energy efficient micro combustion system for power generation and fuel processing" presents a design of integrated micro-scale power converter which includes a micro machined combustor to convert hydrocarbon fuel into thermal energy and a micro machined thermoelectric generator to convert the thermal energy into electrical energy.

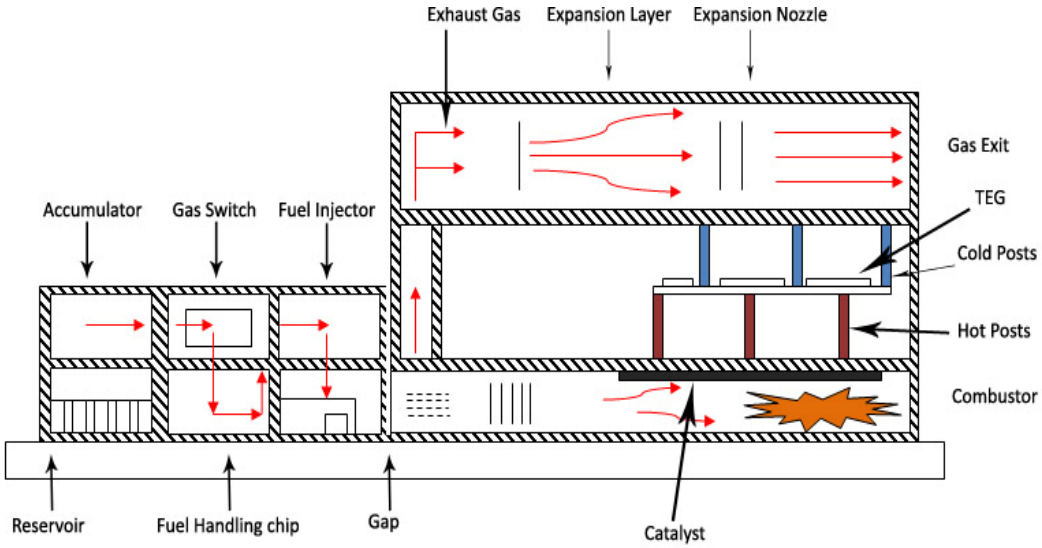

Figure 2.34: Schematic of integrated micro-scale power converter patented by developer Hsu Y

Figure 2.34 shows main components and schematic of the thermoelectric integrated catalytic combustor developed by Hsu Y. Its design and structure aims to increase or maximise the heat flow into the thermoelectric generator. Pneumatic liquid dispenser technology is used as a fuel injector and atomiser. It used passive micro-channels and capillary force to transport fuel in the liquid phase. Air for combustion is introduced into the combustor by the flow momentum of injected fuel. The injected fuel and oxidant are mixed and pre-heated in a mixing chamber. A catalyst was coated on the top surface of the combustion chamber. To increase combustion efficiency, it is important to increase combustion residence time. One of the main features of this design is the use of exhaust gas for cooling the thermoelectric generator. The exhaust gas is suspended via a nozzle over the cold side of the TEG to create large temperature difference [80].

Mueller et al. [81] conducted a research on employing porous burners in thermoelectric generators which included design, assembly, and testing a super-adiabatic combustor integrated with a thermoelectric module.

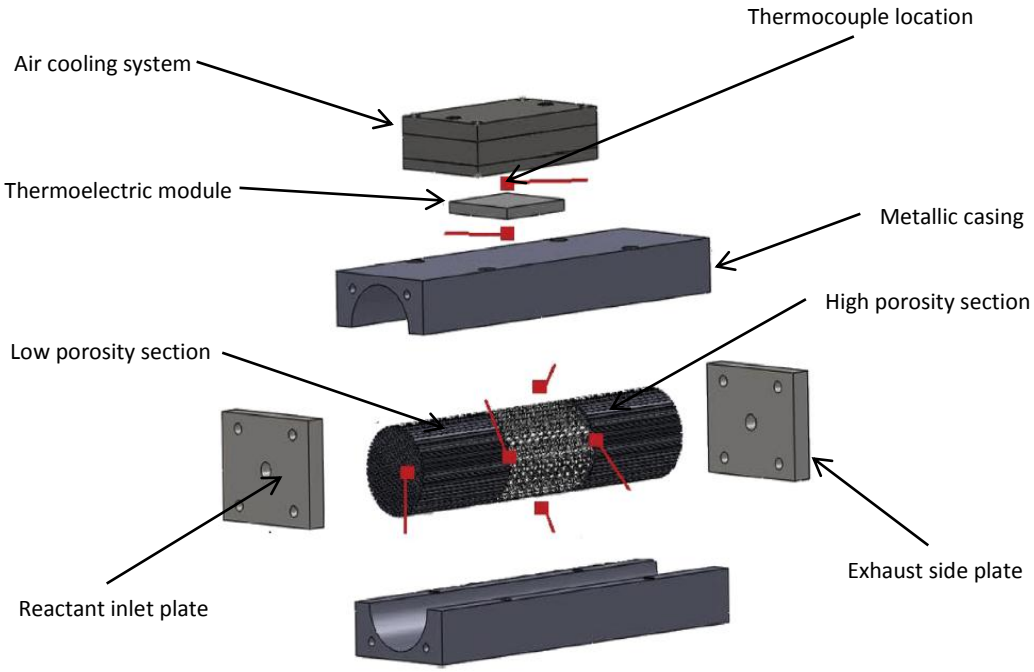

Figure 2.35: Schematic of porous burner assembly [81]

Figure 2.35 shows the schematic of the thermoelectric generator employing a porous burner. The main components of the assembly were Air cooling system which was employed to dissipate heat at the cold side of the thermoelectric module, a thermoelectric module, metallic casing consisting of top and bottom parts, inlet and exhaust plates, porous burner and thermocouples located at various position as shown in the figure. The combustor consisted of a super-adiabatic highly-porous alumina with 80% porosity with a pore size of 3-4 mm. The central combustion chamber had honeycomb structure to stabilise the combustion zone in the porous section. The material used for central combustion chamber was either a pure Al_2O_3 or a catalytic (SiC) active Al_2O_3.

Experiments were performed with stoichiometric and lean mixtures. Results showed that equivalence ratio of 0.589 for the inert porous section and 0.634 for the SiC coated combustion section is the minimum achieved lean limit. The results further showed that SiC might be a good promoter of the combustion for the stoichiometric fuel/air ratio, but SiC coated porous media did not outperform the inert Al_2O_3 matrix where the lean mixtures were used. Thermoelectric module was placed between the steel casing in contact with the porous alumina and air cooler.

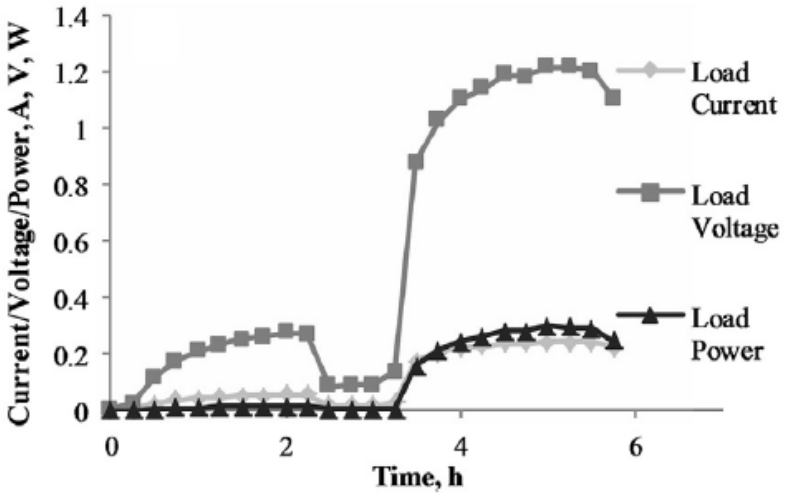

Figure 2.36: Graph showing thermoelectric performance [81]

Figure 2.36 shows power generated during a particular run using the stoichiometric methane to air mixture. It can be seen that the maximum power was recorded to be around 0.3 W after 5 hours of operation.

2.7 Summary

This chapter starts by giving an introduction on premixed combustion and some of the work carried out by authors in the past which relates to the current meso-scale premixed burner integrated with thermoelectric generator under investigation. This is followed by a theoretical study of small scale combustion systems which includes some of the major issues such as quenching and flame stabilisation. Previous work shows that heat recirculation and catalytic combustion has been employed to overcome quenching and heat loss issues in small scale burners. An attempt has been made to define the scale of the burner to be investigated in the current based on the previous work carried out on small scale. The research suggested that premixed burner in the current study can be defined as a small scale burner having operating parameters of a micro-scale burner while having physical characteristics of a meso-scale burner. This was followed by a study of literature on backward facing step which includes an analysis of its effect on the burner wall temperature and an insight on the flow mechanism and interaction that takes place at the step. Backward facing step has been identified as one of the important features which can be implemented in the premixed burner of current research work for the purpose of enhancing mixing of reactants and flame stabilisation. Addition of secondary into the combustion chamber in macro-scale burners has shown to improve flame stability.

The principles of thermoelectrics were studied which includes the three effects, namely, Seebeck effect, Peltier effect and Thomson effect. Seebeck effect will be applicable in the current research which will involve converting heat of combustion in electrical power output. An analysis of different configurations, which can be obtained by varying the arrangement of heat source, thermoelectric generator(s) and cold side heat exchanger, was carried out. This is important in terms of achieving the optimum power generation from the given inputs which in the case of current study are the limited heat availability and cost. The final topic covered in this chapter is an investigation into power generation systems which employ combustion as the heat source and thermoelectric as a method of power conversion. This provided an insight into the design, construction and working principle of the work carried by various authors and inventors.

The present study will involve investigation into flame stabilisation in small scale burners without using a catalyst and heat recirculation, contrary to the previous work done. The following chapters will investigate the effect of secondary air injection in small scale burner having BFS, which previously has been tested on comparatively large scale

burners. Literature revealed that previous combustion based thermoelectric devices were mainly micro-scale and employed a catalyst, the present research will focus on developing and investigation a system which integrates a non-catalytic premixed burner which is meso-scale in terms of its size but operates at micro-scale due to its application, with thermoelectric power generation modules.

Chapter 3

Research Methodology

3.1 Introduction

This chapter explains the research approach followed for development and investigation of the non-catalytic meso-scale premixed burner integrated with thermoelectric generator. It will include the a description of the experimental data obtained to study flame behaviour and data obtained to satisfy design and operating requirements of the burner and thermoelectric generator unit. The test rig constructed for the purpose has been illustrated and a description of major tools and equipment used to collect and analyse the experimental data. Thermoelectric characterisation has also been presented along with a description of main thermoelectric components used in the research.

3.2 Experimental Setup

The initial tests were carried out at Suterra's premises situated at the Treforest Industrial Estate, Wales with some additional investigations into the burner carried out at various facilities at Cardiff School of Engineering. A test rig was constructed to allow two modes of operation of the burner, namely 'self-aspiration mode' and 'forced air supply mode'. As the burner was required to be a self-aspirating type due its application and low cost design, the 'self-aspiration mode' involved natural entrainment of combustion air through the primary air holes by the downstream moving fuel, thus eliminating the use of any expensive means of forced air supply such as pumps etc. The arrangement is shown in the schematic diagram of the experimental setup shown in Figure 3.1. The test rig was built using a Maytech aluminium profiles to allow flexibility; and aluminium sheet as base. Propane was used as fuel which was supplied from a 13 kg bottle through a low pressure (37 mbar) gas regulator. The fuel was regulated using NGX PLATON GTF flowmeter ranged 40-300 mL/min calibrated for propane and was procured from Roxspurs Measurement and Control Ltd. Tests were performed with TEG modules integrated with the burner in self-aspiration mode. Arrangements were made to use FTIR (Fourier transform infrared spectroscopy) to analyse the combustion products which involved taking samples from the top of the burner (exhaust) using a stainless steel probe through a pump.

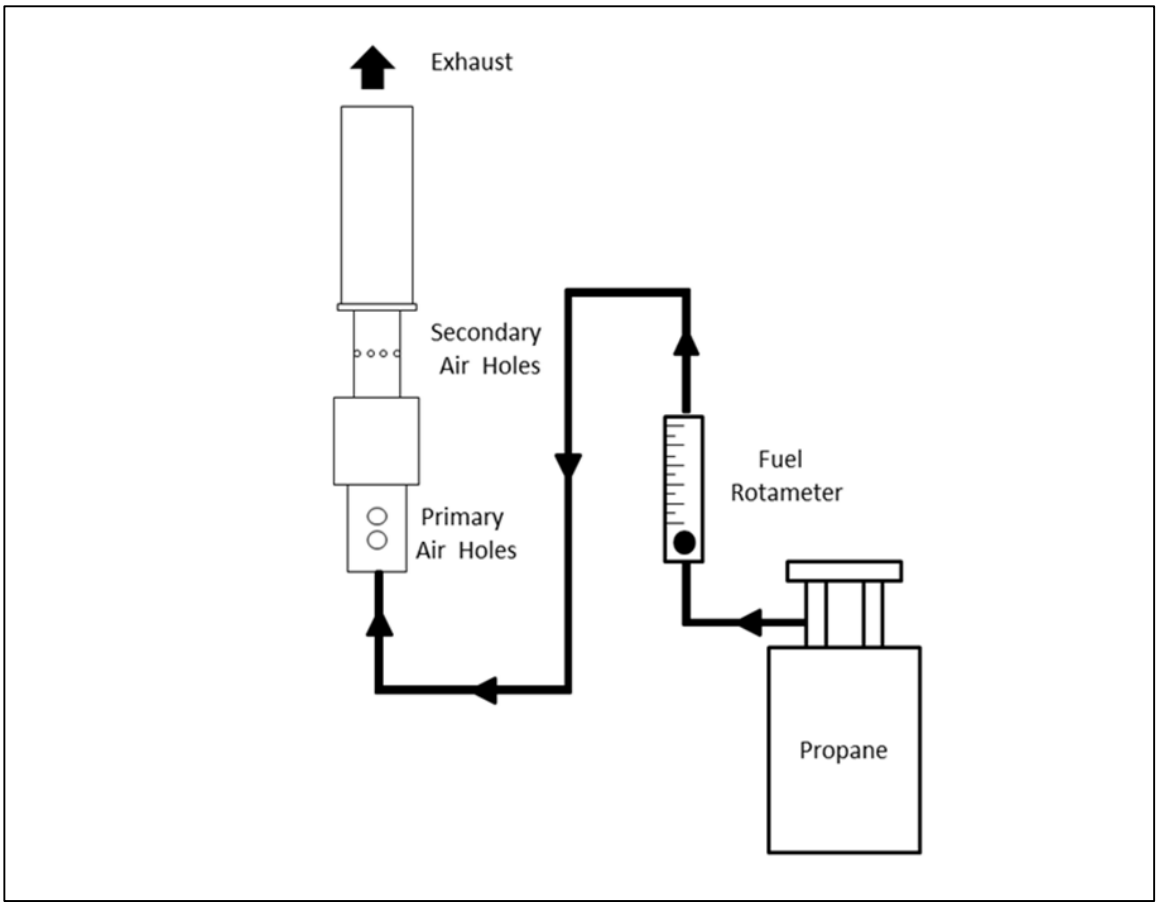

Figure 3.1: Schematic diagram of experimental setup for 'self-aspiration mode'

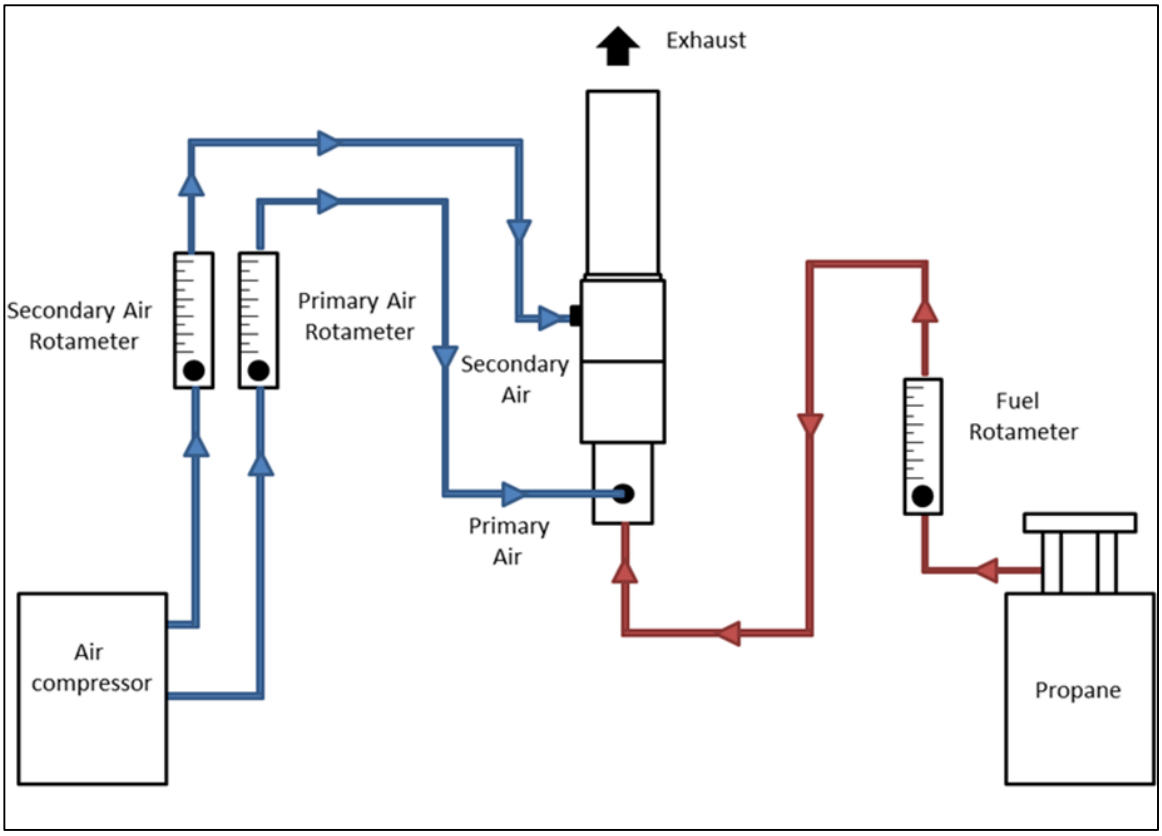

Figure 3.2: Schematic diagram of experimental setup for 'forced air supply mode'

Figure 3.2 shows schematic of test rig with 'forced air supply mode'. This rig was equipped with two separate air flowmeters NGXV PLATON GTF ranged 1-12 L/min and 0.5-12 L/min, to regulate primary and secondary air to the burner. This mode of operation was required to operate the burner at different equivalence ratios to produce results which would contribute towards investigation into the effect of secondary air addition into the combustion chamber on flame stabilisation and also the minimum secondary air required to achieve a stable combustion. Primary air was supplied through the same air holes which are present in the self-aspiration mode while the secondary air supplied to a secondary air chamber where it was forced into the burner through the existing secondary air holes. Similar arrangements for exhaust gas analysis have been done on this configuration as well. This test rig is used to perform experiments to study the effect of secondary air on flame stabilisation.

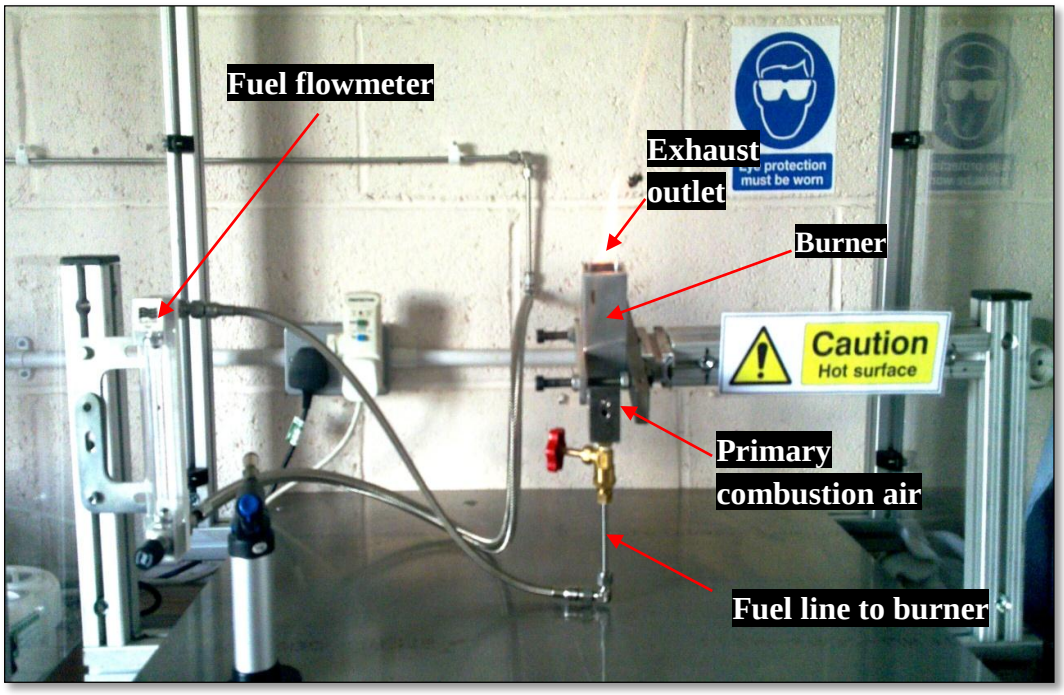

Figure 3.3: A photograph of Test Rig at 'self-aspiration mode' in which the combustion air is entrained in the burner by downstream moving fuel stream, hence eliminating the need of additional components such as a pump etc.

Figure 3.4(i) shows a photograph of rig with tests being carried out on a particular burner and TEG configuration while Figure 3.4(ii) shows a photograph from later stages with endurance tests on one of CO_2 generator prototypes consisting of external housing and exhaust chimneys. Figure 3.5 shows a photograph of main components of the burner and thermoelectric assembly and measurement tools such as Thermocouple Reader and Multimeter.

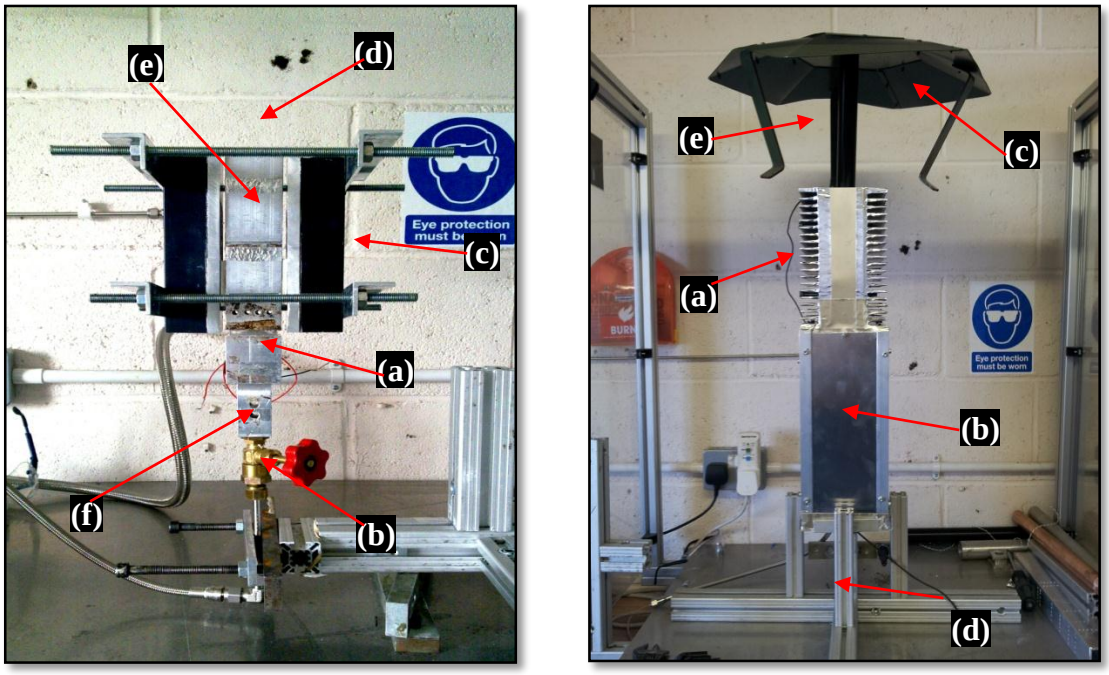

(i) (ii)

Figure 3.4: (i) A photograph of test being carried out on burner and TEG assembly. The main components shown are: (a) Burner, (b) Fuel supply valve, (c) Heat exchanger, (d) Exhaust outlet, (e) Square burner chimney, and (f) Primary combustion air holes. (ii) A photograph of one of the prototypes of the CO_2 Generator being tested in the rig. Main components of this prototype shown are: (a) Heat exchanger, (b) Housing, (c) exhaust chimney, (d) Stand, and (e) CO_2 outlet tube.

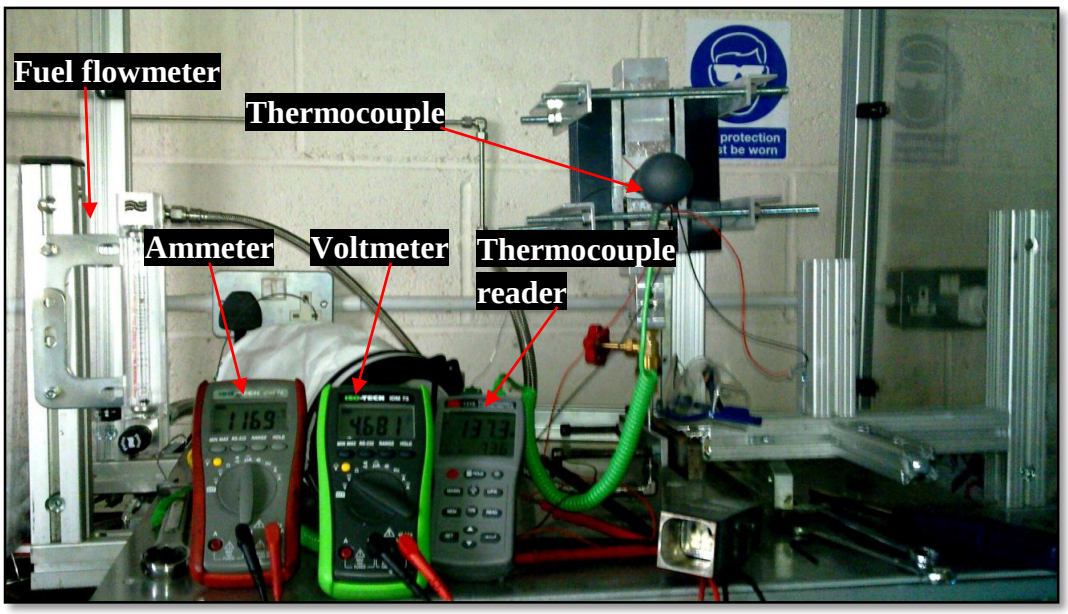

Figure 3.5: A photograph showing main components of the assembly and measurement tools.

3.3 Parameters Analysed

The main parameters analysed during the development and optimisation of the premixed burner integrated thermoelectric generator of the present research are discussed below. In terms of combustion, flame location and products of combustion were the main parameters studied while hot/cold side temperatures and power generation were the main parameters recorded and analysed from the thermoelectric integration.

3.3.1 Flame Location

The location of the flame is important in the combustion chamber as it determines the heat flow into TEG modules. The flame was required to be enclosed, in other words the flame needed to stabilised inside the combustion chamber enclosed by four sides of the burner which accommodates TEG modules. Three different design prototypes of the burner were experimentally investigated which showed varying flame behaviour and location with changes in the geometry of the burner.

3.3.2 Fuel and Air Flow Optimisation

The combustion in the burner was optimised by varying the equivalence ratio to obtain a stable combustion. The fuel and air were supplied by flowmeters manufactured and calibrated by Roxspurs Measurement Ltd. The flowmeters are 'Glass Variable Area Flowmeters', Series NGX with ±1.25% FSD standard accuracy and have 100 mm long scales. The fuel flowmeter was a NGX PLATON GTF with flow range 40-300 mL/min calibrated for propane. The combustion air flowmeters used in the 'forced air supply mode' were also NGX PLATON GTF having flow range 1-12 L/min.

3.3.3 Products of Combustion

The products of combustion were analysed using FTIR at various stages of the research to ensure the burner is not producing compounds in significant amount other than CO_2 and water with changes in design and on integration with TEG modules.

Fourier Transform Infrared Spectroscopy

When infrared radiation is passed through a sample of gaseous molecules, it can be observed that certain wavelengths of the infrared radiation are not transmitted through the gas effectively which is due the fact that the gas absorbs some specific wavelengths of the infrared radiation. The gas molecules on interaction with infrared radiations get energy and start to vibrate or rotate with increasing amplitude. This energy transfer from

the infrared radiation to the gas molecules can be seen as decreased intensity of some wavelengths of the transmitted infrared radiation. If the infrared source sends a broad band of wavelengths of infrared radiation through the sample, some of the wavelengths will be partly absorbed by the gas sample [91].

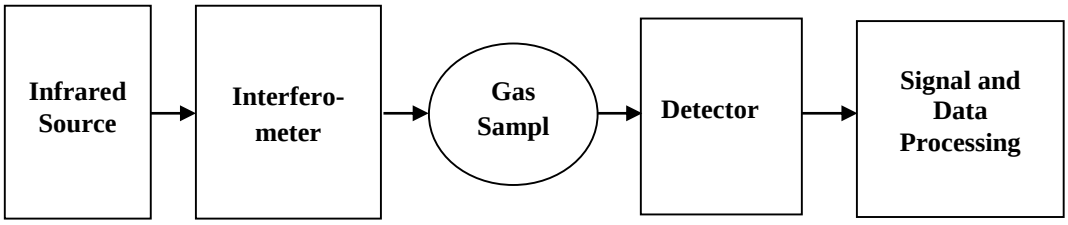

Figure 3.6: Components of Fourier Transform Infrared Spectroscopy

The first component is the infrared source that emits a broad band of different wavelengths of infrared radiation. The infrared radiation then goes through an interferometer whose function is to modulate the infrared radiation. The infrared radiation goes through an inverse Fourier transform on entering the interferometer. The modulated infrared beam passes through the gas sample and the intensity of the infrared beam is detected by a detector. The instrument's processor transforms the detected signal to get the IR-spectrum of the sample gas.

Different gas molecules have unique infrared absorption spectrum and hence it is possible to identify specific gas components from the spectrum of the sample. An example of infrared absorbance spectrum of CH_4 is shown in Figure 3.7 [91].

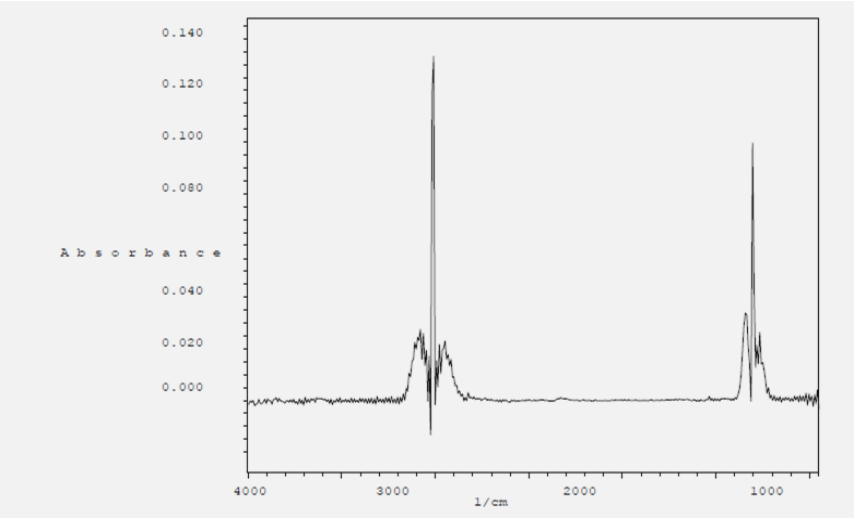

Figure 3.7: Infrared absorbance spectrum of CH4

The FTIR used in this work to analyse combustion exhaust was a GASMET DX 3000.

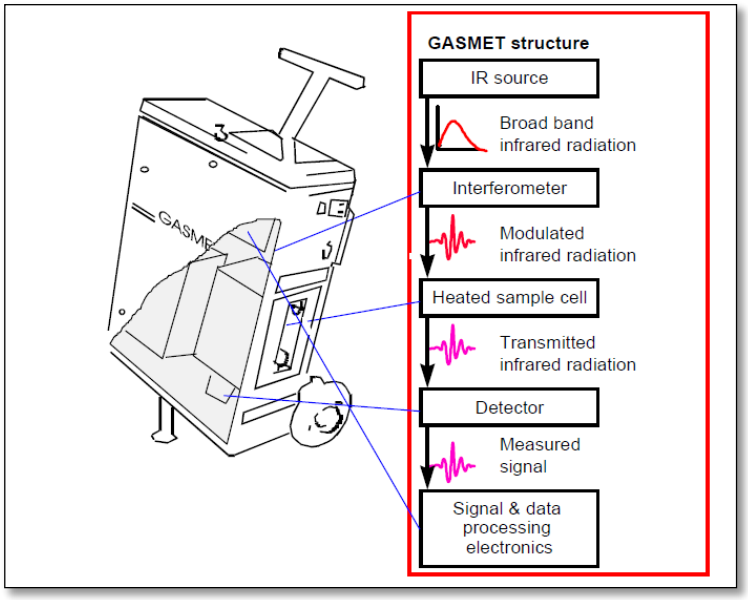

Figure 3.8: An outline of the GASMET DX 9000 analysis system [92]

The Gasmet FTIR gas shown in the Figure 3.8 can measure any gas except Noble (or Inert) gases, Homonuclear diatomic gases (e.g., N_2, Cl_2, H_2, F_2, etc) and H_2S.

Reference Spectrum

The reference spectrum, which forms the basis for the calibration, is an infrared spectrum of a known concentration of the target substance. The analysis is done by comparing the sample spectra to the reference spectra available. The Calcmet analysis software uses the reference spectra to identify and quantify the target components.

The software - Calcmet

The Gasmet gas analyser used in this study uses Calcmet analysis software which allows up to 50 gas compounds to be analysed at the same time. It uses sophisticated and patent protected multi-component algorithms to analyse the sample spectrum. The software is capable of real-time detection, identification and quantification of up to 50 different gas components. Complex gas mixtures involving spectral overlapping are accurately analysed by the software by compensating cross-interference effects and the results can also be compensated for the correct oxygen levels. The results can be shown on either a "wet" or "dry" basis as water content of the sample gas is always measured. The software supports both analog 4 - 20 mA outputs and digital protocols such as MODBUS, PROFIBUS etc. [92].

3.3.4 Burner Wall Temperature (TH, Hot Side Temperature)

The temperature of the burner walls is important as higher wall temperatures would mean higher hot side temperature of the TEG module and hence higher temperature difference can be achieved which would eventually produce higher electrical power output[72][13]. Important to mention here is that the wall temperature cannot be simply increased by increasing the fuel flow rate into the system as it is limited by the operating requirements of 150 ml/min of propane supply and 30 day longevity of the fuel bottle. To measure the hot side temperature, a k-type thermocouple, having a 0.20mm probe diameter, was placed inside a groove cut on the burner wall where TEG was placed while making sure the TEG module and burner wall were in thermal contact with each other. The temperature readings were recorded using a handheld digital thermocouple reader, RS-2063728, supplied by RS Components. The reader had an accuracy of ±0.2% and resolution 0.1^{o}C.

3.3.5 Heat Exchanger Temperature (TC, Cold Side Temperature)

The cold side temperature is important in terms of thermoelectric power generation. Low heat sink temperature is desired to achieve higher temperature difference and hence higher electrical power output [71-75] [13]. T_C depends upon the heat dissipation capacity of the heat exchangers, hence various different shapes and sizes of heat sinks were tested to find the optimum heat sink which is low cost, durable and fits well with the overall size and shape of the unit. To measure the cold side temperature, a k-type thermocouple, having a 0.20 mm probe diameter, was placed between the TEG and cold side heat exchanger while maintaining a thermal contact between them.

3.3.6 Voltage and Electrical Power Output

The Seebeck effect states that when two dissimilar metals or semiconductors are joined together, a voltage V is produced when temperature difference is applied across the two junctions [71-75][13], as shown in the Figure 3.9(a).

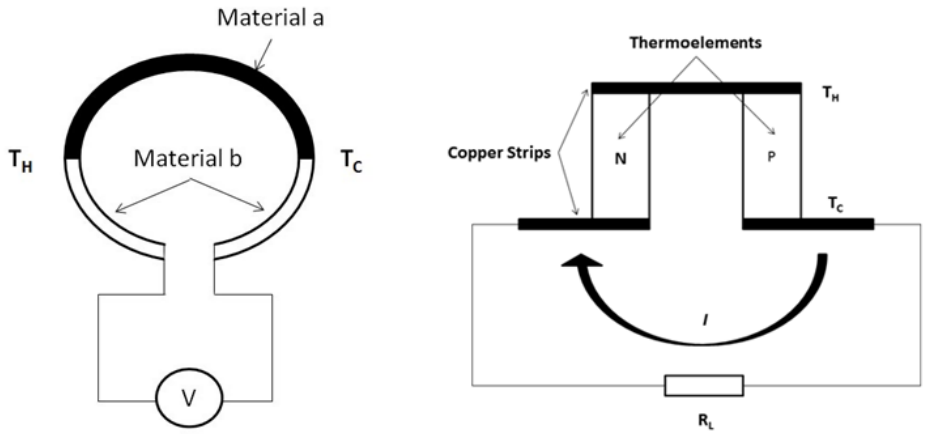

(a) **(b)**

Figure 3.9: (a) Seebeck effect: generation of voltage upon temperature difference being applied at the junctions of two dissimilar metals, a and b (b) Circuit of a thermoelectric module.

Figure 3.9(b) shows the power output circuit.

The Seebeck voltage is given by:

$$Vo = \propto_{np} \Delta T \qquad \text{Equation 3.1}$$

where, subscripts n and p represent n-type and p-type thermoelements which forms the thermocouple junctions; and $\Delta T = (T_H - T_C)$ is the temperature difference across the two junctions and α_{ab} is referred to as Seebeck coefficient.

The power is calculated as:

$$Pmax = \frac{(\propto_{np} \Delta T)^2}{4R} \qquad \text{Equation 3.2}$$

where R is the total resistance of n and p-type thermoelements [96].

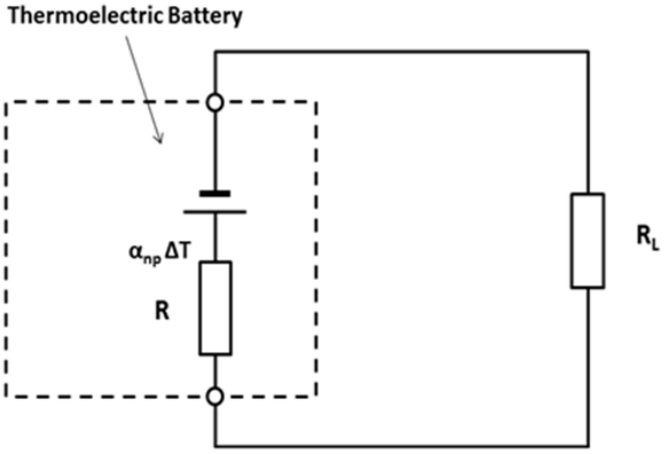

Figure 3.10: Circuit for maximum power output

The thermoelectric power output depends upon the temperature difference achieved between the cold and hot side of the module as shown in the formula for P_{max}. Ideally a higher temperature difference is desired as it would produce higher electrical power.

As mentioned before, the amount of fuel input is fixed which limits the amount of heat available at the hot side, hence focus has been given on looking for methods or mechanisms to capture as much heat as possible at the hot side and dissipate as much as heat as possible from the cold side of the module. Various different configurations have been tested which consists of different arrangements and orientations of heat sinks and heat exchangers.

The electrical measurements were taken with the help of a handheld multimeter supplied by RS Components. ISO-TECH 70 Series Compact Multimeter CAT IV IDM73 was used which has a DC Voltage Accuracy of ±0.5%, DC Current Accuracy ±1%, and Resistance Accuracy ±0.7%. The meter was calibrated by RS Components.

3.4 Properties of TEG

The TEG modules, model GM250-127-14-16, integrated with the meso-scale premixed burner was obtained from European Thermodynamics Limited, UK. The properties are shown in Table 3.1.

Table 3.1: Properties of TEG module used in the research work [93]

Parameters for Hot Side Temp 250 ℃ and Cold Side 30 ℃	
Matched Load Output Power	6.99 W
Matched Load Resistance	3.65 Ω ± 15%
Open Circuit Voltage	10.11 V
Matched Load Output Current	1.38 A
Matched Load Output Voltage	5.05 V
Heat Flow Through Module	~139.8 W
Maximum. Compress. (non-destructive)	1.2 MPa
Max Operation Temperature	Hot side : 250 ℃
Max Operation Temperature	Cold side :175 ℃

The modules are rated for a maximum of 250 ºC hot side temperature which means that the burner wall temperature after placing the TEG module on it should not reach above this temperature. The ideal performance of the module as claimed by the manufacturer is Matched Load Output power 6.99 W, Match load resistance 3.65 Ω±15%, Open Circuit Voltage 10.11 V, Matched Load Output Current1.38 A and Matched Load Output Voltage 5.05 V and Heat Flow ~139.8 W. The Maximum Allowable Compression Force on a module is 1.2MPa; hence care was taken while assembling the TEG module between the burner and heat exchanger to prevent any physical damage to the module [93]. The dimensions of the module are 40±0.5 mm x 40±0.5 mm x 3.4±0.1 mm, as shown in Figure 3.11.

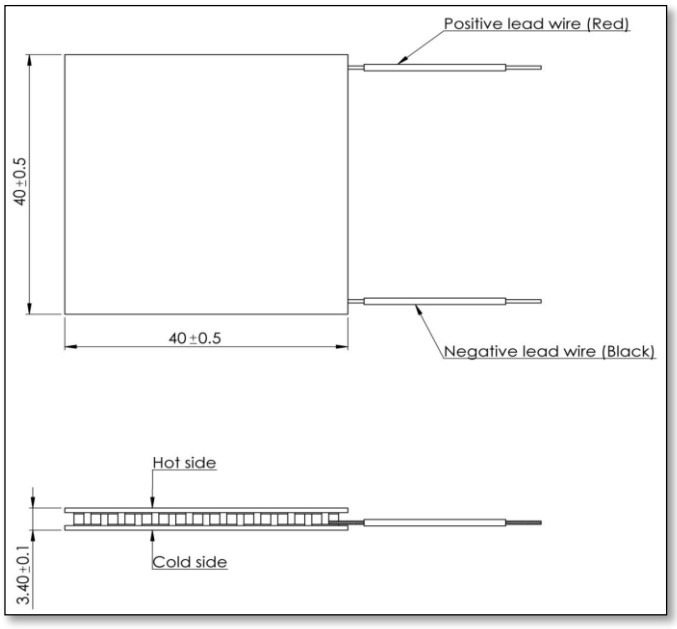

Figure 3.11: Thermoelectric module - GM250-127-14-16

3.4.1 TEG Electric Circuit

As mentioned earlier, various different configurations have been tested in the present research which consists of using a combination of one or more TEG modules. They are connected in series when more than one module is used. The figure below shows two modules connected in series.

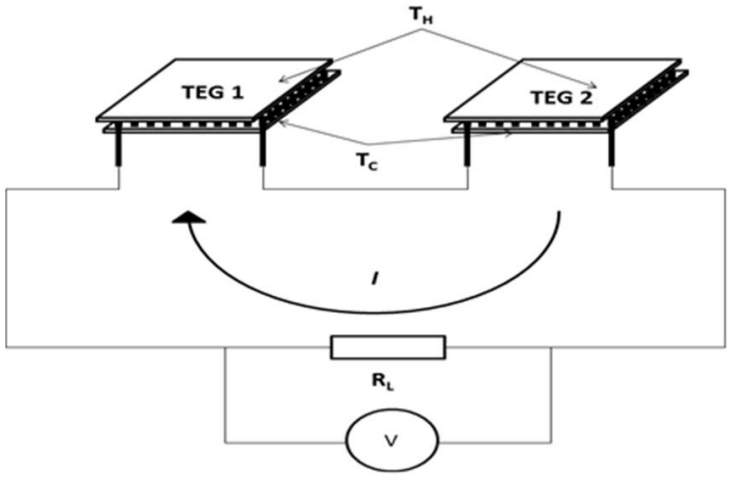

Figure 3.12: Two TEG modules connected in series

The voltmeter is connected in series to the load resistance R_L while measuring load voltage V.

The net potential difference generated is the sum of individual potential differences, therefore in the above case when two modules are used:

$$V = V_1 + V_2$$

Similarly for ‘n’ number of modules used:

$$V = V_1 + V_2 + \cdots \ldots \ldots \ldots + V_n \qquad \text{Equation 3.3}$$

A load resistance R_L is applied to calculate power output:

$$P = \frac{V^2}{R_L}$$

To calculate maximum power output, R_L=Ri, where Ri is the internal resistance of the module [96]:

$$P = \frac{V^2}{R_i} \qquad \text{Equation 3.4}$$

3.4.2 TEG Characterisation

Laboratory characterisation was carried out to determine the internal resistance of the module which is required when measuring the maximum power which can be generated by the thermoelectric burner assembly.

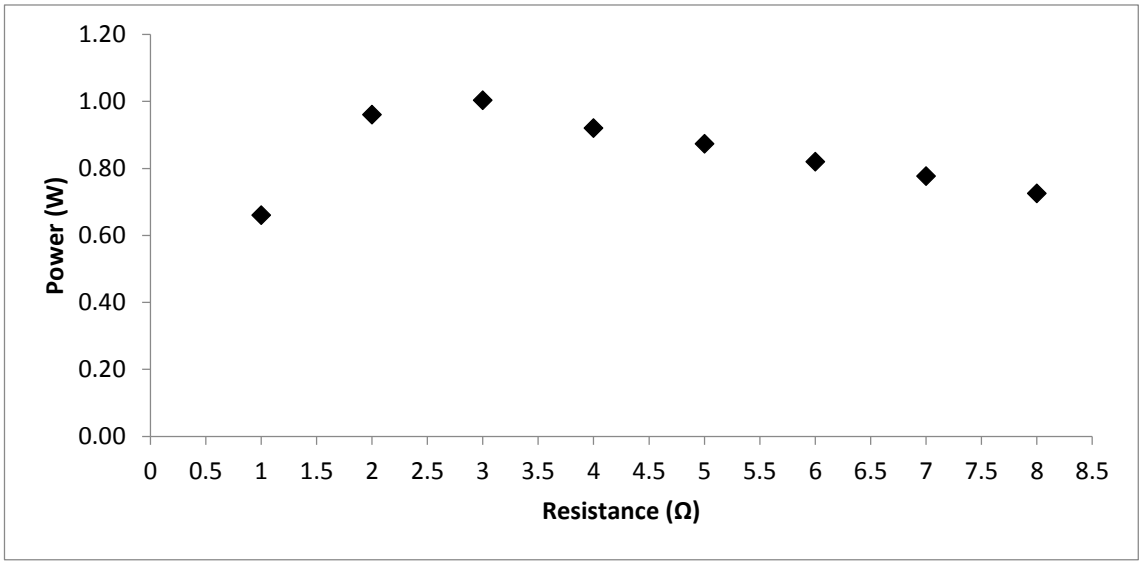

Figure 3.13: Graph showing power output at different resistance values. Internal resistance of a TEG module is the resistance at which P_{max} is obtained i.e. 2.6 Ω in this case.

The graph in Figure 3.13 shows electrical power generation at different resistance values. Experiments were performed to measure the internal resistance of the modules which involved measuring electrical power output at various values of resistance. For each test run, the temperature difference was kept constant by varying the heat input at hot side of the module and heat removal at the cold side. The hot side was kept in thermal contact with a copper block which was in thermal contact with an electrical heater. According to

theory, electrical power generation is maximum at internal resistance of the module [95][94]. In this case, the electrical power was found to be highest at 2.6 Ω resistance. Therefore, in the experiments performed in the research for measurement of electrical power, 2.6 Ω resistor was connected in series with the thermoelectric module as load on the system to calculate P_{max}.

Silicon thermal paste was used in the experiments to maintain a good thermal contact between TEG and burner wall on the hot side of the module and TEG and heat exchanger on the cold side of the module. Thermal paste helps in removing air gaps, making sure there are no hot spots and uniform heat supply to TEG's. The thermal paste used in this experimental study is 'Heat Sink Compound Plus' obtained from RS components. The composition of the paste is 60-80% Aluminium Oxide and 10-30% of Zinc Oxide. The thermal conductivity of the paste if 2.9 W/mK.

3.5 Testing Flame Stabilisation Mechanisms

The plan of experiments to test the flame stabilisation mechanisms will be discussed in this section. Experimental studies were performed to study the effect of backward facing step and secondary air on flame stabilisation in meso-scale burners along with the aim of development of the previously mentioned burner integrated thermoelectric generator device. An in-depth experimental study has been carried out to look into flame stabilisation issues observed in the development part of the research. It was observed that backward facing step and secondary air supply helps to stabilise flame and retain it inside the combustion chamber, so in this section focus has been given on investigating the aerodynamic and chemical behaviour of the flame in the presence and absence of the backward facing step and secondary air, the results and discussion are available in Chapter 7. Three stainless steel burners were constructed having different step heights as shown in the Figure 3.14.

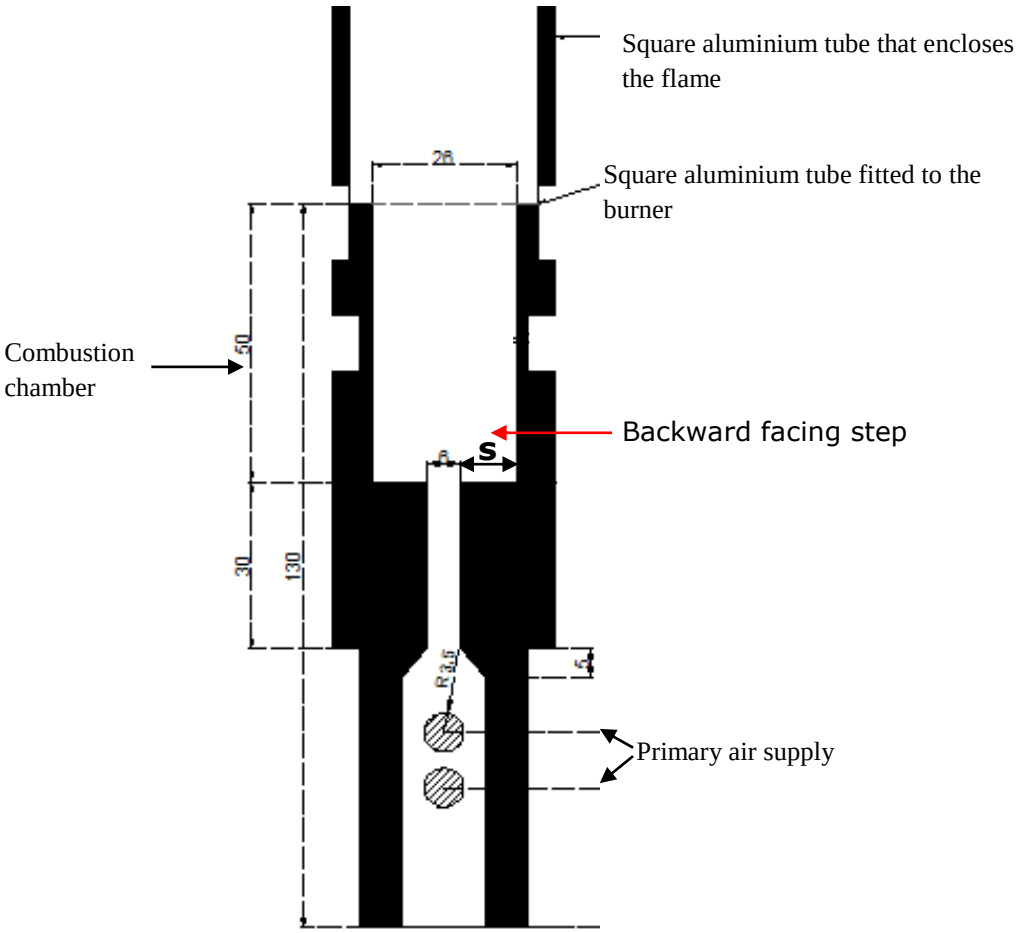

Figure 3.14: A diagram showing the burner with BFS. Experiments were conducted on three Step Heights, 'S'=7, 10 and 15 mm.

The Figure 3.14 shows the burner tube having step height 'S'. Three values of 'S' were studied: 7 mm, 10 mm and 15 mm. Flammability limits were determined by varying the fuel flow as well as air flow and a stable flame region was determined.

The first phase of experiments involved determining the flammability limits, flame positioning and burner wall temperatures of the three burners with different step heights. These experiments were conducted with arrangement made to the design of the burner to facilitate forced supply of combustion air. So unlike the burner included in the product developed for the KTP project, this part of the research had arrangements to vary, and meter, the air flowing through the system. The second phase of experiments involved experiments carried out on combustors with a backward facing step along with secondary air supply as shown in the Figure 3.15.

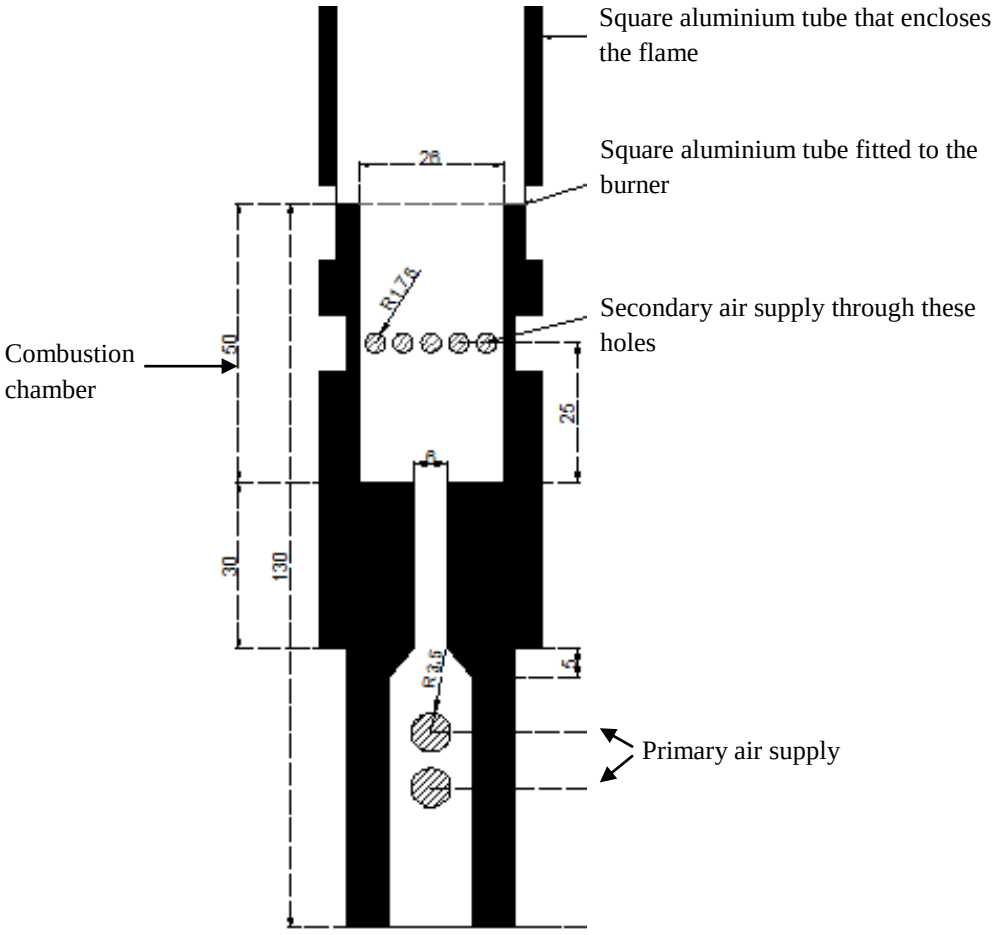

Figure 3.15: A diagram showing the burner with BFS and secondary combustion air supply. Experiments were conducted on three Step Heights, 'S'=7, 10 and 15 mm.

Secondary air holes have been provided downstream of BFS with the aim of anchoring the flame or in other words obtaining an enclosed flame. The measured parameters are minimum secondary air requirement for flame stabilisation for each step height, the overall equivalence ratios, flammability range, stream velocity profiles and burner wall temperature.

3.6 Effect of Variation of Ambient Temperature

The device has been tested in the Environmental Chamber facility at Cardiff University. The device is supposed to be marketed in countries like UAE where temperatures may reach up to 40 ^{0}C and hence it was necessary to test the unit under hot ambient condition to determine its reliability. Endurance tests were performed to investigate flame behaviour and thermoelectric performance of the burner and power generator unit.

Figure 3.16: Environment Chamber at Cardiff School of Engineering

The figure above shows a picture of environment chamber based in the school of engineering at the university campus. The chamber allows various settings for temperature and humidity. Tests were performed for 8 hours of continuous operation of the unit and temperature and voltage readings were periodically recorded. The focus in endurance tests were given its ambient temperature as it is the main variable that can have an effect on both combustion and thermoelectrics. At higher temperatures the inlet combustion air can change the combustion characteristics and affect the flame stabilisation as well as combustion efficiency. In terms of thermoelectrics, at higher ambient temperatures, the cold side temperature of TEG module would be higher due to less heat dissipation to the environment, hence causing the temperature difference across the TEG module to be low and therefore reducing electrical power generation.

The main measurement were hot and cold side temperatures and load voltage. One of the operational requirements is that the external housing and chimney should not exceed permissible temperature for safety reasons, thermocouple were placed on various locations of the housing and chimney.

As shown in the table above, the unit was tested for three different ambient temperature settings of chamber 20 ^{o}C, 30 ^{o}C and 40 ^{o}C. The measurements taken were temperature of cold and hot sides of the module, temperature difference, load voltage, power output, exhaust temperature and temperature of the chimney.

3.7 Summary

This chapter discusses the research approach undertaken to achieve project objectives which includes development of a meso-scale premix burner integrated thermoelectric generator and study of effect of secondary air on flame stabilisation. A description of test rig has been presented with pictures showing experiments been carried out. Arrangements were made to test rig to conduct experiments on self-aspiration mode and forced air supply mode. System development and design optimisation is the next stage which describes the experiments performed during the product development stages and the data collected. Properties of TEG modules have been presented which makes one of the main components of the unit. This section covers a description of design of TEG's and the electrical circuit used for voltage measurement and power calculation. Characterisation of TEG modules has been explained which involved determination of internal resistance of the module which is an important parameter when determining maximum power generation. A description of equipment used in analysing the products of combustion has also been presented which includes description of the principles of Fourier Transform Infrared Spectroscopy and its main components.

Chapter 4

Challenges and Design Issues

4.1 Introduction

This chapter explains the major challenges faced during the product development phase of the project. These challenges presented opportunity to look into combustion and thermoelectrics working together in one system at meso-scale, contrary to previous studies which concentrated on micro-scale as discussed in the literature review. The observations mentioned in the following sections will become the basis of experimental study which has been presented in the later chapters. Before challenges are presented, it is important to understand the design and features of the burner.

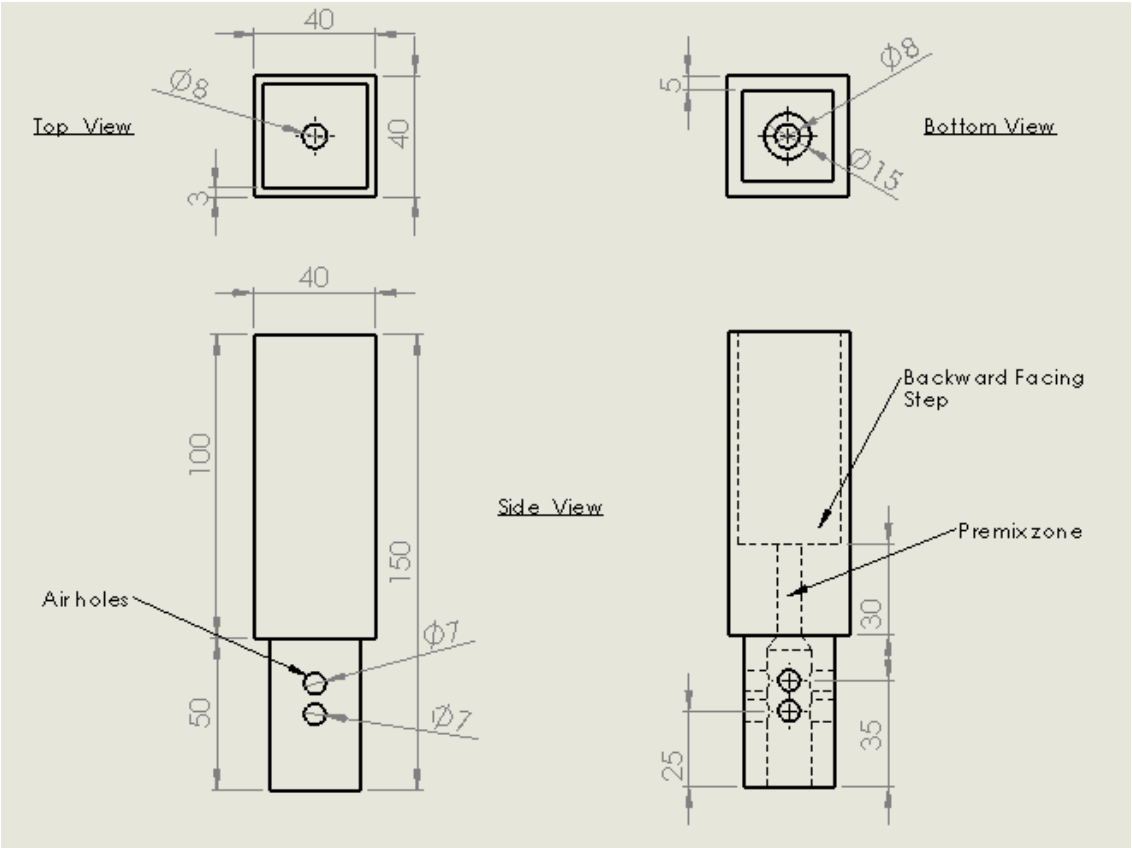

Figure 4.1: A 2D drawing of the burner designed according to operating requirements and thermoelectric integration

The Figure 4.1 shows a technical drawing of the burner which is made up from 40mm square Stainless Steel-316 bar. The square shape is to accommodate thermoelectric power generation (TEG) modules. These modules to be integrated on the burner walls are 40mm

square and hence restrict the size of the burner walls to be no less than 40 mm wide and square in shape.

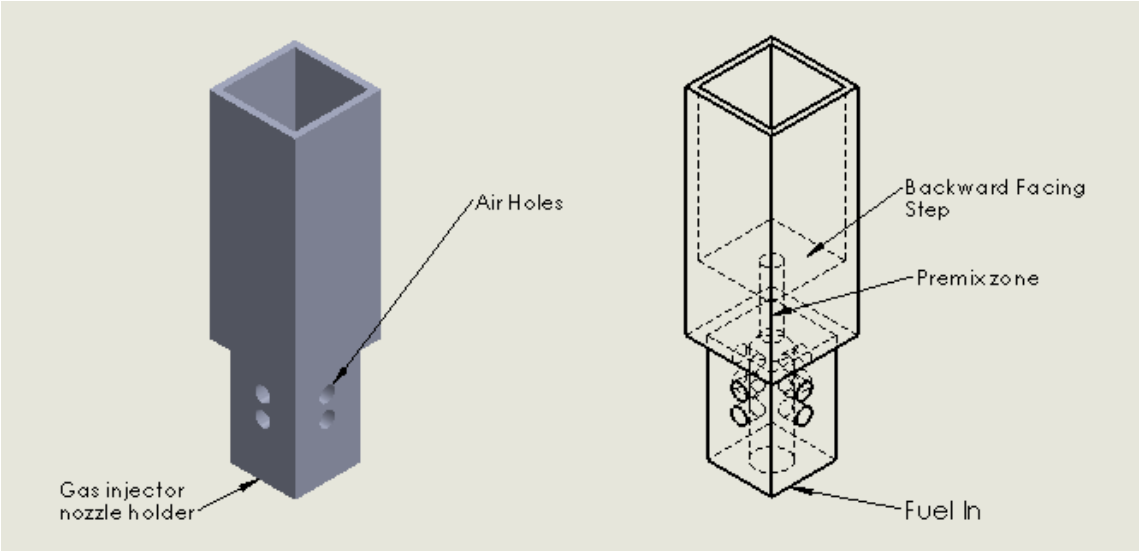

Figure 4.2: A 3D model of burner showing the design features based on the operating requirements and TEG integration

Figure 4.2 shows a three dimensional drawing of the self-aspirating premix burner with premix zone, combustion air holes and backward facing step. The backward facing step has been introduced to enhance mixing of reactants to achieve better combustion in terms of carbon oxidation to CO_2. This burner has been explained in detail in chapters 5 and 6. The major challenges are given below.

4.2 Non Catalytic

The first challenge was the requirement of a catalyst free burner which at the same time should not produce any large amounts of CO, UHC and NOx. Due to the application of the burner in insect attraction, the concentrations of the compounds mentioned should be minimised. Market research was carried out to find the operating characteristics and design specifications of similar devices marketed by competitors and it was found that the only way the company could market this device without violating intellectual property of its competitors is by making it catalyst free. The basic operation of these devices involves combustion of propane or butane to produce CO_2 and H_2O at required rate [2-11]. Various companies in the field of pest management and control are marketing these devices generating insect attractants of CO_2, heat and water vapour through catalytic conversion of a hydrocarbon fuel in a combustion chamber[5][6][7]. These catalytic converters are similar to those widely used in automobile industry for the abatement UHC, CO and NOx from the internal combustion engines [104]. The success of catalytic

converter has provided a strong basis of confidence in using them for many other applications in the vital role of cleaning our environment.

A typical combustion process in a catalytic burner of Mosquito Magnet, a mosquito and midge trapping apparatus, is explained as: Gas flows from a gas bottle through the bottles shutoff valve and flexible line to a regulator which drops the pressure to 15psi. The gas continues at this pressure to the input of a gas safety device which is a flame sensing type of device. The gas flows out of the nozzle at a rate of 0.5 kg in 36 hours.

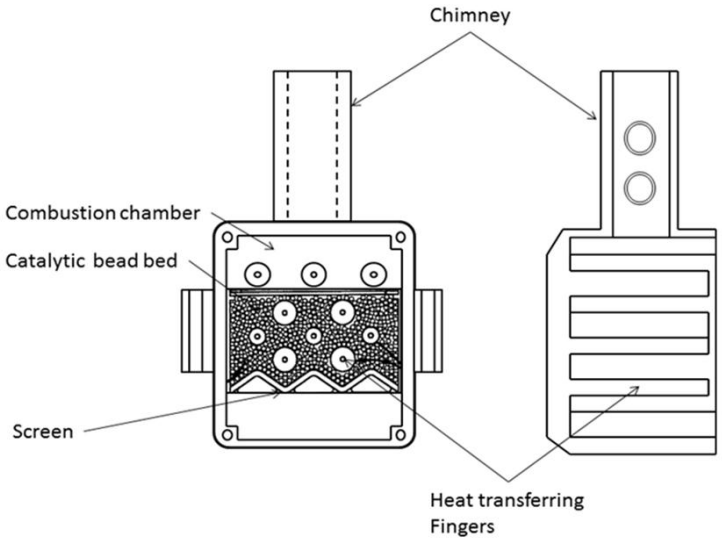

Figure 4.3: A catalytic burner included in '*Mosquito Magnet*' mosquito trapping apparatus

Atmospheric air is entrained into carburettor by pressure difference created by two diameters of flow. An adjustment screw is provided to vary the airflow. The air fuel mixture enters combustion chamber and flows through screen into catalytic bead bed filled with platinum coated alumina beads. These beads have diameter no larger than about 3.175 mm. The flame is initiated above bead bed with a piezoelectric spark ignitor. As the flame burns, heat generated from the combustion warms the combustion chamber and bead bed. After the flame has been going for some 30 seconds to 45 seconds, the heat is reflected down into catalytic bed. The catalyst is warmed up and as the catalyst is warmed up it achieves a surface combustion temperature and the flame converts to a catalytic surface combustion bed. As a greater amount of the fuel air mixture oxidises in bead bed, the flame becomes starved of fuel and is extinguished. The combustion continues entirely on a catalytic basis [5].

A low cost design

One of the objectives of the research project is a low cost design. Similar devices available in the market can cost between $ 500 to $ 1000 in the European and American market [2-11]. The company aims to sell this device anywhere between $ 150 and $ 200, which is less than half of the price of cheapest device available in the market. An analysis of competitors products showed that the major cost associated with the manufacturing of their devices is the machining complexity of the catalytic combustion chamber along with the cost of the catalyst and thermoelectric power generation modules. So the company came up with the research proposal of developing a carbon dioxide generator which would not have expensive catalyst, simple to manufacture, assemble and market and provide an opportunity to the company to have its own intellectual property.

4.3 Self-Aspiration of Combustion Air

The burner was intended to be a self-aspirated, which means that the combustion air to the burner is required to be supplied without the use of any pump or other forced means. The reason behind this requirement is cost associated with air compressors and design complexity. The self-aspiration mode of the burner presented major difficulties in testing as the amount of air supplied or sucked in could not be determined throughout the design phase. Hence, the equivalence ratios could not be determined due to unavailability of mass of combustion air flowing through the system. The only way to vary combustion air was through the opening and closing of air holes on the burner walls as shown in Figure 4.2.

4.4 Design Challenge: micro-scale operating regimes versus meso- scale dimensions

The need to eliminate the catalyst presents an opportunity to study burner design principles associated with achieving complete combustion. The design of the burner is restricted to have 40 mm square sides to facilitate thermoelectric power generation modules as the modules to be used are 40 mm square. This shape and size of the combustion chamber was considered as the foundation of designing the remaining burner sections such as mixing zones, backward facing step height and chimney etc. This provided a basis for designing and experimentally investigating a burner integrated with thermoelectric power generation modules where the general design principles of micro-scale combustion and large scale combustion do not directly apply, giving an opportunity to study flame stability and thermoelectric power generation at a scale where the operating

regimes are small while the design requirements are of macro-scale, which has not been done previously in academic literature.

4.5 Enclosed Flame

The burner is required to have an enclosed flame so that it heats up the walls of combustion chamber which have thermoelectric module accommodated on them. The modules use this heat to produce electrical power via Seebeck effect [13][72-74][95]. Also, the burner is supposed to operate constantly i.e. 24x7 in all-weather conditions due to its application with mosquito catching apparatus, enclosed flame would mean no rain water or strong wind affects the operation of the device. Another reason to have an enclosed flame was safety hazards as pets and small children could be vulnerable to an open flame. So, obtaining a stable flame in a burner having specific design requirements are restricted to thermoelectric integration; need for an enclosed flame and robustness was a big challenge and the following chapters will present the results and analysis of the techniques/methods used to achieve a stable enclosed flame under the conditions considered.

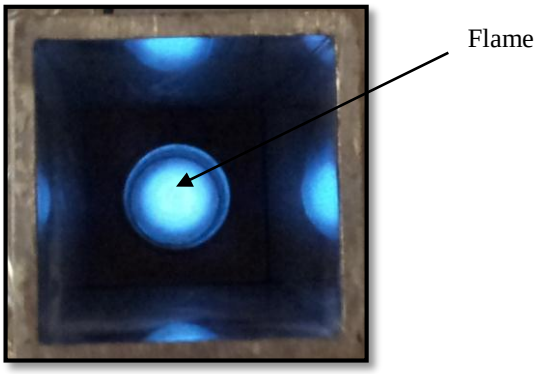

Figure 4.4: Figure showing the desired enclosed flame in a square burner

Figure 4.4 showing an ideal (desired) flame which is enclosed by the burner walls and hence, heating them up which is required for electrical power generation. Arrangements were made at the top of the burner to make sure water or wind doesn't come inside causing the flame to extinguish. The problems in obtaining this flame have been mentioned in the next section.

4.6 Flame Stabilisation

Flame stabilisation is one of the most important aspects of any combustion process. According to the previous work carried out in the field of small scale combustion, the burner of the present research falls under the category of micro-scale burners in terms of the amount of fuel required to be oxidised, however the size of the burner is restricted to have at least 40 mm wide burner walls so that TEG modules can be placed on them to achieve optimum hot side temperature (T_H).

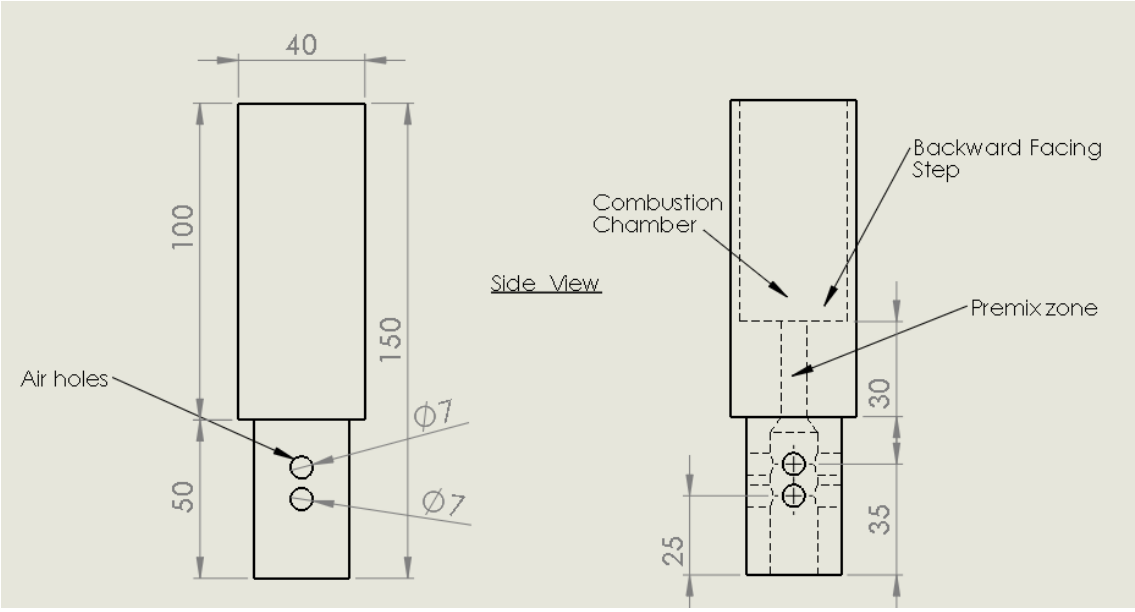

Figure 4.5: Figure showing the expansion ratio between premix zone and combustion chamber, causing problems in flame stabilisation.

The Figure 4.5 shows the design requirements of the burner, which includes a premix zone of diameter 6 mm for mixing of reactants and the square combustion chamber having 40mm width where the TEG modules are required to be accommodated. The desired flame location is at the step height so that the heat from the flame is transferred to the 40 mm wide burner wall and hence to the TEG module. During ideal operation, the fuel should enter through a nozzle at the bottom of the burner as shown in the figure, entrain primary combustion air from the primary air holes while moving downstream and enter into the premix zone which is a constrained passage. The fuel then should enter the combustion chamber which has a backward facing step for enhancing reactant mixing through turbulence created by the recirculation of the stream at the sudden expansion.

It can be seen that the expansion ratio i.e. the ratio of the diameter of the premix zone and the combustion chamber, is large considering the amount of fuel supplied and air entrained. This caused major design issue as the dimension of the premix zone needed to

be small for good mixing of reactants before they enter the combustion chamber as the flow mass of the stream is small.

The tests on the burner designed with the necessary operating and design requirements showed very unstable combustion with occasional occurrences of flame in the burner. The results showed flame resting at the extreme downstream of the burner tube at the top as shown in the Figure 4.6.

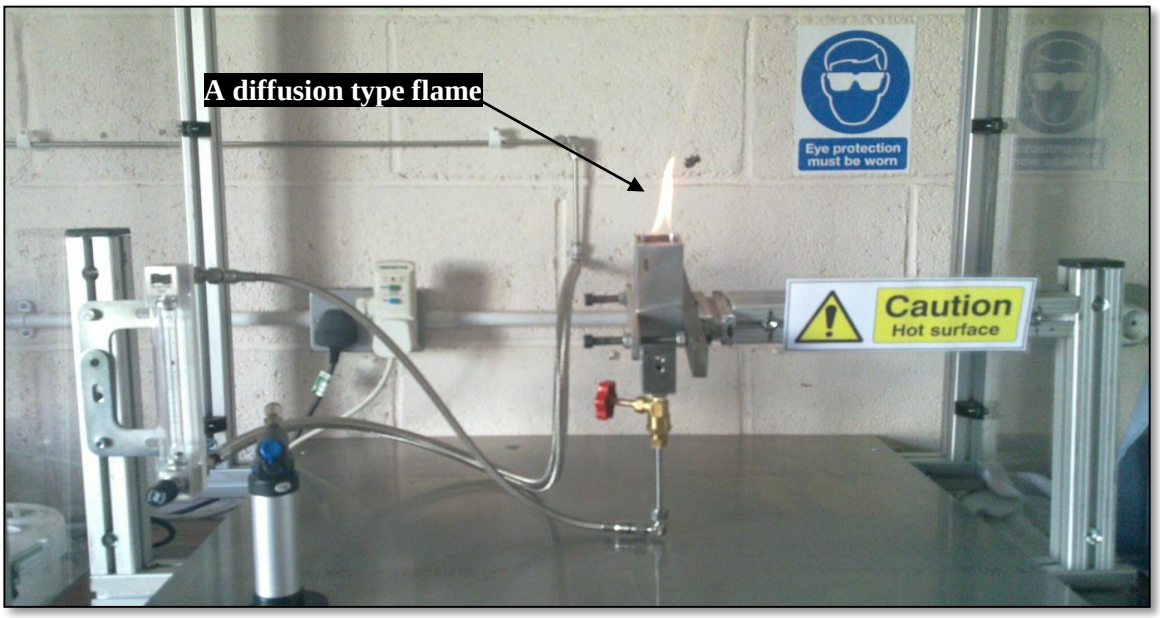

Figure 4.6: A photograph of the flame obtained with the burner. Flame can be seen stabilising itself at the extreme downstream

Figure 4.6 shows an unstable diffusion type yellow flame on top of the burner which turned out to be a major challenge. Therefore, a flame stabilisation mechanism was required to facilitate combustion at the desired location shown in the Figure 4.4.

4.7 Integration: Combustion and Thermoelectrics

Past research on the subject of integration of combustion and thermoelectrics has been mainly focused on micro-scale combustors having capability of generating few milli-watts of electrical power. The size of combustion chambers of these micro combustors can be between 100 microns to few millimetres. Some of these micro combustors have been discussed in detail in the literature review section of present study. So, one of the challenges under the integration of the two mentioned fields of science was the lack of literature on meso-scale devices. This gave an opportunity to present and explore new scientific data on performance and analysis of meso-scale power generator using thermoelectric and combustion.

Another challenge under the integration issue was the low cost design of the device. As previously mentioned the proposed selling price of unit is 75% cheaper than the currently available similar devices. Major cost contributing to the manufacturing cost is the cost of thermoelectric power generation modules which can vary anywhere between $20 and $50 depending upon the required specifications. The competitor's devices utilise 4 thermoelectric modules to generate 4-5 watts electrical power. So, one of the ways to reduce the manufacturing cost is to reduce the number of modules to be integrated with the combustion chamber by making improvements in the system. The present work investigates various configurations with the aim achieving 3-5 W electrical power output using a minimum number of thermoelectric modules at a restricted or limited heat supply from the combustion chamber. Major issues were heat extraction from the combustion chamber at the hot side, heat dissipation at the cold side the thermoelectric module to have a large temperature difference and hence power output, consistent power output and robustness issues. The device is to be marketed in various parts of the world where weather could have an impact on the performance. The machine will be sold in Scotland where the ambient temperatures can be as low as 1 ^{o}C during mosquito season or in United Arab Emirates where ambient temperatures can reach up to 45 ^{o}C making the operating conditions worse in terms of combustion efficiency and electrical power output. In this regard, the device has been designed considering environmental factors and has been tested in an environmental chamber with varying ambient conditions. Further, the device is supposed to operate under heavy rain as mosquitoes become active under such conditions; the device has been tested in the field where it had to withstand strong wind and rain. All this gave an opportunity to gather data of a meso-scale combustor integrated with a thermoelectric generator which was not available before. The recorded data can be used by future researchers who may wish to undertake similar results.

4.8 Summary

This chapter presents the challenges and problems faced during the development, design and testing of the meso-scale burner integrated thermoelectric generator. Firstly, the burner geometry and its features have been explained followed by the major design factors which include designing an efficient burner without a catalyst due to cost and intellectual property issues, self-aspiration operation of the burner, design issues involving a vast difference in the scale of operation and geometrical requirements, flame stabilisation and integration with thermoelectrics. Various observations have been presented which gave opportunity to look into the scientific side of events such as flame positioning at the exit. Flame stabilisation has been one of the most important challenges in this self-aspirating burner having size and shape restrictions due to integration with thermoelectrics. This research work contributes in developing literature on behaviour of flame in an aspirating mode operating at meso-scale. The next chapter will explain the stages of development of the burner and its integration with thermoelectrics which will present the solutions to the challenges or problems mentioned in this chapter.

Chapter 5

Development and Investigation of a Meso-Scale Burner

5.1 Introduction

As mentioned in the previous chapters, the aim of this research work carried out under KTP project was to develop, test and validate a carbon dioxide generator which basically consists of a meso-scale premixed burner integrated with thermoelectric modules. This device has been successfully developed through various stages of product development and has been intensely tested in the laboratory and actual field. This section will cover the technical development stages from design of initial test burner to the final commercial one to the final assembly with thermoelectric generators.

The meso-scale combustor integrated thermoelectric generator which constitutes an insect catching apparatus was carefully designed according to operating requirements which were based on a thorough market research, analysis of competitor's products, entomological experts and customer requirements.

5.2 Meso-Scale Premixed Burner

This section covers development stages of the burner and thermoelectric assembly and presents experimental results from parametric studies on three different prototypes. Firstly, emphasis has been given on optimising the burner to satisfy operating characteristics and obtaining a stable flame. Next, experiments have been performed to optimise most suitable thermoelectric power generation modules and heat exchanger configuration to obtain the required consistent electrical power output. This will include identification of the location of TEG modules on the burner as well as methods to extract maximum heat from the exhaust through the burner wall in order to achieve highest possible hot side temperature without affecting combustion side of the device.

5.2.1 Prototype 1

Based on the literature review, a premixed burner was designed keeping focus on the design requirements. One of the main features of the Prototype 1 was a backward facing step to enhance mixing and square shape of the burner as shown in the Figure 5.1.

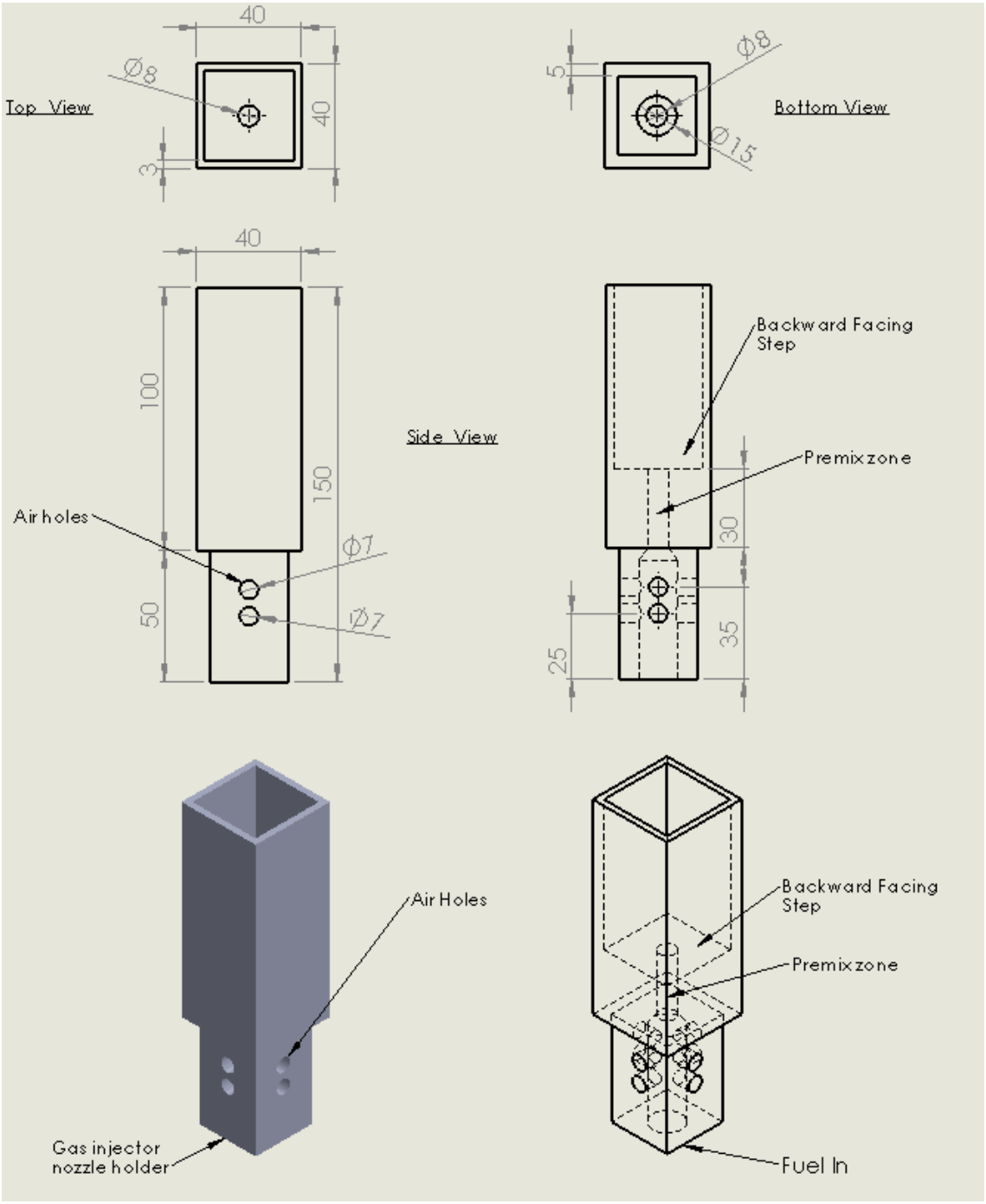

Figure 5.1: Drawing of Prototype 1

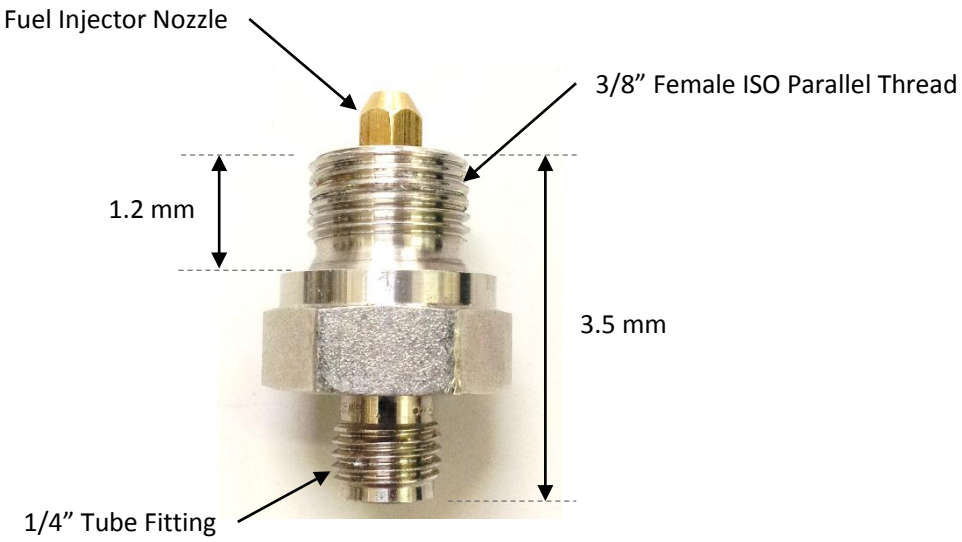

Figure 5.2: Details of fuel injector nozzle holder

The drawing in Figure 5.1 shows internal and external geometry of Prototype 1 which is made up of 316 Stainless Steel. Figure 5.2 shows the details of the injector holder which was a stainless steel compression fitting with one end had 3/8" 'Female ISO Parallel Thread' connection whereas the other end had a ¼" tube fitting. The burner was machined out from a single 150 mm long, 40 mm square bar. The square shape has been chosen to accommodate TEG modules on its sides as these modules are 40 mm square and 3mm thick flat plate types (Technical drawing is available in Chapter 3 – Research Methodology).

The motivation behind the design of the first prototype was a premixed gas burner which offers good mixing mechanism for the reactants and can accommodate TEG modules on its sides. A backward facing step was introduced based on the literature review which has shown that it enhances mixing of reactants due formation of recirculation zones. Another feature of this burner is self-aspiration of combustion air, the need of which is previously explained in the operational requirements in this chapter. So for this purpose, a hole having diameter 7 mm on all the sides of the burner were machined to vary the air supply as shown in the Figure 5.2. The burner was provided with a premixed zone which is a smaller diameter passage which compresses the fuel and air to mix it before it enters into the combustion chamber. As mentioned previously, focus is given on utilising or capturing the optimum heat from the exhaust gas to convert it into electricity using TEG modules. The more heat available at the module's hot side, higher the temperature difference would be across its sides and greater electrical power can be obtained. So, the idea was to keep the shape of the burner square and its width same as the width of TEG

module which would ensure that the TEG module covers the maximum surface area of the burner's side and hence less heat losses. In operation, the fuel is supplied through a flow meter to the nozzle which injects it into the primary mixing zone where it entrains air from outside through air holes due to creation of a low pressure zone inside. The stream further moves downstream into the mixing zone and finally into the combustion chamber which consists of the backward facing step. The burner was initially designed with the aim of obtaining the flame on the backward facing step which would heat the walls supplying heat to the TEG modules under ideal conditions.

It should be noted here that these experiments were carried out without any forced air supply i.e. the burners were operating under self-aspiration mode as required by the application of the final product. The only way to vary the air supply was to change the effective area of the air holes provided in the primary mixing zone.

Table 5.1: Effective area of primary combustion air holes

No. of Primary Air Holes	Effective area available for primary air entrainment (mm^2)
1	38.5
2	77
3	115
4	154

The effective area available for primary air entrainment corresponding to the number of primary air holes kept open for a particular experiment is shown in Table 5.1. This means that it was not possible to directly measure the fuel air ratios and hence equivalence ratios, which have been determined later when the experiments have been carried out under 'forced air supply mode' and gas analysis with FTIR. As mentioned in the operating requirements, the burner is supposed to combust 150 mL/min of propane to produce the required carbon dioxide. Upon setting up this fuel rate at the flow meter, no combustion was observed until the air supply was reduced to just 2 air holes open. Even at this composition, the combustion was very occasional with unstable fluctuating flame (Figure 5.3) in the combustion chamber which was not the desired outcome.

Figure 5.3: A photograph of flame obtained with Prototype-1

The burner was then tested for various flow rates of fuel and air supplies which showed similar behaviour of occasional and very unstable combustion. Flashback was also observed at small flow rates between 100 mL/min to 150 mL/min. Hence, it was evident at this point that the current design would not yield a stable combustion and modifications will be required.

Various bluff bodies were then inserted in the combustion chamber to see their effect on the flame stabilisation. Following are some photographs indicating the type of bluff body and the flame obtained with them:

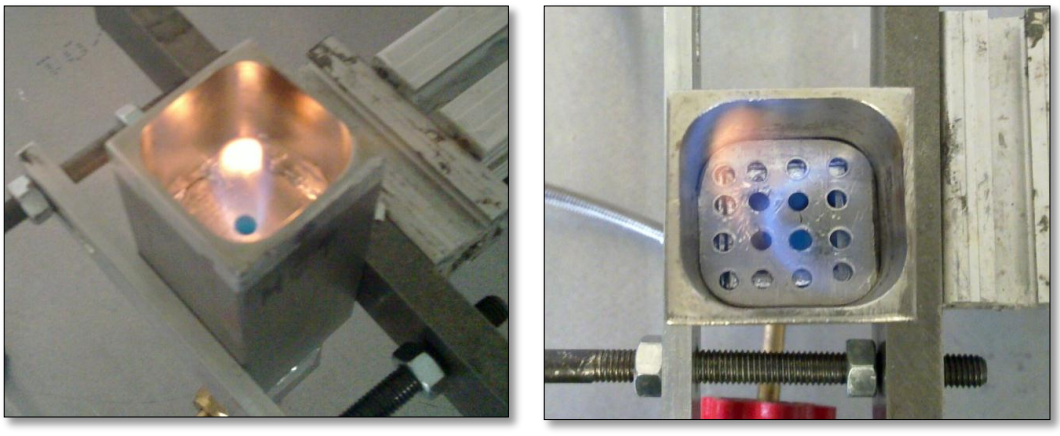

(a) **(b)**

Figure 5.4(a): A photograph showing diffusion type flame with a plate having 3mm hole inserted to act as a bluff body, (b) Combustion with another type of a bluff body insert which consisted of a plate with several 3mm holes

The bluff body shown in Figure 5.4 (a) is an aluminium plate with a 3 mm diameter opening at the centre and another bluff body tested was an aluminium plate with a series of 3mm diameter openings as shown in the Figure 5.4 (b). These tests were performed to observe the behaviour of burner upon making changes in the flow of fluid as a result of inserting these bluff bodies in the combustion chamber.

Figure 5.4 (a) shows a photograph of flame obtained with the bluff body placed in the combustion chamber making an additional mixing zone after the backward facing step. Diffusion type yellow flames were observed. Figure 5.4 (b) shows the flame obtained with the aluminium plate with number of opening placed in the combustion chamber, a diffusion type unstable flame was observed in this case too.

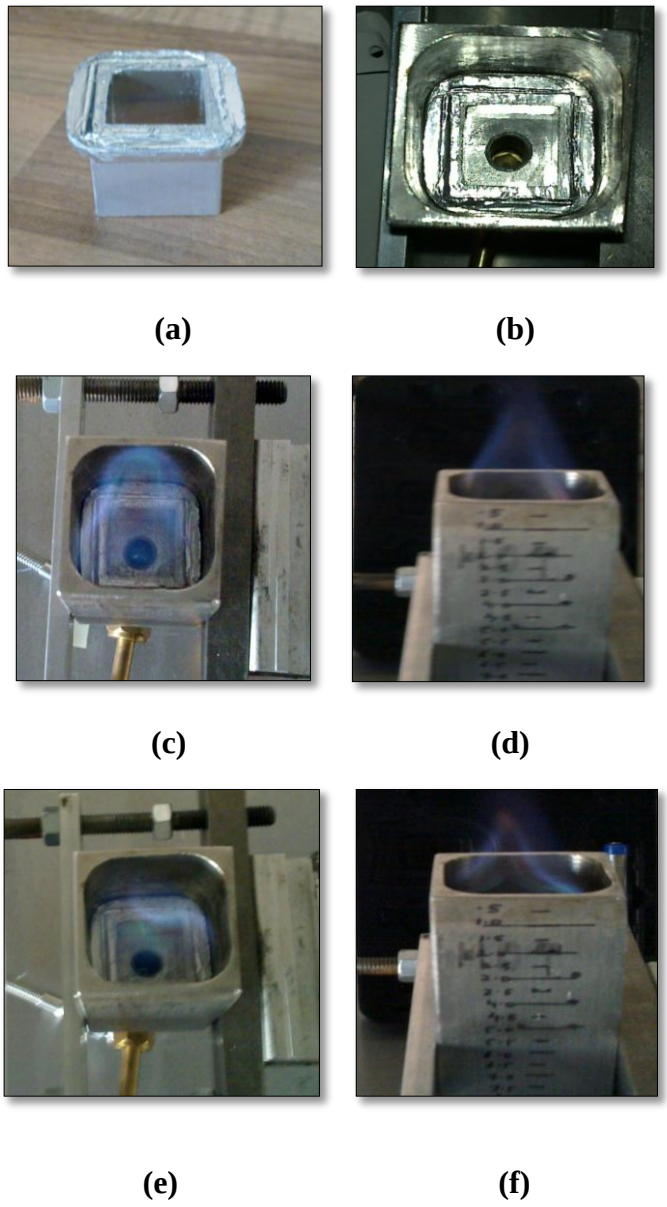

(a) **(b)**

(c) **(d)**

(e) **(f)**

Figure 5.5: (a) and (b) Aluminium 'seat' was inserted in the combustion chamber; (c) and (d) Flame pictures at Vf=200 mL/min and 4 air holes open , (e) and (f) Flame pictures at Vf=150 mL/min, 4 air holes open

Figure 5.5 (a) and 5.5 (b) shows another type of bluff body which is aluminium 'seat' placed in the combustion chamber in order to reduce the step height i.e. reducing the expansion ratio. This bluff body showed some signs of combustion in the desired location which is inside of the combustion chamber rather than flame resting on the extreme downstream of the burner which was the case with the Prototype 1. The photographs of flames obtained with this type of bluff body at fuel supply of 200 mL/min are shown in Figure 5.5 (c) and 5.5 (d). Similarly photographs of burner operating at 150 mL/min are shown in Figure 5.5 (e) and 5.5 (f).

5.2.2 Prototype 2

Based on the results from Prototype 1 with an aluminium 'seat' which showed some signs of combustion and flashback, Prototype 2 was designed with the same requirements and aims as the previous one but focus was given on reducing the height of backward facing step which would reduce the expansion ratio. Flame flashback was also observed in the Prototype 1 which suggested that the stream velocity was lower than the burning velocity of the flame. In order to address this issue, the diameter of secondary mixing zone was reduced which would prevent the flame from travelling upstream. When the stream is moving downstream in a smaller diameter channel its velocity is higher as compared to a stream moving downstream in a bigger diameter channel. So the motivation behind this modification was to increase the downstream flow velocity so that it is higher than the burning velocity. As the final product will be mass produced, emphasis has been given on designing the unit in a way which reduces manufacturing cost and simplifies the manufacturing process. The internal geometry of the combustion chamber in the first prototype is square which was designed to facilitate uniform heat transfer to burner walls where TEG modules will be placed. The internal geometry was made cylindrical instead of square to make mass manufacturing simple and economical.

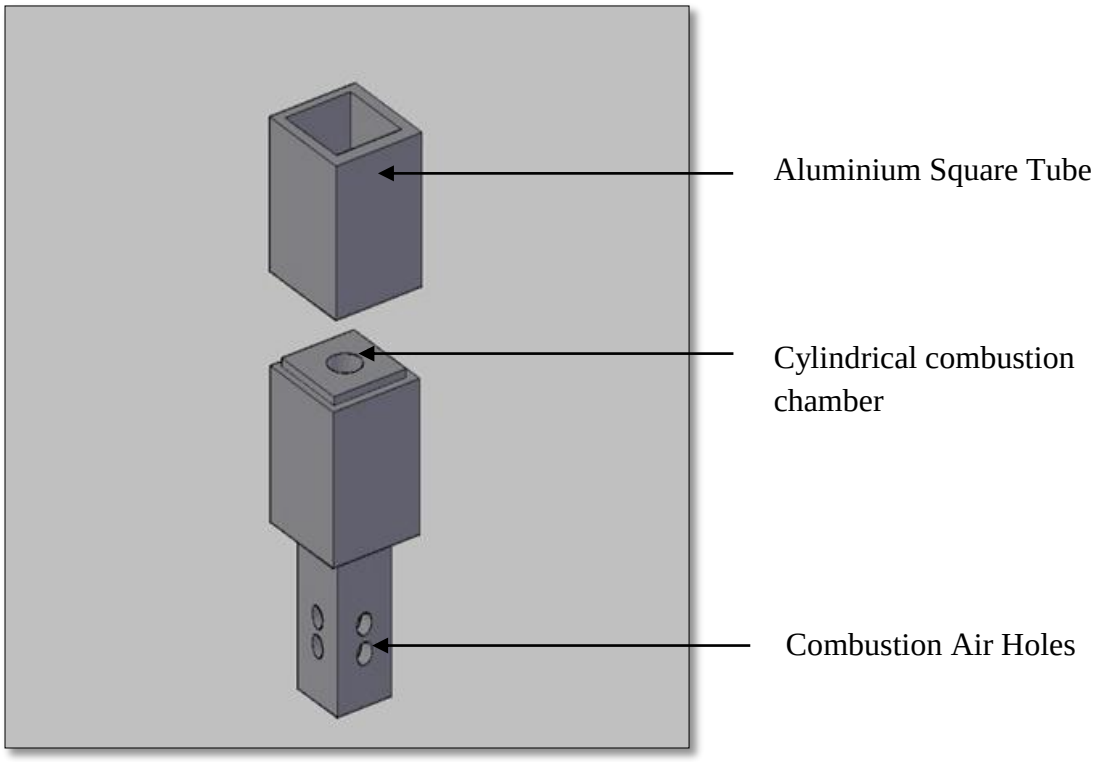

Figure 5.6: A 3-D CAD model of Prototype-2

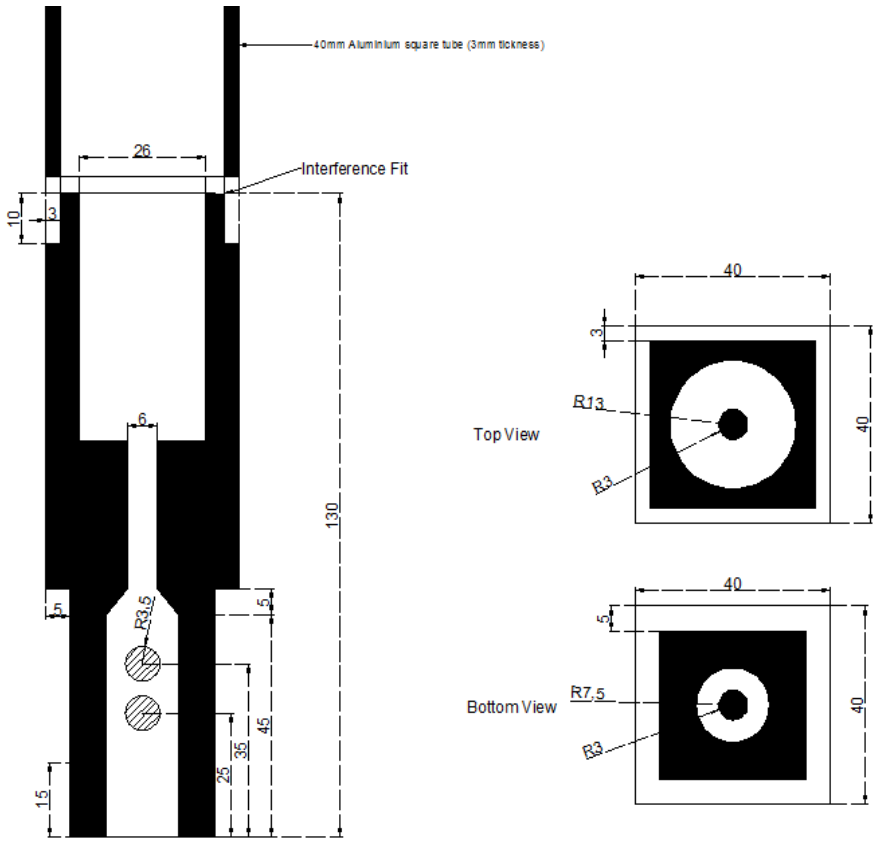

Figure 5.7: A 2-D CAD Drawing of Prototype-2

The burner is made up of two sections as shown in the 3-D drawing in Figure 5.6; the first section is made of stainless steel which consists of the mixing zones and backward facing step and the second section is 40 mm square aluminium tube having thickness 3 mm. The aluminium square section is where the TEG modules will be placed later.

As shown in Figure 5.7, the major design changes are reduction in the step height from 13 mm to 10 mm, diameter of the secondary mixing zone is reduced to 6 mm from 8 mm and the internal geometry of the combustion chamber is cylindrical instead of square which was the case in Prototype 1. In operation, propane is injected in the primary mixing zone through a 0.28 mm brass injector; the stream flowing downstream entrains combustion air in the similar way as in Prototype 1. The aim is to anchor the flame in 50mm long cylindrical combustion chamber just after the backward facing step with its tip entering in the aluminium tube. The exhaust gas would move downstream and exits the burner from the top.

As was the case with Prototype 1, it is important here to note that the burner was operating on 'self-aspiration mode' i.e. the air was naturally entrained through air holes on the sides of primary mixing zone/chamber. The only way to vary the air was to change the effective area of air holes; hence it was not possible to determine the equivalence ratio which would be determined later by performing gas analysis using FTIR and operating the burner under 'forced air supply mode'. The burner was set up to run at the desired mass flow rate i.e. 150 mL/min of propane. On lighting the burner, there was no stable flame observed inside the combustion chamber which was similar to the prototype 1 results. Upon ignition, the mixture would ignite in combustion chamber but soon the flame would start to move downstream until it reaches the top of the aluminium tube as shown in the Figure 5.8. Various different gas supply rates were tested but similar results were obtained with flame travelling all the way downstream to anchor on top of the burner which is not the desired location for the flame. The flame is more like a diffusion one than a premixed with yellowish orange colour as shown in the Figure 5.9 (V_f=200 mL/min).

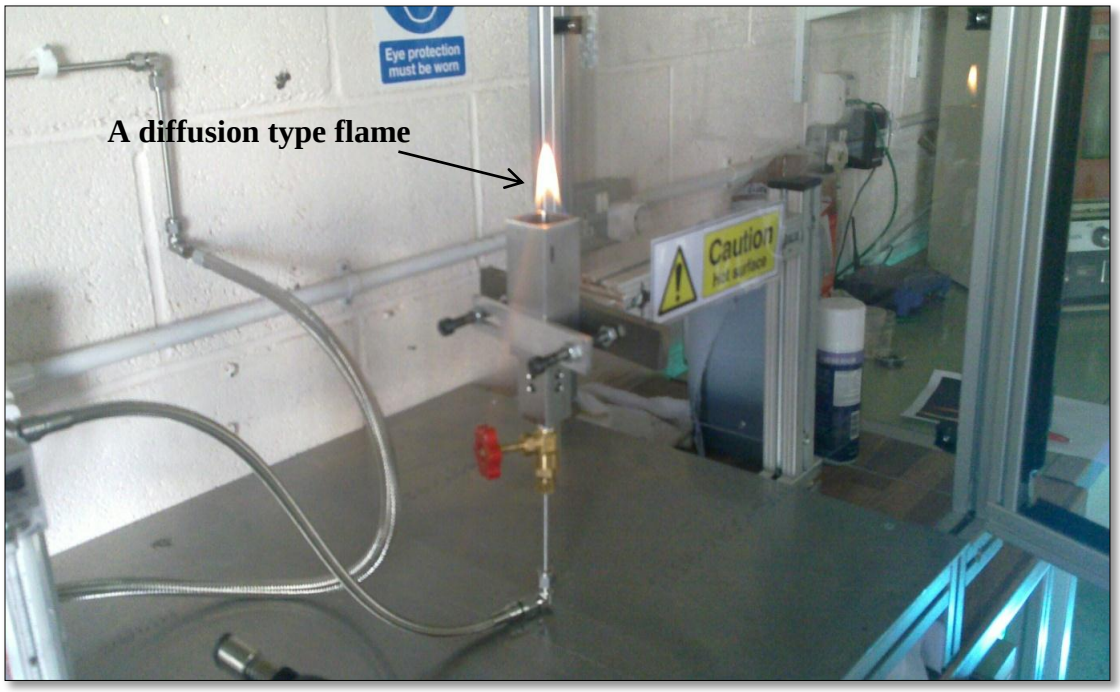

Figure 5.8: Photograph showing flame stabilising itself at the exit at 200 mL/min of propane.

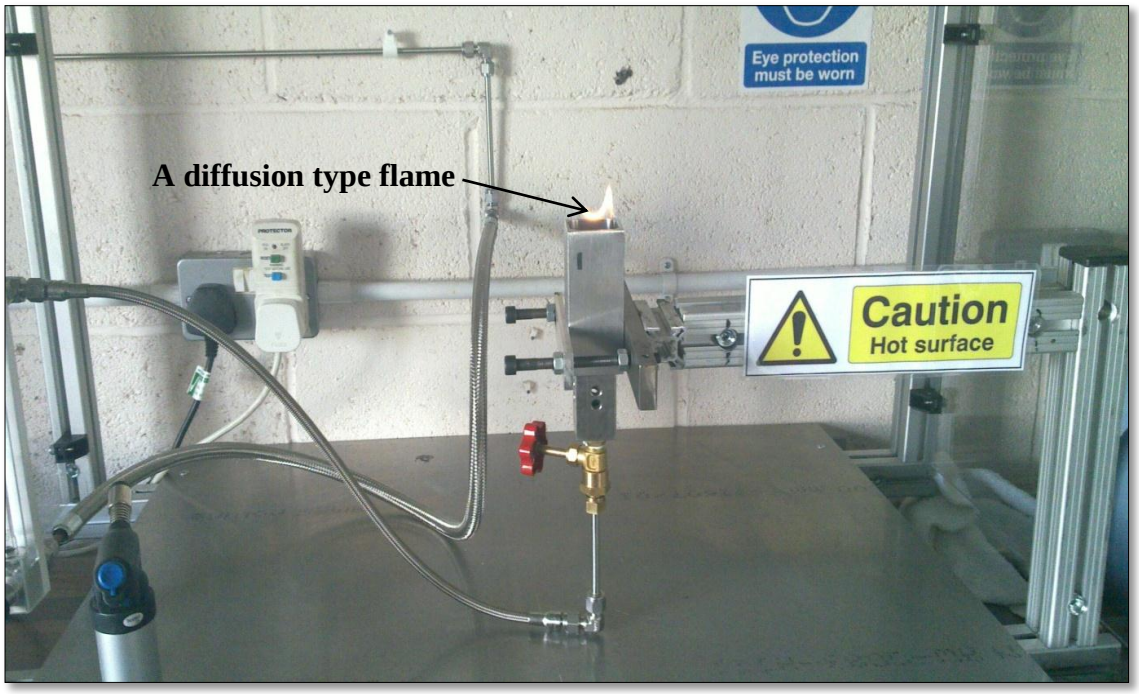

Figure 5.9: Photograph showing flame stabilising itself at the exit at 150 mL/min of propane

As seen in the above two pictures, regardless of the mixture composition, the flame was either not present or it was stabilised on top of the burner.

5.2.3 Prototype 3

The only design change in prototype 3 is the introduction of secondary combustion air with the aim of stabilising the flame in the combustion chamber over the backward facing step. As shown in the Figure 5.10, 15 air holes having diameter 3mm were machined 25mm above the backward facing step.

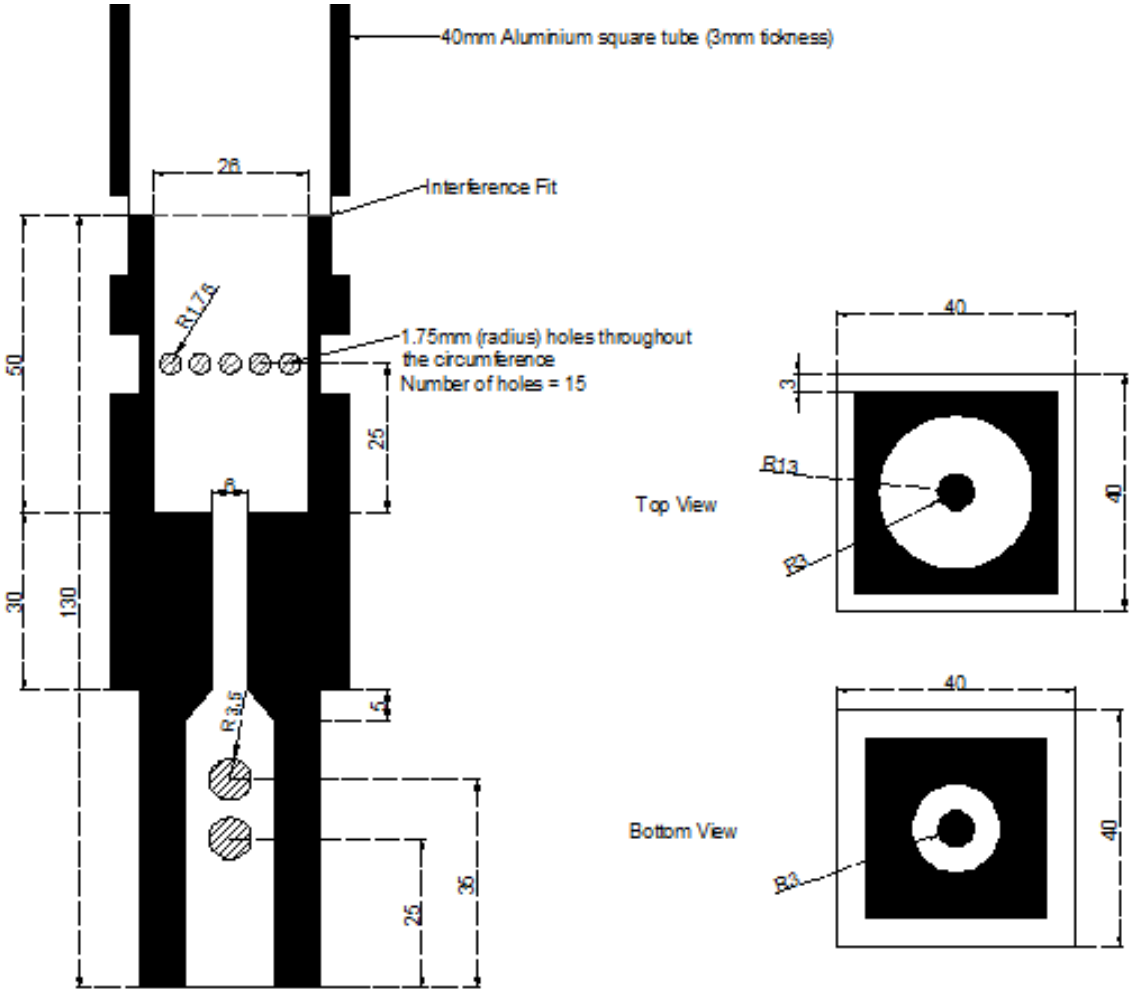

Figure 5.10: A 2-D CAD model of Prototype-3

Figure 5.10 shows a 2-D drawing of Prototype 3 with main feature introduced was secondary air holes.

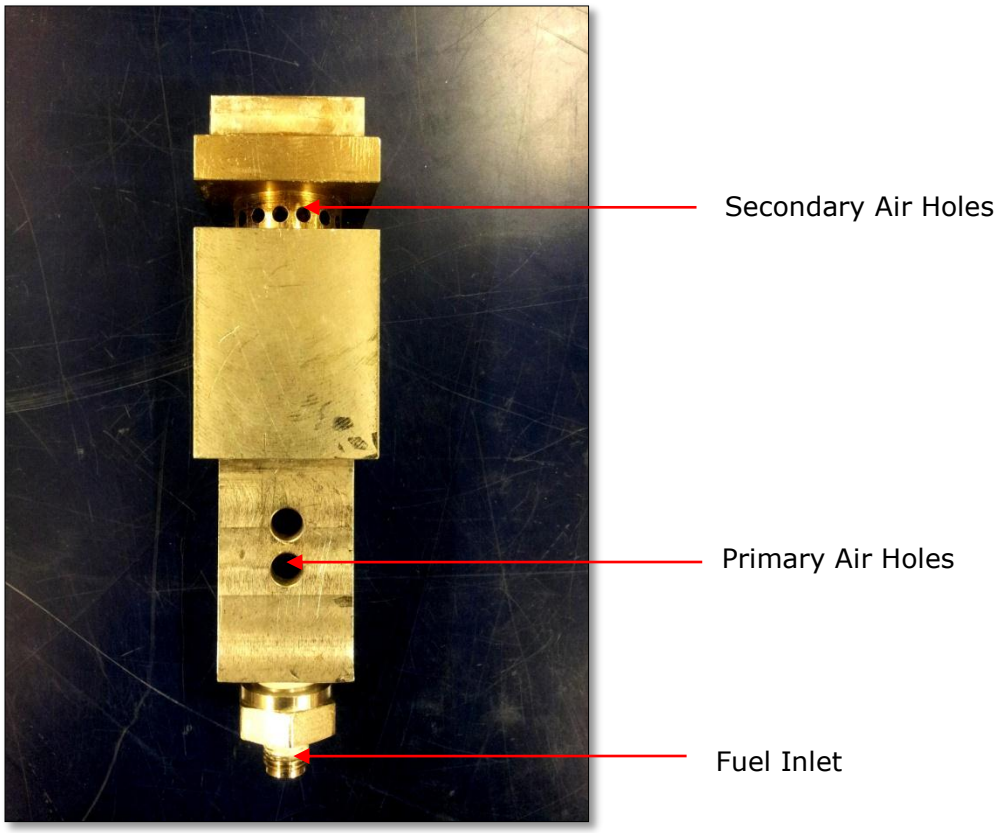

Figure 5.11: Prototype-3 with secondary air holes

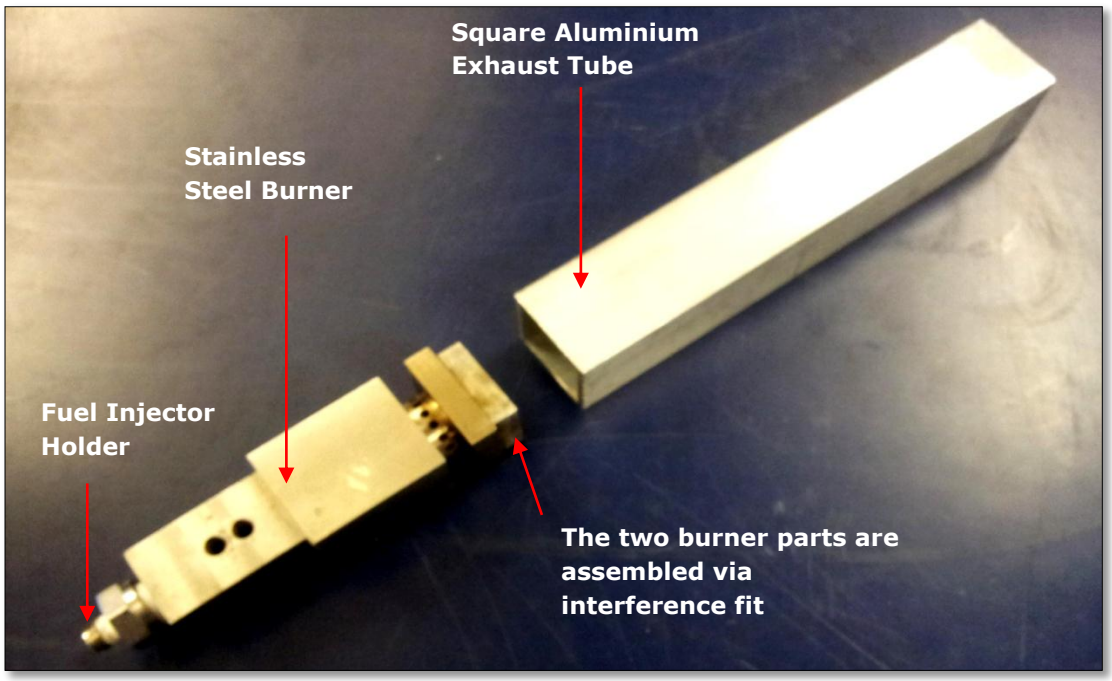

Figure 5.12: A photograph of Prototype-3 with Aluminium square chimney tube

The stainless steel Prototype 3 with secondary air holes is shown in the Figure 5.11. The remaining design of the stainless steel burner is nominally the same as Prototype 2 except

the reduction of wall thickness where the secondary air holes are made. The method of secondary air supply is same as primary air supply i.e. the air is entrained into the combustion chamber by the downstream moving fuel and air mixture formed in the primary and secondary mixing zones. The operation of burner and fuel supply is also same as the previous version. Similar to previous two prototypes, it was not possible to determine the equivalence ratio as the air supply could not be metered due to operating requirements of the unit. When the burner was ignited upon setting the burner at the required fuel supply, a stable flame was observed at all air supplies. The flame is anchored on the secondary air holes and do not show any fluctuation at the required flow rate of 150 mL/min propane and 2 air holes open.

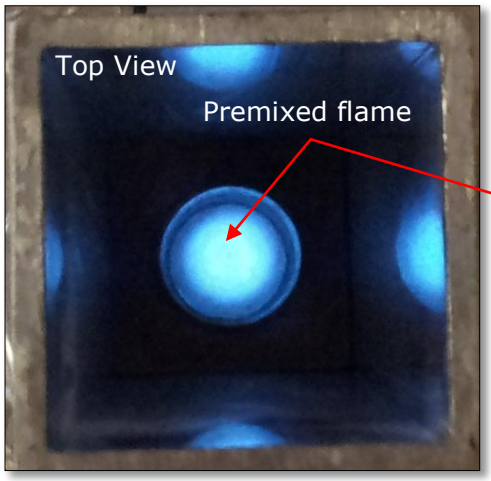

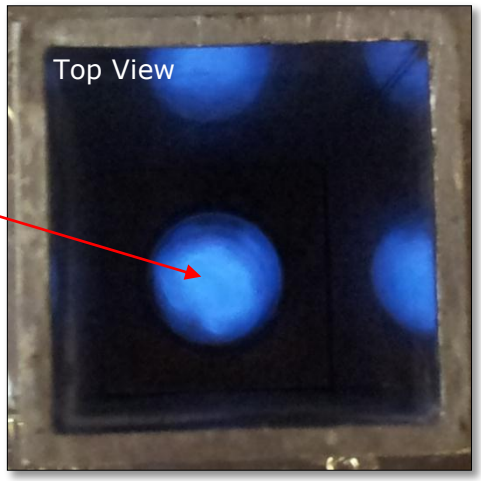

Figure 5.13: V_f=150 mL/min, 2 air holes

Figure 5.14: V_f=125 mL/min, 2 air holes

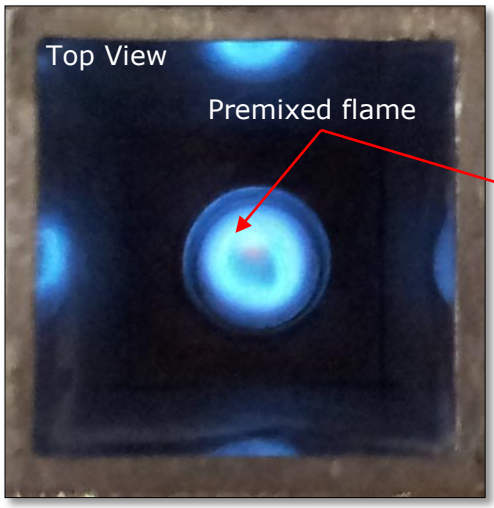

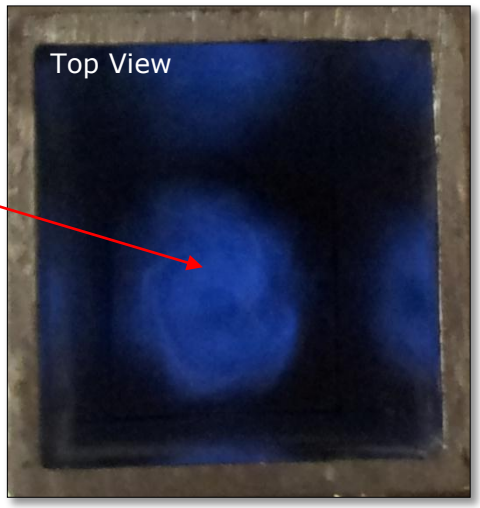

Figure 5.15: V_f=200 mL/min, 2 air holes

Figure 5.16: V_f=100 mL/min, 2 air holes

Figure 5.13-16 shows photographs of flame obtained with Prototype 3 at fuel flow rate ranging from 100 mL/min to 200 mL/min. It is evident from the above pictures that

secondary air supply had a significant effect on flame stabilisation inside the burner. A detailed experimental analysis has been done in the later chapters to study this phenomenon. This method of flame stabilisation can be very useful in self-aspirating premixed burners.

5.3 Exhaust Gas Analysis

The quality of CO_2 is of utmost importance due to its application in insect attraction which is purely dependent upon CO_2 production rate while other compounds in the exhaust plume such as CO or NOx can repel the insects. To analyse the products of combustion, gas analysis was performed. The burner was set at the required operating parameters and using a probe, exhaust sample was sent to the gas analyser through a compressor pump.

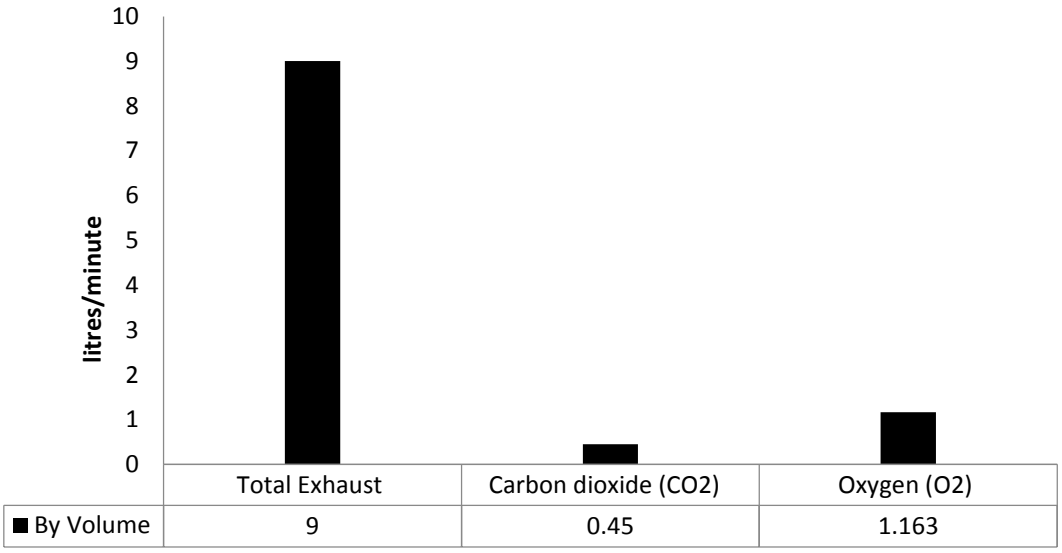

Figure 5.17: FTIR results showing concentrations of CO_2 and O_2

The Figure 5.17 represents average production of CO_2 and O_2 over continuous operation of the burner for 1 hour. Two primary air holes and all the 15 secondary air holes were kept open as this provided the most stable flame in the combustion chamber. Again in this experiment there was no metering of combustion air due to its application as a self-aspirating burner. The average percentage of CO_2 in the exhaust shown by the gas analyser was 5.2% while average O_2 was 12.93%. The total exhaust is determined using stoichiometric equation of propane. The burner was set up at 150 mL/min of propane which should produce 450 mL/min of CO_2 at stoichiometric conditions. Using the stoichiometric equation for propane, the total exhaust is calculated to be ~ 9L/min as the burner is producing 0.450 L/min of CO_2 at stoichiometry which is 5.2% of total exhaust shown by gas analyser.

The Figure 5.18 shows average concentration of CO, NOx and THC present in the exhaust. The concentration of CO was 72.5ppm which corresponds to 0.65mL/min by volume and average NOx was 29ppm corresponding to 0.25mL/min. There were no traces of any un-burnt hydrocarbons in the exhaust indicating complete combustion of propane.

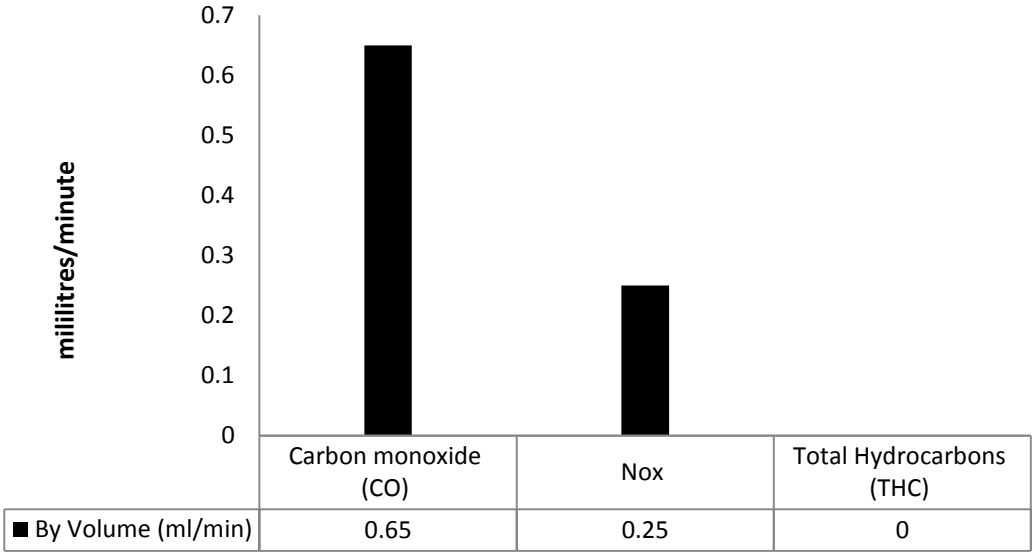

Figure 5.18: FTIR results showing concentrations of CO, NOx and THC

The production of CO can be attributed to the cooling of flame due to secondary air supply near the secondary air holes which was introduced to facilitate flame stabilisation.

According to entomological experts working alongside the project, the gas analysis results were good enough to go ahead to the next stage of product development i.e. integration with thermoelectrics. The CO and NOx concentrations produced in these experiments were not a sign of concern in terms of its application as the concentration shown by the analyser was in the sample taken from exhaust chimney which gets diluted in the atmosphere as soon as exhaust exits the burner.

The absence of un-burnt hydrocarbons and low concentration of compounds such as CO and NOx shows that the addition of secondary air not just only helps in achieving a stable combustion but also contributes towards clean and efficient combustion. Further analysis was performed after integrating the burner with thermoelectric modules and heat exchangers. The results will be shown later in the thesis.

The primary air supply was varied by changing the effective area of primary air holes and gas analysis was performed which showed similar productions rates for the compounds. The CO and NOx were not significantly high and the CO_2 production was sufficient for the application.

5.4 Summary

This chapter presented results from development and investigation of a premixed meso-scale self-aspirating burner. Three stainless steel prototypes were tested with focus on obtaining a stable flame at the desired location and operating at the required fuel supply i.e. 150 mL/min. The main features of the burner in all the three prototypes were a backward facing step to enhance mixing of reactants by generating recirculation zones and square shape of the burner to accommodate TEG modules. The experimental results showed that the Prototypes 1 and 2 were unable to provide a stable flame with combustion taking place at the extreme downstream i.e. the flame was resting at the exit on top of the burner. Prototype 3 was designed with the addition of secondary combustion air at the step; the results showed a stable premixed blue flame at the desired location and at the required fuel input.

After satisfying results shown by Prototype 3, the burner was tested for the concentration of products of combustion by FTIR. The results showed that the combustion was complete with no UHC present in the exhaust. The CO_2 production rate was found to be 450mL/min, which satisfies the CO_2 production requirement for the device. The concentrations of CO and NOx were found to be 72 ppm and 29 ppm respectively which were not considered significantly high for the application of the device.

Chapter 6

Integration with Thermoelectrics

6.1 Introduction

One of the main design requirements is 3.5 W electrical power output, which is the power required to operate a DC fan. This fan is an integral part of the insect catching apparatus which captures and holds the insects inside a catch bag as described in the Chapter 1. The cost of the final product is also a major factor as thermoelectric power generation modules are the most expensive component of the unit. Hence, the number of modules to be employed affects the overall cost of final product. So the design consideration in thermoelectrics optimisation has been to achieve higher electrical power with minimum number of modules used through an efficient means of heat dissipation at the cold side and heat absorption from the combustion exhaust at the hot side to maximise temperature difference. Higher temperature difference is desired as power output is directly proportional to temperature difference. In this section, optimisation of the hot side of the module has been experimentally performed which includes identifying a mechanism to increase the hot side temperature of the module to achieve higher temperature difference. Subsequently design configurations were tested, which consisted of varying the arrangement of TEG modules and heat exchangers. After identifying the ideal design configuration, optimisation of the cold side of the module was experimentally performed, this consisted of testing various shapes and sizes of cold side heat exchangers.

6.2 Hot Side Optimisation

As mentioned in the literature review, the power generation of a TEG module is directly proportional to temperature difference across the two sides of the module [71-75]. One way to optimise temperature difference is by optimising the hot side to attain maximum possible temperature. A higher temperature of the hot side of the module is desired which would result in higher temperature difference across the two sides of the module and hence higher power output.

The hot side of a TEG module is the side which is in contact with the burner wall as shown in the Figure 6.1.

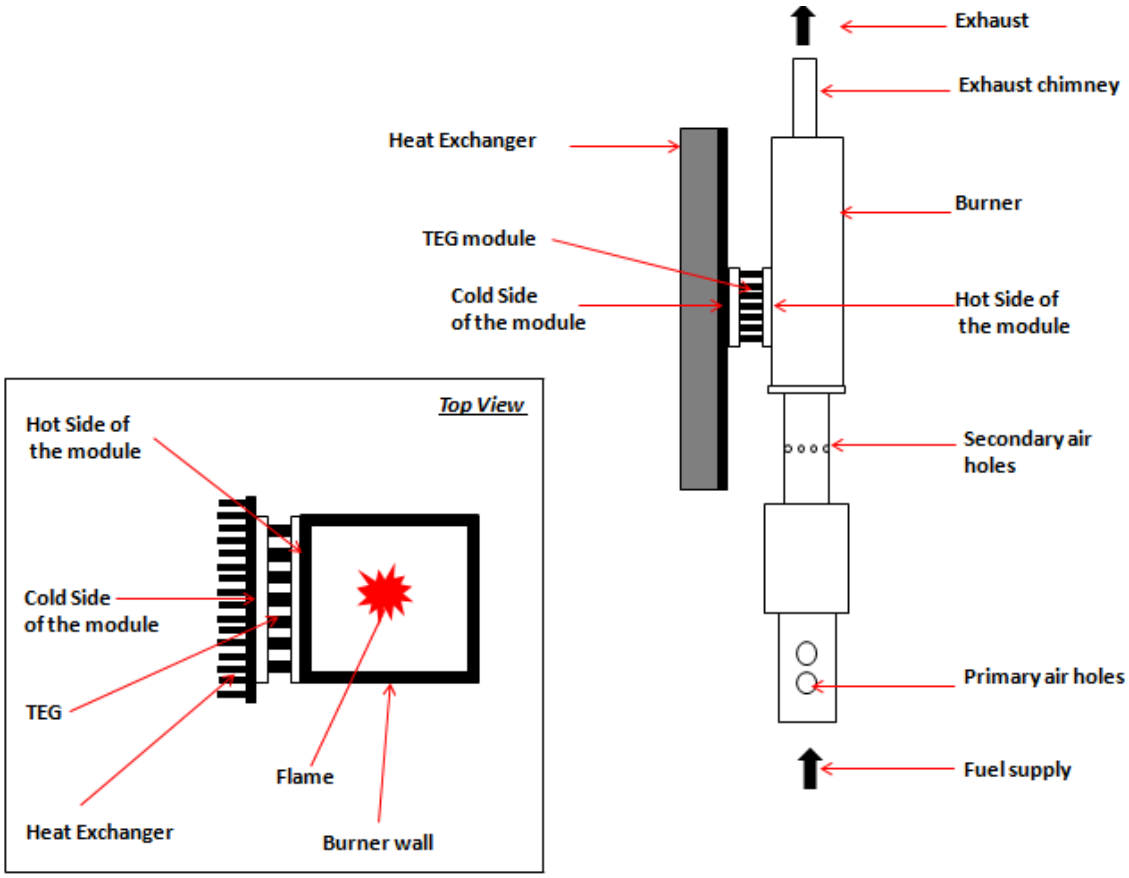

Figure 6.1: A schematic diagram of burner and TEG assembly

Figure 6.1 presents the schematic diagram showing hot and cold sides of the TEG module in a burner TEG assembly. The hot side is in contact with the burner wall while the cold side has been provided with a heat exchanger. The focus has been given on achieving optimum hot side temperature by extracting maximum heat from the combustion exhaust. The important factor to consider here is that the heat output of the burner is fixed due to operating requirements. This means that the fuel supply to the burner cannot be increased as it would reduce the number of days a 13 kg gas bottle would last. So, a design feature was sought which would help in achieving a high hot side temperature of the module by extracting limited heat available from the burner.

Figure 6.2 shows the burner unit which consists of two parts; stainless steel base consisting of the fuel nozzle, mixing zones and combustion chamber, and the square aluminium tube. The two parts were assembled through interference forming a single unit. The tests were performed to find out the wall temperatures of the square chimney without integrating the TEG modules. The next test consisted of obtaining temperature profiles of the wall of the burner after integrating the TEG modules on the sides of square chimney.

The fuel inlet to the burner was kept at 150 mL/min propane resulting in 250 W heat output.

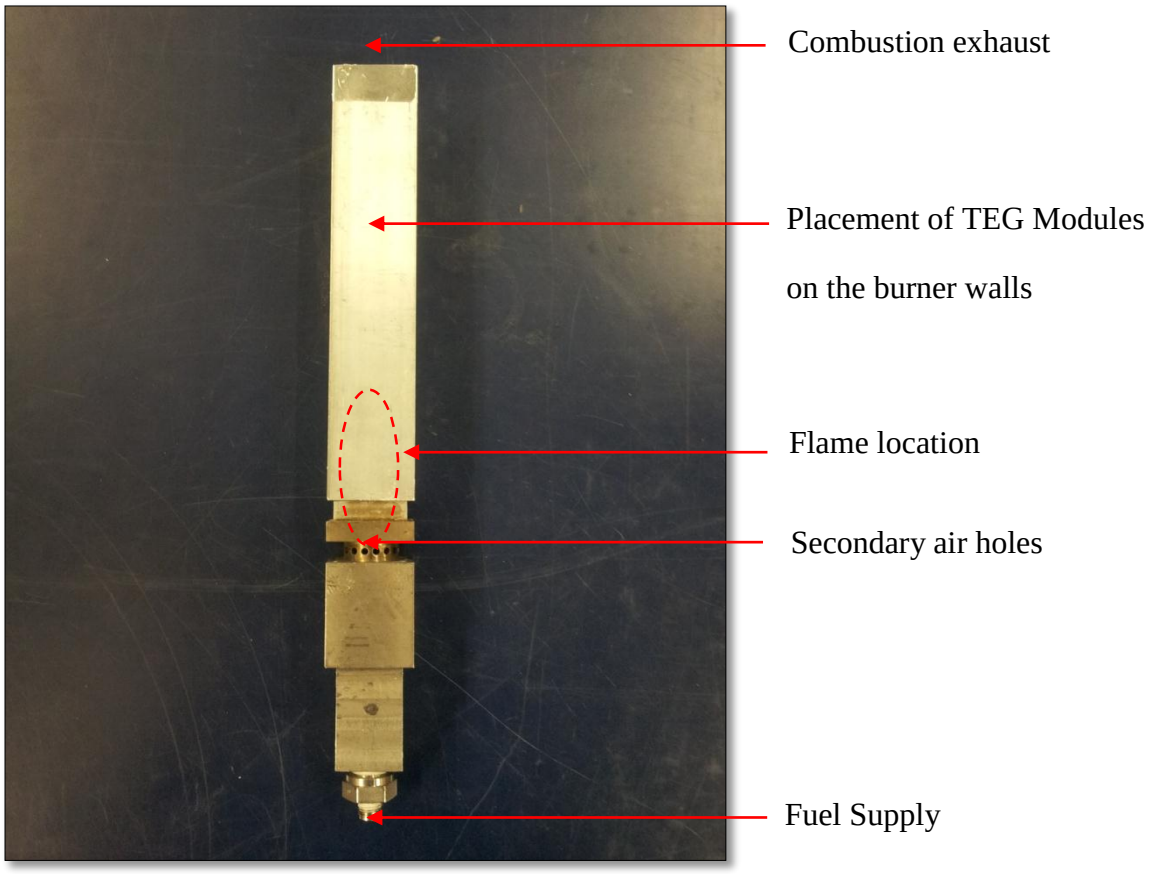

Figure 6.2: A photograph indicating placement of TEG modules on the burner tube

The placement/location of TEG module on the burner is important as it determines how much heat is flowing through it. In this regard, modules were placed as different location on the burner exhaust tube.

The graph in Figure 6.3 shows temperature of the wall of the burner (T_H without TEG and HE) and wall temperature after integrating the TEG module on the burner wall (T_H with TEG and HE). The burner TEG assembly used for this test is shown in Figure 6.1.

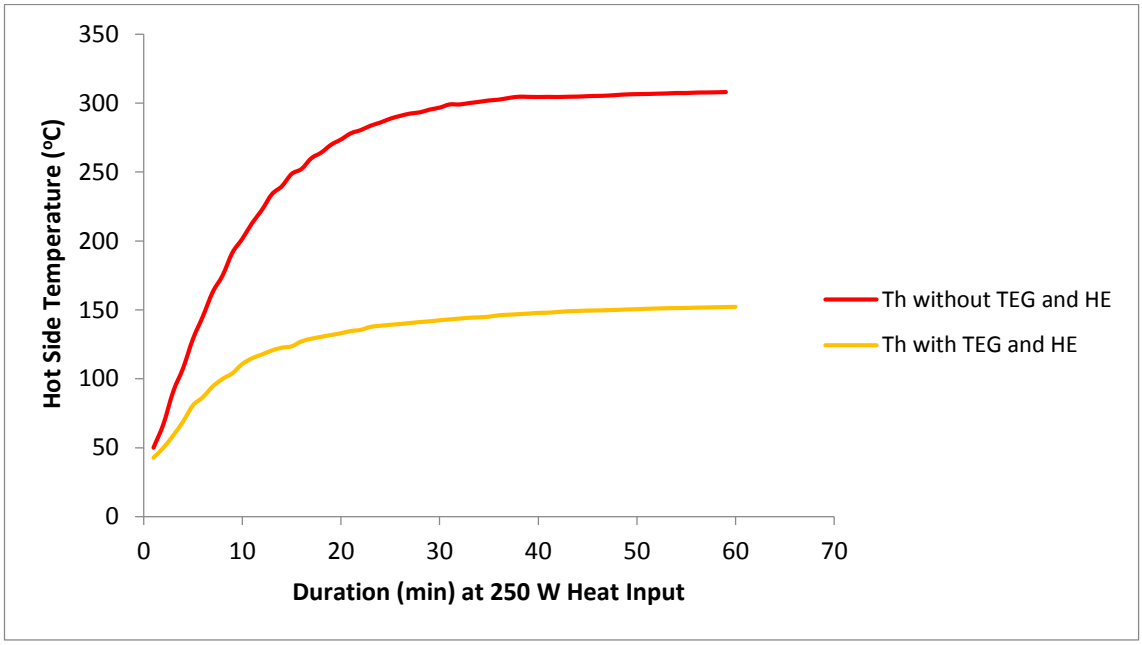

Figure 6.3: Graph showing wall temperature (T_H) with and without integration with TEGs

It can be seen in Figure 6.3 that T_H without TEG modules is around 300 °C and the T_H after placing TEG modules on the burner wall is around 140 °C. There is a significant drop in the wall temperature when modules are placed on the burner wall. Therefore, the objective of optimisation of the hot side was to find a method to increase or in other words optimise the temperature of the hot side of the module. An aluminium square profile having internal fins (referred as Internal Heat Sinks hereafter) was connected to the burner tube with the aim of extracting more heat from exhaust gases as shown in the Figure 6.4.

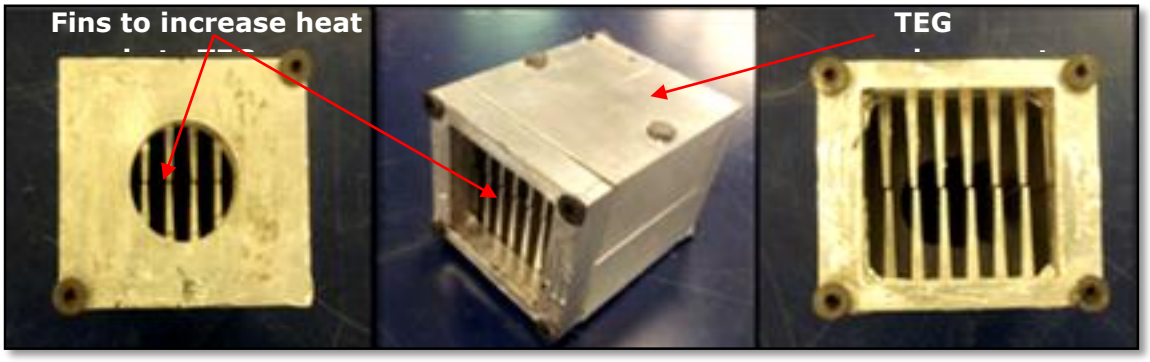

Figure 6.4: A photograph of Aluminium Internal Heat Sinks

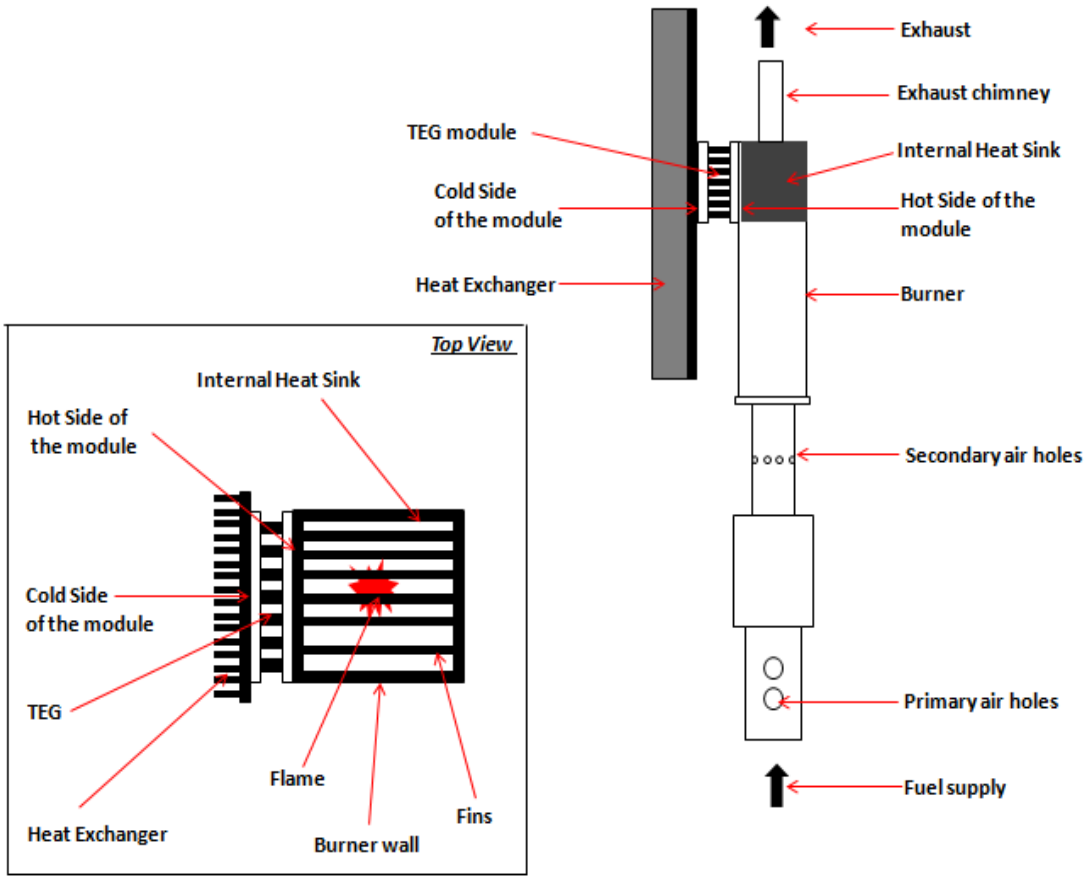

Figure 6.5: A schematic diagram of burner and TEG assembly with IHS

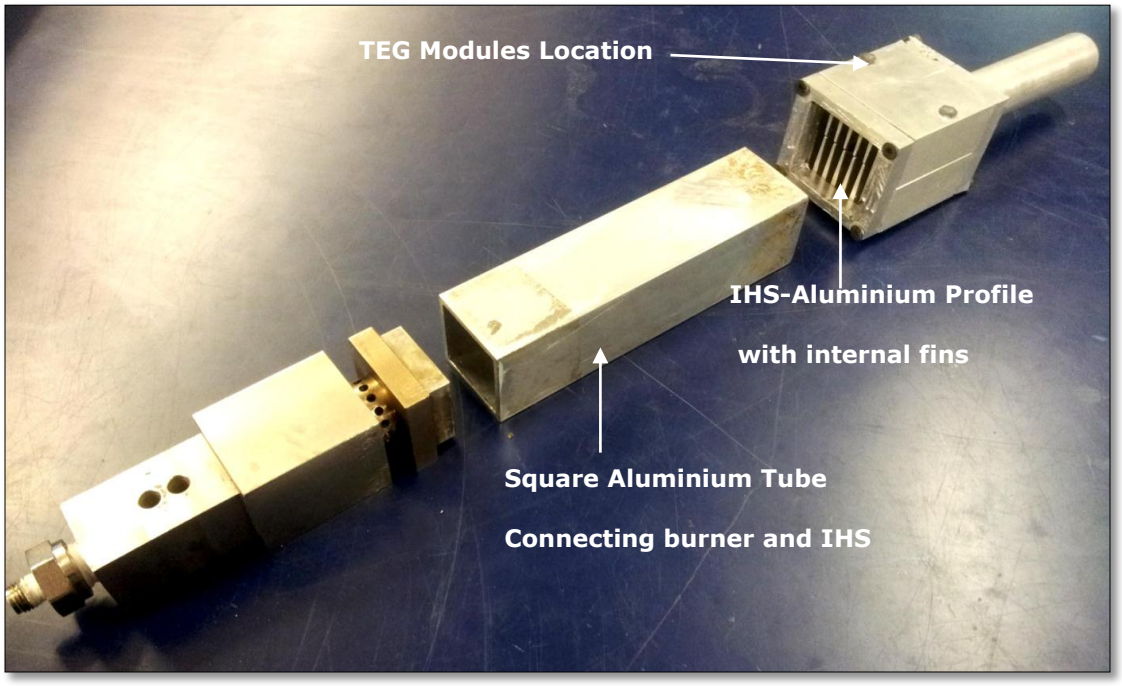

Figure 6.6: A photograph showing burner equipped with square aluminium tube and IHS

Figure 6.5 shows the schematic of the burner and TEG assembly with Internal Heat Sink connected on top of the aluminium square tube. Figure 6.6 shows a picture of the burner

and thermoelectric power generator assembly which are connected together by the square aluminium tube. The internal fins are provided to absorb heat from the hot exhaust gases flowing downstream of the burner tube. The TEG modules were placed on the two sides having internal fins so that more heat is absorbed by the fins and hence supplied to the TEG modules.

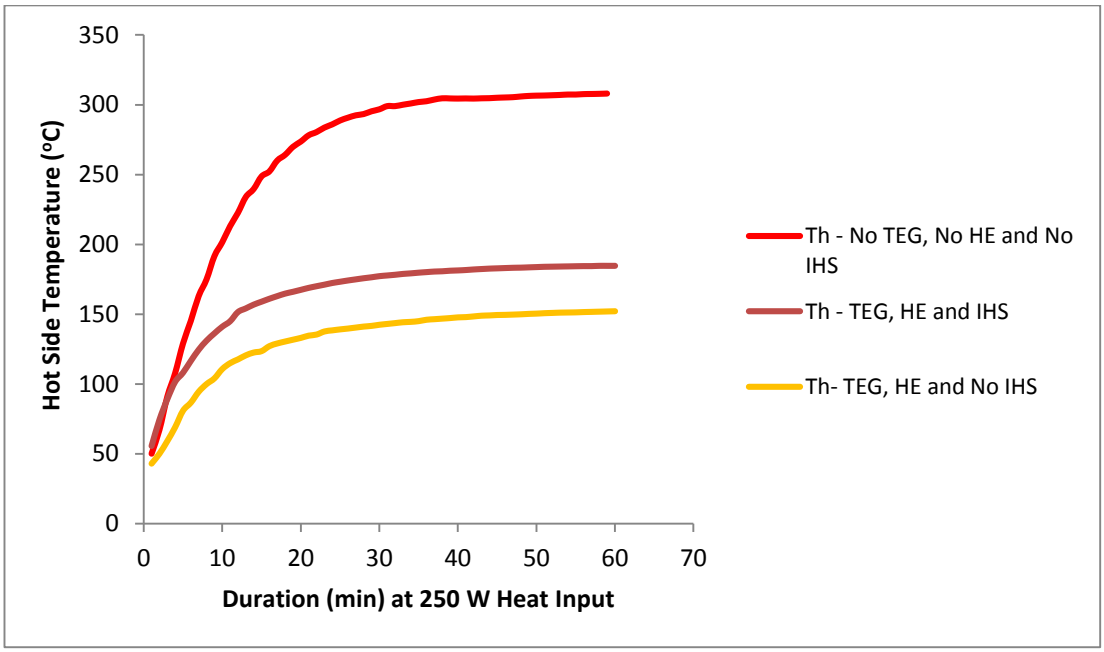

Figure 6.7: Graph showing T_H without TEG integration, T_H with TEG integration and T_H with TEG on IHS

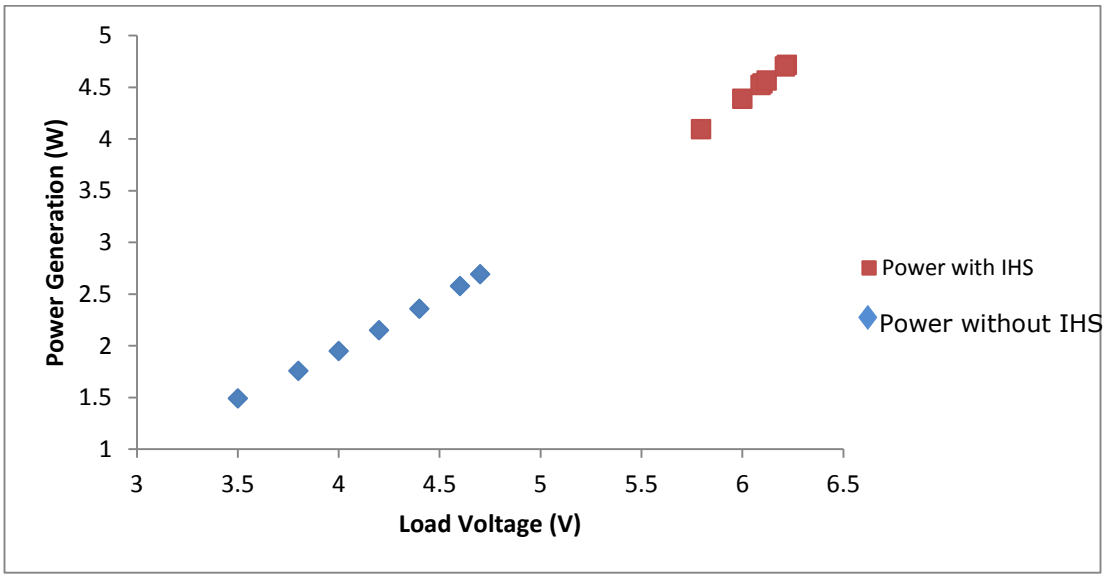

Figure 6.8: Graph for Power Generation with and without IHS

Figure 6.7 shows a comparison of temperature profiles i.e. T_H with no TEG and no IHS, T_H with TEG but no IHS and T_H with TEG and IHS. For same amount of fuel supply in all the three mentioned cases, it can be seen that the hot side temperature was increased

with IHS. The increase in hot side temperature has clearly shown improvement in temperature difference and hence power generation and load voltage output shown in Figure 6.8.

It was clearly evident that an increase in power generation and voltage output is achieved with internal heat sinks employed.

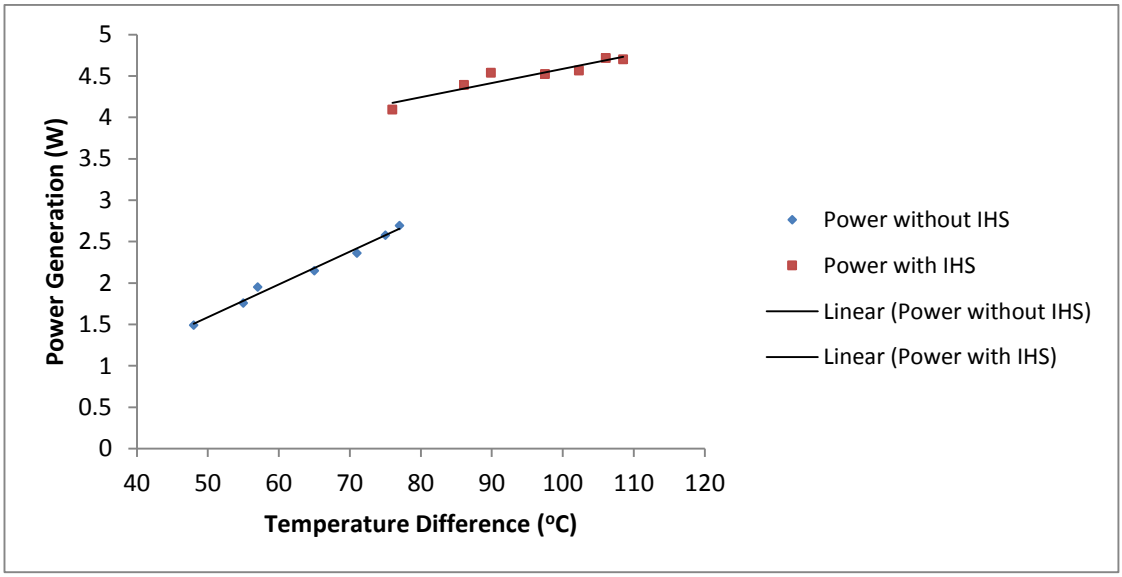

Figure 6.9: Graph comparing Power Generation and Temperature Difference with and without HIS

Figure 6.9 shows temperature difference and corresponding power generation with and without IHS. The results showed that higher temperature difference could be achieved with IHS. It can be seen in the graph that at the same temperature difference, the power output was higher with IHS than without IHS. This can be attributed to the fact that the placement of the thermocouple was at the centre of the TEG, which suggests that the TH was same around the centre of the TEG for both with and without HIS configurations, but was lower towards the sides for without IHS configuration. Hence, this suggested that the heat supplied to the TEG in without IHS configuration was not uniform over the whole area of the module and some of the thermo-elements, located away from the centre of the TEG, were operating at a lower temperature difference than the others. On the other hand, when IHS was employed, fins of the IHS facilitated uniform heat supply to the whole area of the module thus producing more power. Thus, the IHS not only increased the heat supply to the TEG module but it also enabled a uniform heat supply to the whole area of the module.

The burner tube was subsequently made up into two pieces; an aluminium square tube and a square aluminium profile having internal fins, both connected to each other via interference fit.

6.3 Design Optimisation

Various different configurations were tested with the objective of improvement in power generation keeping the cost of the final product in focus. These configurations differ from each other on the basis of heat sink orientations, number of heat sinks and internal heat sinks used and number of TEG modules employed and thus a comparison between these configuration options was essential in defining the operation of the system.

Table 6.1: Summary of the configurations

Configuration	Cooling Heat Exchangers	Internal Heat Sink(s)	TEG modules
Nominal	2	1	2
C1	2	1	2
C2	2	2	4
C3	2	2	4
C4	4	1	4
C5	3	1	3

Table 6.1 provides details on the main components used in various configurations investigated in the present study. Along with the number of each component used in the configurations, the arrangement and orientations of these components have been varied too.

Firstly, the ‘Nominal Configuration’ will be described, the schematic diagram of which is shown in the Figure 6.10 and a photograph of tests being carried out on the Nominal Configuration is shown in Figure 6.11, it is constructed and assembled based on the results from the ‘Hot side optimisation design stage’. This design configuration was kept as the nominal design which consisted of 2 TEG modules placed on the opposite sides of internal heat sink as described in the previous sections. The cold side heat sinks were two 500 mm long, 40 mm wide aluminium profiles and the height of the fins was 70 mm. Experiments were performed on various modified versions of the ‘Nominal Configuration’ and a comparison of results was done.

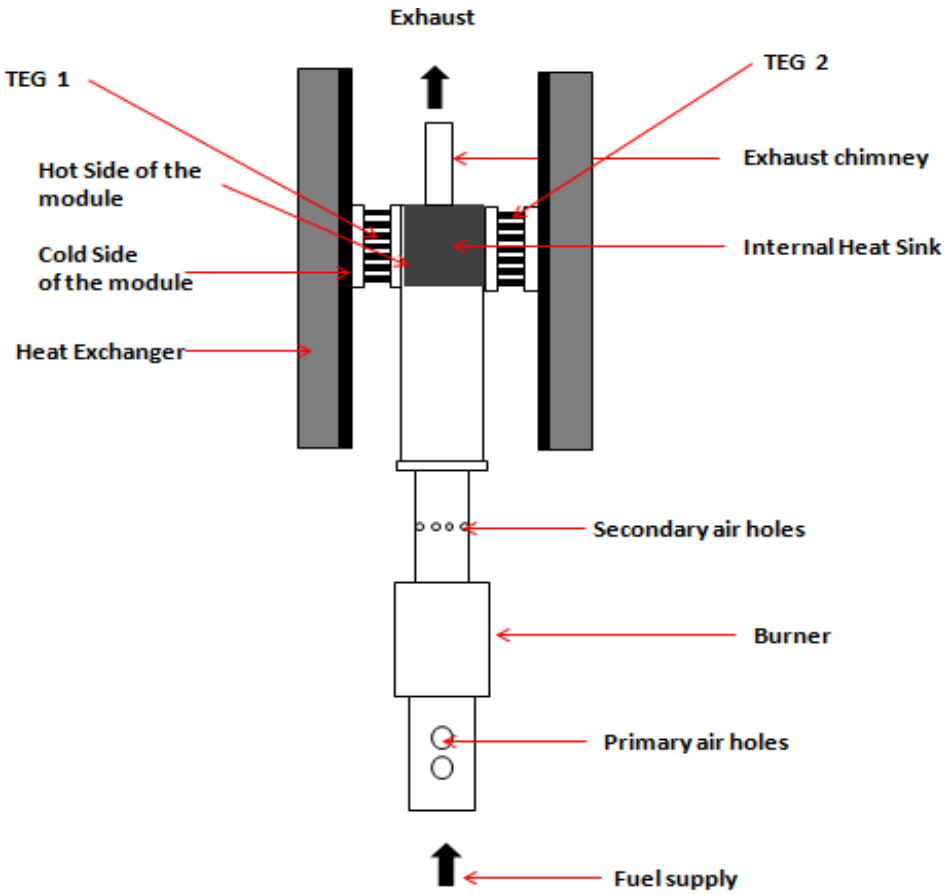

Figure 6.10: Schematic diagram of Nominal Configuration

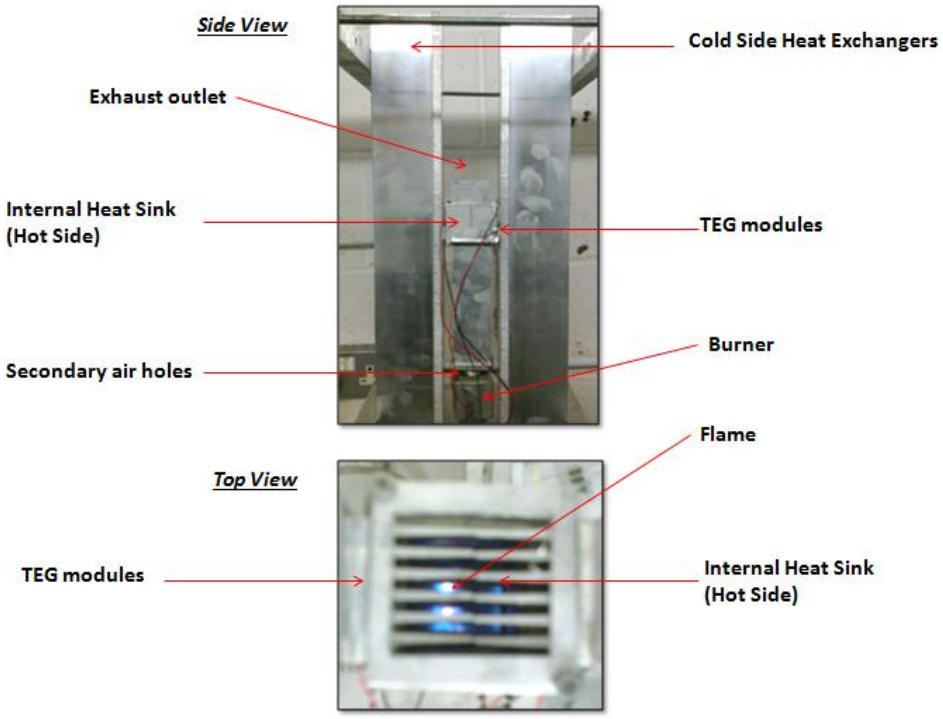

Figure 6.11: A photograph of Nominal Configuration

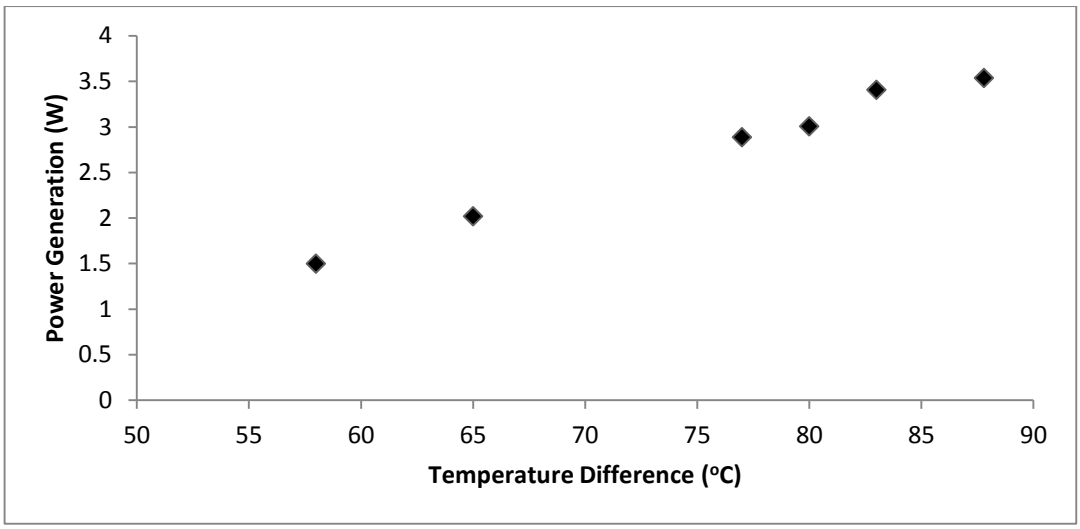

Figure 6.12: Graph showing Power generation at respective Temperature Difference for Nominal Configuration

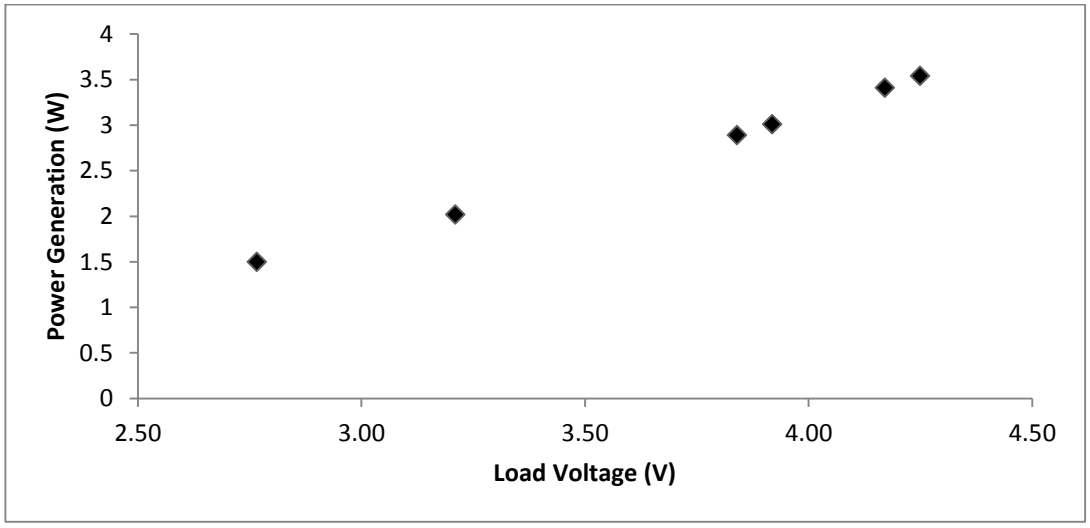

Figure 6.13: Graph showing Power Generation and Load Voltage output of Nominal Configuration

Figure 6.12 shows power generation at various temperature differences and Figure 6.13 shows power generation and load voltage output for Nominal Configuration.

It can be seen in the graphs above that at a duration of 30 minutes from ignition at 250 W heat input, the electrical power generation was around 3.54 W corresponding to a 4.25 V of load voltage at a temperature difference of 87.8 ^{o}C. These results were considered as a basis of comparison with the results from various modified versions of nominal configuration.

It should be noted that the term 'power generator' will be used from hereafter which refers to an assembly of internal heat sink and thermoelectric module(s).

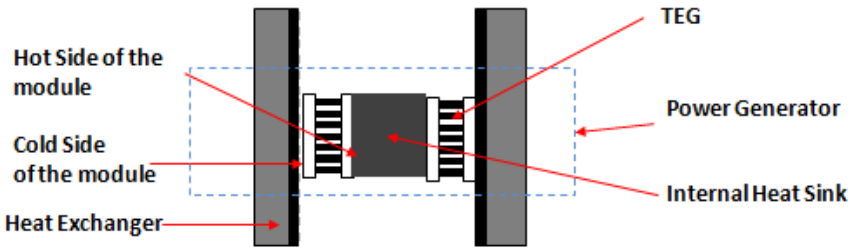

Figure 6.14: Schematic diagram of a 'Power Generator'

A power generator is shown in the Figure 6.14 which in this case consists of 2 TEG modules placed on the opposite sides of the IHS. The hot side of the modules is the wall of IHS where the modules are accommodated. The cold side of the modules has a heat exchanger. This assembly will be referred as a power generator in this research.

6.3.1 Configuration 1

This configuration is similar to the nominal one but differs in terms of density of fins on the internal heat sinks. The internal heat sink has more fins as compared to the Nominal Configuration; the aim is again to extract more heat from the combustion exhaust. Two TEG modules were employed with a cold side heat sink on each module.

As shown in the Figure 6.15, Configuration 1 consists of one power generator having 2 TEG modules. Each TEG module is sandwiched between hot side which is the side of internal heat sink having internal fins and cold side heat exchanger. Figure 6.16 shows a photograph of the arrangement of main components in Configuration 1.

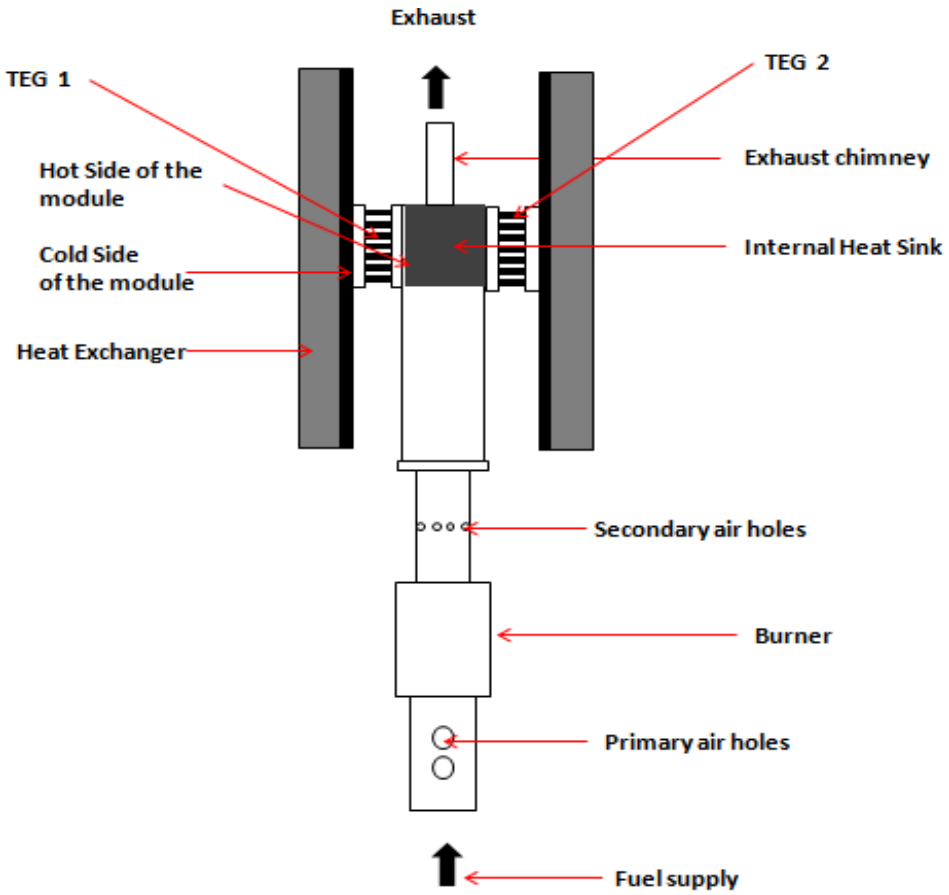

Figure 6.15: Schematic diagram of Configuration 1

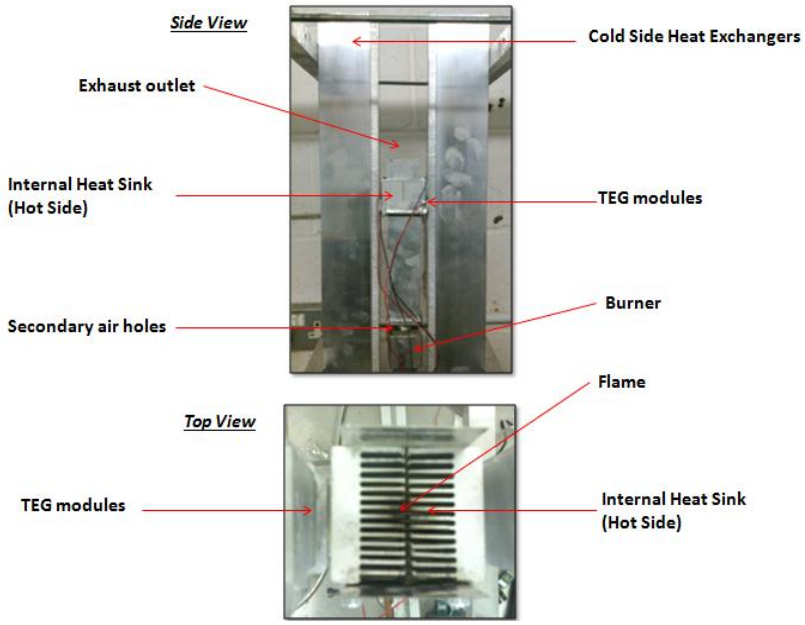

Figure 6.16: Picture showing arrangement of TEGs, Heat Exchangers and Power Generator in Configuration 1

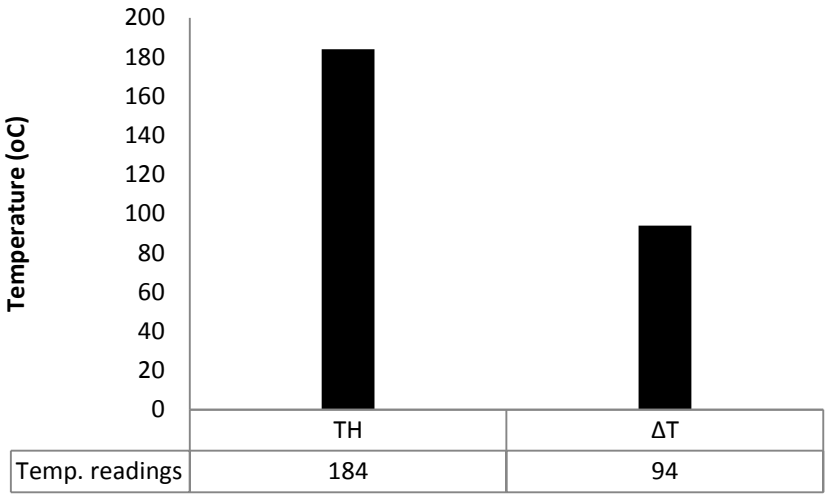

Figure 6.17: Hot side Temperature (T_H) and Temperature Difference (ΔT) for Configuration 1

Figure 6.17 shows T_H achieved by the unit operating at150 mL/min of propane input to the burner. As expected, the results showed higher T_H and ΔT than they were in Nominal Configuration.

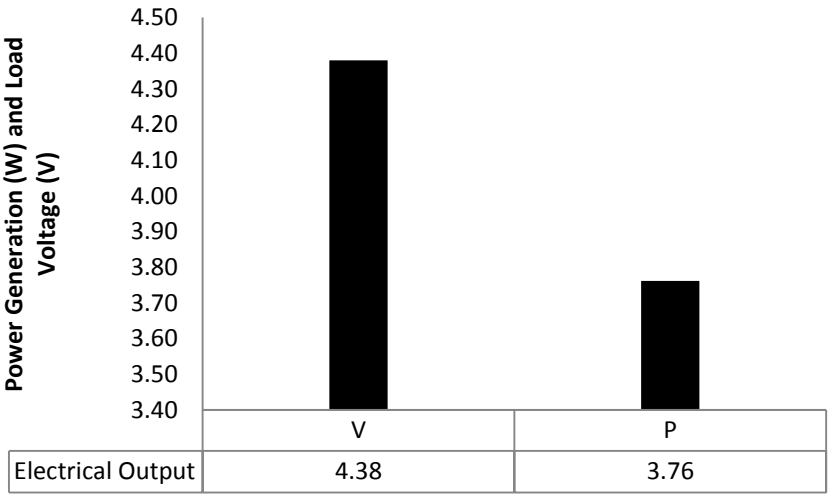

Figure 6.18: Power Generation and Load Voltage output for Configuration 1

Figure 6.18 shows electrical output of the Configuration 1. The result from this configuration showed a slight increase in the power generation from 3.54 W in nominal configuration to 3.78 W in Configuration 1. The increase in power can be attributed to the increase in hot side temperature of the module which resulted in an increased temperature difference of 94 ^oC from 87.8^oC in Nominal Configuration.

6.3.2 Configuration 2

Figure 6.19 shows the schematic of Configuration 2 which consists of two power generators connected downstream of the burner tube as compared to one in Nominal Configuration and Configuration 1. Each power generator has 2 TEG modules; therefore this configuration employs four modules in total. The location of TEG modules is same as Configuration 1 but in this case each cold side heat exchanger is shared by two modules as shown in the figure.

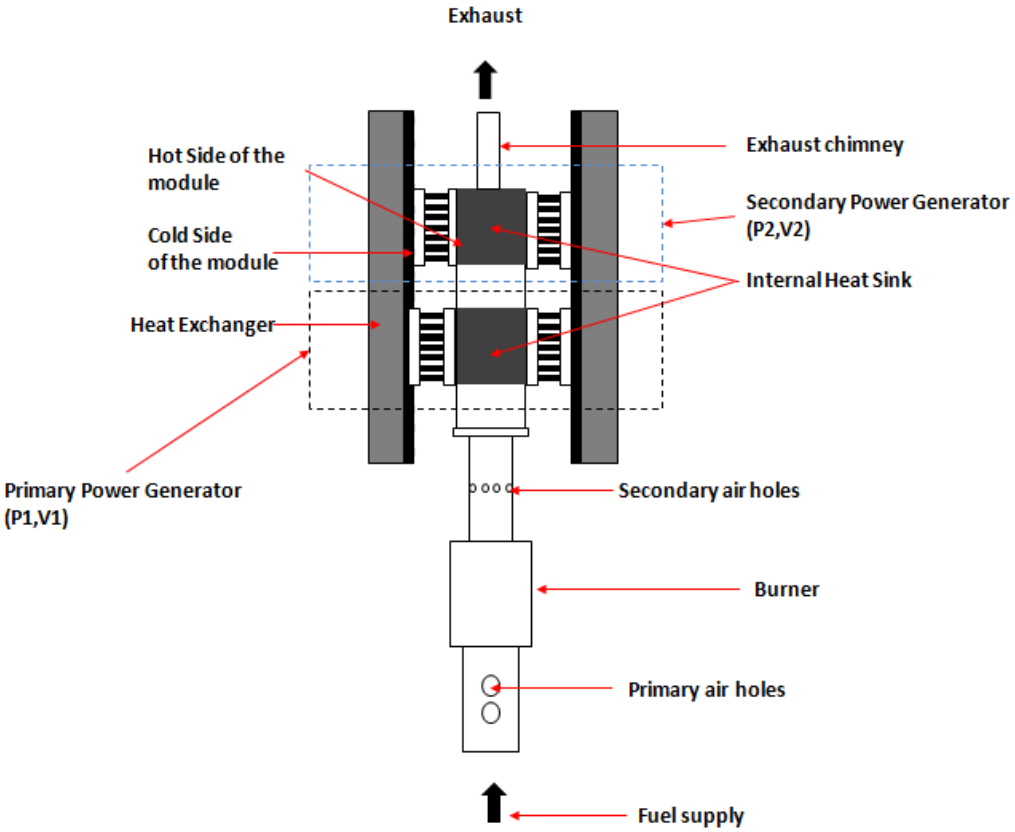

Figure 6.19: Schematic diagram of Configuration 2

The concept behind this design change was to extract the remaining heat from the exhaust which has passed over the first internal heat sinks and using two additional TEG modules to convert this extra additional heat into electricity.

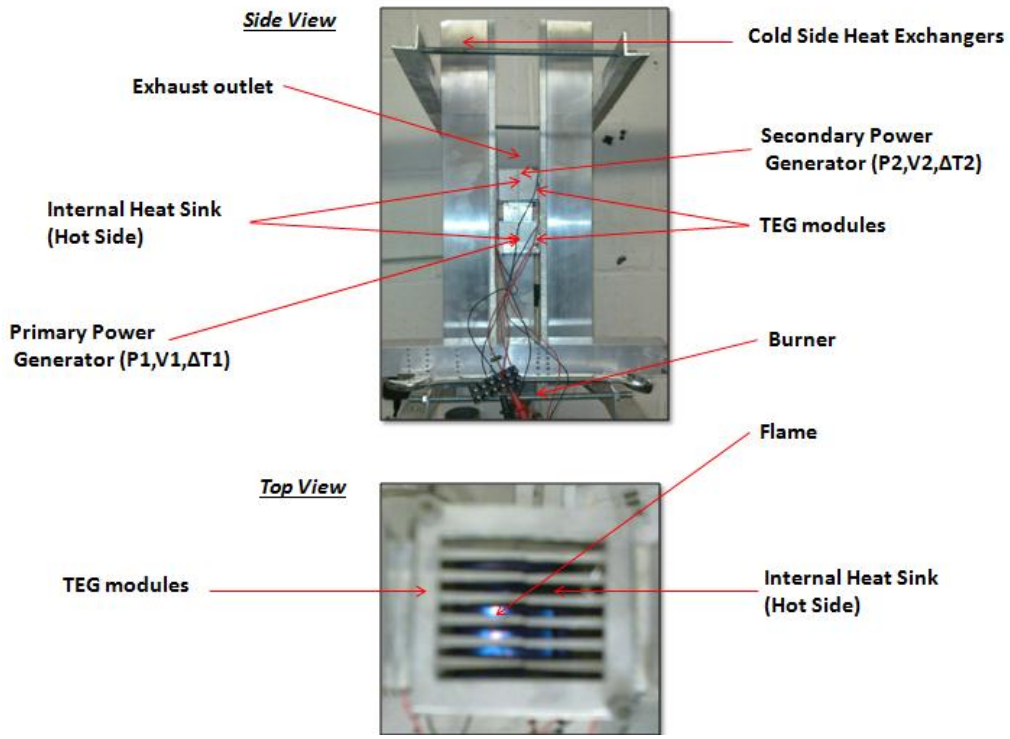

Figure 6.20: Photograph showing arrangement of TEGs, Heat Exchangers and Power Generators in Configuration 2

The Figure 6.20 shows a photograph of Configuration 2, the following results were obtained at propane inlet to the burner fixed at 150 mL/min, same as previous two configurations.

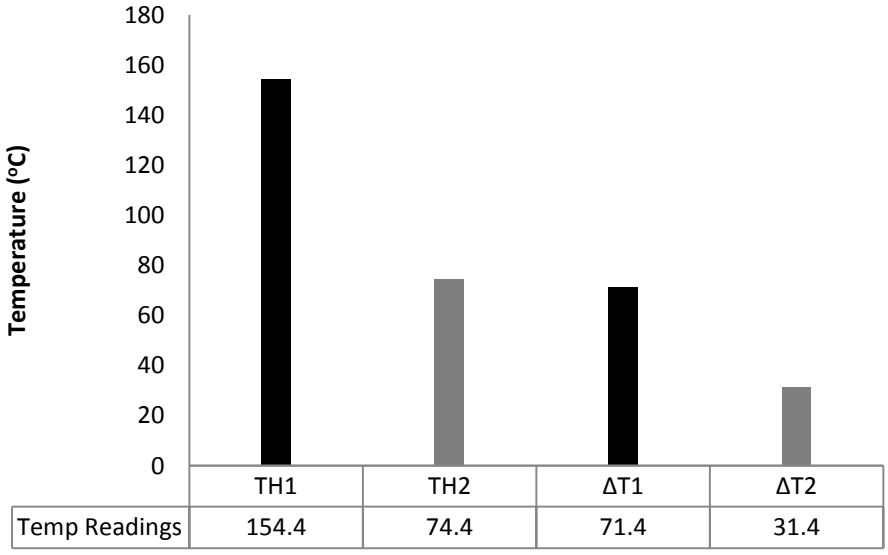

Figure 6.21: Hot side Temperature (T_H) and Temperature Difference (ΔT) for Configuration 2

The Figure 6.21 shows hot side temperatures (T_{H1} and T_{H2}) and temperature differences (ΔT_1 and ΔT_2) obtained from the two power generators. The hot side temperature (T_{H2}) of the secondary power generator is significantly less than that of the primary power generator (T_{H1}). Similar results for temperature difference were shown by the two power generators with primary (ΔT_1) having more than double the temperature difference achieved by secondary (ΔT_2).

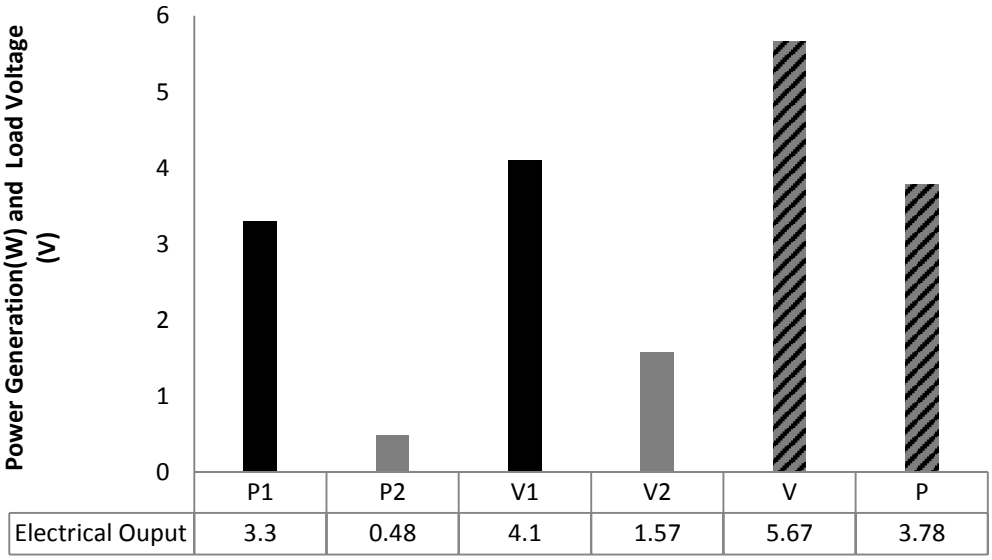

Figure 6.22: Power Generation and Load Voltage output for Configuration 2

The electrical performance of the Configuration 2 is shown in Figure 6.22. The power generation and load voltage of primary power generator (P_1 and V_1) are higher than the secondary (P_2 and V_2). The average power generation from the secondary power generator having heat output of 250 W is 0.48 W which is around 85% less than the power generation of 3.3W by the primary generator. Similarly, load voltage output of the secondary generator is around 60% less than the primary generator. The combined power generation and load voltage output is 3.78 W and 5.67 V respectively.

It is evident that having two power generators does not contribute significantly towards improvement in electrical power output because the amount of heat available is limited to 250 W. The secondary power generator does not receive enough heat to achieve a significant temperature difference, thus producing very little power. So, considering the cost of using two extra modules and the resulted a small increase in power, this configuration is not a practical solution at achieving higher performance from the unit.

6.3.3 Configuration 3

The results from Configuration 2 did not show any significant heat extraction by the internal heat sink of the secondary power generator. This configuration differs from Configuration 2 in terms of number of fins available on the second internal heat sink profile as shown in the photograph in Figure 6.24. The second internal heat sink was provided with a high density of fins in order to increase the surface area over which the exhaust would flow.

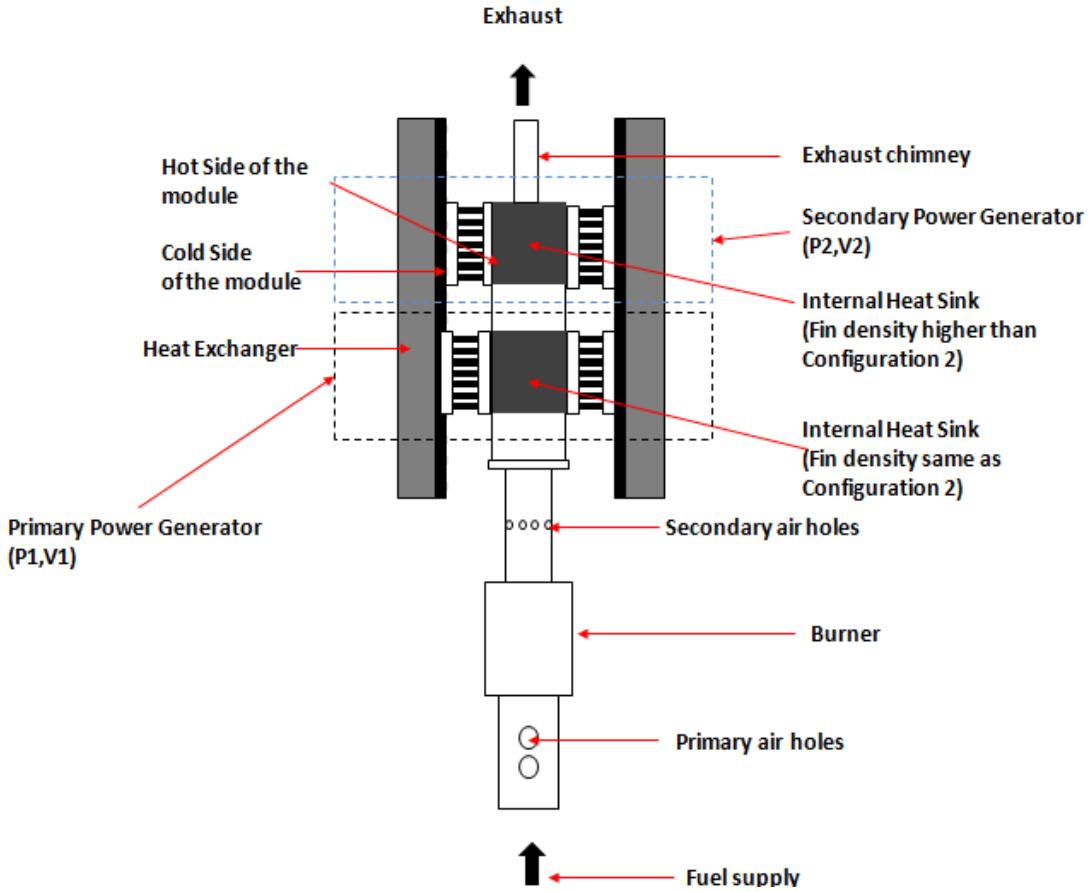

Figure 6.23: Schematic diagram of Configuration 3

The Schematic diagram is shown in Figure 6.23, it can be seen that the configuration is exactly same as Configuration 2 but the only difference is the IHS of secondary power generator which has higher fin density as. Similar to previous configuration, each heat sink was shared by two TEG modules.

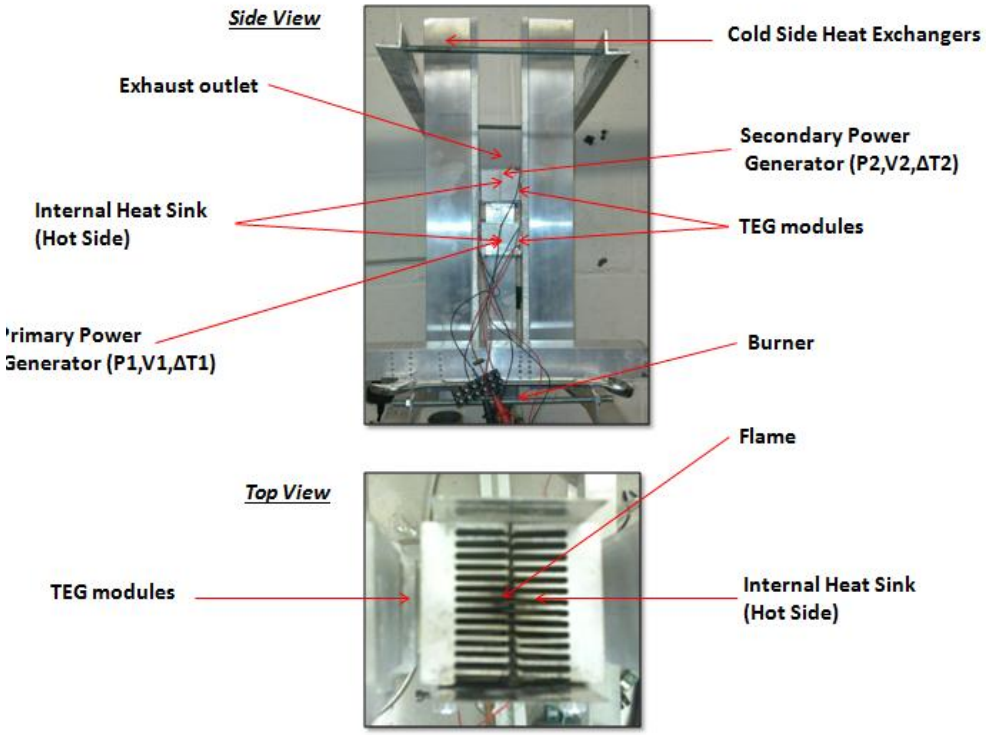

Figure 6.24: Photograph showing arrangement of TEGs, Heat Exchangers and Power Generator in Configuration 3

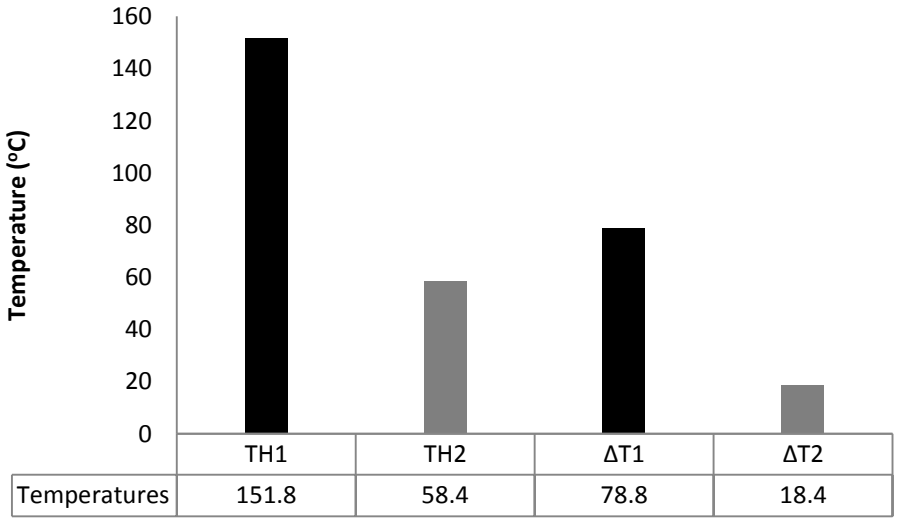

Figure 6.25: Hot side Temperature (T_H) and Temperature Difference (ΔT) for Configuration 3

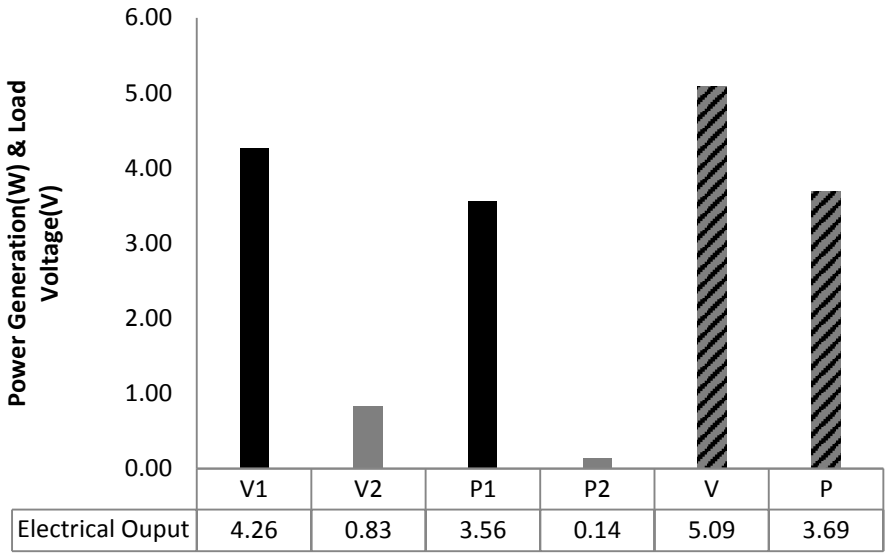

Figure 6.26: Power Generation and Load Voltage output for Configuration 3

The temperature profiles are shown in Figure 6.25 while Figure 6.26 presents the electrical output of Configuration 3. The results showed a similar trend as Configuration 2, the P_1, V_1 and ΔT_1 are higher than P_2, V_2 and ΔT_2. The combined power generation (P) and load voltage output (V) are recorded to be lower than Configuration 2. One of the reasons could be lower temperature difference achieved due to higher cold side temperatures of the heat sinks. As each cold side heat sink is shared by 2 modules, having denser fins in the secondary power generator is actually increasing the heat input to the heat sinks causing its temperature to rise.

6.3.4 Configuration 4

This configuration again consists of 4 TEG modules, but in this case the placement of modules on the burner is different. The primary power generator does not consist of an internal heat sink which means the two modules have been placed directly on the sides of the burner exhaust tube. The secondary power generator consists of internal heat sinks which accommodates the other 2 TEG modules. The difference has been the use of 4 cold side heat sinks in place of 2, which means each TEG module has its own cold side heat sink as shown in the schematic diagram in Figure 6.27.

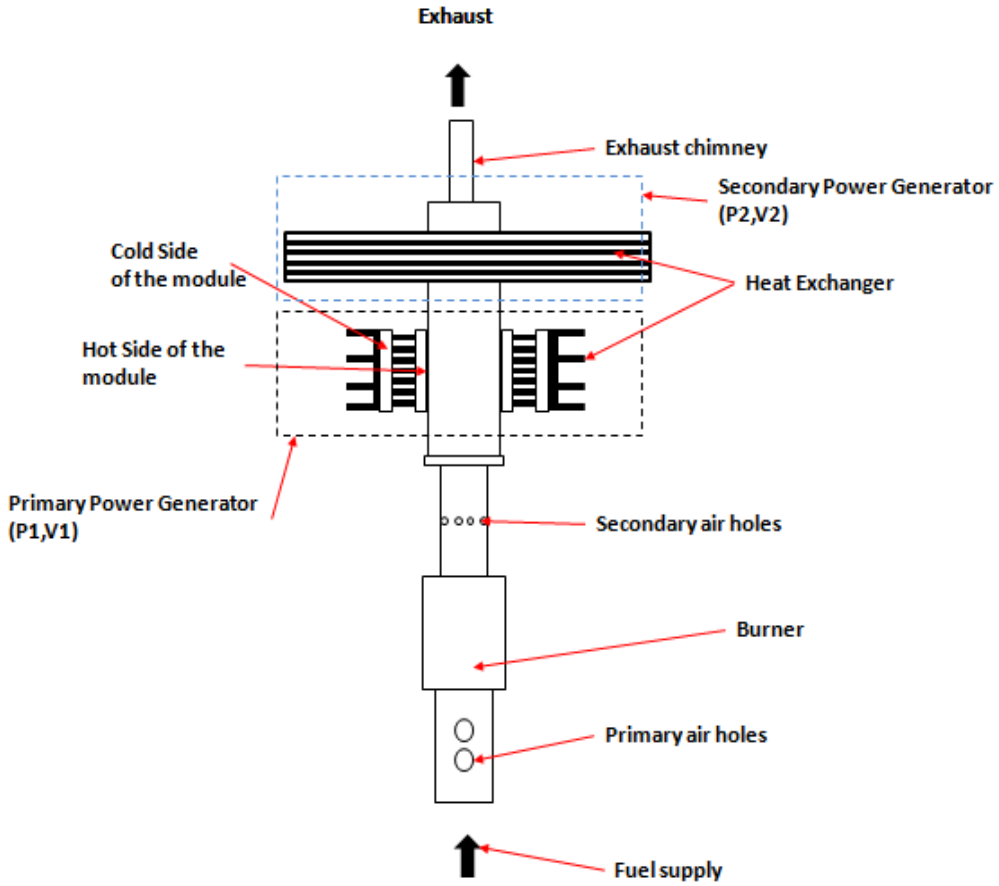

Figure 6.27: Schematic diagram of Configuration 4

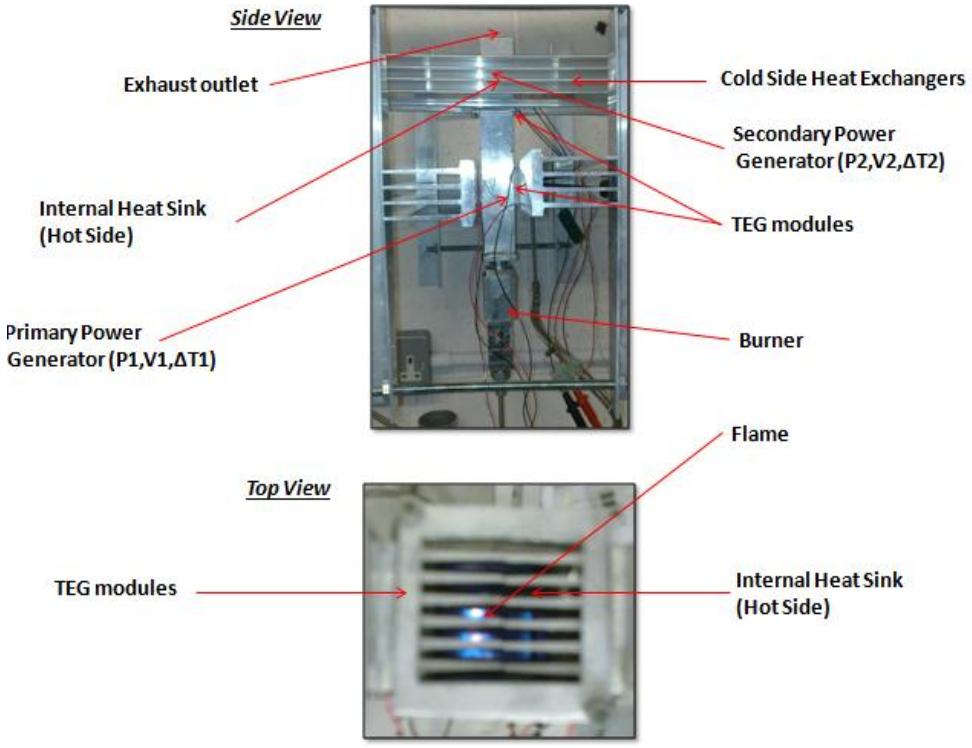

Figure 6.28: Photograph showing arrangement of TEGs, Heat Exchangers and Power Generator in Configuration 4

The aim of testing this configuration was to achieve higher temperature difference by providing a separate heat exchanger for each module but this means the overall cost of the unit would increase quite significantly as this also involves the use of 4 TEG modules. Tests were conducted and results were obtained to make a comparison for selecting the ideal configuration based on cost and electrical output. The Figure 6.29 shows the hot side temperatures and temperature differences obtained with Configuration 4, it can be seen that the hot side temperature of the secondary power generator (T_{H2}) is higher than T_{H2} of any other configuration involving two power generators. This is obviously because of the presence of the IHS in the secondary power generator which is capturing more heat as compared to the primary power generator which does not have IHS. Also, in contrast to Configuration 2 and 3, this configuration has a higher T_{H2} than T_{H1}. The primary power generator as mentioned earlier is directly placed on the walls of the burners without having internal fins, and hence does not get hotter than 112 ^{o}C, which is lower than T_{H1} of Configuration 2 and 3. The temperature differences achieved by the two power generators are however in a similar range on the lower side as shown in the Figure 6.29.

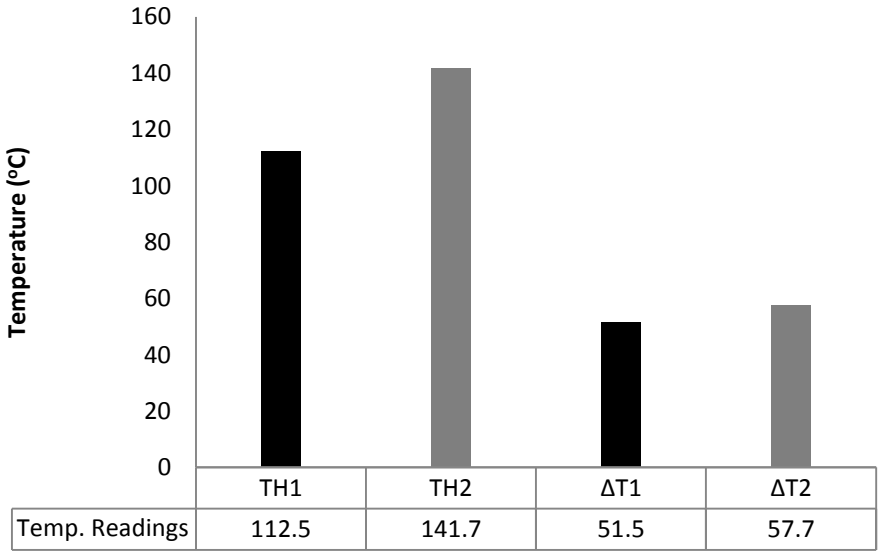

Figure 6.29: Hot side Temperature (T_H) and Temperature Difference (ΔT) for Configuration 4

Figure 6.30 shows the voltage output and corresponding power generation with Configuration 4. Due to the lower temperature difference, power generation and load voltage output are recorded to be comparatively low, 2.63 W and 5.18 V respectively.

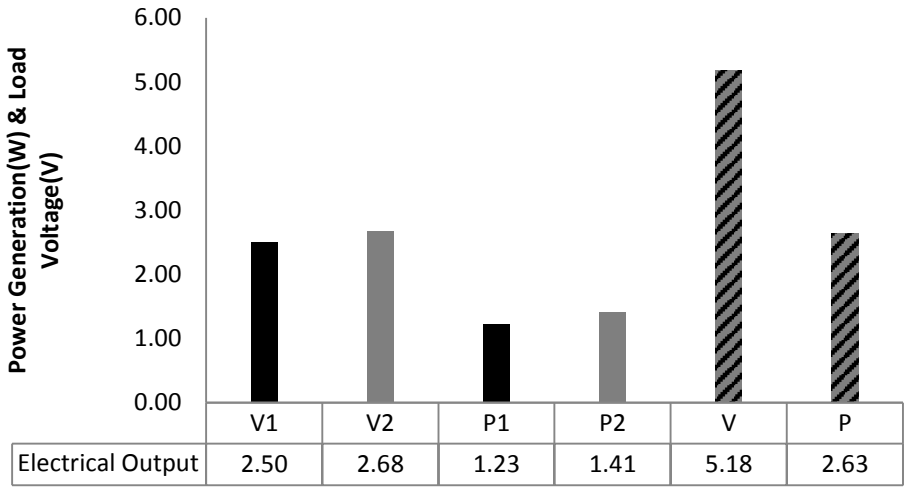

Figure 6.30: Power Generation and Load Voltage output for Configuration 4

The reason behind this inferior electrical output can be attributed to the heat extraction pattern of the two power generators. The primary power generator being closer to the flame is achieving a T_{H1} of around 112 ^{o}C without IHS which is lower than any other configuration, hence ΔT_1 is low but it is more than any other power generator without IHS. Hence, the ΔT_1 in this case is not as low as it has been in the previous configuration where a power generator does not have IHS. The remaining heat available for the secondary power generator is on the lower side but due to the presence of internal fins, it is able to achieve around 141.7 ^{o}C of T_{H2} which is higher than any T_{H2} achieved by any secondary power generator.

6.3.5 Configuration 5

This design configuration consists of 3 TEG modules, two on the side faces of the burner tube while one on top of the chimney as shown in the Figure 6.31. This configuration was aimed at increasing heat extraction from the exhaust. A chimney has been made in this configuration which allows the exhaust to impinge upon the top surface and leave the burner from the front as compared to the top in previous design configuration. The idea is to extract the remaining heat from the exhaust which is impinging on the top surface of the chimney after travelling through the IHS of primary heat sink.

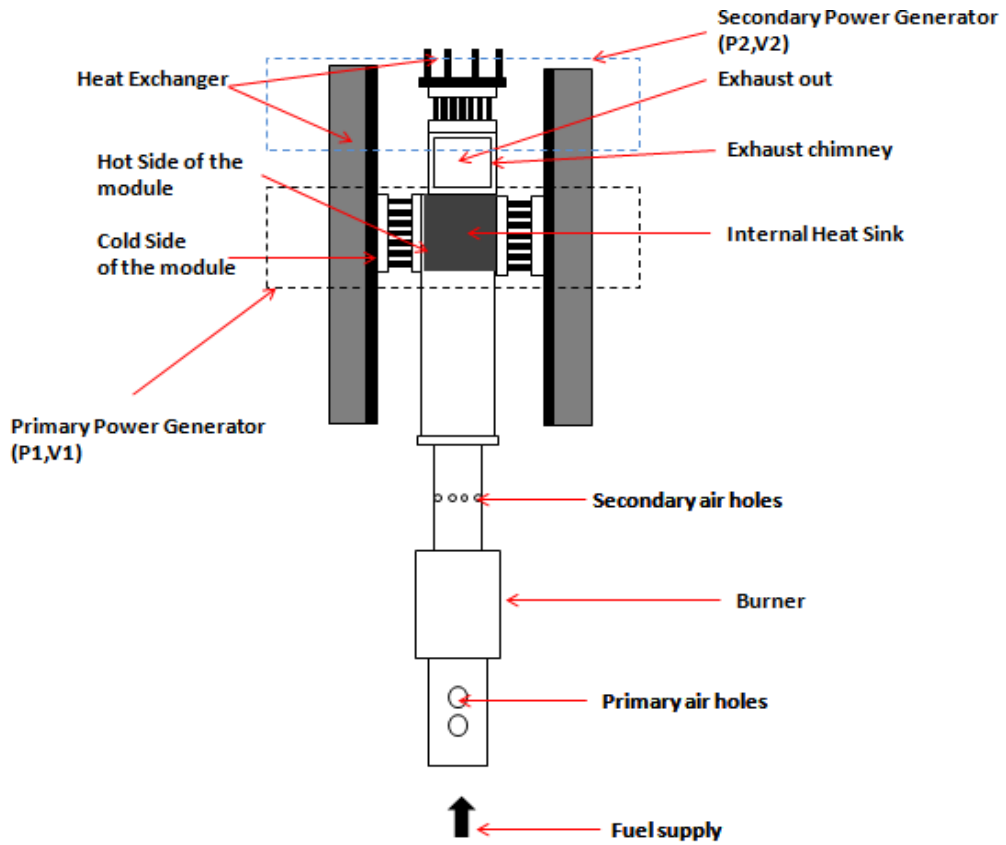

Figure 6.31: Schematic diagram of Configuration 5

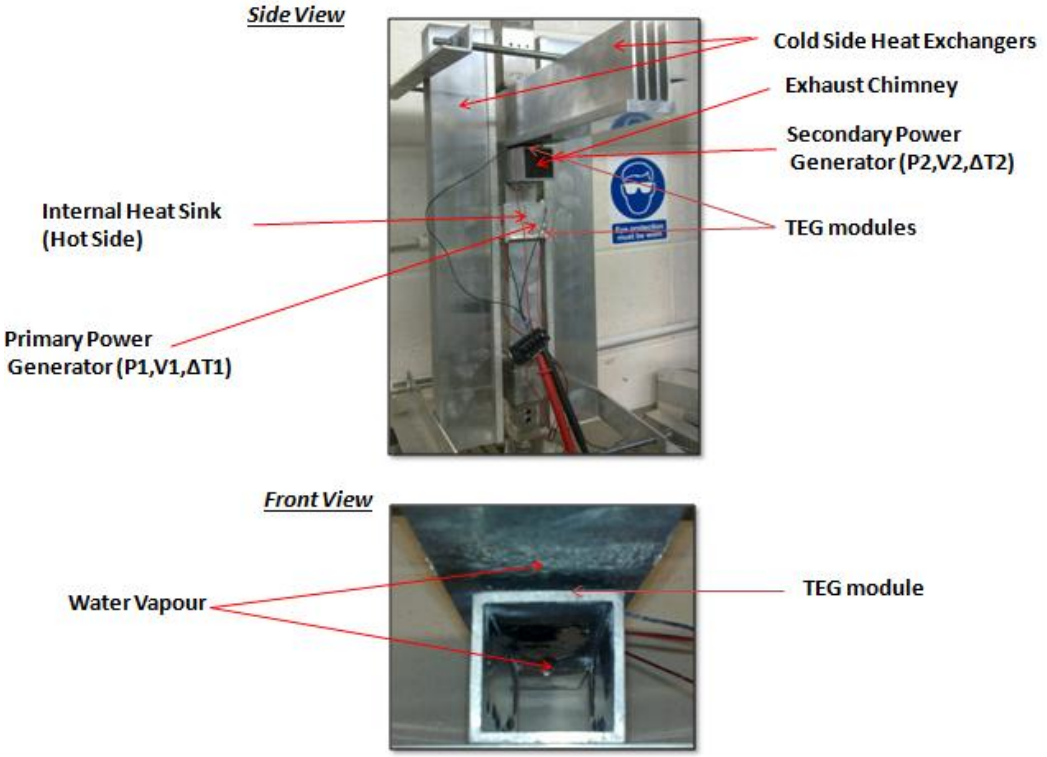

Figure 6.32: Picture showing arrangement of TEGs, Heat Exchangers and Power Generator in Configuration 5

Figure 6.32 shows a photograph of the Configuration 5 being tested with 150 mL/min of propane supply to the burner, it can be seen that water vapour was observed to accumulate on the top wall of the chimney tube where the exhaust is made to change direction and come out from the front. This is due to the fact that the exhaust has already been cooled below the H_2O dew point because of heat lost in the primary power generator and along the passage where it has to travel before reaching the top of the chimney.

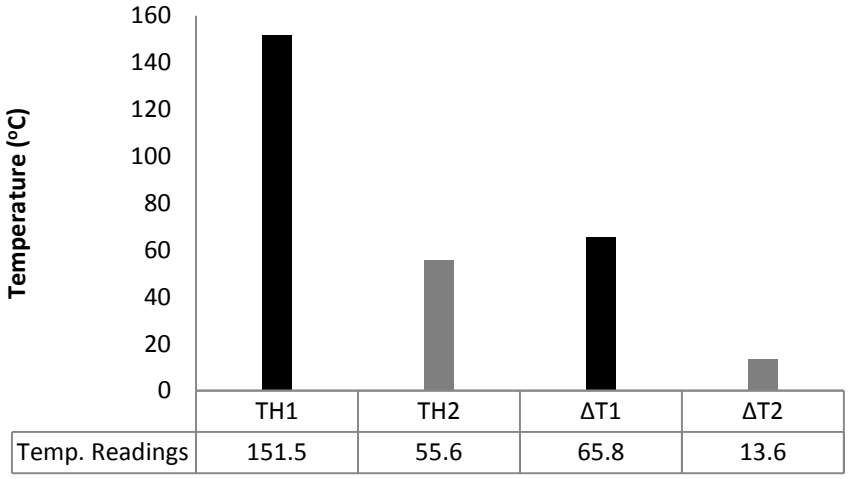

Figure 6.33: Hot side Temperature (T_H) and Temperature Difference (ΔT) for Configuration 5

Figure 6.33 shows the T_H and ΔT results of Configuration 5, similar to Configuration 2 and 3, the T_{H2} is significantly lower than T_{H1} and hence ΔT_2 being lower than ΔT_1.

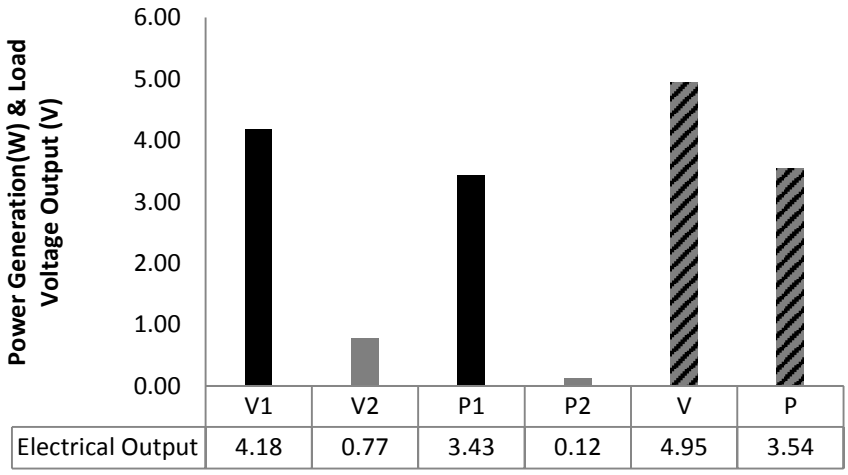

Figure 6.34: Power Generation and Voltage output for Configuration 5

The electrical performance of this configuration (shown in Figure 6.34) is closer to the output of Configuration 1 while slightly less than the output of Configurations 2 and 3, while it is more than the Configuration 4. The individual performance of power generators is again similar to Configurations 2 and 3; the primary power generator was outperforming the secondary one by a significant margin. The ΔT_2 achieved was low because of lower T_{H2} and hence lower P_2 which is eventually causing the combined power output to be lower.

Apart from a comparatively low electrical power output considering the use of 3 TEG modules and a separate heat sink for each of them, water vapour was accumulated on top of the burner chimney which on a few occasions has been interfering with the combustion. In some test runs water vapour was seen to fall back in the combustion chamber causing the flame to extinguish.

6.3.6 Summary

The Figure 6.35 shows a comparison of all the configurations in terms of electrical power generation and load voltage output obtained at a fuel input of V_f =150 mL/min propane, two air holes open for combustion air and presence of secondary air supply and backward facing step for flame stabilisation.

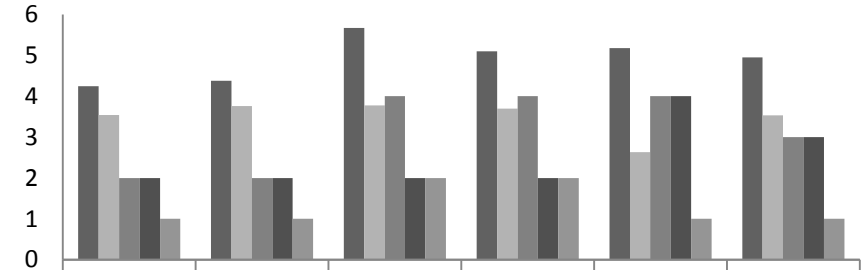

	BC	C1	C2	C3	C4	C5
Voltage Output (V)	4.25	4.38	5.67	5.1	5.18	4.95
Power Output (W)	3.54	3.76	3.78	3.7	2.63	3.53
No. of TEG	2	2	4	4	4	3
No. of HE	2	2	2	2	4	3
No. of IHS	1	1	2	2	1	1

Figure 6.35: Comparison of various configurations

It can be seen in the above comparison that the power and load voltage output was not significantly different in all the configurations investigated. The power output of all the configurations except Configuration 4 is between 3.5 W to 3.80 W which satisfies the power requirement. This implies that the power output was not affected by a significant

amount by the number of TEG modules used in the configuration. For instance, the Configuration 2 employed 4 TEG modules and generated 3.78 W power whereas the Nominal Configuration employed only 2 modules and generated 3.54 W of power, the difference in power generation being a mere 0.24 W with additional 2 modules used in Configuration 2. The reason could be attributed to the fact that the amount of heat available was limited to 250 W as the burner was allowed to combust only 150mL/min of fuel in order to satisfy the operating requirements and hence employing more number of modules in the system does not increase the power generation by a large sum. This means that the more the number of modules integrated on the burner, less will be the heat available to each module and hence less temperature difference leading to lower power output per module. As cost was an important aspect in this product development project because the product will be mass produced to be sold to domestic consumers, the Nominal Configuration (NC) has proved to be the optimum design configuration because it uses the minimum number of TEG modules i.e. two and hence requires minimum number of heat exchangers and has shown to generate enough power for the application.

6.4 Optimisation: Cold Side

Various different shape and size of heat exchangers were tested with the burner to find out the best performing ones which produced maximum electrical power, were economical to procure and fits in with the overall design of the final product. This section presents a comparison of electrical power output, load voltage, hot side and cold side temperatures obtained with 4 different types of heat exchangers with the same TEG modules used for each of the types to make a decision on the type of heat exchanger to be used in the final product. Due to high cost of customisation of these heat exchangers, commercially available ones were obtained and tested. The number of TEG modules used in the following configurations was 2; hence a heat exchanger was integrated on the cold side of each module. The electrical load applied was a 6 Ω resistor which was required in order to replicate the operating conditions and measurement of maximum power output.

Table 6.2: Description of the heat exchangers

	Type 1	Type 2	Type 3	Type 4
Length (mm)	200	300	500	200
Width (mm)	40	40	40	150
Height (mm)	40	70	70	40
Surface finish	Black anodised	Plain	Plain	Black anodised

Table 6.2 gives physical description of the 4 types of heat exchangers employed in this part of the investigation of the thermoelectric combustor. The Type 1 and Type 2 heat exchangers were black anodised while the Type 2 and Type 3 had plain surface finish. The type 3 heat exchangers were the longest whereas the Type 4 had the largest width. The Type 2 and Type 3 had the highest height among all the heat sinks. It is worth mentioning here that one of the reasons for performing heat exchanger optimisation was unavailability of heat dissipation capabilities of various types and shapes of heat exchangers. As cost is a major consideration, expensive commercially available heat exchangers were difficult to procure in small numbers, hence, large heat exchangers were cut down to small desired shapes and sizes which made it difficult to predict their performance.

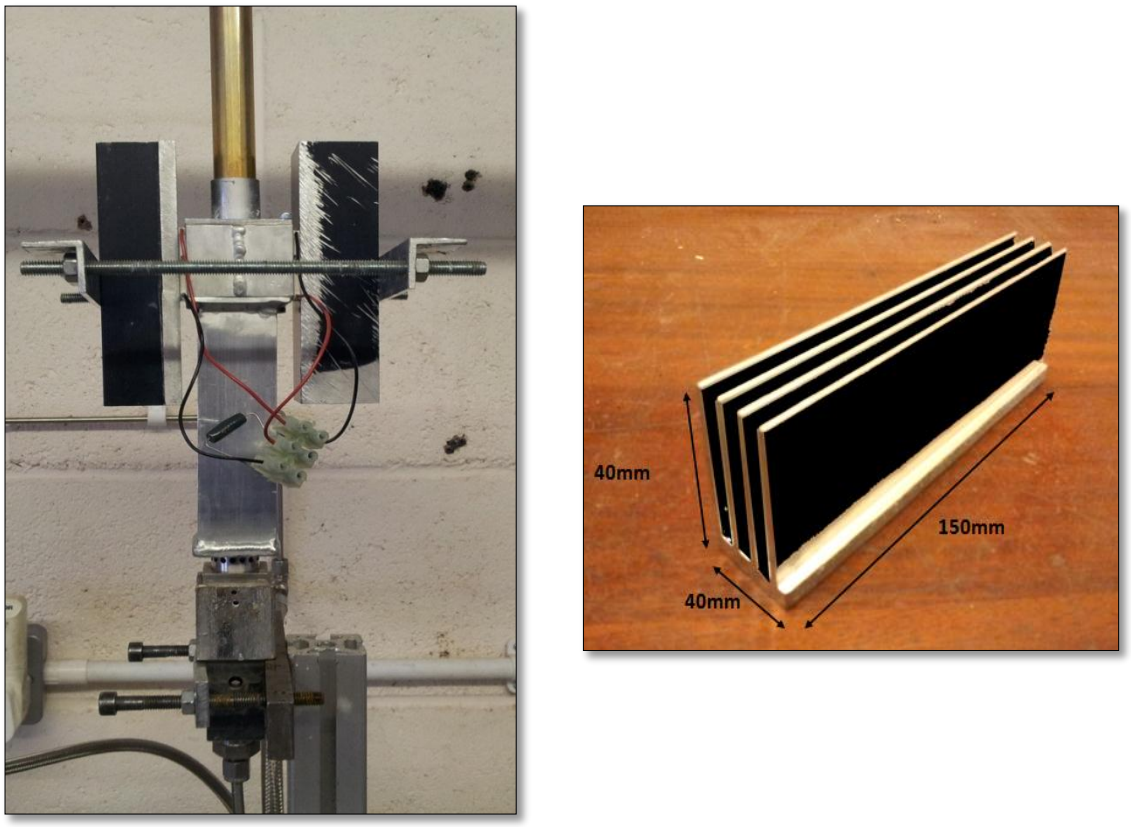

Figure 6.36: Type 1 Heat Exchanger

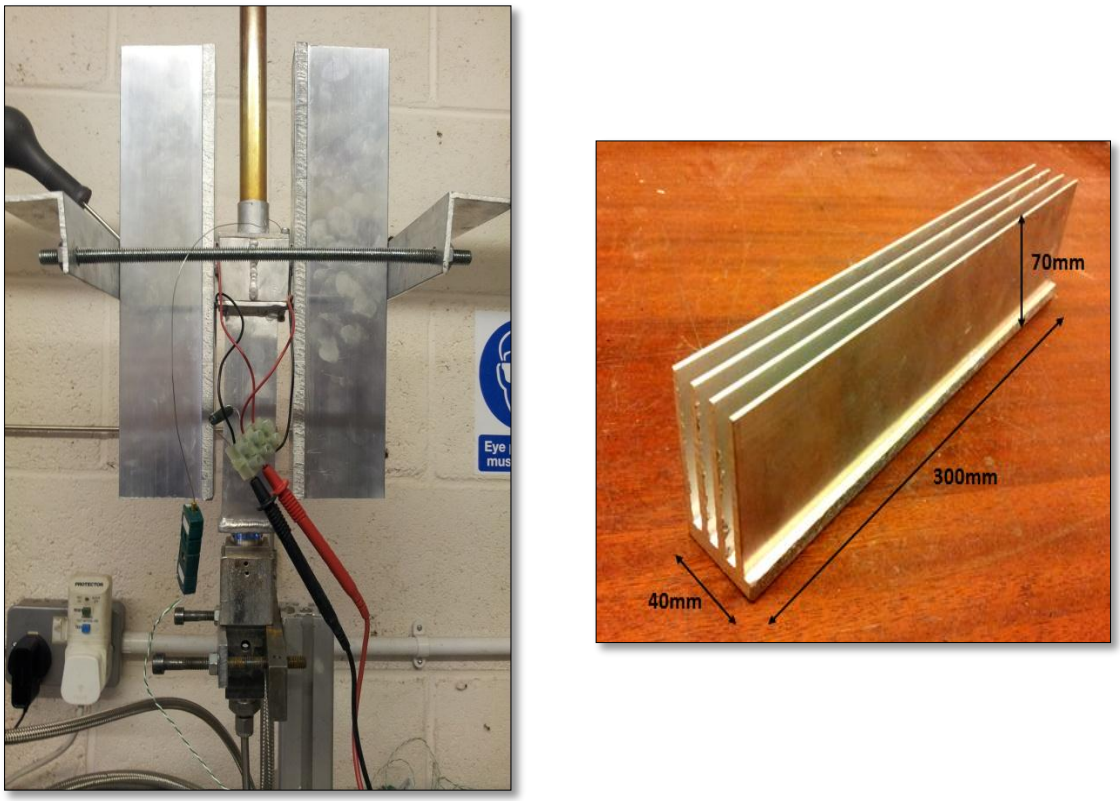

Figure 6.37: Type 2 Heat Exchanger

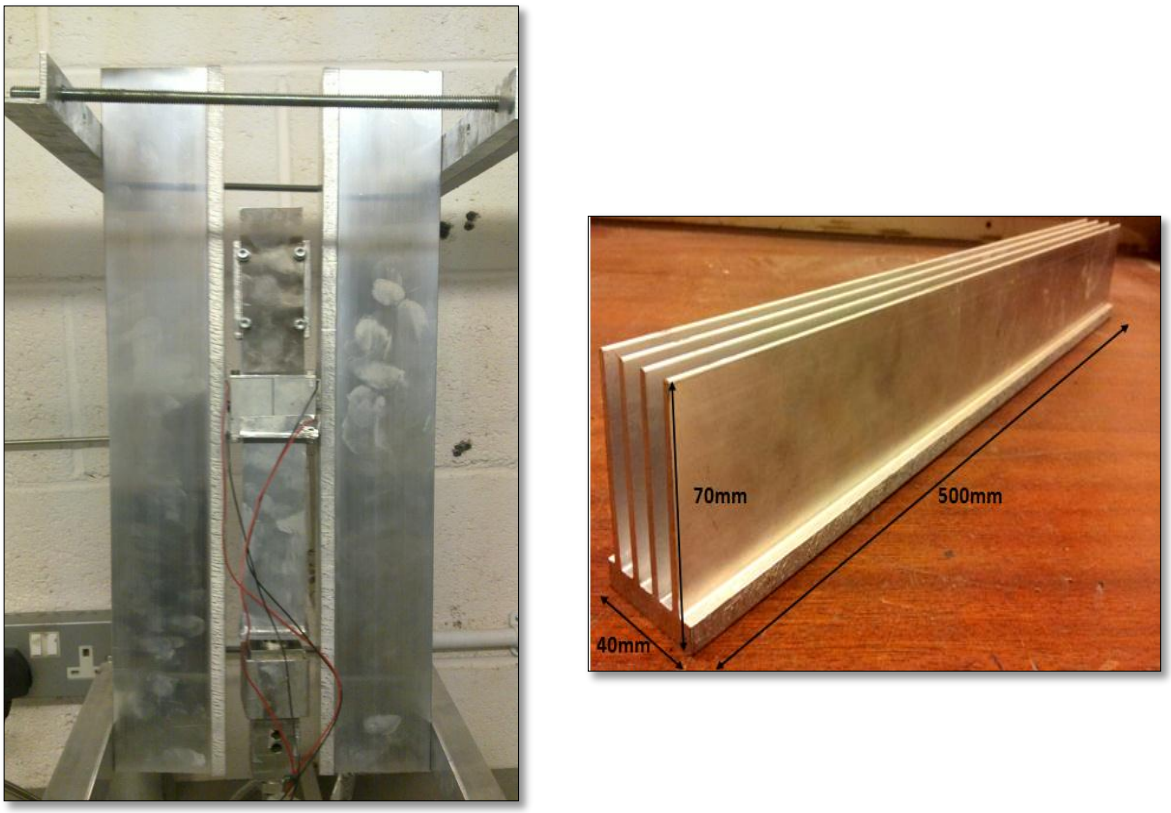

Figure 6.38: Type 3 Heat Exchanger

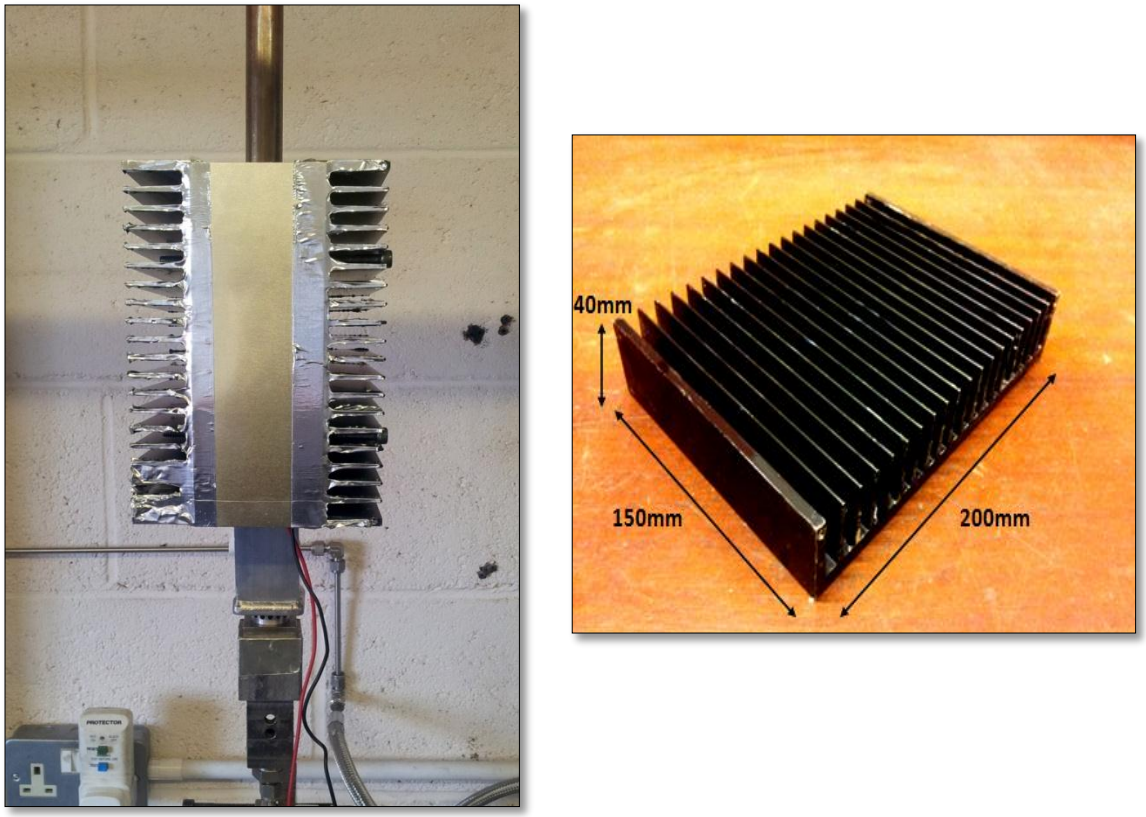

Figure 6.39: Type 4 Heat Exchanger

Following were comparison results

The graph in Figure 6.40 compares cold side temperatures (T_C) achieved by the four different types of heat exchangers. The results are obtained for first 60 minutes of device in operation. It can be seen in the graph below Type-4 heat exchanger showed lowest T_C while the Type 1 recorded the highest. The aim was to achieve a high temperature difference which would result in higher electrical power generation, in this regard, low cold side temperatures are desired which would help in achieving higher temperature difference. Hence in this comparison of T_C with different type of heat exchangers, for a specified duration of operation at 150mL/min of propane supplied to the burner, Type-4 heat exchanger came out to be superior to the others.

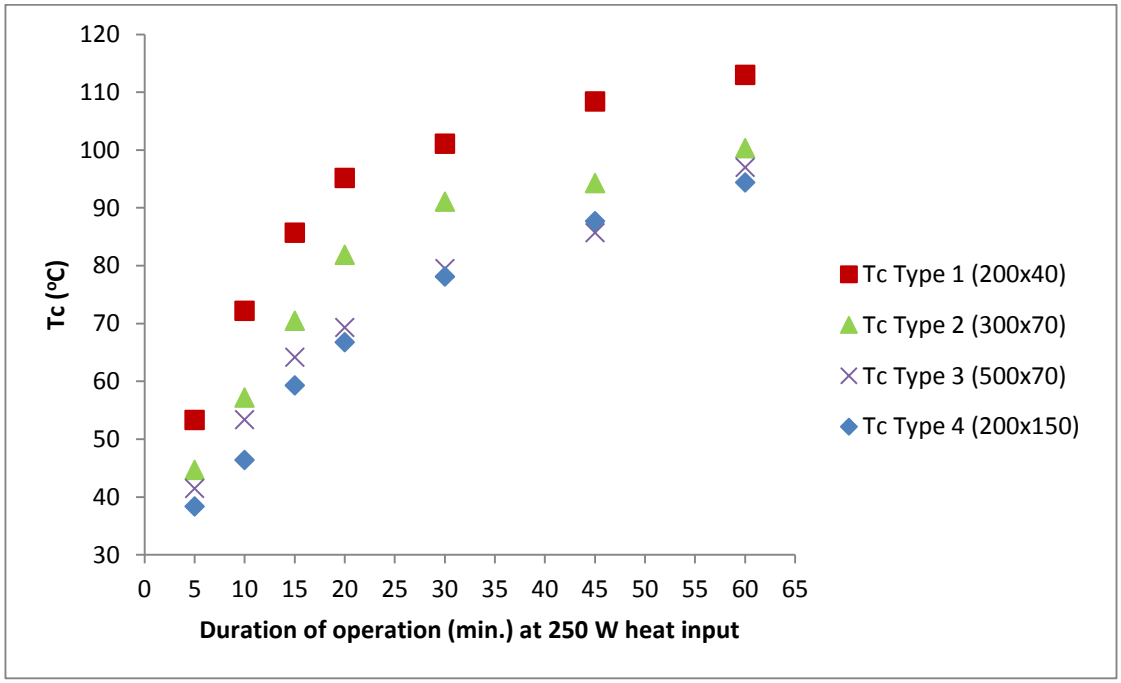

Figure 6.40: A graph comparing Cold Side Temperature (T_C) achieved with different types of heat exchangers

Next, measurements were taken for electrical power generation, load voltage output and temperature difference obtained by using all four types of heat exchangers and a comparison was made which is shown in Figure 6.41.

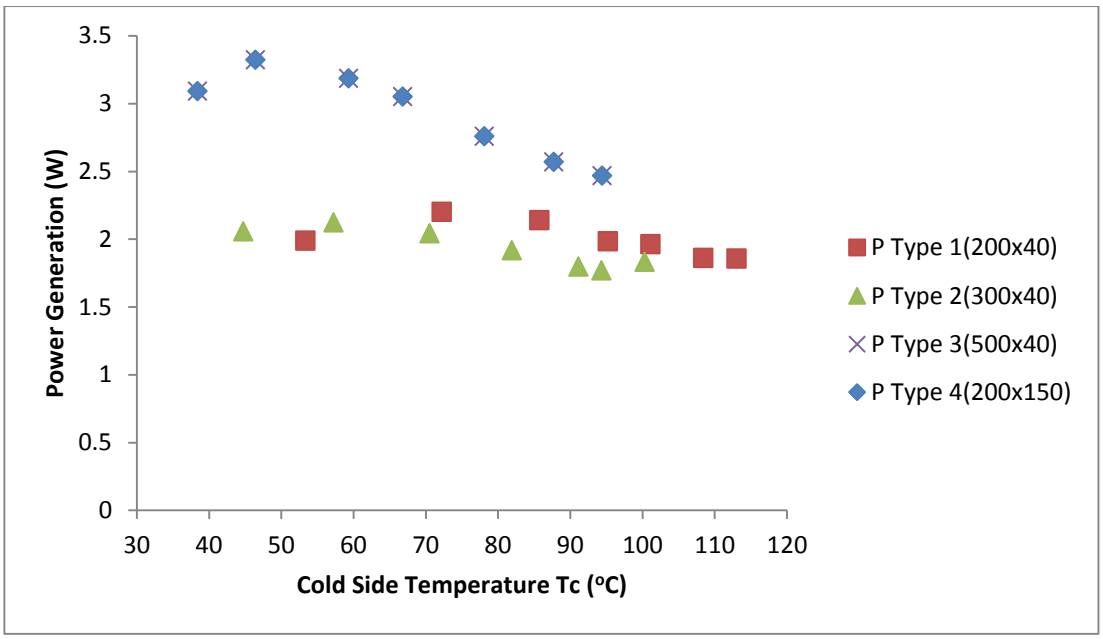

Figure 6.41: Comparison of Power (P) Generation with different heat exchanger types

The graph in Figure 6.41 shows a comparison of power generation with different types of heat exchangers. The Type-4 heat exchanger showed highest power generation for the specified duration of time.

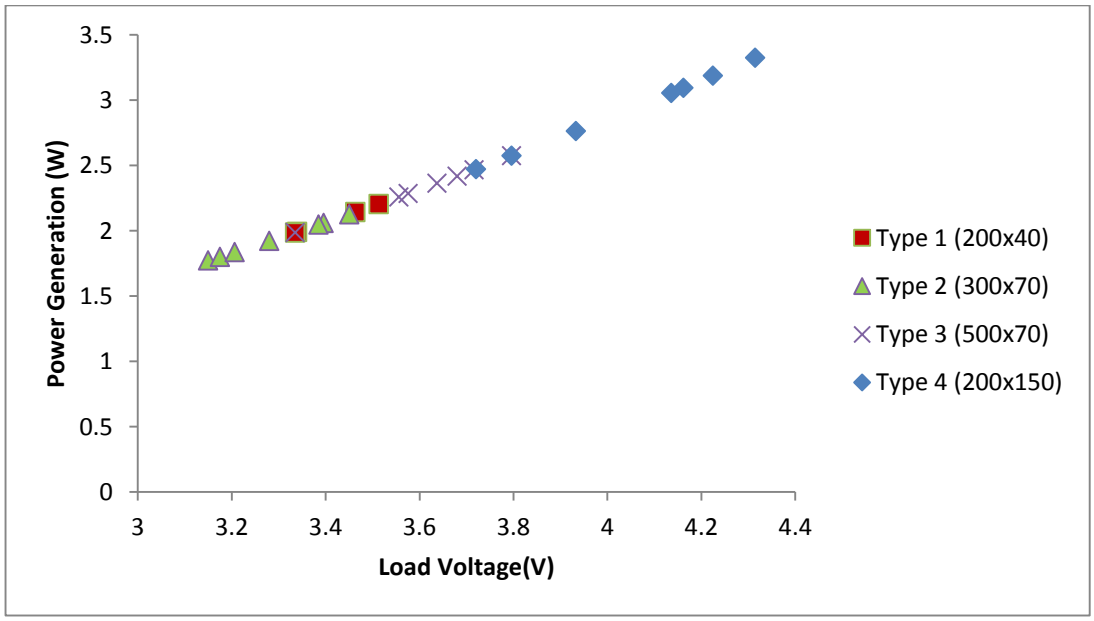

Figure 6.42: Power and Load Voltage output for different heat exchanger types

The graph in Figure 6.42 compares power generation against load voltage for the four types of heat exchangers. Again it was quite evident that power generation and load voltage output both were higher when Type-4 heat exchangers were employed.

The comparison results showed that Type-4 heat exchangers outperformed others in terms of electrical power generation and voltage output. The only other heat exchangers which performed similarly were Type-3. However due to ease of availability and a standard design model, Type 4 were more desirable as Type-3 were required to be cut down from a large size heat exchanger thus involving some customisation. Another factor which favoured this heat sink was the orientation of the fins which allowed wind to pass through them enhancing heat dissipation via natural convection. Based on the results from heat optimisation and economic factors, Type-4 heat exchangers were considered as the optimum.

6.5 Summary

This chapter has presented results from the integration of the meso-scale premixed burner developed and tested in the previous chapter with thermoelectric power generation modules in order to harvest the heat of combustion available from the burner walls enclosing the flame. The aim of the tests was to optimise the temperature difference through optimising hot and cold sides of the module, as power generation is directly proportional to temperature difference or in other words higher temperature difference between the cold and hot side of the module would yield higher power output. The hot side of the module was optimised by employing IHS in the burner tube which helped in extracting more heat from the exhaust as the internal fins on the IHS increased the surface area in contact with the exhaust gas and transferred heat to the IHS wall where TEG module is placed. The temperature of the hot side of the module was increased from 150^{o}C without IHS to 185 ^{o}C, which resulted in an increase in temperature difference thus a higher power output of 5.5 W with IHS than 3.5 W without IHS.

The next experiments consisted of testing various configurations consisting of different number and arrangement of main thermoelectric components which are TEG module, heat exchangers and IHS. The total number of configurations tested was 6 including a Nominal Configuration which consisted of 2 TEG modules, 2 heat exchangers and 1 HIS, the remaining configurations were constructed by making modifications to the Nominal configurations. The results showed that increasing the number of TEG modules in the system does not increase the power generation as the amount of heat available is limited to a 250 W burner output. More number of modules in the system meant less heat available to each module and hence lower power generation per module. Based on the results, Nominal Configuration was chosen to be the final design configuration as it generated the required amount of power with only 2 modules making it economical as well.

The cold side of the module was optimised by testing different type of heat exchangers within the system to find out the ones which generated highest power by dissipating most heat. Four different types of heat exchangers were tested and the Type 4 heat exchangers which have the dimension as 150 mm width, 200 mm length, 40 mm height of the fins and black anodised surface finish, outperformed others in terms of highest power output and low cost design.

Chapter 7

Effect of Secondary Air Addition on Flame Stabilisation

7.1 Introduction

The effect of secondary air supply on the flame stabilisation will be experimentally investigated in this chapter. It was found in the development stages of the self-aspirating meso-scale premixed burner (Chapter 5 of thesis) that the addition of secondary air has a significant effect in stabilising the flame inside the combustion chamber. This chapter will focus on an in-depth analysis of the flame behaviour in the presence and absence of secondary air supply. Firstly, three burners, each of different step height will be tested for various equivalence ratios in order to find flammability range and then secondary air will be added to explore the flammability range at different equivalence ratios.

7.2 Experiments Without Secondary Air Supply

This section of the research will focus on the experimental investigation of effect of step height on the flame stabilisation in a small scale burner which operates at micro-scale operating parameters but has macro-scale size requirements as mentioned in Chapter 3: Challenges and Design Barriers, and Chapter 5: Development and investigation of a meso-scale premixed combustor. As previously mentioned in Chapter 5, the present research involved development of a premixed burner which included a step height for enhancement of reactant mixing. As literature suggested, recirculation zones are created at the step which helps in improving the degree of mixing of reactants, eventually contributing towards completeness of combustion. Firstly, the premixed burner of Prototype 2 will be considered. The burner description can be found in Chapter 5 and the detailed drawing is available in Figure 5.6: A 3-D CAD model of Prototype-2 and Figure 5.7: A 2-D CAD Drawing of Prototype-2.

.

The main features of this burner were square shape and most importantly a BFS.

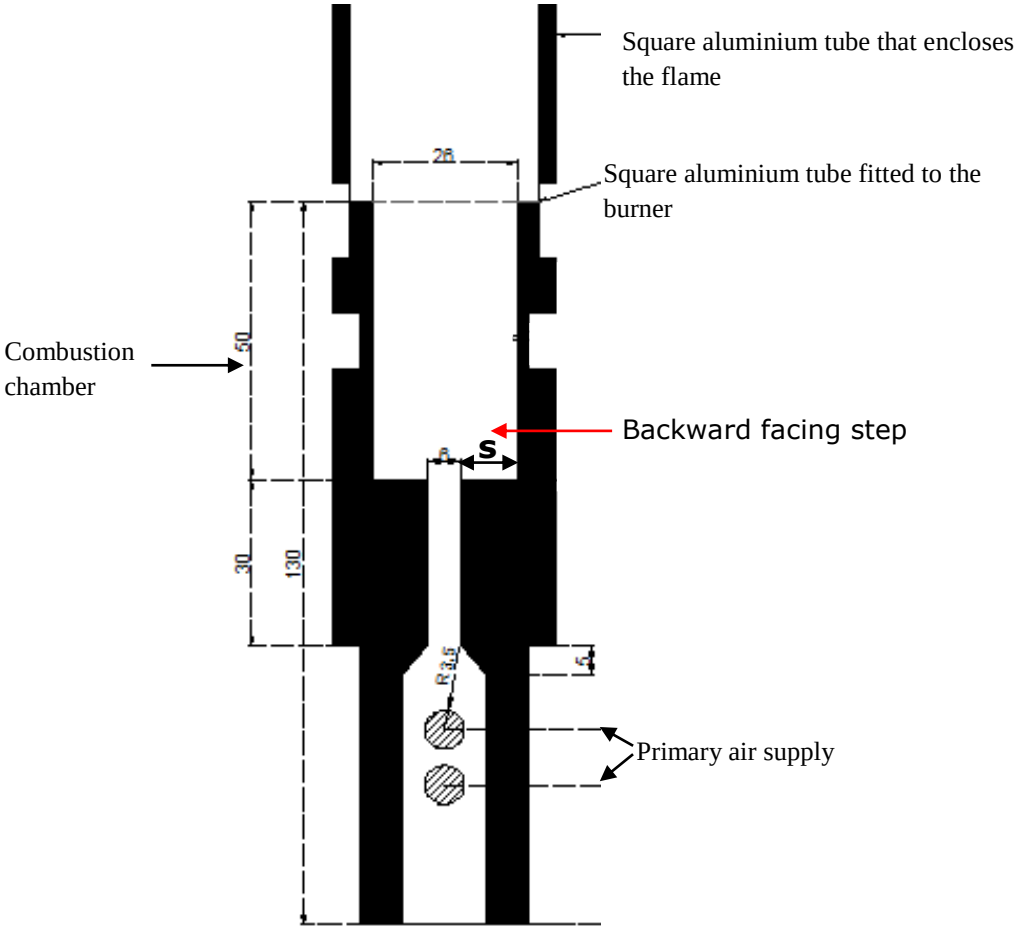

Figure 7.1: A diagram showing the burner with BFS, Step Heights (S) =10 mm.

Figure 7.1 shows the meso-scale non-catalytic burner with a BFS to enhance mixing of reactants and to provide a means of flame stabilisation mechanism. The burners were tested under 'forced air supply mode' of operation as discussed in the Chapter 3: Research Methodology. It meant that the combustion air was regulated and metered using flowmeters and therefore, equivalence ratios could be calculated unlike the 'self-aspiration mode' where the combustion air was not metered and equivalence ratios was calculated using combustion product analysis by FTIR. The volumetric flow rates of propane considered were in a range from 50 mL/min to 300 mL/min. The volumetric flow rates of primary combustion air were in a range of 1 L/min to 7 L/min.

7.2.1 Results

Step Height, S=7 mm

The burner in this test was the one shown in Figure 7.1 with a BFS having a step height (S) of 7 mm.

The test results of the burner with step height 10mm, discussed in Chapter 5 showed no flame inside the combustion chamber at all equivalence ratios. The flame was observed to stabilise itself at the extreme downstream end of the burner or in other words blowoff was observed with burner having step height 10 mm. The test results of burner with step height 7 mm showed different behaviour with the flame location being inside the combustion chamber.

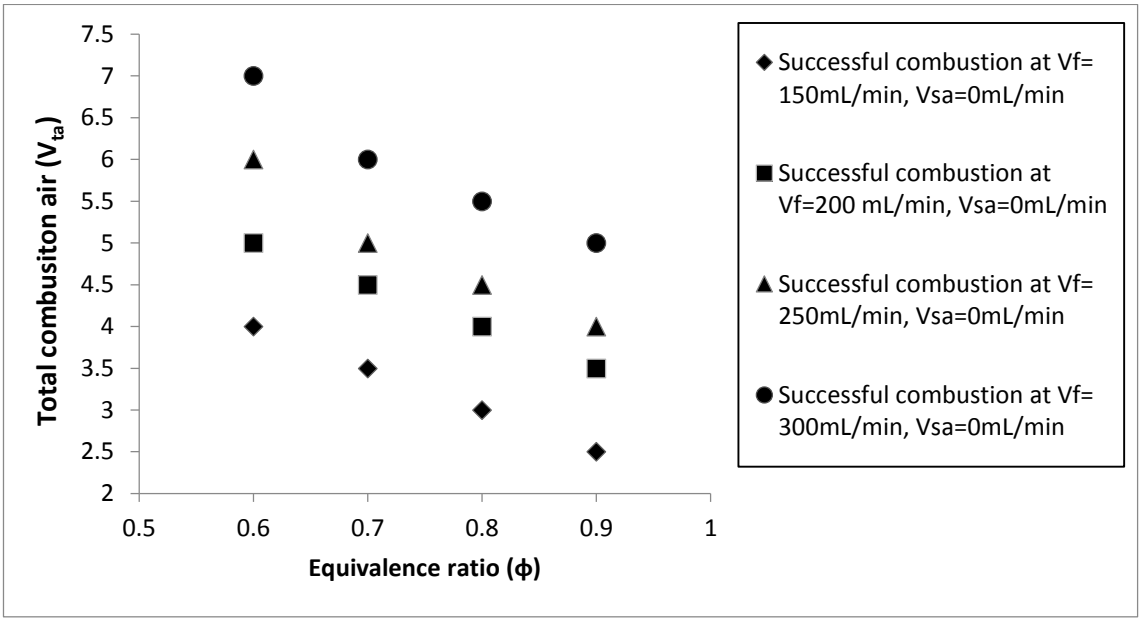

Figure 7.2: Equivalence ratios for various V_f where a flame was observed inside the combustion chamber of the burner with S=7 mm (without secondary air).

Figure 7.2 shows the equivalence ratios at corresponding total combustion air supply for various volumetric flow rates of propane at which a flame was observed in the combustion chamber without secondary air addition. The graph shows the equivalence ratios at which propane was oxidised inside the combustion chamber or the primary combustion air at which combustion took place in the combustion chamber without the need of secondary air injection.

Even though the flame was located inside the combustion chamber, the flame was observed to be unstable. The flame was seen flickering and making noise throughout the operation of the burner at all the equivalence ratios at which combustion was taking place inside the burner. So in terms of the location of the flame, reducing the step height aided in preventing the downstream movement of the flame but due to high noise and flicker, the reduction in step height did not yield a stable premixed flame inside the combustion chamber.

Step Height, S=10 and 15mm

Similar to the results shown in Chapter 5 with the burner having step height 10mm operating at self-aspiration mode, the results with the burner having step height 10 and 15mm showed blow-off at all equivalence ratios when the burner was operated at forced air supply mode in these tests. The flame was found to be stabilising itself at the extreme downstream of the burner i.e. the top of the burner or the exit as mentioned in the Chapter 5. This phenomenon resulted in a very unstable diffusion type yellow flame similar to ones shown in Figure 5.12.

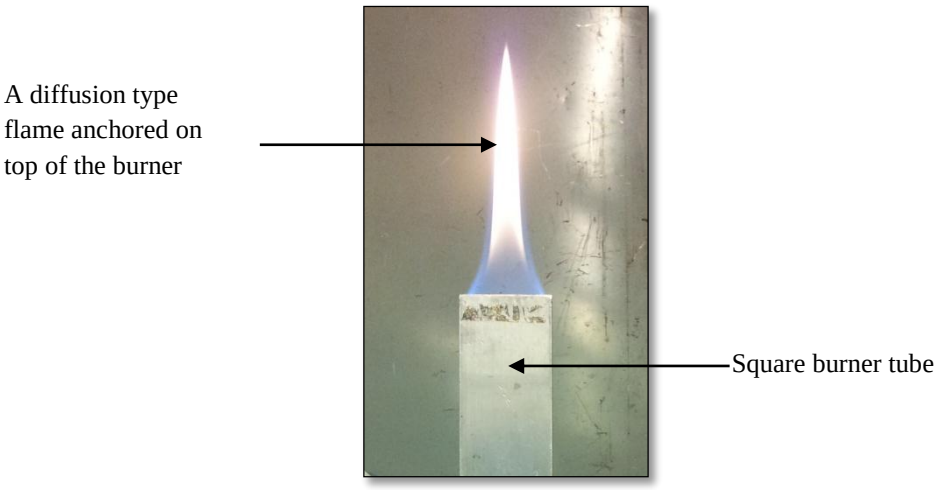

Figure 7.3: A photograph of flame with no secondary air, i.e. V_{sa}=0 L/min and V_f=300 mL/min.

A photograph of flame can be seen in Figure 7.3 with burner having step height 15mm. It can be seen that the flame tends to travel downstream and stabilises itself at the extreme downstream which was not the desired location of the flame. A stable premixed flame could not be achieved at any equivalence ratios for step heights 10 mm and 15 mm. The flame was observed to either completely absent from the combustion chamber or a successful ignition of reactant mixture inside the combustion chamber leading to the flame moving to the extreme downstream. The flames obtained were yellow in colour and were appeared like diffusion flame as shown in the Figure.

7.2.2 Discussion

The graph in Figure 7.4 shows the equivalence ratios at different volumetric flow rates of propane. The equivalence ratios considered in this analysis are the ones which were nearer to stoichiometry.

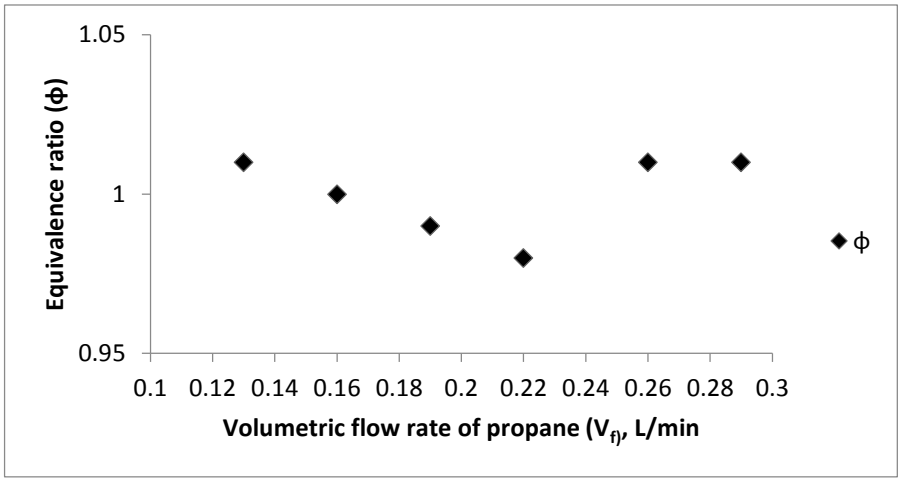

Figure 7.4: Graph showing equivalence ratios near to stoichiometry at different volumetric flow rates of propane

It can be seen that the premixed reactants contained the right amount of oxidant to burn the fuel completely to obtain a premixed flame at these equivalence ratios. Therefore, it can be concluded from these results that even at the stoichiometric conditions, stable combustion did not occur which means that a flame stabilisation mechanism was required which would help anchor the flame inside the combustion chamber.

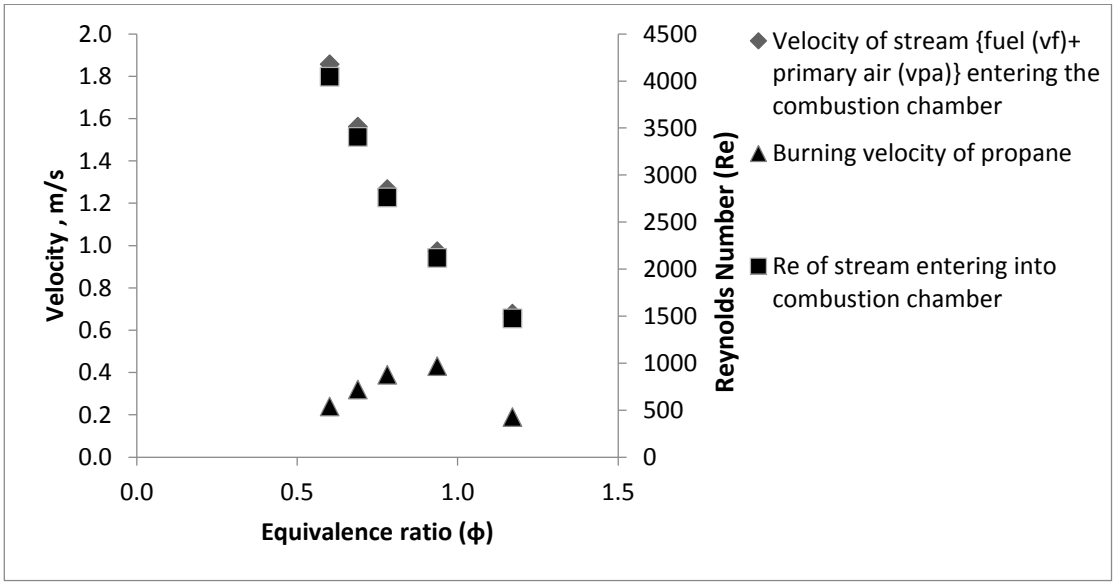

Figure 7.5: Graph showing the Reynolds Number and velocity of the stream i.e. propane and air mixture at different equivalence ratios compared with the burning velocity of propane.

The graph in Figure 7.5 shows the velocity of fuel and primary combustion air stream entering into the combustion chamber of burner having step height 10 mm operating at 150 mL/min of propane injection and the burning velocity of propane. A comparison of the velocities, for instance at ϕ=0.9, shows that the stream velocity is 1.27 m/s whereas at the same ϕ the burning velocity is 0.39 m/s. It can be seen that velocity of the fuel and air stream is significantly higher than the burning velocity of the propane which explains the flame behaviour observed in the burners where the flame was seen to move downstream and experience blowoff where the flame is anchored completely out of the burner.

The results from these tests have shown that a change in step height affects the combustion characteristics in meso-scale burners. It was found that reducing the step height does help in obtaining a flame or combustion inside the combustion chamber or in other words flame blowoff was absent with the step height 7mm, however the flame was seen to experience flickering with consistent high noise. On the other hand, increasing the step height from 10 mm to 15 mm resulted in a very unstable flame which was similar to the flame produced by the burner of step height 10mm. It can be concluded that neither reducing nor increasing the step height resulted in a stable flame inside the combustion chamber. The velocity profiles of the stream and burning velocity of propane have shown that the stream velocity is significantly higher than the burning velocity and hence causing flame blowoff.

It was therefore decided that secondary air holes should be added in order to explore the effect of modifying the flow field in the combustion zone. It was postulated that the inclusion of secondary air jets would affect the momentum flux in the chamber and hence provide a region of low momentum under which stable combustion could take place.

7.3 Experiments with addition of Secondary Air

The addition of secondary combustion air was employed in the burner in order to create a flame stabilisation mechanism. The location of the secondary air injection was at the step while all other design features of the burner were kept same. A detailed drawing of the burner can be found in Figure 5.10 in Chapter 5.

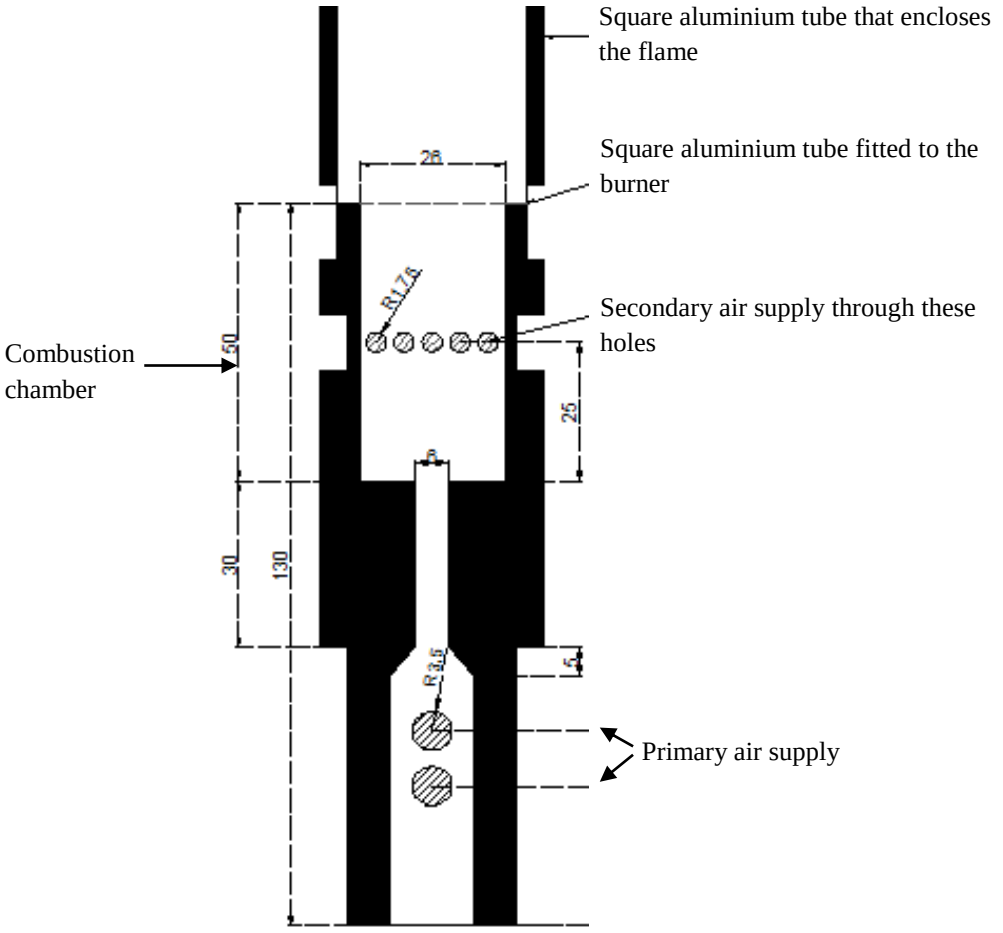

Figure 7.6: Premixed burner with secondary combustion air and BFS (S=10 in this drawing)

The drawing of the burner with secondary combustion air supply and BFS is shown in Figure 7.6. The secondary air is injected via 3.5 mm diameter secondary air holes which are present throughout the circumference of the burner tube and are 25 mm above the BFS. Two separate air rotameters were used to supply the primary and secondary combustion air respectively. The radial photographs with secondary air addition are shown in Figure 7.7.

7.3.1 Results

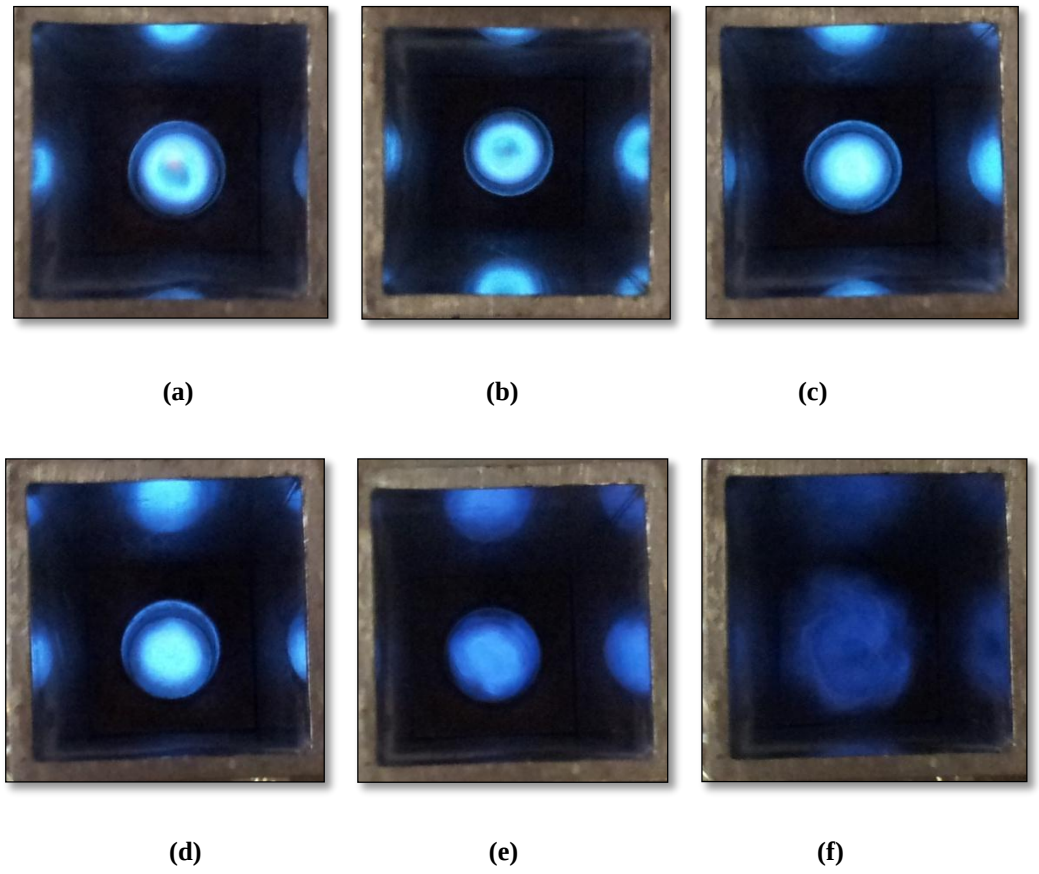

Figure 7.7: Photographs of flames obtained with the premixed burner having step height 10mm (a) V_{pa}=2.5 L/min and V_{sa} =0.5 L/min, (a) V_{pa}=2.5 L/min and V_{sa} =1 L/min, (c) V_{pa}=2.5 L/min and V_{sa} =1.5 L/min, (d) V_{pa}=4 L/min and V_{sa} =0.5 L/min, (e) V_{pa}=4 L/min and V_{sa} =1 L/min and (f) V_{pa}=4 L/min and V_{sa} = 1.5 L/min.

The photographs of the flame at different primary and secondary air addition rates are shown in Figure 7.7. The burner was supplied with 2.5 L/min (Figure 7.7 (a), (b) and (c)) and 4 L/min (Figure 7.7 (d), (e) and (f)) fixed primary combustion air whereas the secondary air was varied from 0.5 L/min to 1.5 L/min. It is apparent from the pictures that the flames produced by the burner on addition of secondary air were stable premixed flames having major part of the flame in blue colour with a small yellow tip at lower secondary air supply rates. The flame was very stable with no noise and no flickering of the flame was seen unless the secondary air was increased to 3.5 L/min. The flame produced no noise as was the case without secondary air addition in the burner with step height 7 mm which produced a flame in the combustion chamber without secondary air addition but the flame was very unstable, noisy and flickered for most of the time. Similar flame characteristics were observed for the burner having step height 15 mm. The

minimum secondary air requirement to obtain a stable flame with burner having step height 10 mm is shown in Figure 7.8. The grey area represents 'no combustion zone' while the white area is the 'zone of combustion'

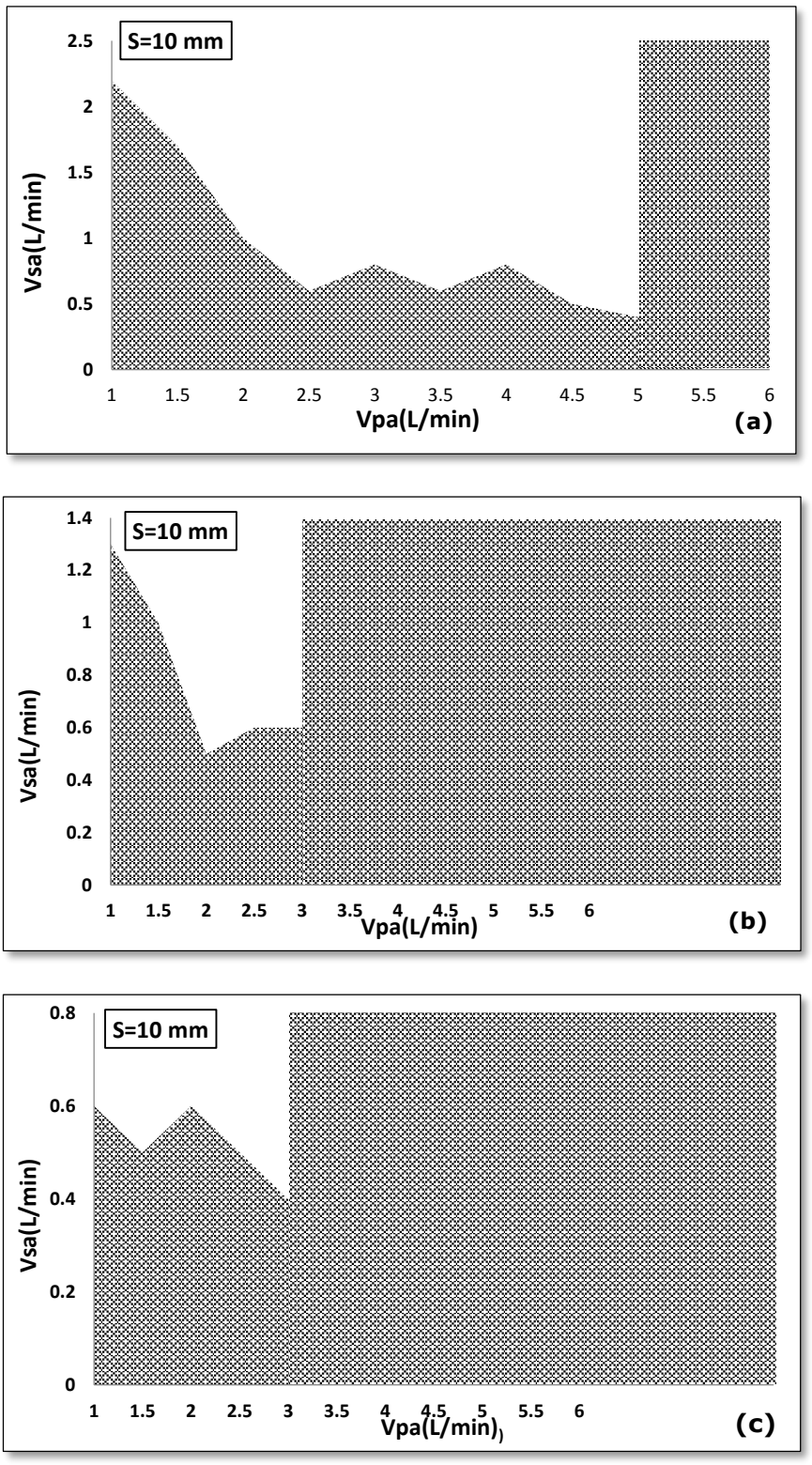

Figure 7.8: Minimum Secondary Air Requirement for stable combustion for step height 10 mm (a)V_f= 250 mL/min. (b) V_f=200 mL/min and (c) V_f=150 mL/min.

Similarly, experiments were conducted to find the minimum secondary air requirement for stable combustion for step height 15 mm at different propane injection rates. The results are shown in the graphs below.

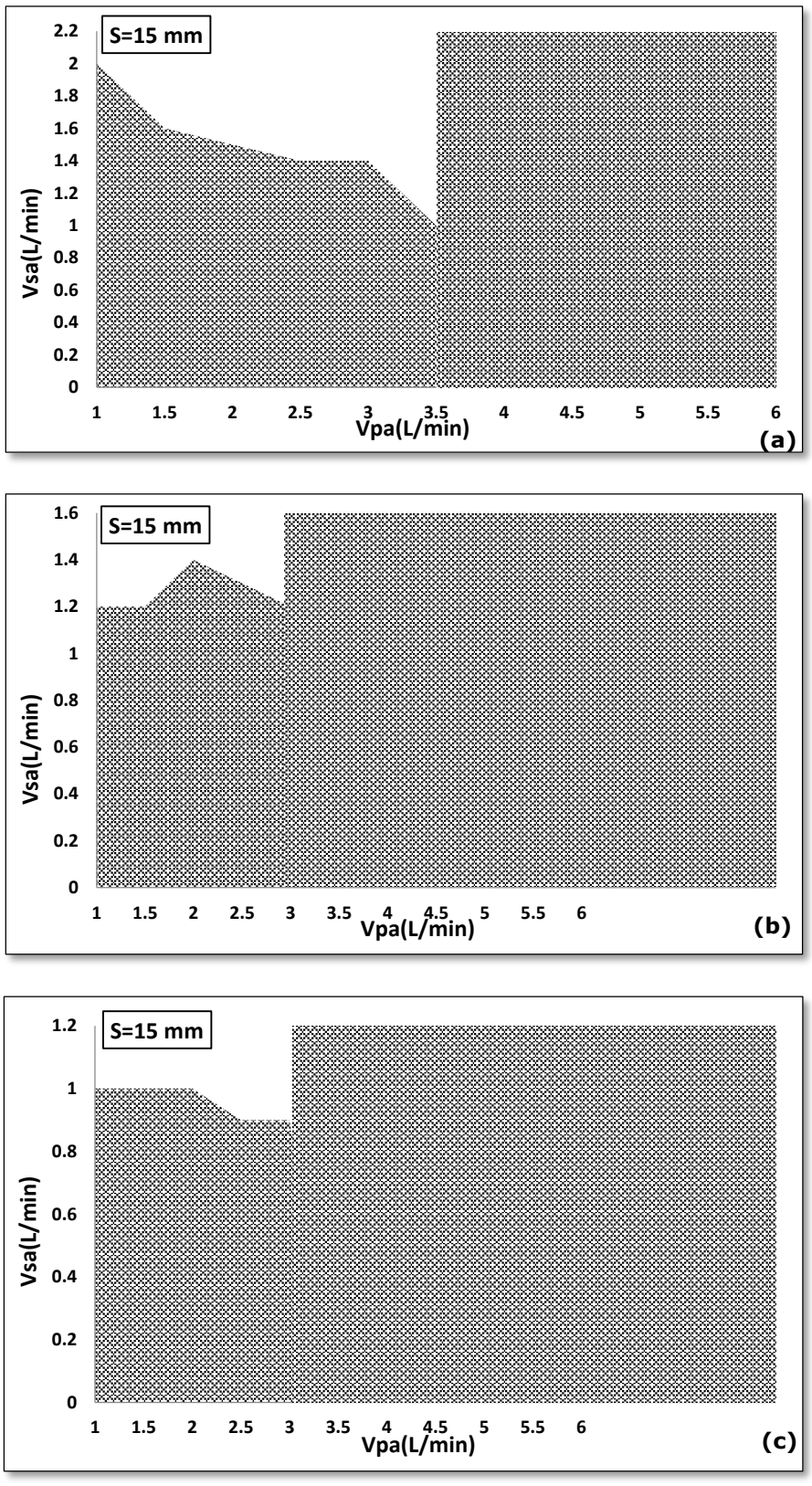

Figure 7.9: Minimum Secondary Air Requirement for stable combustion for step height 15 mm (a) V_f=250 mL/min, (b) V_f=200 mL/min and (c) V_f=150 mL/min

Figure 7.10 below shows the secondary air requirement and corresponding equivalence ratios at which the flame was stable inside the combustion chamber for the burner with step height 10 mm.

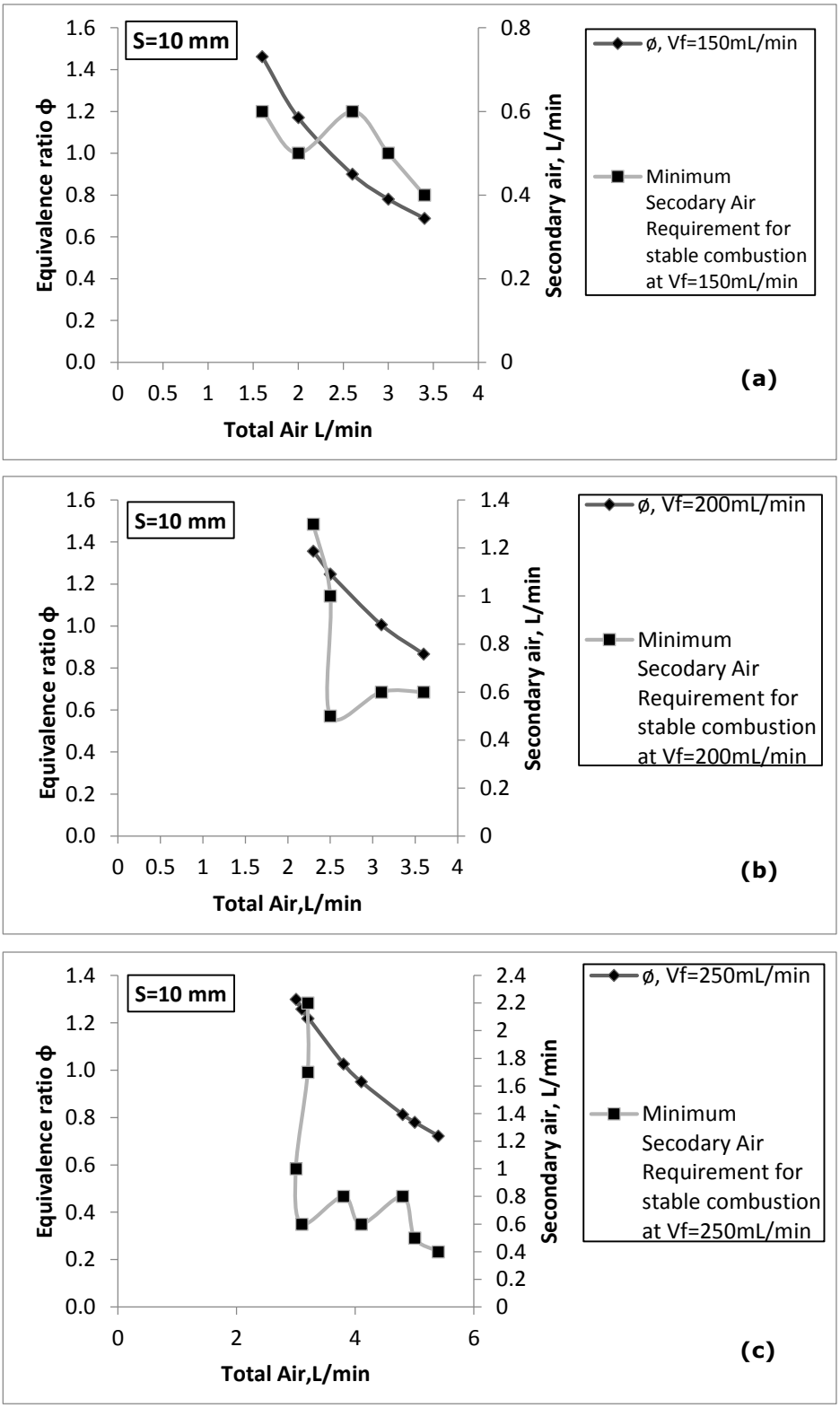

Figure 7.10: Minimum secondary air requirement for stable combustion and the corresponding equivalence ratio at different Total Air supply rates for various propane injection rates for S=10 mm.

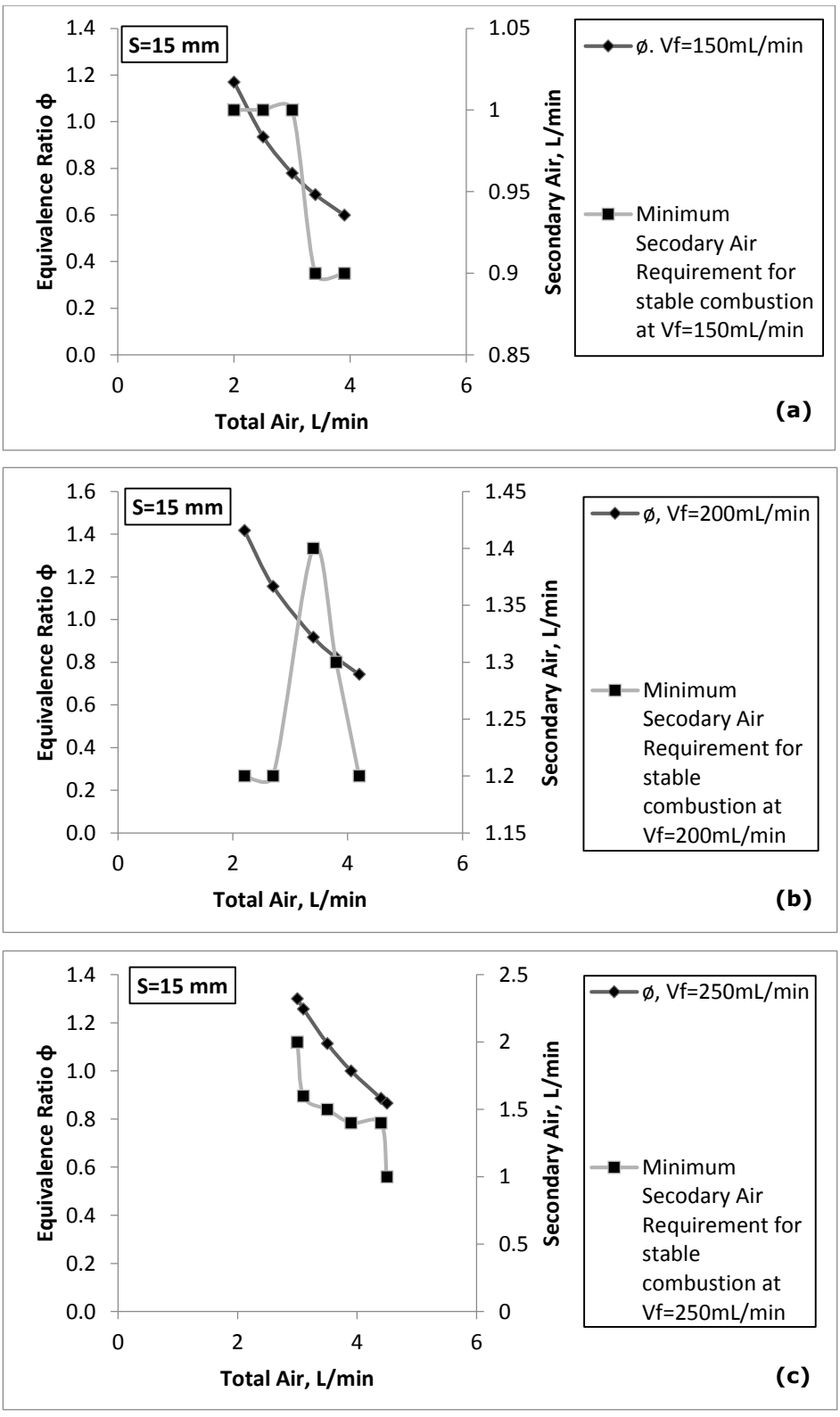

Figure 7.11: Minimum secondary air requirement for stable combustion and the corresponding equivalence ratio at different Total Air supply rates for various propane injection rates for S=15 mm.

Figure 7.11 shows the secondary air requirement and corresponding equivalence ratios at which the flame was stable inside the combustion chamber for the burner with step height 15 mm.

7.3.2 Discussion

The results shown in the Figure 7.8 to Figure 7.11 presents the window of operation of the burner with step heights 10 mm and 15 mm. The graphs in these figures show the minimum flow rate of secondary air required to sustain combustion in the combustion chamber resulting in a stable premixed flame similar to ones shown in the photographs available in Figure 7.7. The results clearly indicate that the addition of secondary air has an effect on flame stabilisation in a small scale burner which has operating characteristics of a micro-scale burner but having geometry of a domestic gas burner required due to its application as explained in the thesis previously in Chapter 1, 3 and 5. The minimum secondary air requirements were obtained for both 10mm and 15mm step height burners which previously showed flame blowoff in the absence of secondary air even though the reactant mixture was near to stoichiometry at some operating conditions.

The velocity profiles will be analysed now in an attempt to understand the flow modification in the combustion chamber that takes place when secondary air is added.

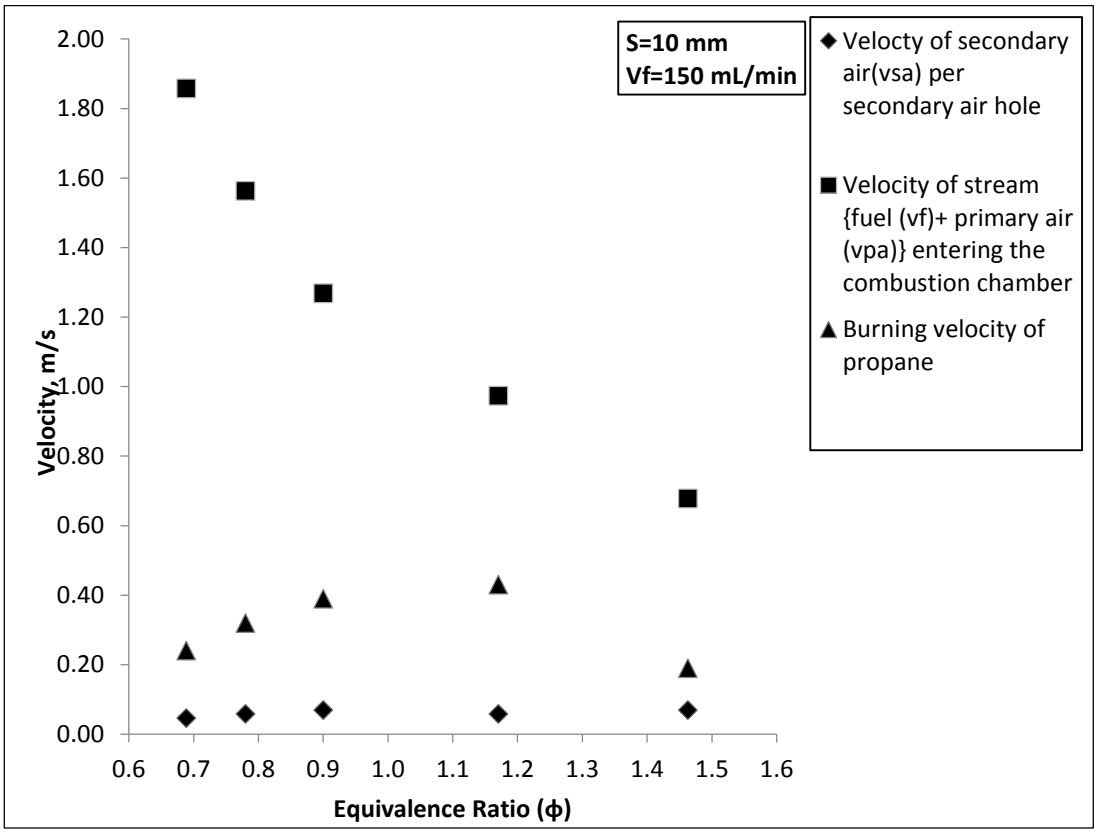

Figure 7.12: The velocity profiles of the fuel and primary combustion air stream, burning velocity of propane and secondary air through each secondary air hole (S=10 mm).

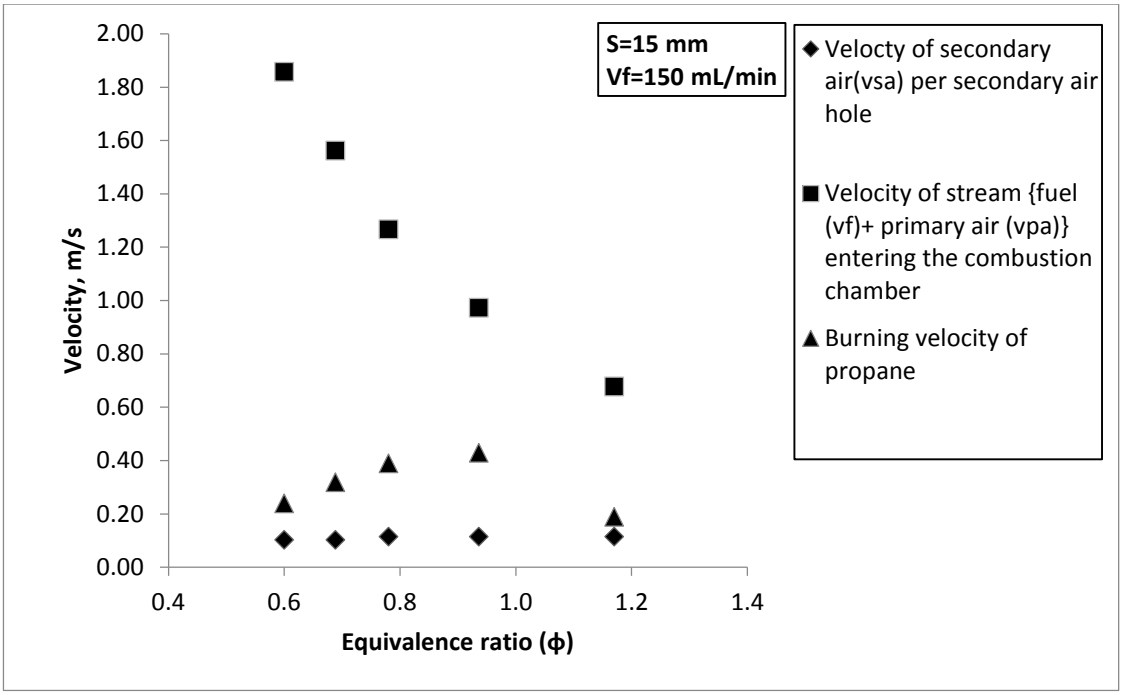

Figure 7.13: The velocity profiles of the fuel and primary combustion air stream, burning velocity of propane and secondary air through each secondary air hole (S=15 mm).

The graph in Figure 7.12 shows the velocity comparisons of the reactant stream which consists of the fuel and the primary combustion air, the secondary air and the burning velocity of the propane at different equivalence ratios for the burner with step height 10mm operating at 150 mL/min propane injection. For a particular equivalence ratio, for instance ϕ=0.9, the velocity of the stream is 1.27 m/s, the burning velocity of the propane is 0.39m/s and the velocity of the secondary air injected is 0.07 m/s per hole. There are 15 secondary air holes at the circumference of the burner tube as shown in the diagram in Figure 7.6, so each hole is injecting secondary air into the burner at a velocity of 0.07 m/s and the total secondary air injection in this case was 0.6 L/min. Similar results were seen with the burner with step height 15mm as shown in Figure 7.13, the reactants stream velocity is same as the burner with step height 10 mm as the premixed zone upstream the combustion chamber has the same diameter in both the burners. Also, the velocity of the reactant stream is same with and without secondary air addition as the secondary air is added later in the combustion chamber. However, the velocity of the secondary air was different as the minimum secondary air required to have combustion was different for different step heights.

According to combustion theory, flame blowoff occurs when the velocity of the reactant stream is higher than the burning velocity of the fuel [27]. This phenomenon can be seen in the velocity profiles shown in the above graphs which clearly show that the velocity of

the reactant stream is significantly higher than the burning velocity of propane and hence causing flame to blowoff. However, as soon as secondary air is added, the flame blowoff does not take place which is clear evidence in itself that the velocity of the reactant stream is reduced in the 'flow interaction zone' which is preventing the flame to blowoff. Hence, we can conclude that the secondary air injection into the combustion chamber perpendicular to the axis of the burner acts as an aerodynamic bluff body which creates a restriction into the flow of reactant stream and thus reducing its velocity and preventing flame blowoff.

Now, the Reynolds Number will be studied to analyse the flow field inside the combustion chamber.

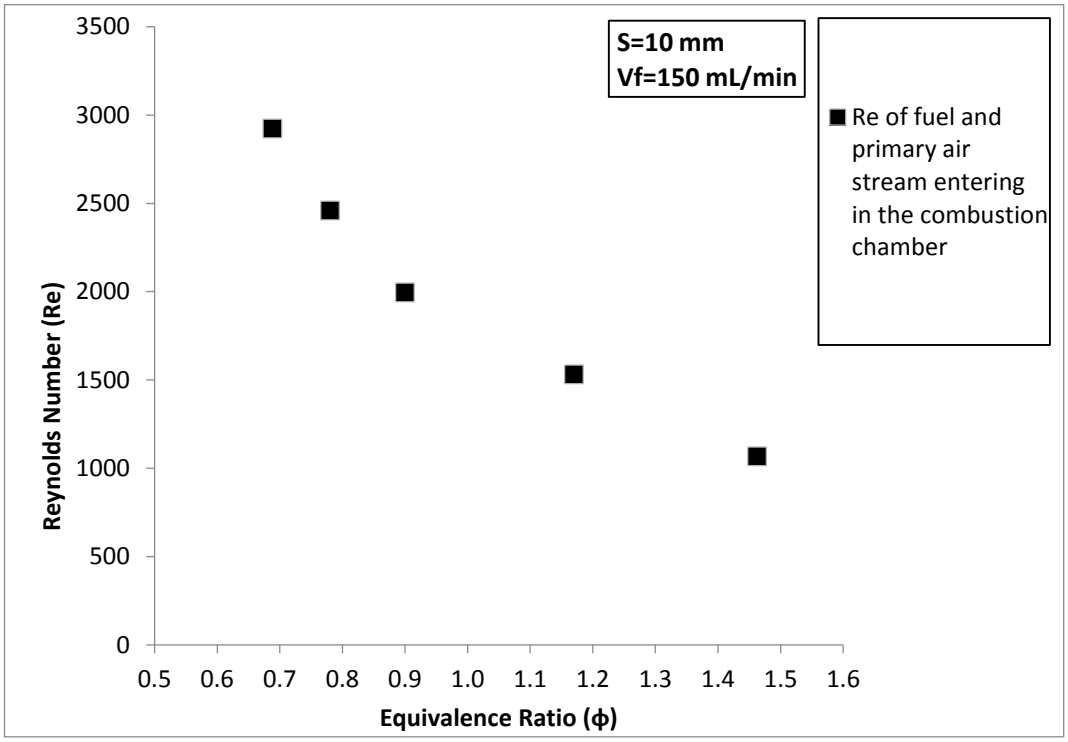

Figure 7.14: Reynolds Number of the fuel and primary combustion air stream (S=10 mm).

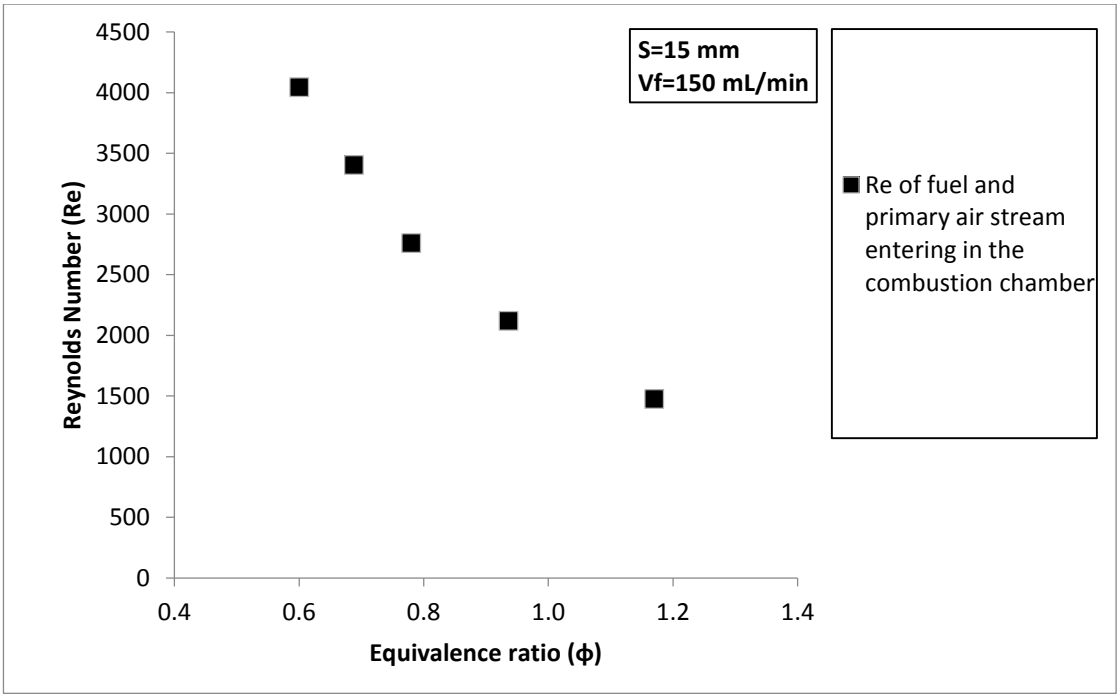

Figure 7.15: Reynolds Number of the fuel and primary combustion air stream (S=15 mm).

Figure 7.14 shows the Reynolds Number (Re) of the reactant stream entering into the combustion chamber at different equivalence ratios for the burner with step height 10 mm. Figure 7.15 shows the respective values of Re but for the burner with step height 15 mm. The Re of the reactant stream entering into the combustion chamber, for instance at ϕ=0.7, is close to 3000 for the step height 10 mm whereas the Re for 15 mm step height is 3500. These values suggests that the flow is turbulent when it enters into the combustion chamber as Re>2300. The difference in the Re for the two burners can be attributed to the difference in the diameters of the combustion chambers.

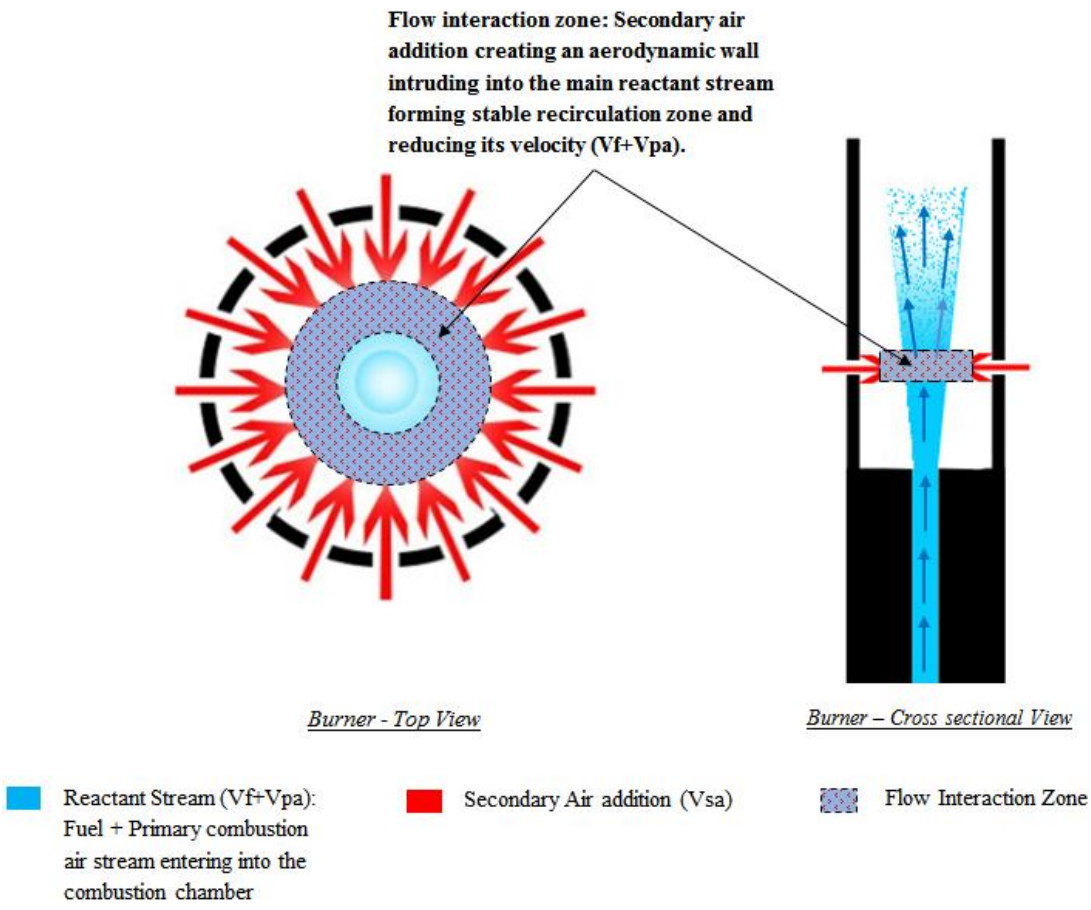

Figure 7.16: Diagram explaining the effect of Secondary Air Addition in the combustion chamber. Secondary Air acting as a 'bluff-body' or a wall intruding into the main reactant stream thus reduces its velocity.

The diagram in Figure 7.16 explains the effect of secondary air addition in the combustion chamber on flame stabilisation. It can be seen that the secondary air injected through air holes added into the periphery of the burner tube in a direction perpendicular to the flow of main stream. This creates a zone of flow interaction where the secondary air intrudes into the main reactant stream and this collision of the two streams forms small recirculation zones of high turbulence. The addition of secondary air increases the net volume flux in the combustion chamber, therefore according to theory the average bulk velocity of the reactants should increase. This suggests that the secondary air forms stable recirculation zone inside the 'flow interaction zone' where the local velocity of the reactants is slower as explained in the Figure 7.16. This shows that the secondary air introduces aerodynamic stability or in other words the secondary air injection helps in slowing down the local velocity of the main stream in the flow interaction zone and hence producing a balance between the propane burning velocity and the reactant stream velocity so that the fuel is oxidised inside the combustion chamber rather than at the

extreme downstream or at the exit as observed without secondary air. The addition of secondary into a 33 kW premixed burner having a BFS has been studied by Atley et al [66]. The findings of the present study are in agreement with their work where they have suggested that the addition of secondary air near the step in a direction perpendicular to the stream helps in reducing thermoacoustic instabilities. In another experimental research on premixed burner with BFS carried out by Ghoniem et al.[65] found that injection of air perpendicular to the stream in the flame anchoring zone helps in stabilising the flame by overcoming pressure oscillations and reduces the NOx concentration as well. Also, in the case of burner with 7 mm step height which produced a flame inside the combustion chamber without secondary air addition, it can be argued that due to small step height the stream of reactants coming into the combustion chamber impinges on the chamber walls hence reducing its velocity and therefore combustion was taking place inside the combustion chamber though with some instabilities. On the other hand when the step height was increased to 10 mm or 15 mm, the reactant stream do not collide with the chamber walls due to its distance from the burner centre and hence the velocity is not reduced and is greater than the burning velocity of propane and hence resulting into flame blowoff without the addition of secondary air.

7.4 Summary

This chapter presented results from tests aimed at investigation into the effect of secondary air addition in the combustion chamber on flame stabilisation. The initial tests were conducted on three burners having different step heights without secondary air addition and operating at forced air supply mode as opposed to the tests performed under self-aspiration mode mentioned in Chapter 5. This was followed by addition of secondary air into the combustion chamber of the burner with step height 10mm and the results were confirmed with similar trends shown in the results of burner with step height 15mm. The following can be concluded from the test results presented in this chapter:

- The reduction in step height from 10 mm to 7 mm resulted in a visual flame inside the combustion chamber; hence the flame blowoff did not occur with the step height 7mm as was the case with 10 mm step height. The flame was observed to have acoustic instabilities along with continuous flickering and hence the flame could not be classified as a stable premixed flame.
- The increase in step height from 10 mm to 15 mm resulted into similar results as were seen with the step height 10 mm i.e. flame blowoff was observed for all equivalence ratios and the flame was absent from the combustion chamber for all operating conditions.
- The addition of secondary air has significant effect on flame stabilisation. The burners with step height 10 mm and 15 mm showed a stable premixed flame inside the combustion chamber with no acoustic instabilities and no flame flickering observed when secondary air was added. The velocity of the reactant stream calculated was significantly higher than the burning velocity of propane; therefore flame blowoff was occurring without secondary air addition. The possible reason could be the secondary air stream acting as an aerodynamic bluff body causing the velocity of the reactant stream to reduce and hence preventing blowoff. This reasoning can be validated based on the fact that the velocity of the reactant stream entering into the combustion chamber is same with and without secondary air supply as the secondary air is supplied later into the combustion chamber, hence the only logical explanation could be the secondary air generating aerodynamic wall which is intruding in the reactant stream and hence reducing its velocity and preventing flame blowoff.

Chapter 8

Optimised Design Validation

8.1 Introduction

This chapter presents results from tests conducted on the final prototype of the CO_2 Generator device consisting of a premixed burner integrated with two TEG modules. The aim of these tests was to obtain evidence which would help in the validation of the concept of integrating combustion and thermoelectric for small scale power generation application such as a CO_2 Generator of the present research. The CO_2 Generator developed and investigated in this study has its application in insect control industry, the premixed burner produces CO_2 which is a proven attractant for insects such as mosquitoes and TEG modules integrated with the burner produces power to run the electrical components of the insect trap. Thus, the tests carried out were aimed at investigating the performance of combustion and thermoelectric integrated unit operating under real environmental conditions, providing operational reliability and robustness analysis of these devices. A series of tests were performed with the aim of determining conformation of the operation of the unit as per design and operating requirements mentioned in Chapter 5, Development of the CO_2 Generator. Following are the main objectives of tests carried out and subsequent results reported in this chapter:

- The focus has been given on investigating the products of combustion of the premixed burner after integrating it with the TEGs.
- The device was tested in an environment chamber where it was operated under varied ambient temperatures and results were compared and analysis was performed to see the effect of ambient temperature on power generation.
- To gather further evidence on the completeness of combustion, amount and quality of CO_2 production, the unit was tested with live mosquitoes by using an Olfactometer. As the application of this CO_2 generator is with insect attraction (mentioned in detail in the Introduction chapter), the unit was tested to find out the behaviour of mosquitoes towards the CO_2 produced by the premixed burner.
- At last, the CO_2 generator was tested in actual field at various sites at North Wales, UK. A number of working prototypes were constructed and were placed at test sites where they were allowed to operate for a certain amount of time to capture

mosquitoes. The results were compared with competitor's mosquitoes catching apparatus.

8.2 Exhaust analysis

This section presents an exhaust composition of the unit after integrating the burner with TEG modules for power generation. The purpose of analysing the exhaust has to make sure that after integrating with thermoelectrics the combustion in the premix burner was not affected in terms of concentration of products of combustion. The final unit was designated as a CO_2 Generator and is shown in the photograph below:

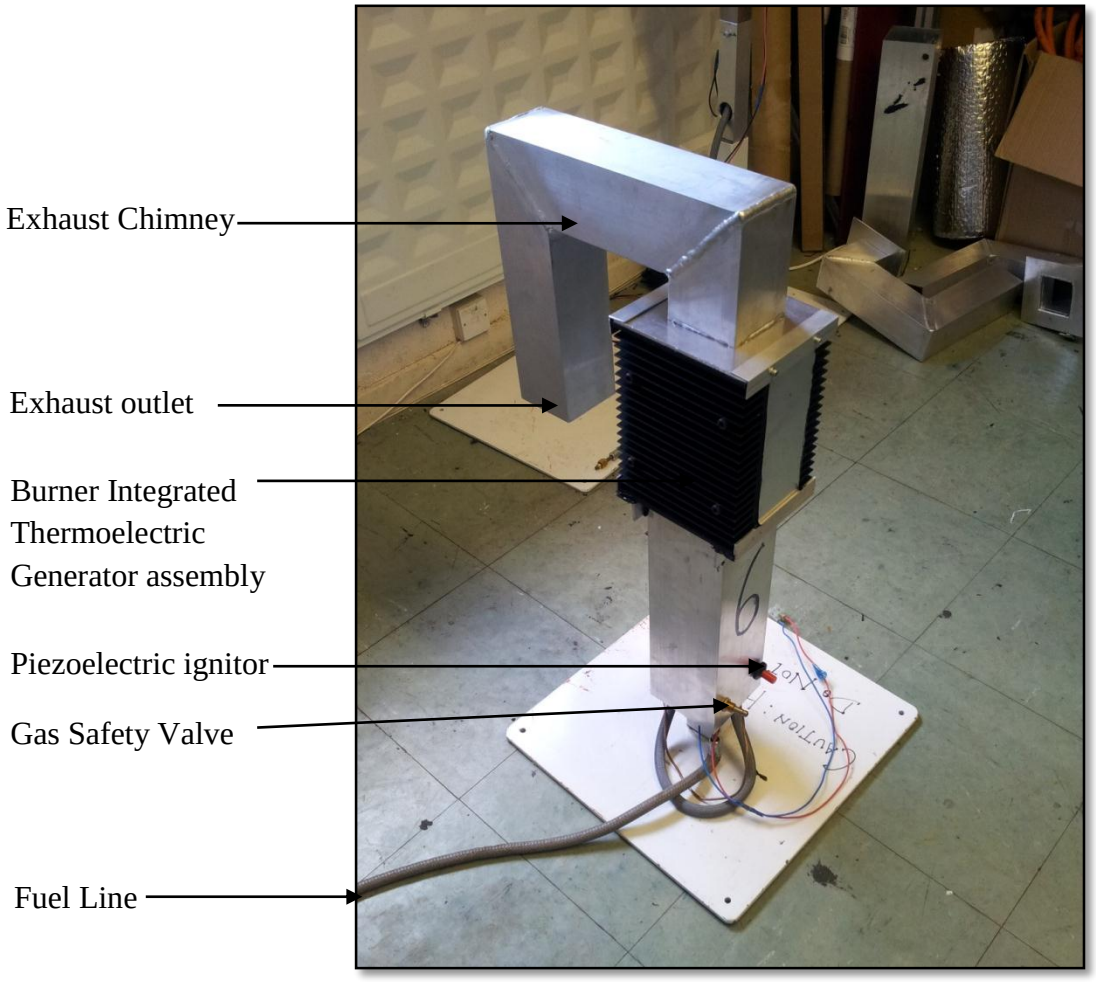

Figure 8.1: A CO_2 Generator assembly consisting of meso-scale premix burner integrated thermoelectric generator

The final design of the CO_2 Generator is shown in Figure 8.1 which consists of a brass nozzle designed to allow ~150 ml/min of fuel supply. The accuracy of machining nozzle orifice was not 100%, hence, the percentage volume of CO_2 production shown in the graph below is higher than the gas analysis results presented in Chapter 5 in which case the fuel was accurately measured and supplied at a fixed required rate via a gas flowmeter

while in the final assembly the fuel supply is fixed by the size of the orifice which as mentioned has machining errors causing higher fuel to flow through.

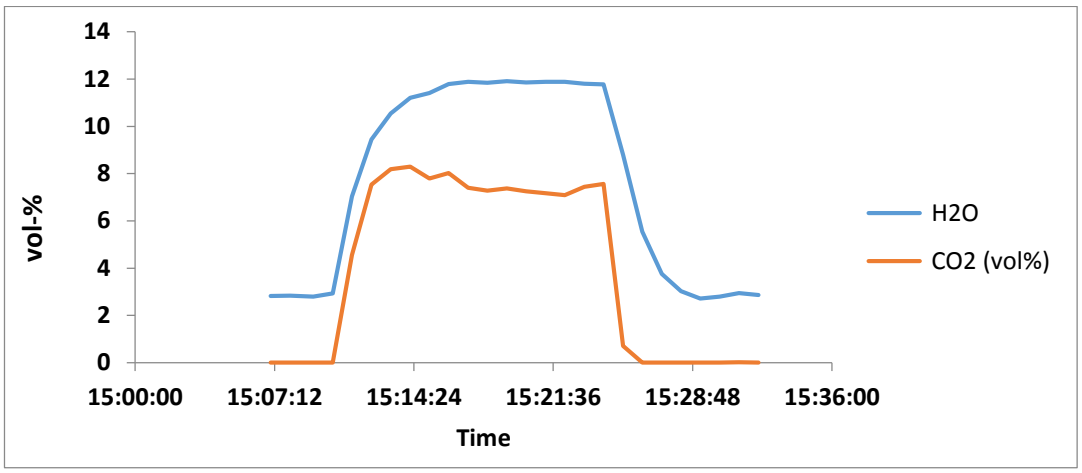

Figure 8.2: H_2O and CO_2 Concentrations

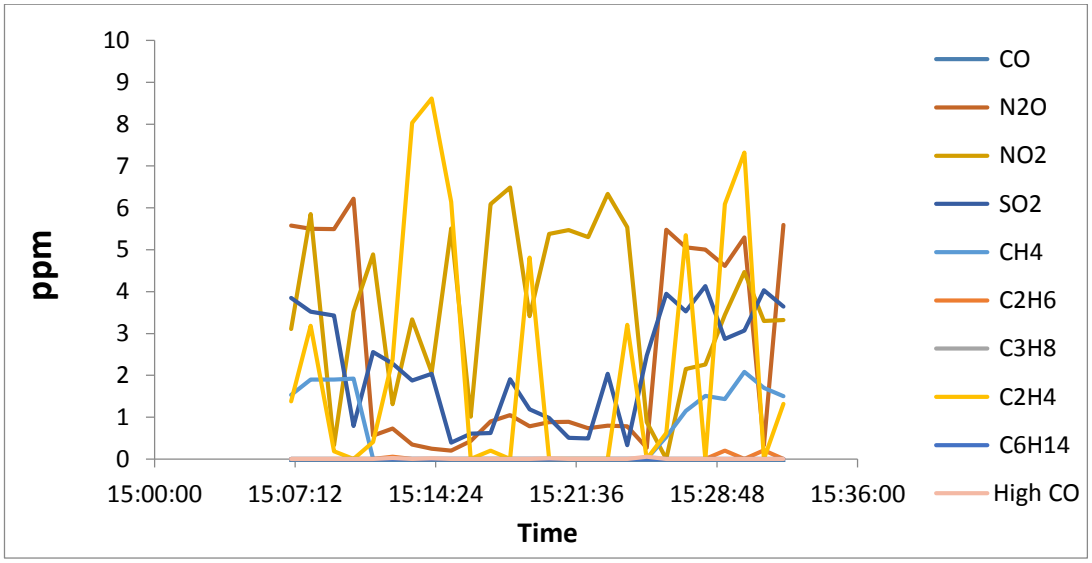

Figure 8.3: Concentration of various compounds (ppm)

Figure 8.2 shows the production of CO_2 and H_2O, the percentage volume of CO_2 shown by the FTIR was approx. 7 % while H_2O was approx. 12 %. Figure 8.3 shows volumetric concentrations in ppm of various compounds other than CO_2 and H_2O in the burner exhaust. The purpose of this analysis was to make sure that compounds such as CO and NOx are not present in significant amounts after integration of the burner with thermoelectrics. CO, N_2O, NO_2, SO_2, CH_4, C_2H_6, C_2H_4, and C_6H_{14} were found to be less than 10ppm. There were no signs of un-burnt C_3H_8 in the exhaust indicating complete combustion. Considering the absence of C_3H_8 in the exhaust and assuming 150 ml/min of C_3H_8 supplied to the burner, the CO_2 production rate should be around 450 ml/min. The CO_2 production rate was considered to be satisfactory. The exhaust analysis has

shown that integrating thermoelectric power generation devices to burner walls does not affect the flame stability and combustion characteristics.

8.3 Effect of Ambient Temperature

Experiments were carried out for power output from two thermoelectric modules connected in series, sandwiched between burner wall and heat sinks (Nominal Configuration, Figure 6.10, and Chapter 6). The device was operated for a minimum of 8 hours continuously at a given chamber temperature.

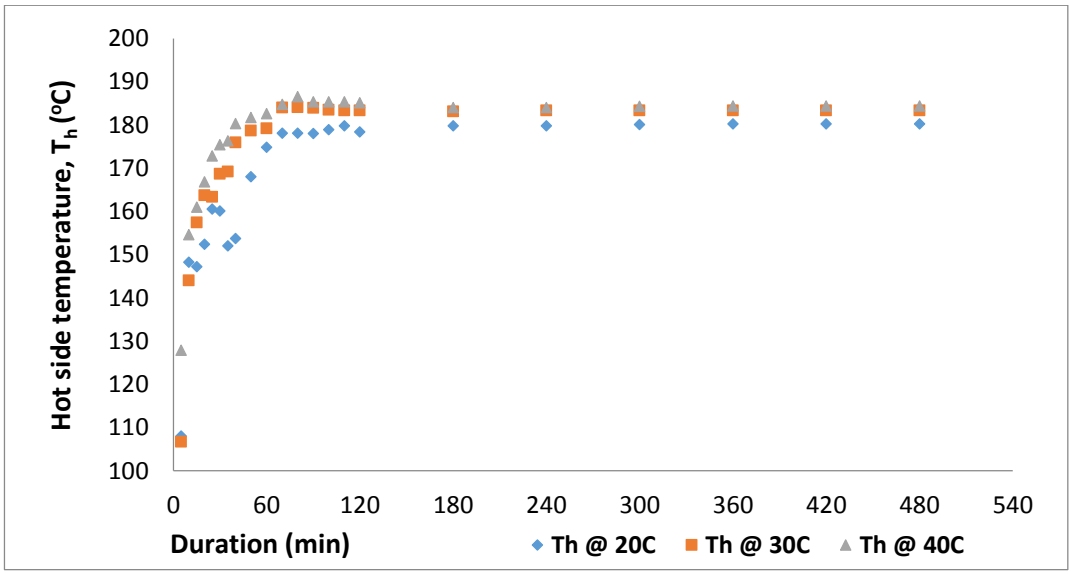

Figure 8.4: Hot side temperature, T_H at different Ambient Temperature settings in the Environmental Chamber

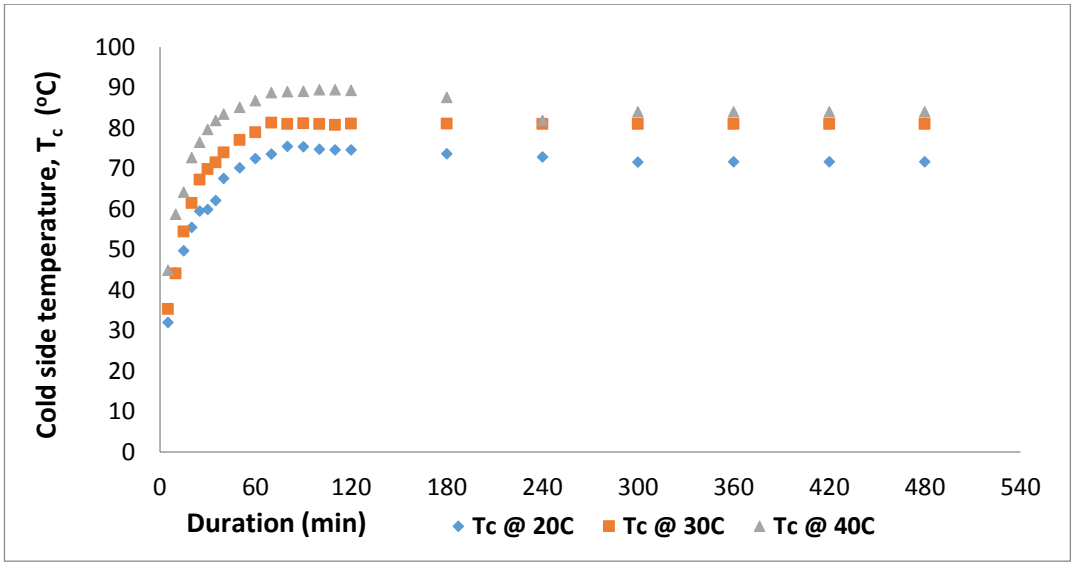

Figure 8.5: Cold side temperature, T_C at different Ambient Temperature settings in the Environmental Chamber

Three values of chamber temperature were considered: 20 ^{o}C, 30 ^{o}C and 40 ^{o}C.

The graph in Figure 8.4 shows T_H at different ambient temperatures set inside the Environmental Chamber. It can be seen that there is around 2.3 % increase in hot side temperature with increase in the chamber temperature from 20 ^{o}C to 40 ^{o}C. This increase in the hot side temperature is attributed to the fact that at higher chamber temperatures, the inlet air to the burner is warmer causing the combustion temperature to increase. On the other hand, an approximately 17 % increase in the cold side temperature was observed when the chamber temperature was increased from 20 ^{o}C to 40 ^{o}C as shown in the graph in Figure 8.5. This is an effect caused by low dissipation of heat by heat sinks at higher chamber temperatures. The increase in both hot cold and hot side temperature has an effect on the temperature difference and hence, output voltage and maximum power output of thermoelectric modules.

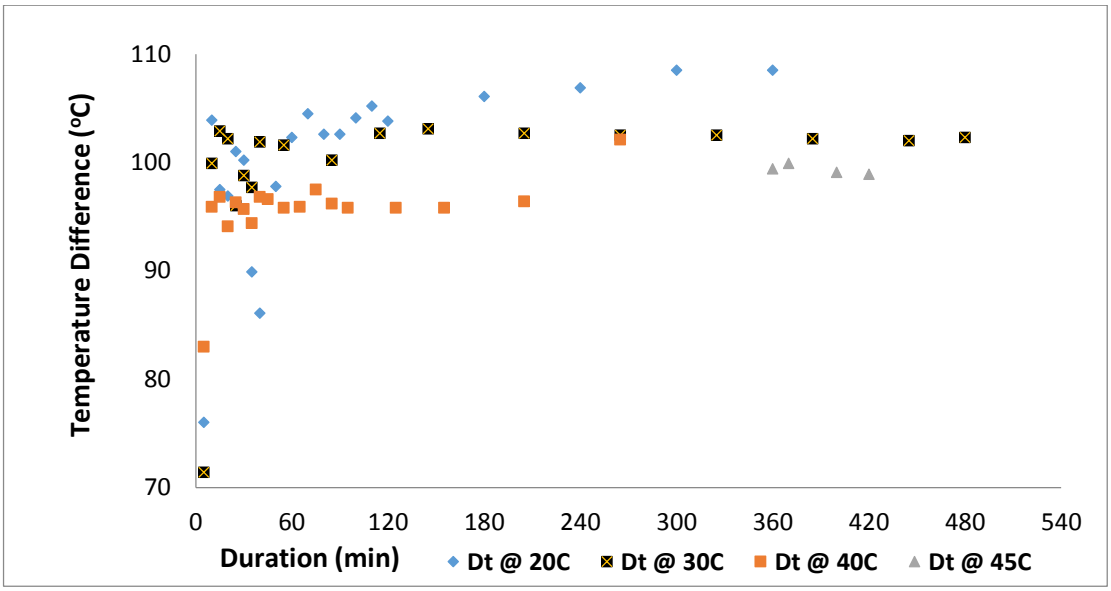

Figure 8.6: Temperature difference at various Ambient Temperature settings in the Environmental Chamber

The graph in Figure 8.6 shows temperature difference at different chamber temperatures. It is evident that the temperature difference decreases with increasing chamber temperature. This can be attributed to the higher cold side temperature causing the temperature difference to decrease. The initial 60 minutes show some non-uniformity in the data which can be referred to as stabilisation phase. After that the temperature difference is consistent for the remaining duration of the test. This test proved the feasibility of generating electrical power using thermoelectric power generation principle

even at conditions where temperature is above 40 ^{o}C. The corresponding maximum power at different chamber temperatures is shown in the Figure 8.7.

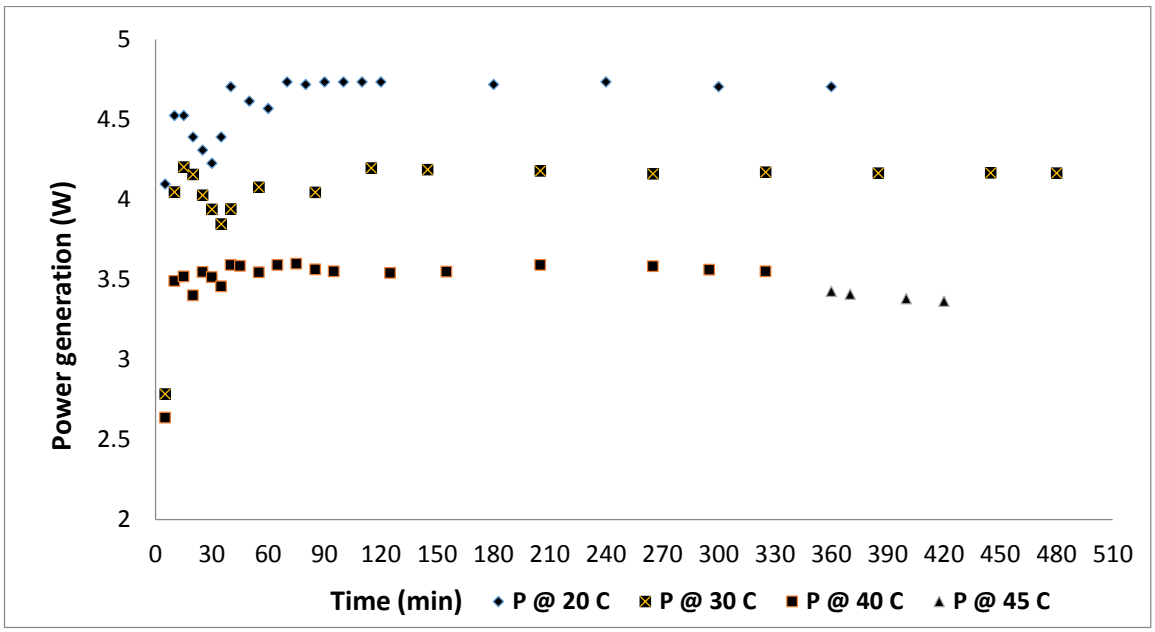

Figure 8.7: Power generation at different Ambient Temperature settings in the Environmental Chamber

It can be seen in the Figure 8.7 that maximum power decreases with increasing chamber temperature which is expected as power output is directly proportional to temperature difference. The decrease in temperature difference at elevated chamber temperatures will decrease the power output as well. A similar trend is seen in the power curves also, uniform power is achieved after the initial stabilisation phase. Again, this shows the feasibility of this concept at places where ambient temperature is just above 40 ^{o}C.

The experimental analysis of thermoelectric generators integrated with meso-scale burners operating at different ambient temperatures have shown that that the electrical power output decreases with increasing ambient temperature because of decrease in temperature difference. This study proves the operational feasibility of thermoelectric and combustions systems working together to generate enough electrical power to run small scale electronic devices while maintaining complete combustion for long durations. The results can be used as a reference for future work on similar meso-scale thermoelectric generator combustors.

8.4 Olfactometer Tests

The CO_2 Generator was tested with live insects at a testing facility at Biogents AG in Regensburg, Germany. The objective of the tests was to determine the effectiveness of CO_2 in terms of attracting insects, in this case mosquitoes as they have proven attraction towards CO_2; hence, providing evidence that the CO_2 Generator produces the required amount CO_2 and the combustion exhaust does not contain harmful compounds such as CO, UHC or NOx in significantly higher amounts.

The tests were carried out using an Olfactometer designed by Biogents AG. [101][102]. According to Biogents, an Olfactometer is an equipment to investigate the level of attraction or repulsion of mosquitoes to volatile stimuli in choice experiments.

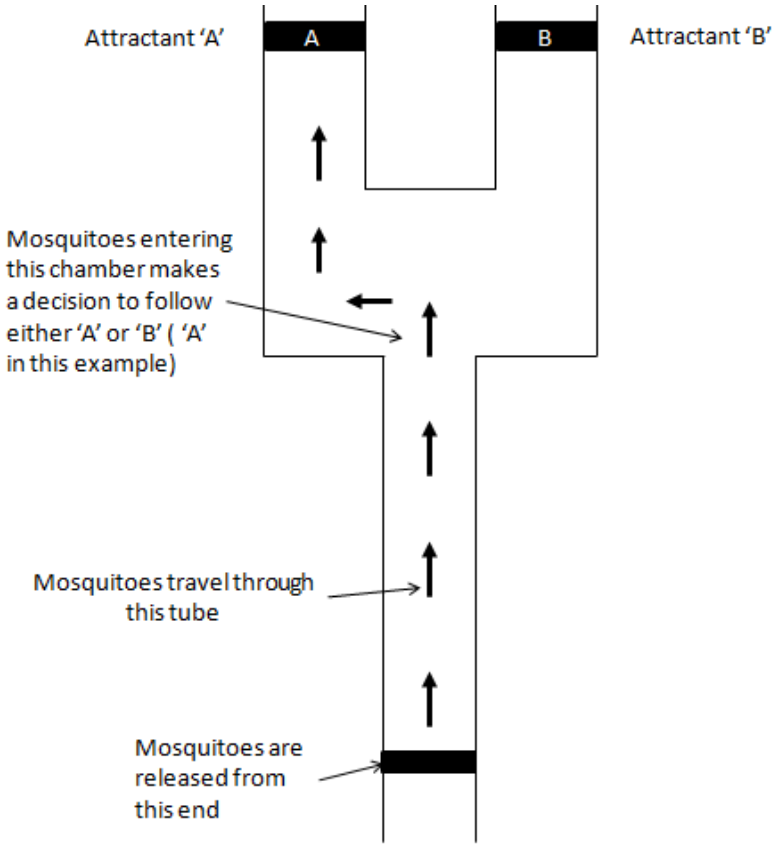

Figure 8.8: Olfactometer developed by Biogents AG, Regensburg, Germany

An Olfactometer is a Y-tube shaped equipment which has mosquitoes at one end while the end contains attractants, Attractant 'A' and Attractant 'B'. A constant flow of clean and conditioned air is maintained through the apparatus towards the end where blood-hungry mosquito females are connected as shown in the Figure 8.8. During tests, mosquitoes are freed and allowed to enter the tube system where they choose between 'A' and 'B'.

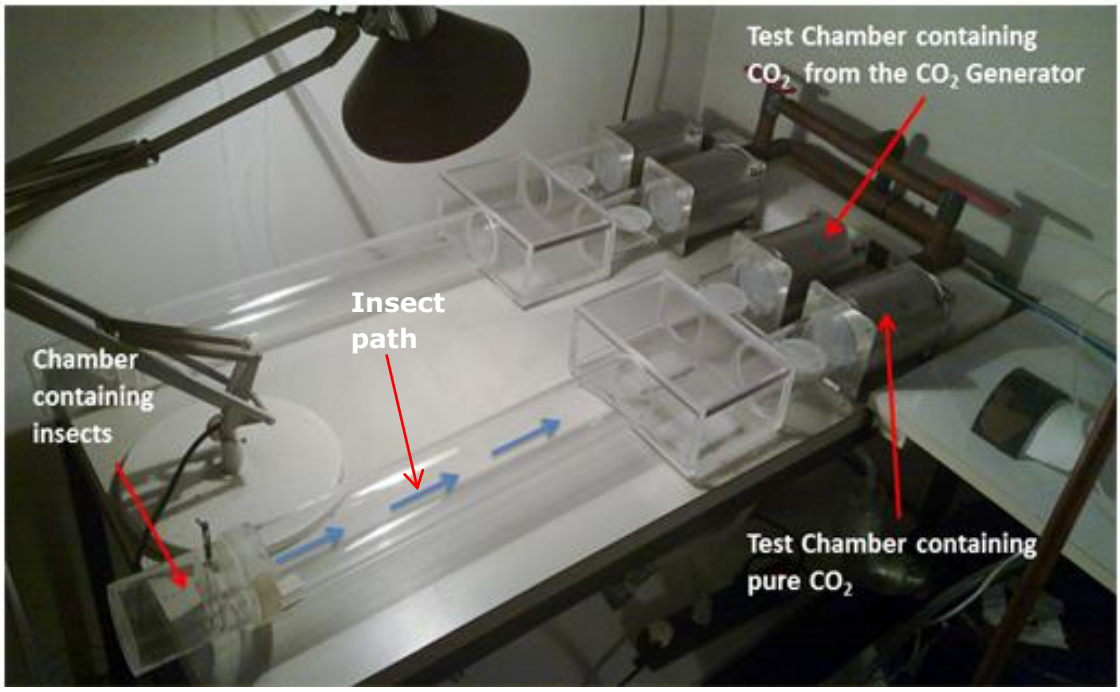

Figure 8.9: A photograph showing an Olfactometer used for determining insect behaviour towards particular attractants

Figure 8.9 shows a photograph of tests being carried out in the Olfactometer equipment. As it can be seen in the picture, one test chamber is always supplied with clean air only while the other test chamber is provided with pure CO_2, a human finger as a source of attractant and CO_2 produced by the CO_2 Generator in each set of test. Mosquitoes were released and the results are shown in the Figure 8.10.

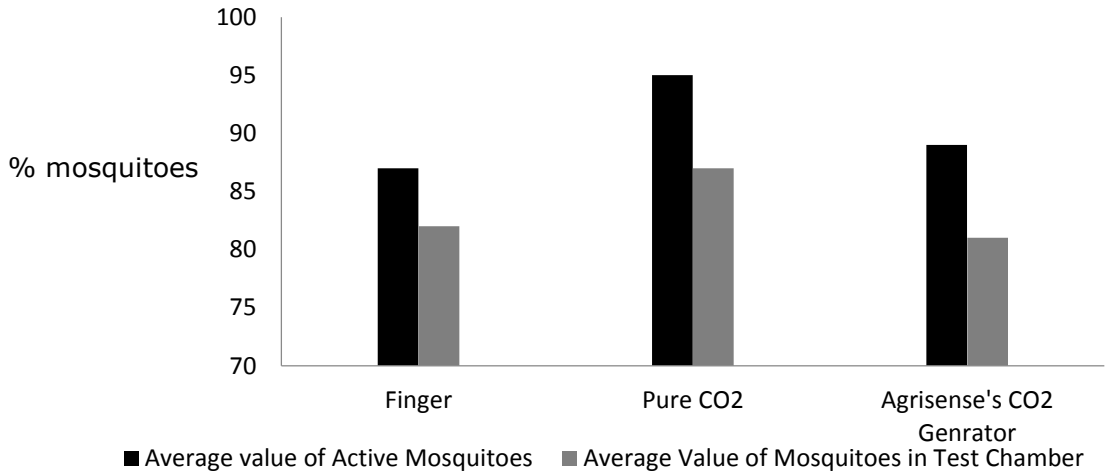

Figure 8.10: Results from Olfactometer with three attractants tested – Human Finger, Pure CO_2 and CO_2 produced by the CO_2 generator (Agrisense's CO_2 Generator) investigated in the current research

The ‘Average value of Active Mosquitoes’ is the percentage of mosquitoes which left the mosquito chamber upon release, while the ‘Average mosquitoes in Test Chamber’ are the percentage of mosquitoes who chose to enter the chamber containing either finger, Pure CO_2 and CO_2 from CO_2 Generator. It can be seen in the figure that the result for the CO_2 generator was positive with 89 % of the mosquitoes stimulated and left their initial location, 81% followed the chamber containing CO_2 from the CO_2 Generator whereas only 8% chose to head towards the test chamber containing air only. These results were similar to Pure CO_2 in which case the percentage of mosquitoes entered the test chamber with air was 8 % too even though the average number of active mosquitoes were higher at 91 %. The results with finger showed the least percentage of mosquitoes choosing to enter the test chamber with air which in other words mean that most of the mosquitoes entered the test chamber having the human finger.

The results with finger showed least difference in the percentage of mosquitoes leaving their initial chamber and the percentage of mosquitoes entering the chamber having the finger, this can be attributed to the explanation that the finger contains a combination of attractants such as human body temperature and human sweat which is the most effective combination according to entomological experts conducted these tests. The tests with pure CO_2 have showed quite similar results as with CO_2 from the burner which further adds to the evidence that the quality of CO_2 produced by the burner is not too far off being pure CO_2. The results from laboratory testing showed that the exhaust of the premixed burner designed and investigated in the present study produces the required amount and quality of CO_2. The high percentage of mosquitoes choosing to enter the test chamber containing the exhaust from the burner shows there is no or very little CO, NOx and UHC which is in agreement with the results from gas analysis performed using FTIR.

8.5 Field Trials

After obtaining satisfactory results from laboratory tests, which showed no repulsion of mosquitoes from the exhaust of the burner, working prototypes of the CO_2 generator were constructed for field trials. The objectives of these trials were to obtain data on mosquitoes/midges catch, performance of thermoelectric generator and robustness of the unit. Data on mosquitoes/midges trapped by the unit is important to determine if the CO_2 production is as per requirement but also for marketing purpose. Robustness of the unit in terms of its capability to withstand high wind, fluctuation in ambient temperatures and rain were the main considerations. The thermoelectric performance is important as the fan of the mosquito catching apparatus needs to be operating all the time for mosquitoes

to be held inside the trap. The thermoelectric data obtained earlier was recorded in a confined environment so it was important to analyse its performance in the actual field environment.

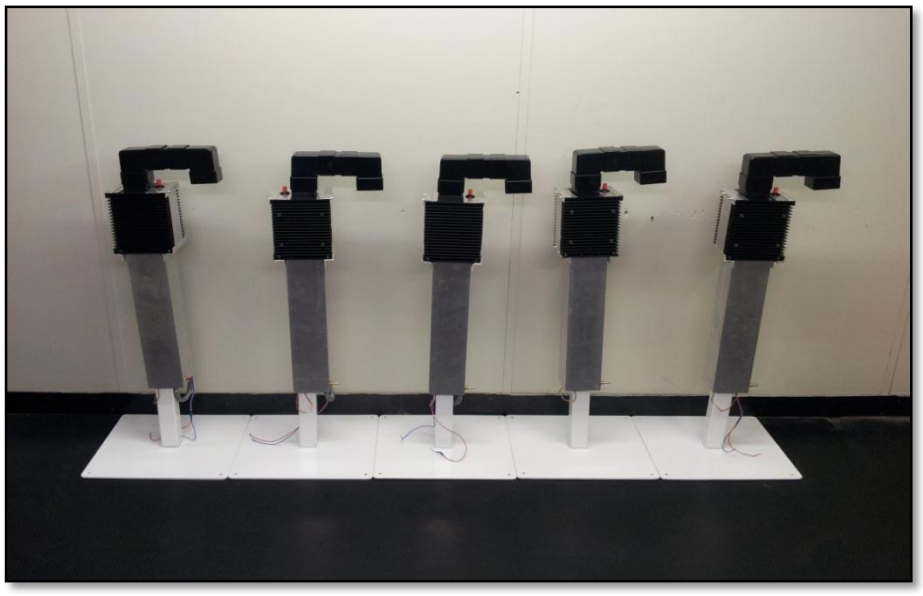

Figure 8.11: CO_2 Generator Prototypes

Figure 8.11 shows 5 prototypes being constructed for the field trials. The location of field trials was chosen to be at Swansea, UK. The test plan included comparison of the unit of the present study with a commercially available mosquito trap. The trap used for comparison was a Skeetervac SV5100 marketed by Blue Rhino [11], the working concept of this trap is similar to the CO_2 generator of the present research in terms of combustion of a hydrocarbon fuel and thermoelectric conversion as a means on power generation but the combustion is catalytic.

Figure 8.12: A CO_2 Generator connected to a 13 kg propane bottle, placed at a test site near Swansea

Figure 8.13: A CO_2 Generator placed at one of the test sites having ideal conditions for mosquito breeding

The CO_2 Generator shown in the Figure 8.12 and 8.13 was operating at around 250 W burner thermal output, around 150 mL/min of propane was supplied from a 13 kg propane bottle, was producing around 450 mL/min of CO_2 and was capable of generating approx. 3.5W of electrical power output. The mosquito catching apparatus used in these trials was Sentinel mosquito Trap manufactured by Biogents AG, the working principle of the trap can be found in the Chapter 1 Introduction. The units were placed in the field at a distance of 10m apart from each other. It should be noted here that due to the location being coastal, strong wind and rain was observed throughout the trials. The reason behind choosing this particular location was the unavailability of mosquito species at other sites due to weather and mosquito breeding season almost coming to an end. Due to time limit on completion of the tests and obtaining the data, tests had to be conducted at this site even though the ambient conditions were not exactly in the favour. The catch results can be seen in the Figure 8.14.

Figure 8.14: A photograph of mosquitoes captured by the CO_2 Generator

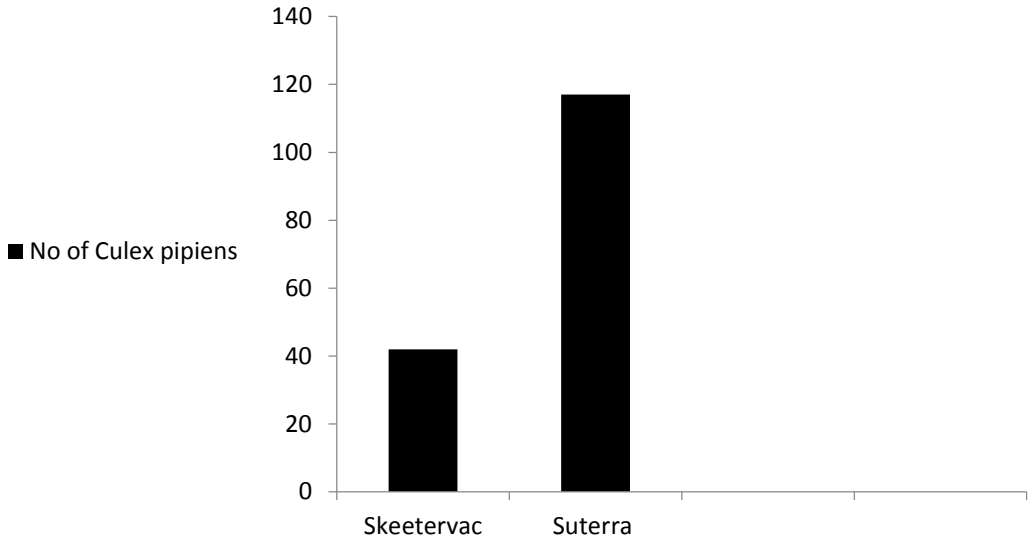

Figure 8.15: A comparison of Culex Pipiens captured by Skeetervac and CO_2 Generator

Figure 8.15 shows a comparison of mosquito catches of Skeetervac and the CO_2 Generator in a period of 24 hours of continuous operation. The species found at that particular site was Culex Pipiens. The number of Culex Pipiens caught by Skeetervac was 42 for this particular test period while 117 Culex Pipiens were found to be present in the mosquito catching apparatus employing CO_2 generator of the current study. The results from this particular test site showed that the CO_2 generator outperformed the competitor's product by a significant amount which was a clear indicator that the mosquitoes are attracted by the CO_2 produced by the CO_2 generator device, hence, providing evidence of clean and stable combustion. It should be noted here that an enormous amount of field trials are required to compare the results and obtain a definite conclusion on which trap is more efficient as various factors can affect the number of mosquitoes trapped by a trap, for instance the location of the trap. Given the limited resources available to perform the field trials, these results were encouraging as they confirmed that mosquitoes were attracted by the CO_2 produced by the device and that there was no evidence suggesting presence of any compound in the exhaust which would repel them. The mosquito catch also confirms the required electrical power generation as the fan's suction power holds the mosquitoes in the insect catch bag, an insufficient voltage generation would mean the fan speed is low and hence the mosquitoes would escape out. It can be concluded that the results indicate fulfilment of operational requirements.

8.6 Cost Analysis

As previously mentioned in the Chapter 1, project motivation and design requirements section, one of the main objectives of designing the CO_2 generator was a low cost design. The similar mosquito catching apparatus available in the market costs between $ 500 and $1000 [2-11], the CO_2 generator was proposed to be manufactured under $ 100. The design of the unit and material selection has been based on this manufacturing cost. This section of the thesis will discuss the breakdown of the cost of manufacturing which includes the material and labour costs.

Table 8.1: A cost breakdown of the CO_2 Generator

Manufacturing in China and procurement of material from China and UK				
S. no.	Item	Quantity	Unit Price,$	Total Cost,$
1	Burner	1	10	10
2	Cooling Heat Sink	2	10	20
3	Internal Heat Sinks	2	1	2
4	Chimney Square Pipe	1	3	3
5	TEG	2	7	14
6	Injector	1		0
7	Fuel Control Valve	1	5	5
8	Thermal Paste	1	0.5	0.5
9	Exhaust Tube	1	1	1
10	Gas Fittings	1	10	10
11	Igniter	1	3	3
12	Safety thermocouple	1	2	2
13	Electricals	1	0.5	0.5
14	Housing			
	Side Plates	2	1	2
	Base Plate	1	10	10
	Outer Square Sections	1	5	5
15	Assembly cost/Hr	4	1.5	6
		Cost per unit for first 1000 units		94

The Table 8.1 presents the list of materials, cost per unit and the quantity required for each item. The costs shown in the table are based on the market research and quotations obtained from the suppliers in UK and China. The number of hours required to assemble are based on the experience of engineers working in Suterra. The procurement of the material, except TEG, was proposed to be done from China due to lower cost. The TEG was decided to be procured from a UK supplier. The assembly of the unit was decided to

take place in China because of significantly lower labour cost per hour as compared to UK. The estimated manufacturing cost per unit of CO_2 Generator was $ 94, which is under the proposed manufacturing cost. This cost is estimated when the material is ordered for 1000 units. Hence, the objective of a low cost design was fulfilled.

8.7 Summary

The CO_2 generator has been subjected to series of tests and this chapter has presented the important results which helps in investigating the performance of the unit. Results from gas analysis has shown that the unit produces the right amount of CO_2 and also confirms the absence of any other compound in the combustion exhaust in significant amounts, hence indicating complete combustion is taking place in the premixed burner. The CO_2 generator was then tested in an environmental chamber where the ambient temperatures were varied from a lowest being at 20 ^oC while the highest at 45 ^oC. The results have shown a decrease in temperature difference with increase in the ambient temperature which eventually causes a decrease in the power generation, as temperature difference across the sides of a TEG module is directly proportional to the power generation. It must be noted that even though the power generation at higher ambient temperature was low as compared to power generation at lower ambient temperatures but it was still capable producing the required power output of 3.5 W.

As mentioned previously, the application of the unit is in insect control so it was important to test the unit with insects. A laboratory test was carried out which involved testing the behaviour of the mosquitoes towards the CO_2 produced by the CO_2 generator. Olfactometer equipment was used to determine whether the mosquitoes follow the CO_2 plume and results were satisfactory with 87 % of mosquitoes showed attraction towards the CO_2. These tests not only helped in finding out the responsiveness of mosquitoes with the CO_2 but also confirmed absence of compounds such as CO, NOx and UHC in the combustion exhaust because presence of any of these compounds would repel mosquitoes as per entomological experts working alongside the project.

Next were field trials carried out to investigate the performance of the CO_2 generator in terms of flame stabilisation under real environmental condition involving wind, rain, temperature fluctuations etc., thermoelectric performance in terms of operation of the electrical components of the insect trap and most importantly the number of mosquitoes attracted and trapped by the insect trap which is the ultimate indication of the successful design and development of the CO_2 Generator. According to results from field trials, the CO_2 generator trapped 117 mosquitoes as compared to 42 by a Skeetervac SV1500, mosquito catching apparatus marketed by a competitor.

The cost breakdown has also been presented and it was estimated that the CO_2 Generator would cost $93 per unit to make, when 1000 units are manufactured in China.

Chapter 9

Conclusions and Recommendations

9.1 Conclusions

This research investigated a meso-scale non-catalytic premixed burner integrated with thermoelectric power generation modules. The research was carried out under a KTP project with the aim of developing and investigating a CO_2 generator which consists of the above mentioned burner and thermoelectric assembly. The working concept of the CO_2 Generator has been explained in Chapter 1 in detail, to summarise, a CO_2 Generator is a device that produces CO_2 by burning a hydrocarbon fuel and generates electrical power by converting the heat of combustion into electrical power via Seebeck effect using thermoelectric power generation modules. This device is intended to be marketed in the insect control market where it will be used as a source of attractant in the form of CO_2 for biting flying insects such as mosquitoes and midges as they have a proven tendency to attract towards CO_2. Following were the main achievements and finding of the research work:

- A non-catalytic self-aspirating premixed burner was designed which had the operating parameters of a meso-scale burner having thermal output of 250W and the size of a macro-scale burner required due to its integration with thermoelectric modules.
- It was found that addition of secondary air into combustion chamber helps in achieving a stable premixed flame. The final specification of the burner were a square shape with a backward facing step, non-catalytic combustion of 150mL/min of propane producing around 450mL/min of CO_2 and operating at a burner thermal rating of 250W.
- The burner was tested for the concentration of products of combustion by FTIR. The results showed that the combustion was complete as no UHC were present in the exhaust. The CO_2 production rate was found to be 450 mL/min, thus satisfying CO_2 production requirement for the device. The concentrations of CO and NOx were found to be 72 ppm and 29 ppm. These results showed that employing a backward facing step aids in the complete combustion of the fuel by enhancing the mixing of reactants by generating recirculation zones in the flow, and addition of secondary air into the combustion chamber has a significant effect of the flame stabilisation in meso-scale premix burners.

- Next, the premixed burner was integrated with thermoelectric. The tests involved optimisation of the hot and cold side of the module. The aim of the optimisation was to achieve a large temperature difference between the hot and cold side of the module as thermoelectric power generation is directly proportional to this temperature difference. The hot side was optimised by introducing internal heat sink (IHS) in the burner tube and placing the TEG modules on it. The idea was to increase the surface area in contact with the exhaust gases through the internal fins of IHS and thus increasing the heat supplied to the hot side of the module. The temperature of the hot side of the module was increased from 150 ^{o}C without IHS to 185 ^{o}C, which resulted in an increase in temperature difference and hence a higher power output of 5.5 W with IHS than 3.5 W without IHS was recorded.
- The results showed that increasing the number of TEG modules in the system does not increase the power generation as the amount of heat available is limited to a 250W burner output. More number of modules in the system meant less heat available to each module and hence lower power generation per module. Based on the results.
- The cold side of the module was optimised by testing different type of heat exchangers within the system to find out the ones which generated highest power by dissipating most heat. Four different types of heat exchangers were tested and the Type 4 heat exchangers which have the dimension as 150 mm width, 200 mm length, 40 mm height of the fins and black anodised surface finish, outperformed others in terms of highest power output and low cost design.
- The integration of TEG modules does not affect the combustion. Results from gas analysis after integration with thermoelectric modules has shown that the unit produces the right amount of CO_2 and also confirms the absence of any other compound in the combustion exhaust in significant amounts, hence indicating complete combustion was taking place in the premixed burner.
- The CO_2 generator was then tested in an environmental chamber and the results showed a decrease in temperature difference with increase in the ambient temperature which eventually causes a decrease in the power generation, as temperature difference across the sides of a TEG module is directly proportional to the power generation.
- The application of the unit is in insect control, therefore laboratory test was carried out which involved testing the behaviour of the mosquitoes towards the CO_2 produced by the CO_2 generator in an Olfactometer. The results were satisfactory with 87 % of mosquitoes showed attraction towards the CO_2. These tests not only helped in finding out the responsiveness of mosquitoes with the CO_2 but also confirmed absence of

compounds such as CO, NOx and UHC in the combustion exhaust because presence of any of these compounds would repel mosquitoes.

- According to results from field trials, the CO_2 generator trapped 117 mosquitoes as compared to 42 by a Skeetervac SV1500, a mosquito catching apparatus marketed by a competitor. The field trials provided evidence that the flame was stable under real environmental condition involving wind, rain, temperature fluctuations etc. The thermoelectric performance was satisfactory in terms of operation of the electrical components of the insect trap. The number of mosquitoes attracted and trapped by the insect trap is the ultimate indication of the success of the CO_2 Generator device and hence the completeness of the combustion and generation of required electrical power output.
- Effect of varying the step height on flame stabilisation was studied. Results showed that reducing the step height from 10 mm to 7 mm helped in preventing flame blowoff or in other words the flame was present inside the combustion chamber as opposed to 10mm step height in which the flame was completely anchored outside the burner. However, the flame showed unstable behaviour with high noise and flickering. The increase in step height from 10 mm to 15 mm resulted into flame blowoff similar to the burner with 10mm step height at all equivalence ratios.
- An investigation into the effect of secondary air addition in the combustion chamber on flame stabilisation was carried out. The addition of secondary air was found to have significant effect on flame stabilisation. With the addition of secondary air into the combustion chamber, the burners with step height 10mm and 15mm showed a stable premixed flame inside the combustion chamber with no acoustic instabilities and no flame flickering. It was concluded that the possible reason could be the secondary air stream acting as an aerodynamic bluff body causing the velocity of the reactant stream to reduce and hence preventing blowoff. This reasoning can be validated based on the fact that the velocity of the reactant stream entering into the combustion chamber is same with and without secondary air supply because the secondary air is supplied later into the combustion chamber, hence the only logical explanation could be the secondary air generating an aerodynamic wall which is intruding in the reactant stream and hence reducing its velocity and therefore preventing flame blowoff.

9.2 Recommendation for Future Work

The present study had various design limitation as it was an Industrial project leading to development of a commercial product. The operating parameters of the burner were restricted to a 250 W burner thermal output required as per the application of the final product. Future studies can include varying the burner thermal output and investigating its effect of thermoelectric performance.

As the power output is dependent upon the temperature difference between the two sides of the TEG, methods of improving the temperature difference can be explored in the future studies. Counter-flow heat exchanger arrangement which is previously tested on micro-scale burners can be proposed to test on the present meso-scale burner. This will involve modifying the current design to facilitate heat transfer from the cooling heat exchangers to the inlet fuel or combustion air. The expected results are an increase in heat dissipation from the heat exchanger leading to increase in temperature difference and hence higher power output, and improvement in combustion efficiency due to preheating of the reactants.

Flow visualisation method such as Laser Doppler Anemometry (LDA) or smoke visualisation are proposed for future work to study the actual flow fields and velocity profiles.

References

1. Biogents. The importance of carbon dioxide. Available: http://www.biogents.com/cms/website.php?id=/de/traps/funktion_wirksamkeit/kohlensaeure_co2.htm. Last accessed: 11th January 2014.
2. Mosquito Traps. Mosquito traps: Outdoors Available: http://mosquitotraps.co.uk/Products/Mosquitotrapsoutdoors/tabid/60/List/0/CategoryID/3/Level/a/Default.aspx?SortField=Free3,ProductName. Last accessed 1st January 2014. Blue Rhino. How SkeeterVac® Traps Exterminate. Available: http://www.bluerhino.com/BRWEB/Outdoor-Living-Products/Mosquito-Traps/How-SkeeterVac-traps-and-Exterminates.aspx. Last accessed: 11th January 2014.
3. Armatron Company. (2011). Flowtron- How it works. Available: http://www.flowtron.com/mm5/merchant.mvc?Screen=SH&Store_Code=F. Last accessed: 11th January 2014.
4. Koolatron. (2010). Bite Shield™ Mosquito Traps and Accessories. Available: http://koolatrononline.stores.yahoo.net/mosquito-control.html. Last accessed: 11th January 2014.
5. Woodstream Corporation. (2014). Mosquito Magnet - How It Works. Available: http://www.mosquitomagnet.com/advice/how-it-works. Last accessed: 11th January 2014.
6. Wigton BE, Jamestown, Miller MH and Hope, American Biophysics Corporation. (2000). Method and Device Producing CO_2 Gas For Trapping Insects. U.S. Pat. 6145243.
7. Bossler MC and CPD Associates Inc. (2004). Insect Trap Apparatus. U.S. Pat. 6718685B2.

8. Ohno S, Araki, Ikari and Fujimori, Jordan and Hamburg LLP. (2007). Insect Trapping Device. U.S. Pat. 2007/0017150A1.
9. Spiro M and Weiss RWJ. Lentek International Inc. (2004). Insect Trapping Apparatus. U.S. Pat. US2004/0123512A1.
10. Mosher II R F and Schmidt F. The Coleman Company Inc. (2005). Gas Tip and Gas Tip Holder for a Mosquito Trap. U.S. Pat. US2005/0066570A1.
11. Blue Rhino. How SkeeterVac® Traps Exterminate. Available: http://www.bluerhino.com/BRWEB/Outdoor-Living-Products/Mosquito-Traps/How-SkeeterVac-traps-and-Exterminates.aspx. Last accessed: 11th January 2014.
12. Biogents. BG-Sentinel: The researchers' mosquito trap. Available: http://www.biogents.com/cms/website.php?id=/en/traps/mosquito_traps/bg_sentinel.htm. Last accessed: 19th January 2014.
13. Rowe DM. (1995). CRC Handbook of Thermoelectrics. Florida, US: CRC Press.
14. Schaevitz SB, Franz AJ, Jensen KF, and Schmidt MA. (2001). A combustion based MEMS thermoelectric power generator. TRANSDUCERS'01. 1, p764-773.
15. Kania T and Dreizler A. (2009). Investigation of Micro Combustion chamber for a Thermoelectric Energy Converter. Proceedings of the European Combustion meeting.
16. Maruta K. (2011). Micro and mesoscale combustion. Proceedings of the Combustion Institute. 33, p125-150.
17. Fu K, Knobloch AJ and Martinez FC. (2001). American Society of Mechanical Engineers. 3, p867–873.
18. Weinberg FJ. (1975). The first half million years of combustion research and today's burning problems. Fifteenth Symposium (International) on Combustion. 15, p1-17.

19. Ahn J, Eastwood C, Sitzki L and Ronney PD (2005). Gas-phase and catalytic combustion in heat-recirculating burners. Proceedings of the Combustion Institute. 30, p2463-2472.
20. Lloyd SA and Weinberg FJ (1974). Nature Publishing Group.
21. Sitzki L, Borer K, Schuster E and Ronney PD. (2001). Combustion in Microscale Heat-Recirculating Burners. The Third Asia-Pacific Conference on Combustion. Seoul, Korea.
22. Mueller KT, Waters O, Bubnovich V, Orlovskaya N and Chen R. (2013). Super-adiabatic combustion in Al_2O_3 and SiC coated porous media for thermoelectric power conversion. Energy. 56, p108-116.
24. Charles E and Baukal JR (2001). The John Zink Combustion Handbook. USA: CRC Press LLC. p363-390.
25. Peters N (2000). Turbulent Combustion. Cambridge, UK: The Press Syndicate of the University of Cambridge. p66-168.
26. Gaydon AG and Wolfhard HG (1970). Flames: Their structure, radiation and temperature. 3rd ed. London: Chapman and Hall Ltd.
27. Mishra DP. (2007). Experimental studies of flame stability limits of CNG-air premixed flame. Energy Conservation and Management. 48, p1208-1211.
28. Hase K and Kori Y. (1996). Effect of premixing of fuel gas and air on NOx formation. Fuel. 75, p1509-1514.
29. Ghoniem AF, Annaswamy A, Park S and Sobhani ZC. (2005). Stability and emissions control using air injection and H2 addition in premixed combustion. Proceedings of the Combustion Institute. 30, p1765-1773.
30. Alliche M, Haldenwang P and Chikh S. (2010). Extinction conditions of a premixed flame in a channel. Combustion and Flame. 157, p1050-1060.

31. Xu B and Ju Y. (2005). Theoretical and Experimental studies on mesoscale flame propagation and extinction. Proceedings of the Combustion Institute. 30, p2445-2453.
32. Kim N, Kataoka T, Maruyama S and Maruta K. (2005). Flammability limits of stationary flames in tubes at low pressure. Combustion and Flame. 141, p78-88.
33. Tang C, Huang Z, Jin C, He J, Wang J, Wang X and Miao H. (2008). Laminar burning velocities and combustion characteristics of propane-hydrogen-air premixed flames. International Journal of Hydrogen Energy. 33, p4906-4919.
34. Li J, Chou SK, Huang G, Yang WM and Li ZW. (April 2009). Study on premixed combustion in cylindrical micro combustors: Transient flame behaviour and wall heat flux. Experimental Thermal and Fluid Science. 33, p764-773.
35. Huang Y and Yang V. (2009). Dynamics and stability of lea-premixed swirl-stabilized combustion. Progress in Energy and Combustion Science. 35, p293-364.
36. Kurdyumov V, Fernandez-Tarrazo E, Truffaut JM, Quinard J, Wangher A and Searby G. (2007). Experimental and numerical of premixed flame flashback. Proceedings of the Combustion Institute. 31, p1275-1282.
37. Akbari MH and Riahi P. (2010). Investigation of the structural and reactants properties on thermal characteristics of a premixed porous burner. Applied Energy. 87, p1433-1440.
38. Wood S and Harris AT. (2008). Porous burners for lean-burn application. Progress in Energy and Combustion Science. 34, p667-684.
39. Maruta K. (2011). Micro and mesoscale combustion. Proceedings of the Combustion Institute. 33, p125-150.
40. Walther DC and Ahn J. (2011). Advances and challenges in the development of power-generation systems at small scales. Progress in Energy and Combustion Science. 37, p583-610.

41. Cooley B, Walther DC and Fernandez-Pello AC. Exploring the limits of microscale combustion. Fall Technical Meeting. Irvine, CA: Western States Section/ Combustion Institute; October 1999.
42. Peterson RB and Hatfield JM. (2001). A catalytically sustained microcombustor burning propane. Proc. 2001 International Mechanical Engineering Congress and Exposition (IMECE). New York.
43. Masel R and Shannon M. (2001). Microcombustor having submillimeter critical dimensions. Patent: US06193501.
44. Spadaccini CM, Zhang X, Cadou CP, Miki N and Waitz IA. (2002). Development of a catalytic silicon micro-combustor for hydrocarbon-fueled power MEMS. MEMS 2001.
45. Maruta K, Takeda K, Sitzki L, Borer K, Ronney PD, Wussow S. (2001) Catalytic combustion in microchannel for MEMS power generation. Third Asia-Pacific Conference on Combustion. Seoul, Korea.
46. Maruta K, Takeda K, Ahn J, Borer K, Sitzki L, Ronney PD and Deutschmann O. (2002). Extinction limits of catalytic combustion in micro-channels. Proceedings of the Combustion Institute. 29, p957-963.
47. Vican J, Gajdeczko BF, Dryer FL, Milius DL, Aksay IA and Yetter RA. (2002). Development of a microreactor as a thermal source for MEMS power generation. Proceedings of the Combustion Institute. 29. P909-916.
48. Peterson RB. Small packages. Mechanical Engineering; June 2001:58e61.
49. Jackson T, Buckmaster J, Lu Z, Kyritsis DC and Massa L. (2007). Flames in narrow circular tubes. Proceedings of the Combustion Institute. 31, p955-962.
50. Maruta K, Kataoka T, Kim NI, Minaev S and Fursenko R. (2005). Characteristics of combustion in narrow channel with temperature gradient. Proceedings of the Combustion Institute. 30, p2429-2436.

51. Evans CJ and Kyritsis DC (2009). Operational regimes of rich methane and propane/oxygen flames in mesoscale non-adiabatic ducts. Proceedings of the Combustion Institute. 32, p3107-3114.
52. Bijjula K, Christensen KT and Kyritsis DC. (2009). Experimental investigation of gaseous reactive flows around catalytically coated micro-wires. Proceedings of the Combustion Institute. 32, p3043-50.
53. Smyth SA, Christensen KT and Kyritsis DC (2009). Intermediate Reynolds number flat plate boundary layer flows over catalytic surfaces for "Micro" combustion applications. Proceedings of the Combustion Institute. 32, p3035-3042.
54. Kaisare NS and Vlachos DG. (2007). Optimal reactor dimensions for homogeneous combustion in small channels. Catalysis Today. 120, p96-106.
55. Yang WM, Chou SK, Shu C, Li ZW and Xue H. (2002). Combustion in micro-cylindrical combustors with and without a backward facing step. Applied Thermal Engineering. 22, p1777-1787.
56. Yang WM, Chou SK, Chua KJ, Li J and Zhao X. (2011). Research on modular micro combustor-radiator with and without porous media. Chemical Engineering Journal. 168, p799-802.
57. Kariuki J and Balachandran R. (2010). Experimental investigation of dynamics of premixed acetylene–air flames in a micro-combustor. Experimental Thermal and Fluid Science. 34, p330-337.
58. Scarpa A, Pironec R, Russo G and Vlachos DG. (2009). Effect of heat recirculation on the self-sustained catalytic combustion of propane/air mixtures in a quartz reactor. Combustion and Flame. 156, p947-953.
59. Kania T and Dreizler A. (2009). Investigation of Micro Combustion chamber for a Thermoelectric Energy Converter. Proceedings of the European Combustion meeting. Vienna, Austria.

60. U S Government. (2000). Micro combustor and combustion based thermoelectric micro generator- US Patent US 20010029974 A1.
61. Wu M, Wang Y, Yang V and Yetter RA. (2007). Combustion in meso-scale vortex chambers. Proceedings of the Combustion Institute. 31, p3235-3242.
62. Belmont EL, Schoegl I and Ellzey JL. (2013). Experimental and analytical investigation of lean premixed methane/air combustion in a mesoscale counter-flow reactor. Proceedings of the Combustion Institute. 34, p3361-3367.
63. Li ZW, Chou SK, ShuC and Yang WM. (2005). Effects of step height on wall temperature of a microcombustor. Institute of Physics Publishing. 15, p207-212.
64. Altay HM, Speth RL, Hudgins D E and Ghoniem AF. (2009). Flame-vortex interaction driven combustion dynamic in a backward facing step combustor. Combustion and Flame. 156, p1111-1125.
65. Ghoniem AF, Annaswamy A, Sobhani ZC and Park S. (2005). Stability and emissions control using air injection and H_2 addition in premixed combustion. Proceedings of the Combustion Institute. 30, p1765-1773.
66. Altay HM, Hudgins DE, Speth RL, Annaswamy A and Ghoniem AF. (2010). Mitigation of thermoacoustic instability utilizing steady air injection near the flame anchoring zone. Combustion and Flame. 157, p686-700.
67. Uhm J and Acharya S. (2004). Control of combustion instability with a high-momentum air-jet. Combustion and Flame. 139, p106–125.
68. Roy V, Majumder S and Sanyal D. (2010). Analysis of the Turbulent Fluid Flow in a Axi-Symmetric Sudden Expansion. International Journal of Engineering Science and Technology. 2(6), p1669-1574.
69. Abu-Mulaweh H I, Chen TS and Armaly BF. (2002). Turbulent mixed convection flow over a backward-facing step—the effect of the step heights. International Journal of Heat and Fluid Flow. 23, p758-765.

70. Ko SC and Sung H J. (2001). Large-eddy simulation of turbulent flow inside a sudden-expansion cylindrical chamber. Journal of Turbulence. 01, p1468-5248.
71. Rowe DM and Bhandari CM (1983). Modern Thermoelectrics. London: Rinehart and Winston.
72. Rowe DM (2005). CRC Handbook of Thermoelectrics: Micro to Nano. London: CRC Press.
73. Rowe DM and Min G. (2006). Conversion efficiency of Thermoelectric Combustion systems. IEEE Transactions on energy Conversion.
74. Rowe DM and Min G. (2001). A novel principle allowing rapid and accurate measurement of a dimensionless thermoelectric figure of merit. Measurement Science and Technology. 12, p1261-1262.
75. Rowe DM, Min G and Kontostavlakis K. (2004). Thermoelectric figure of merit under large temperature difference. Journal of Physics D: Applied Sciences. 37, p1301-1304.
76. Schaevitz SB, Franz AJ, Jensen KF, and Schmidt MA. (2001). A combustion based MEMS thermoelectric power generator. TRANSDUCERS '01. 1, p764-773.
77. Rowe DM and Min G. (2002). On thermoelectric power conversion from heat re-circulating combustion systems. Proceedings of combustion institute. 29, p941-947.
78. Norton DG, Voit KW, Brüggemann T, and Vlachos DG. Portable power generation via integrated catalytic microcombustion-thermoelectric devices. Army Research Laboratory, Weapons and Materials Research Directorate.
79. U S Government. (2000). Micro combustor and combustion based thermoelectric micro generator- US Patent US6613972 B2.
80. Ying H. (2011). Energy-Efficient Micro-Combustion System for Power Generation and Fuel Processing. US Patent US20110083710 A1.

81. Mueller KT, Waters O, Bubnovich V, Orlovskaya N and Chen R. (2013). Super-adiabatic combustion in Al2O3 and SiC coated porous media for thermoelectric power conversion. Energy. 56, p108-116.
82. Ju Y and Maruta K. (2011). Microscale combustion: Technology development and fundamental research. Progress in Energy and Combustion Science . 37, p669-715.
83. Rowe DM and Min G. (2002). Symbiotic application of thermoelectric conversion for fluid preheating/power generation. Energy Conversion and Management. 43, p221-228.
84. Huesgen T, Woias P and Kockmann N. (2008). Design and fabrication of MEMS thermoelectric generator with high temperature efficiency. Sensors and Actuators. p423-429.
85. Hong X, Wenming Y, Chou SK, Chang S and Zhigwang L. (2005). Microthermophotovoltaics power system for portable MEMS devices. Microscale thermophysical engineering. 9, p85-97.
86. Wienberg FJ, Rowe DM and Min G. (2002). Novel high performance small scale thermoelectric power generation employing regenerative combustion system. Rapid Communication. 35, P61-63.
87. Carlos A. (2002). Micro Power Generation Using Combustion: Issues and approaches. Proceedings of combustion institute. 29, p883-899.
88. Abu-Mulaweh HI, Chen TS and Armaly BF. (2001). Turbulent mixed convection flow over a backward-facing step. International Journal of Heat and Mass Transfer. 44, p2661-2669.
89. Pan JF, Huang J, Li DT, Yang WM, Tang WX and Xue H. (2007). Effects of major parameters on micro-combustion for thermophotovoltaic energy conversion. Applies Thermal Engineering. 27, p1089-1095.

90. Li J, Chou SK, Li ZW and Yang WM. (2009). Characterization of wall temperature and radiation power through cylindrical dump micro-combustors. Combustion and Flame. 156, p1587-1593.

91. Gasmet. (1997). Instruction Manual for GASMET On-Site Series: DX-3000 and DX-9000. p6-10.

92. Gasmet Technologies Inc. Calcmet™ - From Spectrum to Results. Available: http://www.gasmet.com/na/products/software/calcmet. Last accessed: 25th February 2014.

93. European Thermodynamics Limited. Thermo Electric Generation Module, MFG Part Number：GM250-127-14-16.p1-6.

94. Rowe DM and Min G. (1998). Evaluation of Thermoelectric modules for power generation. Journal of Power Sources. 73, p193-198.

95. Rowe DM. (1999). Thermoelectrics, an environmentally-friendly source of electrical power. Renewable Energy. 16, p1251-1256.

96. Riffat SB and Ma X. (2003). Thermoelectrics: a review of present and potential applications. Applied Thermal Engineering. 23, P913-935.

97. Garrett SL and Poese ME. (2013). There's (still) plenty of room at the bottom. Applied Thermal Engineering. 61, p884-888.

98. Saidur R, Rezaei M, Muzammil WK, Hassan MH, Paria S and Hasanuzzaman M. (2012). Technologies to recover exhaust heat from internal combustion engines. Renewable and Sustainable Energy Reviews. 16, p5649-5659.

99. Elsheikh MH, Shnawah DA and Sabri MFM. (2014). A review on thermoelectric renewable energy: Principle parameters. Renewable and Sustainable Energy Reviews. 30, p337-355.

100. Kline DL. (2002). Evaluation of various models of propane-powered mosquito traps. Journal of Vector Ecology. 27 (1), p1-7.

101. Biogents. Olfactometer Tests. Available: http://www.biogents.com/cms/website.php?id=/en/contract/test_protocols/olfactometer_tests.htm. Last accessed: 03rd March January 2014.

102. Geier M, Bosch O, Steib B and Rose A. (2002). Odour-guided host finding of mosquitoes: identification of new attractants on human skin. Proceedings of the 4th international conference on urban pests.

103. Dynamic Solutions Worldwide. (2014). How The Dynatrap Works. Available: http://www.dynatrap.com/howitworks. Last accessed: 11th January 2014.

104. Taylor KC. (1987). Automobile Catalytic Converters. Proceedings of the First International Symposium. 30, p97-116

105. Cowley A (2013). Platinum 2013. Johnson Matthey Public Limited Company.